

Speciation Analysis and Environmental Tracer Studies of 129I

Zhang, Luyuan; Hou, Xiaolin

Publication date:
2015

Document Version
Publisher's PDF, also known as Version of record

[Link back to DTU Orbit](#)

Citation (APA):
Zhang, L., & Hou, X. (2015). Speciation Analysis and Environmental Tracer Studies of 129I. DTU Nutech.

DTU Library

Technical Information Center of Denmark

General rights

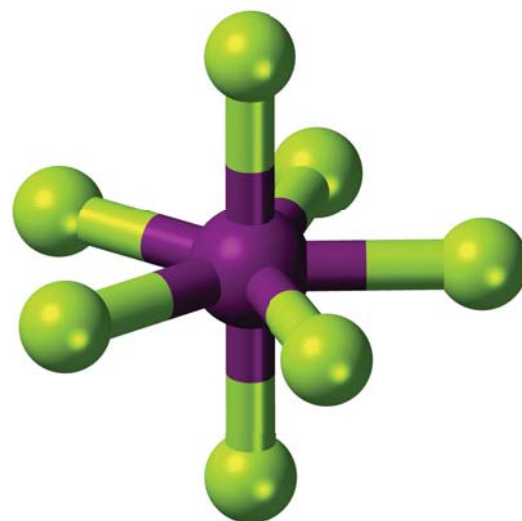
Copyright and moral rights for the publications made accessible in the public portal are retained by the authors and/or other copyright owners and it is a condition of accessing publications that users recognise and abide by the legal requirements associated with these rights.

- Users may download and print one copy of any publication from the public portal for the purpose of private study or research.
- You may not further distribute the material or use it for any profit-making activity or commercial gain
- You may freely distribute the URL identifying the publication in the public portal

If you believe that this document breaches copyright please contact us providing details, and we will remove access to the work immediately and investigate your claim.

Speciation Analysis and Environmental Tracer Studies of ^{129}I

PhD Dissertation



Luyuan Zhang
DTU Nutech Report
June 2015



Dissertation for the Degree of Doctor of Philosophy

Center for Nuclear Technologies,

Technical University of Denmark

**Speciation Analysis and Environmental
Tracer Studies of ^{129}I**

BY

LUYUAN ZHANG

To be presented for public criticism on 3 June, 2015

DTU Nutech, Roskilde, Denmark

Supervisor

Professor Xiaolin Hou

Center for Nuclear Technologies, Technical University of Denmark

Roskilde, Denmark

Opponents

Senior Scientist Sven P. Nielsens

Radioecology and Tracer Studies, Center for Nuclear Technologies, Technical University of Denmark

Roskilde, Denmark

Professor Ala Aldahan

Department of Earth Sciences, Uppsala University
Uppsala, Sweden

Department of Geology, United Arab Emirates University
Al Ain, United Arab Emirates

Reader Dr. Alex R. Baker

Laboratory for Global Marine and Atmospheric Chemistry, School of Environmental Sciences, University of East Anglia
Norwich, United Kingdom

Preface

This dissertation is only a part of my experience in Denmark during the three and half years. I have been devoting myself to those lab works with sweet and tears, but I know it definitely deserves all the efforts I made. I could always feel warm from so many lovely people around me, no matter how harsh the weather outside. I could never forget the cherished times I have spent with my colleagues and my friends, enjoying delicious food in parties and sharing happiness and unhappiness. I could not forget how beautiful the Danish summer is, just like elegant frameless paintings depicted by the well-known Danish fairytale writer Hans. C. Andersen. I will always keep in mind the pain of long separation with my family that makes me grow up and rethink the meaning of family. Thanks to these rewarding experiences and all these unforgettable memories will be appreciated and treasured in my whole life.

Luyuan Zhang

Roskilde, Denmark

June, 2015

Resumé

Jod er et essentielt grundstof for alle pattedyr. Derfor er det vigtigt at undersøge, hvorledes jod opfører sig og transporteres i miljøet. ^{129}I , en langlivet radioisotop af jod (1.57×10^7 år), udledes hovedsageligt til miljøet fra nukleare oparbejdningsanlæg (især Sellafield i Storbritannien og La Hague i Frankrig), som udgør unikke punktkilder med udslip til havet, som er velegnede til sporstofundersøgelser af jod i miljøet. Undersøgelser af kemiske former (speciering) af ^{129}I benyttes ikke kun for at studere jods geokemiske kredsløb, men også for at undersøge processer i miljøet. Denne afhandling præsenterer metoder udviklet til kemisk analyse af speciering af ^{129}I i miljøprøver og biologiske prøver (dvs. havvand, aerosoler, og tang), såvel som anvendelser til at undersøge processer i miljøet og det geokemiske kredsløb for stabilt ^{127}I i havet, atmosfæren og tang.

Baseret på tidligere erfaring blev en metode med nedbrydning med persulfat oxidation udviklet yderligere for at konvertere organisk jod til uorganiske former i naturlige vandprøver. Denne ny metode har vist sig at være effektiv og pålidelig til nedbrydning af organisk jod, og har været anvendt med succes til at bestemme ^{129}I i naturlige vandområder og perkolat indeholdende organisk jod.

En metode er udviklet til analyse af speciering af ^{129}I og ^{127}I i aerosoler indsamlet på luftfiltre af polypropylen. Sekventiel ekstraktion med vand og NaOH-opløsning blev brugt til at udvinde vandopløseligt jod (WSI) og NaOH opløselig jod (NSI), og alkalisk foraskning blev brugt til rester af uopløseligt aerosol jod (RII). WSI blev yderligere adskilt i iodid og iodat ved hjælp af anionbytningskromatografi. Parametre, såsom mængden af udvaskningsmidler, udvaskningstid, foraskningstid og temperatur, og tilsætning af jodbevarende reagenser, der kan påvirke stabiliteten af jodformer og kemisk udbytte af jodformer under kemisk separation, blev undersøgt med henblik på at opnå nøjagtige resultater af ^{129}I -former i aerosoler. Analyseresultaterne af de samlede og forskellige kemiske former for ^{129}I i aerosolprøver viser, at den udviklede metode er pålidelig til præcis angivelse af ^{129}I og ^{127}I i aerosoler.

Fordeling af kemiske former (iodid og iodat) af ^{129}I og ^{127}I i prøver af havvand fra det centrale Arktis, Grønlands kyster, danske kyster og kysten ved Fukushima i Japan blev undersøgt. For både ^{129}I og ^{127}I er iodat den fremherskende form i havvand i det centrale Arktis og ved Grønlands kyster, mens iodid er den fremherskende form for ^{129}I og ^{127}I i danske kystfarvande. Et særligt fordelingsmønster af iod-former blev observeret i prøver af havvand fra kysten ved Fukushima, hvor I/IO_3^- atomforholdet for ^{127}I var i intervallet 0.07-0.27, hvilket

afspejler dominerende mængder af iodat i havvand, mens forholdene for ^{129}I angiver, at iodid er den dominerende form. Disse resultater viser, at sammensætningen af jod-former afhænger af kilden til jod (nukleare oparbejdningsanlæg og nukleare ulykker), transportveje (langs kysten og i åbent område på havet) og biogeokemiske processer. Den bemærkelsesværdig store mængde ^{129}I i det Arktiske Ocean i 2011 medfører, at Arktis virker som en sekundær kilde af ^{129}I med udstrømning til sydligere have, såsom Grønlandshavet og det vestlige Atlanterhav, samt til atmosfæren og det arktiske økosystem.

Aerosolprøver indsamlet to steder (Risø, Danmark, nær kysten, og Tsukuba Japan, 170 km sydvest for Fukushima Dai-ichi atomkraftværket) i løbet af foråret 2011 (kort efter Fukushima atomulykken) og vinteren 2014 blev analyseret for jod-former af ^{129}I og ^{127}I herunder opløselige og uopløselige former. Resultaterne viser, at koncentrationer og kemiske former af ^{129}I og ^{127}I i aerosoler er stærkt relateret til kilder og transportveje for luftmasser, og at ^{129}I fra Fukushima bidrog med under 6% af den samlede mængde ^{129}I i atmosfæren over Nordeuropa under ulykken.

Kemiske former af ^{129}I og ^{127}I i tang (*Fucus serratus* og *vesiculosus*) indsamlet i danske kystområder i 2014 blev bestemt, herunder vandopløselig jod (iodid, iodat og opløselig organisk jod) og vanduopløselig jod. Mulige mekanismer for optag af jod i tang i naturlige marine systemer blev undersøgt ved at kombinere data for kemiske former af jod i prøver af vand og tang indsamlet samtidigt.

Abstract

Iodine is well known as an essential nutrient element for mammals. It has evoked extensive interests in investigation of its behaviours and transportation processes in various environmental components. ^{129}I , a long-lived radioisotope of iodine (1.57×10^7 years), is predominantly discharged to the environment from nuclear reprocessing plants (especially Sellafield in United Kingdom and La Hague in France), providing a unique point source for environmental tracing studies. Speciation analysis of ^{129}I can be used not only for studying the geochemical cycle of iodine, but also for investigating various environmental processes. This thesis presents the methods developed for chemical speciation analysis of ^{129}I in environmental and biological samples (i.e. seawater, aerosols, and seaweed), as well as its applications for tracing environmental processes and investigating geochemical cycle of stable ^{127}I in ocean, atmosphere and seaweed.

Based on the previous work, a persulfate oxidation decomposition method was further investigated for converting organic iodine to inorganic forms in natural water samples. This method was proved to be efficient and reliable for decomposing organic iodine, and has been successfully applied for determination of ^{129}I in natural waters and leachates containing organic iodine species.

A method has been established for speciation analysis of ^{129}I and ^{127}I in aerosol samples collected on polypropylene filter. Sequential extraction using water and NaOH solution was employed to extract water-soluble iodine (WSI) and NaOH soluble iodine (NSI), and alkaline ashing for residue insoluble aerosol iodine (RII). WSI was further partitioned to iodide and iodate using anion exchange chromatography. Parameters, such as amount of leaching agents used, leaching time, ashing time and temperature, and addition of iodine protecting reagent that might influence stability of iodine species and chemical yield of iodine species during chemical separation, were investigated in order to obtain accurate results of ^{129}I species in aerosol. The results on the analysis of total and different species of ^{129}I in real samples demonstrate that the developed method is reliable for accurate determination of ^{129}I and ^{127}I species in aerosol samples.

Distributions of chemical species (iodide and iodate) of ^{129}I and ^{127}I in the seawater from the central Arctic, Greenland coast, Danish coast and offshore Fukushima, Japan were investigated. Iodate for both ^{129}I and ^{127}I is the predominant form for the seawater in the central Arctic and Greenland coast, whereas iodide is the major species of ^{129}I and ^{127}I in Danish coast. A distinct distribution pattern of iodine species was observed in Fukushima offshore seawater, where the I/IO_3^- atomic

ratios for ^{127}I were in the range of 0.07-0.27 reflecting a dominant iodate in the seawater, but the I^-/IO_3^- ratios for ^{129}I indicated that iodide is the major iodine species. These investigations demonstrate that variation of iodine species is dependent on origins of iodine (nuclear reprocessing plants and nuclear accident), transportation pathways (along the coast and open area of ocean) and biogeochemical processes. The remarkably increased ^{129}I inventory in the Arctic by 2011 suggests that it may act as a secondary source of ^{129}I that outflows to the downstream seas, such as the Greenland Sea, and the western Atlantic Ocean, as well as to the atmosphere and the Arctic ecosystem.

Aerosol samples collected at two locations (Risø, Denmark, a coastal site, and Tsukuba Japan, about 170 km southwest of the Fukushima Dai-ichi nuclear power plant) during spring 2011 (shortly after the Fukushima nuclear accident) and winter 2014 were analyzed for iodine species of ^{129}I and ^{127}I including soluble and insoluble iodine. The results indicate that the concentrations and species of ^{129}I and ^{127}I in aerosols are strongly related to the sources and pathways of air masses, and that Fukushima-derived ^{129}I only contributed less than 6% of total ^{129}I in the northern Europe during the accident period.

Chemical species of ^{129}I and ^{127}I in seaweed (*Fucus Serratus* and *Vesiculosus*) collected in Danish coastal areas in 2014 were determined including water-soluble iodine (iodide, iodate and soluble organic iodine) and water insoluble iodine. In combination of iodine species in seawater simultaneously collected with seaweed, possible mechanism of iodine uptake by seaweed was explored in natural marine system.

Acknowledgement

As I wrote down the last character of this dissertation, all the unforgettable moments during the three-year Ph.D. study gradually emerges into my mind. To be honest, studying abroad was completely out of my life schedules, but life is what happens while you are making other plans, and always brings surprises. Since my first day on 6th January, 2012, I have felt at home at the Division of Radioecology (RAS), Nutech of DTU Risø campus. I have been given unique opportunities on this miraculous 2.6 km² peninsula with many splendid scientists. I could not describe how much I obtained throughout these years. Undoubtedly, I have been given invaluable and continuous supports in both science and life aspects from many generous, kind, and loving people.

First and foremost, I would like to thank my advisor, Professor Xiaolin Hou. You are not only my supervisor, but also have been my respected mentor. In the summer six years ago, I was fortunate to make acquaintance with you when I was a fledgling on radiochemistry just after my master graduation. I still clearly remember the first talk with you, when you swept my confusion about future career with your enriched life experiences, and encouraged me to proceed with confidence. Ever since, with your guidance, I, like a toddler, really step into the profound and challenging scientific field. Throughout these years, not only during my Ph.D. study, you have academically supported me by providing a great number of invaluable suggestions and advices on designing experiments, operating instruments, organizing manuscripts, preparing papers and so many I cannot count. The joy and enthusiasm you have for the research was contagious and motivational for me, especially during tough times in my Ph.D. pursuit. Not only in science, but also in life, I was deeply touched by your infinite emotional support and sufficient understanding that enabled me to carry on. I appreciate all of your immense contributions of time and ideas to make my Ph.D. experience productive and stimulating.

I am deeply grateful to Senior Scientist Sven P. Nielsen, the head of RAS, who provided me such a wonderful chance to work in his division. His flexibility in scheduling, gentle encouragement and relaxed demeanor made for such a good working relationship and the impetus for me to finish. My sincerely acknowledgement goes to Professor Weijian Zhou in the Institute of Earth Environment, who agreed me to continue my study and consistently cultivates me to become an excellent researcher. Her careness and understanding during my Ph.D. study are greatly appreciated.

I appreciated very much Senior Scientist Per Roos, who was always patient to answer my questions and gave me solid support with the operation of ICP-MS and vivid expositive teaching on radiometric detections. I was often impressed by his extremely high EQ. His fast understanding on what I expressed greatly increased my confidence with the language, especially at the beginning of my study. Great thanks go to Per also for his encourage and comfort, especially during my burdensome thesis writing. I am much indebted to Dr. Sheng Xu in Scottish University Environmental Research Center, who transferred his abundant AMS knowledge to me, gave me previous suggestions on scientific research and contributed a lot for sample analysis. Discussions with him were always pleasant and instructive, especially during my external research in Glasgow.

A sincere thank is given to Professor Shenghong Hu, my master supervisor in China University of Geosciences for his continuous encourage for many years. He used to say to his students that “Be a true man before do advance!” to teach us how to behave right. I bear firmly in my mind.

During the three and half years, I have shared office with Jixin, who sets a good example for me not only on the academic aspect but also on the family responsibility. I also sincerely thank Keliang, who offered me a number of practical helps to live in Denmark, especially the delicious Lanzhou noodles. Also thanks both of you for the plentiful discussions about my iodine project. All the colleagues in our Radioecology Division, Clause, Liga, Kristina, Susanne, Yusuf, Charlotte, Thomas, Kai are deeply thanked for their help on filed sampling, sample preparation, operation of equipment, ordering of chemical reagents and also for their emotional support during my study.

I also would like to express my gratitude to all my colleagues and the whole Nutech headed by Jens-Perter for all the happy moments, nice chatting, wonderful department trips and strong research atmosphere, monthly morning meetings, summer parties, Christmas parties, etc. Thanks to Birgitte, Helle and Majbrit, our lovely secretaries for their kindness and efficient work, because they were always patient to answer my questions and helped me to fill and transfer a number of documents. Although never met, my thanks also go to these people in Lyngby campus, Susan, Hedi and the Ph.D committee for their great help during on my visa application, study plan and a lot of others.

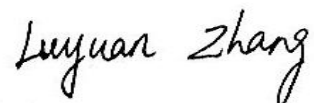
I am grateful to all the colleagues in Xi'an AMS Center, IEECAS for their support in these years. Ning Chen, Yukun, Yuchong, Qi Liu, Senior engineers Zhenkun Wu, Xuefeng Lu, Liping Yang, Linlang Li, Wennian Zhao, Chunhai Huang and many

other people are sincerely acknowledged because of their supports on AMS measurement of ^{129}I and also because of the nice working atmosphere.

I am also grateful to all my friends: Yihong, Haitao, Jinfeng, Yali, Shuangwen, Mingli and Chongyi for their support and friendly atmosphere in our DTU Nutech. I have enjoyed the time spent with them because of the pleasant working atmosphere and the happy parties during weekends. Thanks to all the other nice friends I met in Denmark: Gaoming, Hongsheng, Liying Sun, Li He, Xue Han, Valentina, Xiaodan, Pei Liu, Sunao, Liying Yang, Dela, Lei Feng, etc. for their continuous care and friendship.

The most sincere thanks are given to my family. Words cannot express how grateful I am to my parents, Jianhua and Xiuhong for all of the sacrifices that you have made and for your liberal ideas to let me receive such good education. My deepest gratitude goes to my beloved husband Zheng and my sweetest daughter Youhan for all the support and for your love. Both of you make my life wonderful and distinctive. My dearest sisters and brother, Lufang, Lufei and Lulai for loving me and sharing responsibility for our family.

Finally, this dissertation is dedicated to my grandparents, Fuxiang and Yuxia to express my deeply miss. It has been over ten years since you passed away. Everything is just as if yesterday, playing with you in gardens, being itched by grandfather's prickly beard and having good sleep with grandmother's gentle stroke. I miss you all the time, and always look for you in my dreams. I know wherever I go and whatever I do, you will still be there, standing by me, smiling, hugging and protecting me from the fears and tears. Without your love, I cannot be the one I am today.



DTU Risø, Roskilde

June 2015

List of papers related to the thesis

- I. Zhang L.Y., Hou X.L. Speciation analysis of ^{129}I and its applications in environmental research. *Radiochimica Acta* 2013, 101:525-40.
- II. Zhang L.Y., Hou X.L., Xu S. Speciation analysis of ^{129}I and ^{127}I in aerosols using sequential extraction and Mass Spectrometry. *Analytical Chemistry*, DOI: 10.1021/acs.analchem.5b01555, Publication Date (Web): June 5, 2015.
- III. Zhang L.Y., Hou X.L., Gwynn J. P., Karcher M., Zhou W. J., et al. Depth profile of chemical species of ^{129}I and ^{127}I and implication for water circulation and marine environmental chemistry in the central arctic. Manuscript.
- IV. Hou X.L., Povinec P.P., Zhang L.Y., Shi K.L., Biddulph D., Chang C. et al. Iodine-129 in Seawater Offshore Fukushima: Distribution, Inorganic Speciation, Sources, and Budget. *Environ Sci Technol* 2013, 47:3091-8.
- V. Xu S., Zhang L.Y., Freeman S.P.H.T., Hou X.L., Shibata Y., Sanderson D. et al. Speciation of Radiocesium and Radioiodine in Aerosols from Tsukuba after the Fukushima Nuclear Accident. *Environ Sci Technol* 2015, 49:1017-24.
- VI. Zhang L.Y., Hou X.L., Xu S. Speciation of ^{127}I and ^{129}I in atmospheric aerosols at Risø, Denmark: Insight into sources of iodine isotopes and their species transformation. Submitted to *Atmospheric Chemistry and Physics*.

Conferences

- I. Zhang L.Y., Hou X.L. Speciation analysis of iodine (^{129}I and ^{127}I) in aerosol samples. The 2nd NKS-B Workshop on Radioanalytical Chemistry. Risø, Roskilde, Denmark, 2-6th Sept. 2013, Poster
- II. Zhang L.Y., Hou X.L., Zhou W.J., Li H.C., Chen N., Fan Y.K., et al. ^{129}I Record in the Taal Lake sediment, Philippines: Implication for global fallout of ^{129}I in low latitude. The First Russian-Nordic Symposium on Radiochemistry. Moscow Russia, 21-24 Oct. 2013. Poster.
- III. Zhang L.Y., Hou X.L., Gwynn J. P., Karcher M., Zhou W. J., et al. Distribution, Pathway and Speciation Variation of ^{127}I and ^{129}I in the Central Arctic Ocean. The 13th International Conference on Accelerator Mass

Spectrometry (AMS-13).SEOLANE Centre, Aix en Provence, France, 24-28 Aug. 2014. Oral.

- IV. Zhang L.Y., Hou X.L., Xu S. Determination of iodine species (^{127}I and ^{129}I) in aerosols by Sequential extraction and mass spectrometry detection and its application. Tenth International Conference Methods and Applications of Radioanalytical Chemistry (MARC X). Kailua-Kona, Hawaii, USA, 12-18 Apr. 2015. Oral.

Foundation

Idella travelling grant. Technical University of Denmark. June 2013.

Abbreviations

AES	Atomic emission spectrometry
AMS	Accelerator mass spectrometry
AWL	Atlantic water layer
DIT	Di-iodotyrosine
EXAFS	Extended X-ray absorption fine structure
FDNPP	Fukushima Dai-ichi nuclear power plant
GC	Gas chromatography
HMW	High molecular weight
HPLC	High performance liquid chromatography
HYSPLIT	Hybrid Single Particle Lagrangian Integrated Trajectory Model
IAEA	International Atomic Energy Agency
ICP-MS	Inductively coupled plasma mass spectrometry
INAA	Instrumental neutron activation analysis
LMW	Low molecular weight;
LSC	Liquid scintillation counter
MIT	Mono-iodotyrosine
NAA	Neutron activation analysis
NIST	National Institute of Standards and Technology
NPP	Nuclear power plant
NRP	Nuclear reprocessing plant
NSI	NaOH soluble iodine
PML	Polar mixed layer
RII	Residual insoluble iodine
TIMS	Thermal ionization mass spectrometry
TMAH	Tetramethyl ammonium hydroxide
WSI	Water-soluble iodine
WSOI	Water-soluble organic iodine
WWI	Woodward iodine
XANES	X-ray absorption near edge structure

Contents

Preface	iii
Resumé	iv
Abstract.....	vi
Acknowledgement.....	viii
List of papers	xi
Abbreviations.....	xiii
1. Introduction	1
1.1 Sources, level and radioactive hazard of ^{129}I in the environment	2
1.2 Iodine species and transformation.....	4
1.2.1 Iodine species (^{129}I and ^{127}I) in the environment	5
1.2.2 Transformation of iodine species	7
1.3 Analytical methods for ^{129}I and its species	9
1.3.1 Total ^{129}I	9
1.3.2 Separation techniques for speciation analysis of ^{129}I	12
1.3.3 Techniques for ^{129}I determination.....	14
1.4 Objectives of this research	16
2. Experimental section	17
2.1 Materials.....	17
2.1.1 Chemicals and equipment.....	17
2.1.2 Samples	18
2.2 Determination of total ^{129}I	21
2.2.1 Water samples.....	21
2.2.2 Solid samples	22
2.3 Speciation analysis of ^{129}I and ^{127}I	23
2.3.1 Separation of iodide and iodate from water samples.....	23
2.3.2 Separation of iodine species in aerosol samples.....	24
2.3.3 Separation of iodine species in seaweed.....	25

2.4 Separation of iodine from water samples and iodine fractions for ^{129}I measurement	26
2.5 Measurement	27
2.6 Acquisition of environmental data	30
3. Results and discussion	32
3.1 Methodology development	32
3.1.1 Persulfate oxidation for decomposition of organic iodine in water samples.	32
3.1.2 Determination of ^{129}I and ^{127}I and their species in aerosols.....	38
3.2 Environmental tracing application of ^{129}I and ^{127}I species.....	42
3.2.1 Speciation of ^{129}I and ^{127}I in marine water.....	42
3.2.1.1 The central Arctic	42
3.2.1.2 Greenland coast	47
3.2.1.3 Danish coast	57
3.2.1.4 Offshore Fukushima.....	62
3.2.2 Speciation of ^{129}I and ^{127}I in aerosols.....	63
3.2.3 Speciation of ^{129}I and ^{127}I in seaweed	69
4. Conclusions and perspectives.....	78
4.1 Conclusions	78
4.2 Perspectives	80
Scientific supports	82
References	83

1. Introduction

The discovery of iodine could be traced back to two centuries ago by chemist, Bernard Courtois, in 1811 when he treated seaweed ash. Afterwards, iodine was identified and isolated firstly from brown algae (*Laminaria sp.*) [1]. The content of iodine is only 1.4 mg kg⁻¹ in the Earth's crust, about 60 µg L⁻¹ in the oceans, and up to 1% in dry mass in kelps. Iodine has 37 isotopes but only one stable isotope, and most of radioisotopes of iodine are short-lived with half-life of several days. In 1960, physicist John H. Reynolds discovered that certain meteorites contained an isotopic anomaly in the form of an overabundance of ¹²⁹Xe, and inferred the occurrence of a decay product of long-lived radioactive iodine-129 [2]. ¹²⁹I, with a half-life of 1.57 × 10⁷ years, is the longest-lived radioisotope of iodine, and continuously being produced in the atmosphere primarily by reactions of xenon with cosmic rays, and in the Earth primarily by spontaneous fission of ²³⁸U (Table 1.1) [3]. Since the advent of nuclear age, considerable amount of anthropogenic ¹²⁹I as a fission product of uranium and plutonium has been released into the environment mainly from nuclear weapon testing, nuclear reprocessing plants and nuclear accident, which immensely overwhelmed the natural ¹²⁹I signal.

Table 1.1 Production reactions of ¹²⁹I

Atmosphere	$^{129}\text{Xe} \xrightarrow{\text{Cosmic rays}} ^{129}\text{I}$
Earth	$^{238}\text{U} \xrightarrow{\text{Spontaneous fission}} ^{129}\text{I}$
Meteorites and the Moon	$\text{Te} + \text{n/p} \rightarrow ^{129}\text{I}$ $\text{Ba} + \text{n/p} \rightarrow ^{129}\text{I}$
Nuclear reactors or bomb	$^{235}\text{U} \xrightarrow{\text{fission}} ^{129}\text{I}$ $^{239}\text{Pu} \xrightarrow{\text{fission}} ^{129}\text{I}$

Duo to the high fission yield of ¹²⁹I (0.7% per fission for ²³⁵U) and high accumulation of iodine in thyroid of mammals, initial interests in investigations of ¹²⁹I results mainly from the radioactive hazards to human and transportation pathways of this nuclide in the ecosystem [4, 5]. With the development of detection techniques for ¹²⁹I and increased ¹²⁹I level in the environment, interests extended to geological dating and environmental tracing in various compartments [3, 6]. ¹²⁹I has been successfully applied as a tracer for studying transportation and exchange of water masses, movement of air mass, investigating geochemical cycle of stable iodine, and reconstructing level and distribution of short-lived ¹³¹I [7-10].

As a highly mobile radionuclide, ¹²⁹I is of particular importance in nuclear waste disposal. Migration behaviors, bioavailability, short-term and long-term consequences of ¹²⁹I are not only related to its total concentration, but also remarkably dependent on

its chemical species. The existing limited data have shown different ratios of $^{129}\text{I}/^{127}\text{I}$ for the different chemical species of iodine in water, soil, sediment, and precipitation [11-13], implying that the species of anthropogenic ^{129}I in the environment is different from those of stable iodine. In addition, the reported difference of concentration factors between ^{127}I and ^{129}I by vegetation and seaweed is also attributed to the speciation variation in soil and seawater where these plants grow [14, 15]. Therefore, knowledge on the chemical species of ^{129}I is a key issue for safety assessment of radioactive waste repositories, and for estimation of human exposure through multiple pathways [16]. Moreover, speciation analysis of ^{129}I exhibits a unique potential in investigating species transformation of stable iodine in order to understand the environmental processes such as oceanographic, hydrological and atmospheric processes [11, 17, 18].

Accordingly, accurate and robust determination of ^{129}I species in various environmental samples is necessary to meet the extensive requirements. Due to the low level of ^{129}I and numerous iodine species present in the nature, speciation analysis ^{129}I is rather difficult and thus hinders the investigations and applications. The development of high sensitive accelerator mass spectrometry (AMS) provide a good opportunity to determine low-level ^{129}I , and enables us to establish new methods on ^{129}I speciation analysis, and to explore transportation pathways, processes and conversion among species for radioactive ^{129}I as well as stable iodine.

1.1 Sources, level and radioactive hazard of ^{129}I in the environment

Level of ^{129}I in the environment depends on its release from the human nuclear activities. The main sources of ^{129}I in the environment are listed in Table 1.2.

Table 1.2 Major sources of ^{129}I in the environment by 2009 [15, 19-21]

Source		^{129}I , kg
Nature	Hydrosphere	80
	Atmosphere	0.0005
	Lithosphere	170
Nuclear weapon testing	Atmosphere	50-150
Nuclear accident	Chernobyl, 1986	6
	Fukushima, 2011	1.2
Spent nuclear fuel reprocessing	La Hague, France	4200 in liquid, 75 kg to air
	Sellafield, United Kingdom	1490 in liquid, 180 kg to air
	Marcoule, France	140
	Hanford reservation, USA	274
	Savannah River Site, USA	41
	Mayak, Russia	160
	Seversk, Russia	35
Zhelesnogorsk, Russia	21	
Spent nuclear fuel		14400

On the earth, the naturally produced ^{129}I was estimated to about 250 kg with a production rate of $4.2 \times 10^6 \text{ atoms cm}^{-2} \text{ s}^{-1}$ [22], which results in an initial ratio of $^{129}\text{I}/^{127}\text{I}$ of 1.5×10^{-12} in marine system of the pre-nuclear age [23]. Since the 1940s, continuous and enormous releases of ^{129}I mainly from nuclear weapons testing, nuclear accidents, and spent nuclear fuel reprocessing have drawn attention and been monitored regularly related to environmental hazards. Of these sources, more than 95% of ^{129}I in the environment was discharged into atmosphere and marine from the two European nuclear fuel reprocessing plants (NFRPs), at Sellafield in United Kingdom and La Hague in France [17, 24]. Such huge release of ^{129}I has elevated environmental $^{129}\text{I}/^{127}\text{I}$ ratios by 4-6 orders of magnitude from the pre-nuclear level (see Fig. 1 in Paper I), especially in the Europe [9, 25]. However, the influence of these two major sources to the environmental level of ^{129}I is not so significant in the Asian and North America, especially in the southern hemisphere, where ^{129}I mainly originates from atmospheric nuclear testing with $^{129}\text{I}/^{127}\text{I}$ ratios ranging from 10^{-11} to 10^{-9} [15, 26-30]. In some heavily contaminated areas, for instance, Savana River Site in USA, the ^{129}I concentrations in groundwater were observed up to 37 Bq L^{-1} ($2.64 \times 10^{16} \text{ atoms L}^{-1}$) at present, which are 5-6 orders of magnitude higher than those in seawater in the English Channel ($2 \times 10^{11} \text{ atoms L}^{-1}$) [17] and 9-10 orders of magnitude higher than those in precipitation at the United States continent ($2.5 \times 10^7 \text{ atoms L}^{-1}$) [28]. A comprehensive picture (Fig. 1.1) well depicts the global distribution of ^{129}I .

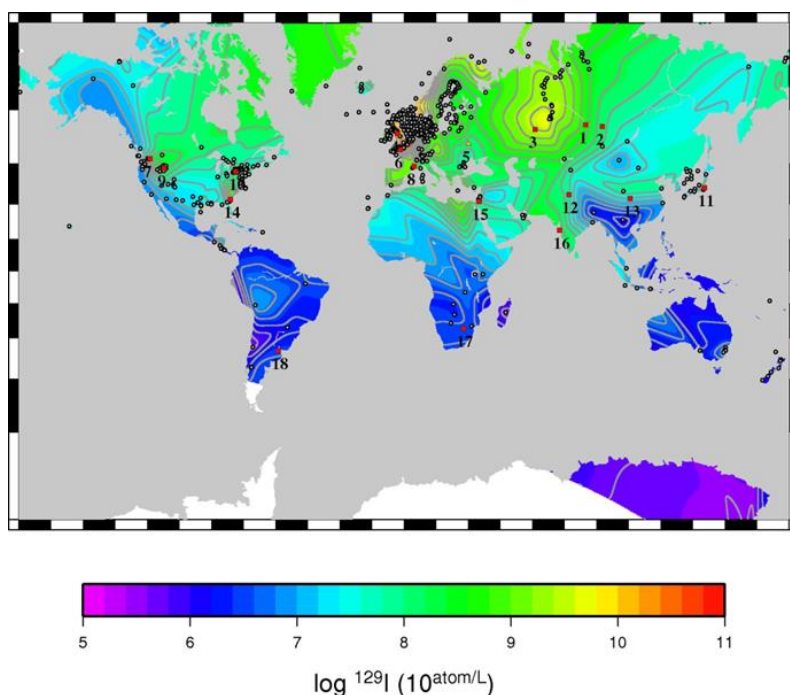


Figure 1.1 Global distribution of ^{129}I in the continent constructed by analysis of river and lake water collected over the world. White circles indicate sampling locations. Red squares and numbers correspond to nuclear reprocessing centers. Yellow triangle corresponds to the Chernobyl accident (Adopted from [5]).

Despite such huge amount of ^{129}I released, radioactive hazard of ^{129}I at present environmental level is still very low and can be negligible. It is recommended by the International Commission on Radiological Protection (ICRP) that the general population dose limits is 1.0 mSv per year [31]. The low energy beta emissions from ^{129}I do not present a significant external radiation exposure because they barely penetrate through the outer layer of skin (Table 1.3). The low energy gamma and X-ray emissions from ^{129}I also present limited penetrating external exposure. Most of iodine (>80%) in human body is primarily accumulated in thyroid. The uptake of ^{129}I to the thyroid is in practice a major path for internal exposure of ^{129}I . Hou et al. (2009) has estimated that the equilibrium annual dose equivalent to the thyroid is about 1 mSv y^{-1} for an adult on a basis of $^{129}\text{I}/^{127}\text{I}$ ratio of 10^{-6} in thyroid and an assumption of 10 mg stable iodine taken from food [16]. This calculation is based on the internal exposure of ^{129}I . However, as stated above, the $^{129}\text{I}/^{127}\text{I}$ ratios varied from 10^{-7} to 10^{-11} in the most of the current environment, implying the radioactive hazards at present could be negligible. It is worthy to note the continuous release of ^{129}I from the nuclear fuel reprocessing and large amount of ^{129}I in the spent nuclear fuel (14400 kg, Table 1.2) as a potential source, which may increase the risk of exposure to high level of ^{129}I in the future. Therefore, it is of much concern for long-term monitoring on the level and distribution of ^{129}I .

Table 1.3 Principal radiation emission of ^{129}I [32, 33]

Maxium Beta Energy	0.152 MeV (100%)
Gamma ray	0.040 MeV (7.5%)
K α 1 X-ray	0.030 MeV (37%)
K α 2 X-ray	0.029 MeV (20%)
K β X-ray	0.034 MeV (13.2%)
L-1 internal conversion Electrons	0.034 (10.7%)
Maximum range of beta in air	23 cm

1.2 Iodine species and transformation

Ocean is a major source of iodine. Iodine in the ocean can be emitted to the atmosphere as volatile gaseous iodine or fine liquid drops by sea-spray, such as molecular iodine and iodocarbons [34, 35], which participate in photochemical processes and formation of new nuclei in the air. Being in gaseous forms, atmospheric iodine could transport long distance and deposited to the land by precipitation and aerosol particles. Iodine in soil is transferred to vegetation, and further taken up by human and animals [36]. Partial iodine in the terrestrial system is translocated back to the ocean via rivers and runoff, meanwhile iodine deposited on the ground can be emitted to the atmosphere in gaseous form through biological activities, such as

vegetation and soil microorganism [37].

1.2.1 Iodine species (^{129}I and ^{127}I) in the environment

In water systems. Iodine in ocean mainly exists in the form of inorganic, organic and particulate iodine [38-41]. Numerous studies on the marine geochemistry of dissolved iodine have focused on the distribution and transformation of iodide, iodate and soluble organic iodine [42-44]. Distribution of iodine species is greatly variable in water systems. Generally, iodate is the predominant specie in open sea, while the thermodynamically unfavorable iodide is also present in oxygenated water, especially in the surface layer and coastal area [39, 45]. Organic iodine is a minor part in open-ocean but found ubiquitously in coastal waters, constituting up to 40% of total dissolved iodine [41]. The concentration of soluble organic iodine is associated with marine suspended matter, showing a decrease trend from up to 127 ng kg^{-1} in the surface to 1 ng kg^{-1} below the euphotic zone [41]. This is attributed to biologically mediated iodination of organic molecules and indirect biologically mediated formation of soluble organic iodine (e.g. HOI and I_2 formed through iodate reduction or iodide oxidation could react with humic substances through abiotic mechanisms) [46-48]. Concentrations of iodine in rivers, lakes, groundwater and precipitation are generally much lower than that in seawater and greatly variable, but generally in the range of low $\mu\text{g L}^{-1}$ to tens of $\mu\text{g L}^{-1}$ depending on the source of iodine. In these fresh waters, iodine species are strongly linked to the redox conditions and biological activity. It is becoming increasingly apparent that organically bound iodine represents a significant fraction in these iodine pools [41, 47, 48]. For examples, Gilfedder et al. (2008) have reported that organic iodine is the dominant specie in the Mummelsee lake, accounting for in average $85 \pm 7\%$ of the total iodine [49]. In the same work, much higher iodide was observed in the hypolimnion, and the formation of iodide was attributed to decomposition of biological materials from the sediments and diffused into the upper water column.

Only few works on the ^{129}I species in seawater have been reported, such as in the North Sea, Baltic Sea, North Atlantic Ocean, and offshore Fukushima, Japan [17, 20, 50-52]. These investigations showed that distribution of ^{129}I species (mainly iodide and iodate) is distinct from that of stable iodine, which is remarkably influenced by their sources. For instance, in the North Sea, the ratios of iodide to iodate were found to be 0.1-0.5 and 0.5-1.6 for ^{127}I and ^{129}I , respectively, in open area, whereas these ratios increased to 0.6-1.3 and 0.8 -2.2, respectively, in coastal waters [17]. In the anoxic Baltic Sea, the distribution of $^{129}\text{I}/^{129}\text{IO}_3^-$ ratios shows more variable than the $^{127}\text{I}/^{127}\text{IO}_3^-$ [52]. Lehto et al. (2013) reported that the fraction of iodide for ^{129}I was slightly higher than ^{127}I in the waters of lakes and rivers in Finland [53]. Such a difference

between ^{129}I species and ^{127}I species has been successfully applied to trace marine currents and to investigate geochemical cycle of stable iodine. In comparison with species of stable iodine, the variation of $^{129}\text{I}^-$ and $^{129}\text{IO}_3^-$ in the North Sea revealed redox rate and processes between iodide and iodate during water exchange. Reduction of iodate to iodide is relatively fast in the European continental coast during transportation of ^{129}I from La Hague but slow in the open sea, while oxidation of iodide to iodate seems an insignificant process [17].

In the atmosphere. Iodine species in the atmosphere is important, which determine the transport of iodine from oceanic source to the continents, influence the oxidizing capacity of the atmosphere through the catalytic destruction of ozone, and play a key role in formation of ultrafine aerosol particles [35]. Ocean provides the main source of iodine to the atmosphere through volatile species of iodine including monohalogenated organic compounds such as methyl iodide (CH_3I), ethyl iodide ($\text{C}_2\text{H}_5\text{I}$), and propyl iodide (1- and 2- $\text{C}_3\text{H}_7\text{I}$), more active polyhalogenated compounds such as chloriodomethane (CH_2ICl), bromiodomethane (CH_2IBr), and diiodomethane (CH_2I_2), and I_2 . These compounds photodissociate rapidly in the atmosphere to generate iodine atoms and various iodine oxides (IO_x) [35]. Through direct trapping and nuclei formation effect, gaseous iodine is accumulated in aerosol particles at the low ng m^{-3} level. In aerosols, iodine exists mainly in the form of iodide, iodate, organic iodine and insoluble iodine probably bound to different components [54, 55]. For instance, soluble organic iodine (SOI) is found the most abundant fraction accounting for approximately 70% of total soluble iodine over Western Pacific Ocean, Eastern and Southern Indian Ocean, and Prydz Bay, coastal Antarctic [56].

Reports on ^{129}I species in the atmosphere are rather scarce. In precipitation collected in Denmark, iodide was observed as the predominant form of ^{129}I accounting for 50-99% of total ^{129}I , while, iodate is the dominant species for ^{127}I , accounting for 43-93% of total ^{127}I [11]. This work showed that data on speciation of ^{129}I and stable iodine could provide valuable information on sources and cycling process despite the complicated atmospheric chemistry of iodine. However, no speciation analysis of ^{129}I in aerosol can be found due to lack of available analytical methods.

In the soil and sediment. Distribution of iodine species in soil and sediment is an integrated consequence of soil pH, Eh, composition and interaction with microorganisms. Iodine was found in soil and sediment in forms of iodide, iodate, organically bound iodine and those associated with oxides and hydroxides of iron and manganese. Of these, a number of experimental observations suggested organically bound iodine is a significant fraction [57, 58]. It is reported that the soluble inorganic iodine as the minor form can be sequestered by soil organic substances, such as humic

acid and fulvic acid [59, 60]. Mobility of iodine species in soil follows the order of $I^- > IO_3^- >$ organic iodine; and for organic iodine, LMW > HMW > particulate organic iodine (LMW, low molecular weight; HMW, high molecular weight) [61-63].

^{129}I species have been investigated in various soil and sediment samples. Because ^{129}I was derived from different sources, and its species showed large variation compared to stable iodine. A relatively higher percentage of ^{129}I was observed in water-soluble (39-49%), exchangeable (7-20%), and residue (25-70%) fractions in the soils collected from a region closed to the WAK reprocessing plant in Germany [64]. Whereas, water-soluble and exchangeable fractions of ^{129}I were less than 10% in IAEA-375 soil (top soil to a depth of 20 cm, collected on the field of the collective farm “Staryi Vishkov”, Novozybkov district, Brjansk region, Russia in July 1990 [65]), soil from Denmark, oxic sediment from the Barents Sea and anoxic sediment from Helvik Fjord, Norway [66, 67]. Iodine associated with soluble humic and fulvic acids accounts for 37-60% of total ^{129}I in these sample and those from Savannah river site [68], even higher up to 80-90% in Chinese loess [30], and 60-80% in a lake sediment from Sweden [69].

In the biological system. Some organisms have the ability to uptake and accumulate iodine with concentration factor of iodine as high as 10^4 (e.g., *Laminaria digitata*). In seaweed, it was observed that iodine is present as inorganic ions (iodide and iodate), and associated forms with mono- and di-iodotyrosine (MIT, DIT), phloroglucinols and phenols, phlorotannins, phlorotannins, fatty acids, terpenes, polysaccharide [70], and distribution of chemical species of iodine in seaweed differs from specie to specie. For instance, up to 92% of total iodine was found in the water-soluble fraction in *Laminaria Japonia*, and 61-93% of the water-soluble iodine is mainly present as iodide [71]. Organic iodine in the seaweed was observed mainly bound to proteins, and less associated with pigments and polyphenol, and iodine is almost not associated with polysaccharides (such as fucoid and cellulose) [72]. After enzymatic hydrolysis of the protein, Shah et al. (2005) determined MIT and DIT in Wakame using size exclusive chromatography coupled with ICP-MS [73] and reported the highest concentrations of MIT and DIT of 900 and 400 ng g⁻¹ in Kombu, respectively, but much lower in other species of seaweed [74, 75]. However, no speciation analysis of ^{129}I in biological samples has been reported up to now.

1.2.2 Transformation of iodine species

Despite many factors are known affecting transformation of iodine species in water, such as pH, Eh, dissolved oxygen, redox reagents (e.g. Fe²⁺, H₂S), biological activity, and light, the conversion mechanism among iodine species is still not well understood. In a redox cycle, iodate and iodide are interconverted, and this is the most pronounced

effect for iodine speciation in oxygenated seawater. The possible mechanisms responsible for iodine species transformation are briefly summarized below.

Reduction of iodate to iodide.

1) Tsunogai and Sase (1969) have proposed that iodate reduction in surface water might be intermediated by nitrate reductase which is presented in various kinds of organisms (like phytoplankton). Reduction of iodate could be an assimilatory process inside the cell or a dissimilatory process at the cell wall [38]. This proposed mechanism is supported by field measurements in the Weddell Sea [76] and in batch culture of different marine phytoplankton species at both ambient and elevated iodate levels [77-79].

2) Microbial respiration was also suggested as a pathway of iodate reduction to iodide, with an evidence of iodide-accumulating bacteria isolated from marine sediment [80, 81].

3) Through observations of the iodate-iodide redox behavior in surface water in the North Sea, Spokes and Liss (1996) proposed that iodide can be photochemically produced through iodate reduction and the organic matter is essential for iodide photoproduction [82].

4) In addition, reductants, such as bisulfides and thiols (e.g. glutathione), which exist under anoxic conditions could be responsible for abiotic reduction of iodate [83, 84].

5) Decomposition of organic matter might release iodine as iodide form or reduce iodate through the formation of reductive sulfide, especially at the sediment-water interface [85-87].

6) A recent work reported that Antarctic diatoms (*diatoms*, *dinoflagellates* and *prymnesiophytes*) can facilitate the reduction reaction of iodate to iodide and iodide levels peaked at the end of the stationary growth phase, and suggested that the iodide production mechanism is connected to cell senescence [88].

Oxidation of iodide. The investigation on the mechanism of iodide oxidation in seawater is relatively sparse. It was suggested that the oxidation of iodide to iodate is an extremely slow process under the prevailing conditions in seawater [43]. The oxidation is biologically catalyzed by vanadium-based haloperoxidases in marine macroalgae to allow hydrogen peroxide to convert iodide through molecular iodine to iodate [42, 89]. However, only one direct evidence was provided that the fungus *Caldariomyces fumago* oxidizes iodide to iodate via the enzyme chloroperoxidase [90]. Oxidation of

iodide in soil water could be mediated by terrestrial enzyme systems, and unlikely to involve the iodine/molecular iodine couple [91].

Transformation of inorganic iodine to organic iodine. Interconversion reactions between inorganic iodine and organic iodine are variable with local redox conditions. In waters with low oxygen concentrations, transformation of iodide and iodate to organic iodine is expected weak due to the absence of intermediate, HIO and I₂, which cannot be maintained at significant levels in seawater [48]. In sulphidic waters, organic iodine compounds could be converted to organic sulfur compound via nucleophilic displacement of iodide by sulphide and/or bacterial decomposition of organic matter to release iodide [48, 86]. In waters containing high oxygen levels, both organic iodine and iodide may be formed probably via reactive intermediates such as I, or HOI, which are probably formed by photochemical processes and/or by hydrogen peroxide from marine plankton extracellularly. In soil and sediment, inorganic iodine can be fixed by soil organic matter, such as humic acid, fulvic acid [58, 92], but this process is reversely mediated by bacteria to release soluble inorganic iodine to soil water [60, 93].

Conversion of iodine species in the atmosphere. In the atmosphere, species transformation among iodocarbons, iodine oxides, gaseous inorganic iodine (I₂ and HIO), particulate iodine is primarily proceeded by phytochemical reaction, interaction with oxygen, ozone, nitrogen oxides, hydrogen oxides and other possible occurring gaseous metal iodine (e.g, (CH₃)Hg⁺) [35].

1.3 Analytical methods for ¹²⁹I and its species

1.3.1 Total ¹²⁹I

Aparting from direct measurement without sample preparation (e.g., gamma spectrometry, INAA), iodine isotopes, ¹²⁹I and ¹²⁷I in water, solid and air samples have to be separated from sample matrix and prepared to appropriate form for instrumental measurement. The analytical methods and required sample size are strongly dependent on the level of ¹²⁹I and sample type. Chemical preparation for ¹²⁹I determination can be summed up as three steps, pretreatment of sample, separation of iodine from sample matrix and further purification of iodine from interferences, and then detection of ¹²⁹I can be carried out by appropriate instruments (Fig. 1.2).

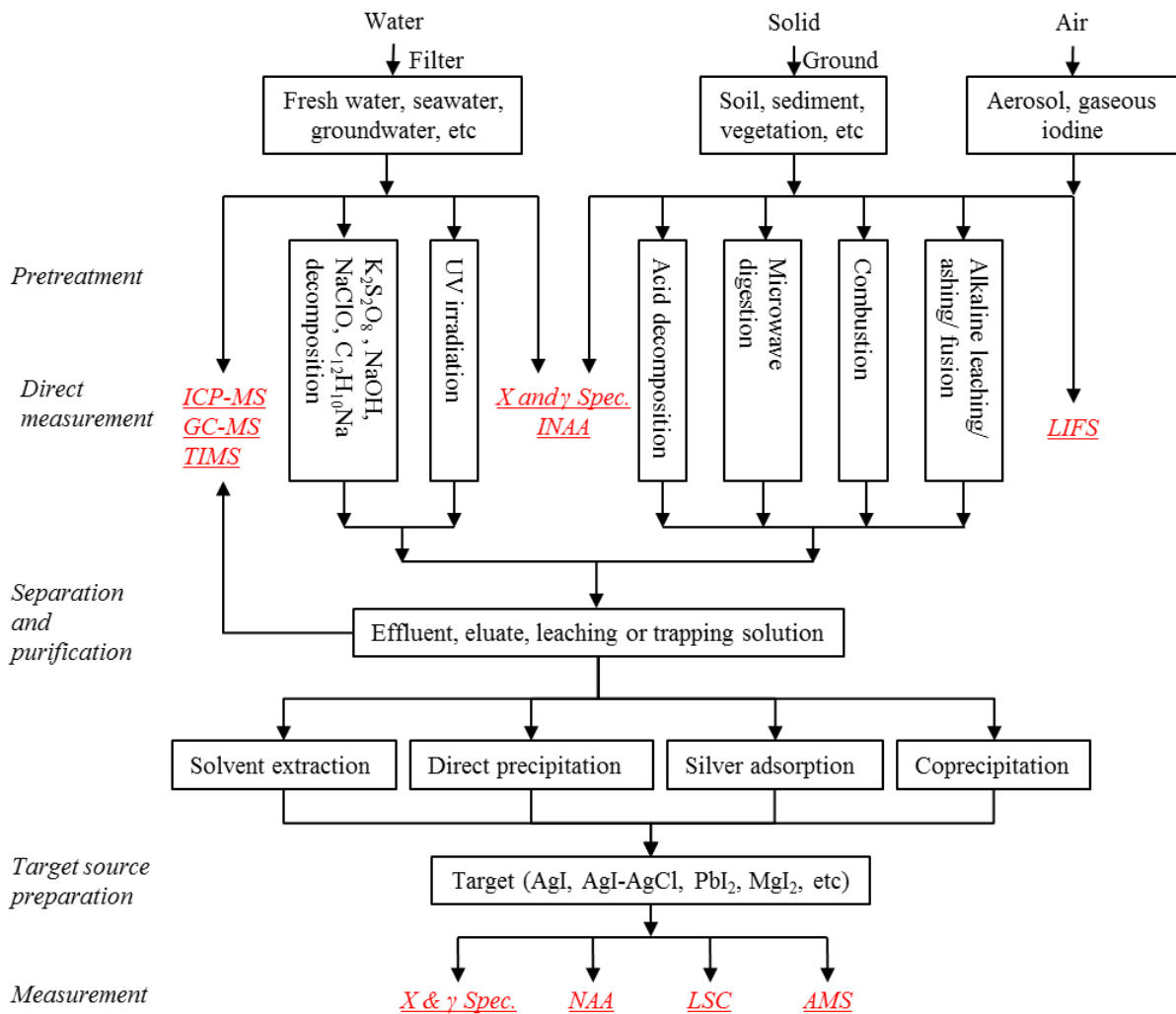


Figure 1.2 Chemical procedures for determination of ^{129}I in environmental and biological samples measurement. X and γ Spec is X-ray and gamma spectrometry, NAA is neutron activation analysis, LSC is liquid scintillation counter, and AMS is accelerator mass spectrometry.

Sample preparation. Large volume of fresh water samples (1-10 L) can be evaporated to small volume for easily handling under protection of alkaline and reductant, such as KHSO_3 and KOH to prevent iodine loss via formation of I_2 . This method is time-consuming [94, 95], meanwhile it is also not suitable for saline water.

The presence of organic iodine in liquid sample could cause underestimation of ^{129}I concentration, because it is hardly extracted by solvent extraction (e.g CHCl_3). Therefore, ultraviolet (UV) irradiation, acid digestion, oxidation by H_2O_2 or $\text{K}_2\text{S}_2\text{O}_8$, and reduction with sodium biphenyl ($\text{C}_{12}\text{H}_{10}\text{Na}$) were utilized to decompose organic iodine to convert it into inorganic ionic forms (iodide and iodate) [96-99]. After transforming all iodine species to iodide, iodine in water can be separated by anion exchange in two ways, batch method and column method. Iodide adsorbed on strong basic anion exchange resin can be eluted with 5-6% NaClO or $2 \text{ mol L}^{-1} \text{ NaNO}_3$.

solution. The chemical yields of iodine are 50-70% for the batch method, and 80-99% for the column method depending on water volume [94, 100-102].

Separation of iodine from solid samples is more difficult than aqueous samples. Combustion using tube furnace is commonly used to release iodine as gaseous iodine (I_2) from solid samples, being oxidized in oxygen flow under high temperature (800-1000°C) and trapped with alkaline solution [103-106]. This method generates a satisfactory chemical yield of more than 95% and low analytical background of ^{129}I . However, low iodine chemical yields of 40-60% are obtained when treating solid samples containing high organic substance. In order to improve the recovery of iodine during combustion of organic matter, catalysts, such as vanadium oxide (V_2O_5) and platinum wire were used [54, 107]. Due to the limitation on specific equipment and its capacity for sample size, combustion method is not suitable for all kinds of solid samples. In such cases, alkaline leaching, ashing and fusion are alternative methods. The main principle is that iodine in solid samples can be dissolved in alkaline solutions. Solid samples can be decomposed or melted in alkaline media under high temperature (400-700°C) and iodine is released from the sample matrix and kept in the mixture under protection of alkaline reagents, such as NaOH. Iodine in the alkaline extracts and leachate is then further treated as aqueous sample. Compared to combustion using tube furnace, the chemical yield of alkali leaching or alkali fusion is slightly lower, about 50-90% related to sample type [15, 94, 108-111]. Microwave digestion based on the principle that sample enclosed in a sealed digestion tank can be decomposed rapidly by acid in high temperature and high pressure produced by microwave heating is a feasible method for trace metal analysis and has been used to treat samples for ^{129}I analysis. High chemical yield of iodine (>90%) using microwave digestion under acidic condition and no iodine loss inside the Teflon digestion canister were reported [112, 113]. Microwave digestion is obviously very effective due to its shorter preparation times and higher automation, but also restricted to small sample sizes. Other methods such as acid distillation [114-116] are rare to use due to either inconvenient procedure or low recovery of iodine.

Chemical separation and purification of iodine. After sample pretreatment, iodine in eluents, leachates or trap solutions needs to be separated and purified to get rid of the sample matrix and eliminate the interference, in order to obtain an appropriate form for measurement. The most conventional method is solvent extraction based on the higher solubility of molecular iodine in organic solvent than that in water. Typically, in a proper separation funnel, ^{127}I carrier, ^{125}I tracer, HNO_3 and reductant (such as H_2SO_3 , $NH_2OH \cdot HCl$, $NaHSO_3$) are sequentially added to 10 -1000 ml of aqueous solution to reduce all iodine forms to iodide. Iodide is oxidized to I_2 by addition of $NaNO_2$ or H_2O_2 , which is extracted into organic phase of CCl_4 or $CHCl_3$ by shaking the funnel.

The molecular iodine dissolved in organic solvent is reduced again and back-extracted into water phase. This extraction and back-extraction procedure is repeated once. Iodide in the back-extracted solution is precipitated as AgI by addition AgNO₃. This method is easy to operate and has been carried out for several decades, but is incapable to analyze samples with low ¹²⁹I/¹²⁷I ratios (< 10⁻¹²), because addition of stable ¹²⁷I carrier introduces additional ¹²⁹I and impairs the detection limit of ¹²⁹I. Recently, a carrier-free method was established based on AgI-AgCl coprecipitation. Using this method, an AMS target containing 5.0 μg iodine can be used for analyzing samples with ¹²⁹I/¹²⁷I > 10⁻¹², and that for samples with ¹²⁹I/¹²⁷I < 10⁻¹³ more than 25 μg iodine is needed [29, 117].

1.3.2 Separation techniques for speciation analysis of ¹²⁹I

Speciation analysis of ¹²⁹I is of particular important to access its short-term and long-term consequences, migration behaviors, and bioavailability. Generally, analytical methods for ¹²⁹I speciation are similar to those for stable iodine, while due to extremely low concentration of ¹²⁹I in the environmental samples, relatively large sample size is normally required. In addition, some ¹²⁷I species, such as iodide, iodate, CH₃I, MIT, DIT, etc, can be determined directly by chromatographic techniques (ion chromatography, HPLC, GC) coupled to detection techniques (UV spectrophotometry, ICP-MS, AES) [118], and can also be directly measured by XANES and EXAFS spectrographic techniques when their concentrations are sufficiently high [119]. A detection limit of 4×10⁻⁹ g L⁻¹ for ¹²⁹I has been reported by on-line introduction of analyte via the gas phase in ICP-MS with hexapole collision cell [120]. However, the level of ¹²⁹I is normally in range of 10⁻¹² to 10⁻¹⁵ g L⁻¹ in environmental water, therefore impossible to be determined by direct detection techniques. This implies that speciation analysis of ¹²⁹I requires considerable separation of iodine species, enrichment of iodine in fractions and finally determined by highly sensitive analytical instrument, e.g. AMS.

Anion exchange chromatography is a commonly used method to separate iodide and iodate based on different affinities of anions on resin (Table 1.4) [121]. Usually, a strong anion exchange resin, AG 1-×4 (Cl⁻ form), is purified with NaClO solution to decrease the background of iodine, and then converted to NO₃⁻ with 2 mol L⁻¹ NaNO₃ [122]. Sample solution is loaded onto a chromatographic column packed with the transformed resin. Due to the different affinity of iodine forms, iodide is adsorbed on the resin, while iodate flow out to the effluent. Iodide on the column is then eluted with 2 mol L⁻¹ NaNO₃ or 5% NaClO. The fractions of iodate and iodide are prepared using the same procedure for the total ¹²⁹I. However, elution efficiency of iodide is variable with eluting conditions, such as eluting solution and flow rate, which may

underestimate iodide concentration. Therefore, radioactive ^{125}I or ^{131}I is often used to monitor chemical yield of iodide during the chromatographic separation. This method has been widely applied for analysis of seawater, fresh water samples [17, 53] and extracts from soil and sediment. It is worthy to mention that for large volume of seawater, the competence of chloride with iodide may deteriorate adsorption efficiency of iodide, even causing a breakthrough of iodide from the resin column. In such case, sufficient amount of resin packed in the column of high height/diameter ratio has to be used.

Table 1.4 Relative selectivity of main anions on the strong basic anion exchange resin [123].

Counterions	Relative Selectivity for AG 1	Counterions	Relative Selectivity for AG 1
OH^-	1.0	BrO_3^-	27
I^-	175	NO_2^-	24
HSO_4^-	85	Cl^-	22
ClO_3^-	74	HCO_3^-	6.0
NO_3^-	65	IO_3^-	5.5
Br^-	50	HPO_4^-	5.0
CN^-	28	F^-	1.6
HSO_3^-	27		

In order to in-situ separate iodine species in seawater, an AgI-AgCl selective coprecipitation method without addition of iodide carrier is developed recently [124]. In this method, iodide is separated from seawater and other iodine species by coprecipitation of AgI with Ag_2SO_3 , AgCl, and AgBr by addition of only $100 \text{ mg L}^{-1} \text{Ag}^+$ and $0.3 \text{ mmol L}^{-1} \text{NaHSO}_3$ at pH 4.2-5.5. The separation efficiency of iodide was more than 95%, and crossover between $^{129}\text{IO}_3^-$ and $^{129}\text{I}^-$ fractions is less than 3%. In addition, a selective oxidation method is primarily established for isolation of iodide from iodate in seawater and fresh water [125]. In this method, iodide in water samples is selectively oxidized to I_2 by a certain concentration of NaClO solution at pH 4-5, which is extracted by CHCl_3 and separated from iodate.

Sequential extraction is an analytical process that chemically leaches iodine out of soil, sediment and sludge samples. The purpose of sequential “selective” extraction is to mimic the release of the selective iodine species into solution under various environmental conditions. Generally, iodine species in solid samples include water-soluble, exchangeable, carbonates, oxides of iron and manganese associated iodine, organically bound iodine and residue, which are extracted with water under room temperature, $1 \text{ mol L}^{-1} \text{NH}_4\text{Ac-HAc}$ at pH 7 under room temperature and pH 5, $0.04 \text{ mol L}^{-1} \text{NH}_4\text{OH HCl}$ in 25% (v/v) HAc at pH 2 under 80°C , $3 \text{ mol L}^{-1} \text{NaOH}$ and 5% NaClO under 85°C , as well as decomposed by combustion or other techniques mentioned above [12], respectively. Iodine in these fractions is further separated by

solvent extraction or carrier free coprecipitation method [30] depending on the ^{129}I concentrations in the samples. Inorganic ions, i.e. iodide and iodate in water extracts can be identified and separated using anion exchange chromatography. Organic iodine can be further divided into eight humic acids fractions and ten fulvic acids fractions by combining with XAD-8 resin [126]. Although sequential extraction has been successfully applied to separate inorganic and organic iodine from seaweed for stable ^{127}I , report on ^{129}I speciation in biological samples is, so far, not available.

A measurement of air-borne iodine species was performed at the island of Foehr in April 2002 [127], in which 18% of the ^{129}I was particle-bound $>0.1\ \mu\text{m}$, 43% inorganic and 40% organic ^{129}I in particle $<0.1\ \mu\text{m}$. A denuder coated with α -cyclodextrin is available for molecular iodine (I_2) with collection efficiency of 95%, which might have the potential to be applied on the ^{129}I [128, 129].

1.3.3 Techniques for ^{129}I determination

As a β decay radionuclide with X- (characteristic X-rays with an energy of 29.8 keV) and γ -ray (39.6 keV) emitting simultaneously (Table 1.3), ^{129}I can be measured by radiometric methods, such as X and γ -ray spectrometry, liquid scintillation counting. Neutron activation analysis is also a radiometric method by activated ^{129}I to ^{130}I in neutron flux to obtain much lower detection limit. The rapid development of mass spectrometry makes it an effective tool for ^{129}I measurement. Both radiometric and mass spectrometric methods have their features and application fields. Table 1.5 lists the detailed information of these techniques for ^{129}I measurement.

Table 1.5 Features of different techniques for measurement of ^{129}I .

Instruments	conditions	Interference	Detection limit		Analyzing Time	Cost	Popularity	Ref.
			^{129}I , atoms	$^{129}\text{I}/^{127}\text{I}$ ratio, atom/atom				
X and γ -ray Spectrometry	a high purity germanium (HPGe)		1.4×10^{13}	10^{-5} - 10^{-6}	> 20 h	Cheapest	not very popular	[130]
LSC			0.7×10^{13}	10^{-5} - 10^{-6}	> 20 h	Cheapest	Very popular for nuclear fission product monitoring	[131]
LIFS			2×10^9 molecules for $^{129}\text{I}_2$	-			Not popular	[132]
NAA		^{82}Br		10^{-10}	> 48 h	middle	Popular before 2000; not popular now	[94, 105]
TIMS	Pure NaI solution		4.7×10^8	2×10^{-8}		Expensive	Not popular	[133]
GC-MS	derivation of iodine to 4-iodo-N,N-dimethylaniline		10.3 ppt	-	~ 25 min	middle	for Speciation, not popular	[128, 134]
ICP-MS	collision cell with oxygen as reaction gas	$^{129}\text{Xe}^+$ and $^{127}\text{IH}^{2+}$	0.4 ppt	1.5×10^{-8}	1-5 min	middle	Popular	[120, 135, 136]
AMS		$^{103}\text{Rh}^{4+}$ and $^{52}\text{Cr}^{2+}$ for $^{129}\text{I}^{5+}$; $^{97}\text{Mo}^{3+}$ for $^{129}\text{I}^{4+}$; $^{86}\text{Sr}^{2+}$ and $^{43}\text{Ca}^+$ for $^{129}\text{I}^{3+}$	5000	2×10^{-14}	30 min	Expensive	Very popular for environmental samples	[137, 138]

1.4 Objectives of this research

The first goal of this thesis is to develop methods for separation of different species of iodine in various environmental samples. The second goal is to investigate the sources, transportation pathways and conversion among various iodine species in the ocean, atmospheric and biological systems by speciation analysis of ^{129}I and stable ^{127}I in environmental and geological samples using the developed methods. This work would be implemented in the following tasks.

- 1) To develop methods for chemical speciation analysis of ^{129}I and stable ^{127}I in seawater, aerosol and seaweed, focus on the effective extraction, identification and separation of different species of iodine from various sample matrix, as well as preparation of appropriate targets for measurement of ^{129}I and ^{127}I .
- 2) To investigate water current movement in the Arctic, Greenland and Danish coast, and offshore Fukushima, to identify the sources and transport pathways of iodine in the atmosphere, as well as to explore uptake and metabolism of iodine in seaweed by employing anthropogenic ^{129}I and its speciation as environmental tracer.

2. Experimental section

2.1 Materials

2.1.1 Chemicals and equipment

Stable iodine carrier (^{127}I), in the form of iodine crystal with low ^{129}I level, was obtained from Woodward Company (Colorado, USA). 0.40 g ^{127}I carrier in the form of solid iodine crystal was dissolved gently in a mixed solution comprised of 0.5 M NaOH and 0.02 M $\text{Na}_2\text{S}_2\text{O}_5$, and diluted with water to 200 mL, which gives a ^{127}I concentration of 2.0 mg mL^{-1} . ^{125}I tracer in iodide form and without reductant in the solution was purchased from PerkinElmer Corporate (Waltham, USA). A working solution of ^{125}I was prepared by dilution with water to radioactivity of 500 Bq mL^{-1} . Two ^{129}I standards with $^{129}\text{I}/^{127}\text{I}$ ratios of 1.138×10^{-10} and 9.954×10^{-12} were prepared by diluting a ^{129}I standard solution (NIST SRM 4949c standard, National Institute of Standards and Technology, Gaithersburg, USA) with ^{127}I carrier. 1000 $\mu\text{g mL}^{-1}$ of $^{127}\text{I}^-$ standard solution (purchased from CPI international, California, USA) was used as calibration standard for determination of ^{127}I by ICP-MS after appropriate dilution with deionized water and 1% ammonia. Silver powder (100 mesh, Sigma-Aldrich Co., Missouri, USA) and niobium powder (325 mesh, Alfa Aesar, Massachusetts, USA) from Alfa Aesar (Karlsruhe, Germany) were used to prepare AgI targets for AMS measurement of ^{129}I . Anion exchange resin (AG1 \times 4, 50-100 mesh) and chromatography columns were obtained from Bio-Rad Laboratories Inc. (Hercules, California, USA).

All other chemical reagents, including nitric acid (HNO_3), ammonia ($\text{NH}_3 \cdot \text{H}_2\text{O}$), sodium hydroxide (NaOH), sodium hypochlorite (NaClO), sodium nitrate (NaNO_3), potassium disulfite ($\text{K}_2\text{S}_2\text{O}_5$), potassium persulfate ($\text{K}_2\text{S}_2\text{O}_8$), used in the experiments were of analytical grade and prepared using deionized water (18.2 $\text{M}\Omega \cdot \text{cm}$).

An ICP-MS instrument (Thermo Fisher, X Series II) was used for determination of ^{127}I in solution, which was equipped with Xt cone and operated under normal mode at Risø campus, Technical University of Denmark. Two AMS systems were used in this work for determination of ^{129}I , one is a 3 MV AMS facility operated by Xi'an AMS center, Institute of Earth Environment, China, and another one is a 5MV AMS facility, operated by Scottish Universities of Environmental Research Center, Glasgow, United Kingdom. A well-type NaI gamma spectrometry (Canberra Inc., Connecticut, USA) was used to measure ^{125}I in energy range of 3.3-58.5 keV for calculation of chemical yield. All other equipment, including balance (Mettler Toledo, Greifensee, Switzerland), centrifuge

(Eppendorf, Germany), oven (Memmert, Bavaria, Germany), furnace (Carbolite, Derbyshire, UK), combustion furnace (Carbolite, Derbyshire, UK) were available at Division of Radioecology, Center for Nuclear Technology, Technical University of Denmark.

2.1.2 Samples

Samples used in this thesis include seawater, lake water, seaweed, sediment and aerosols for method establishment and environmental tracing investigations (Fig. 2.1). The detailed sampling information of these samples is listed below.

2.1.2.1 Seawater

All the seawater samples were filtered by 0.45 µm cellulose membrane (MCE membrane 0.45 UM S-Pak Grid, 47 mm, VWR), and stored in polyethylene bottles in dark prior to analysis for iodine isotopes (^{129}I and ^{127}I) and their species (iodide and iodate).

The central Arctic. The seawater samples were collected by CTD rosette from the central Arctic during the Polarstern expedition ARK-XXVI/3 in August 5-October 7, 2011 [139]. Twelve water profiles from the polar mixed layer to Atlantic water layer (10-800 m) in the central Arctic were analyzed for ^{127}I , ^{129}I and their species (Paper III). The sampling locations stretch over the southeastern Eurasian Basin, North Polar, Makarov Basin, and northern Canada Basin (Fig. 2.1 c).

Greenland coast. Upper layer seawater samples (2 m depth below the water surface) from Greenland shelf of 60-75°N were collected by the Greenland Institute for Natural resources and the National Institute for Aquatic Resources, DTU Aqua in the Arctic Monitoring and Assessment Program (AMAP) during August and September 2012. The temperature and salinity were measured on board for stations 1-6.

Denmark coast. Surface seawater samples were collected from six Denmark coastal sites, covering west coast of Jutland (Hvid Sande and Agger Tange), the Great Belt (Nyborg and Klint), bottom of the Roskilde Fjord and Bornholm at the southern Baltic Sea.

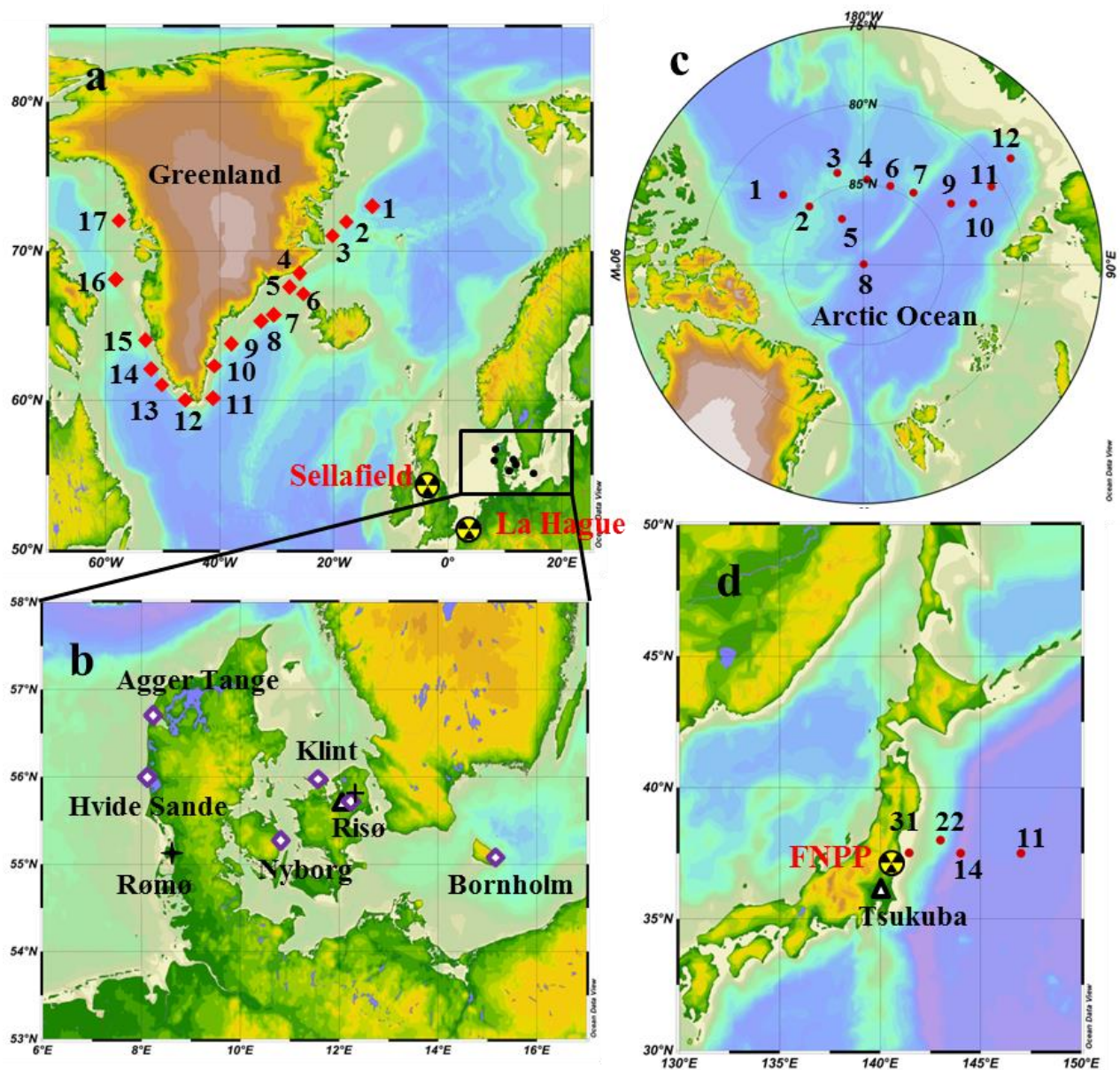


Figure 2.1. Map showing all the sampling stations in this thesis. Seventeen upper layer seawater samples (diamond in red) were collected from the Greenland coastal areas during August-September 2012 (a). Six surface seawater samples and six seaweed samples (hollow diamond in violet) collected from Denmark coastal areas in October 2014 (b). Twelve depth profiles of seawater samples (dots in red) were collected from the central Arctic during August-October 2011 (c) and four depth profiles seawater samples from offshore Fukushima in June 2011 (d). Eight aerosol samples (hollow triangle in black) were sampled at Risø, Denmark during March-May 2011 and December 2014 (b), and four aerosol samples from Tsukuba, Japan in March 2011 (d). One lake water sample (cross in black) was obtained from the Gundsømgle Lake in Roskilde in July 2012 (b). One sediment core samples (star in black) was collected from Rømø, Denmark in August 2012 (b). The nuclear reprocessing plants (a) and the Fukushima Dai-ichi nuclear power plant (d) are indicated by radioactivity symbols.

Offshore Fukushima. Depth profile seawater samples were collected from offshore Fukushima during the research cruise organized by American scientists 3-17 June 2011 using the research vessel *Kaimikai-O-Kanaloa* of the University of Hawaii [140]. The samples were stored in dark at ambient temperature prior to analysis. The four sampling stations are 40-530 km away from Fukushima Dai-ichi nuclear power plant (FDNPP).

2.1.2.2 Aerosols

Risø, Denmark. The aerosol samples were collected using a polypropylene filter (0.45 μm , Type G-3, PTI, Germany) equipped to an in-house aerosol collector (Fig. 2.2b) at Risø campus, Technical University of Denmark, Denmark (55°41.77'N, 12°05.39'E). Of these, seven aerosols were sampled during March to May 2011, and one during 8-15th December 2014. The samples were put into plastic bags and stored in dark.

Tsukuba, Japan. Four aerosol samples were collected on the rooftop of a building at the National Institute for Environmental Studies (NIES) at Tsukuba (36°02'56"N, 140°07'06"E), Japan, located about 170 km southwest of the FDNPP (Fig. 2.2d). The aerosol was sampled using 0.45 μm quartz fiber filter.



Figure 2.2 Aerosol sampler (left for external view and right for internal view) at Risø campus of Technical University of Denmark, Roskilde.

2.1.2.3 Seaweed (*Fucus*)

Seaweed samples were collected simultaneously with seawater at the same sites during October 2014 (Fig. 2.1b). Two species of brown algae, *Fucus vesiculosus* from Kilnt and *Fucus serratus* from the other five locations were collected. The fresh seaweed were rinsed carefully with local seawater and kept in plastic bags. The samples were stored in

refrigerator at -20°C. Prior to analysis, the samples were thaw at room temperature and then ground to fine slurry using a grinder for speciation analysis of ^{129}I .

2.1.2.4 Other samples

One lake water sample was collected from Gundsømgle Lake (55°43'37.00"N, 12°11'45.00"E) at Roskilde on 29 July 2012. One sediment core was collected using a plastic collecting tube (Φ 10cm \times 100cm length) from Rømø, Denmark (55°10'422' N, 8°34'416' E) in August 2012 and stored in a refrigerator at -20°C, and sliced to 2-5 cm intervals.

2.2 Determination of total ^{129}I

2.2.1 Water samples

Labeling natural organic matter with ^{125}I . In order to investigate decomposition efficiency of organic iodine in water samples, ^{125}I was grafted onto natural organic substances extracted from lake water. The organic matter was obtained by evaporating 1000 mL Gundsømgle lake water to about 5 mL. The concentrated lake water was adjusted to pH 6.5 using 3 M HNO_3 first and spiked with 2 mL ^{125}I tracer (110 kBq mL $^{-1}$, prepared on 27th June 2012). 0.5 mL 0.1 mol L $^{-1}$ Chloramine-T solution was added to the solution and the iodination was implemented at room temperature for 30 min. The ^{125}I labeled solution was diluted using deionized water to ^{125}I radioactivity of 500 Bq mL $^{-1}$, and ready for use. The labeled organic ^{125}I in this solution was extracted by chloroform for separation from the remaining inorganic ^{125}I to calculate its fraction of total ^{125}I , which accounts for 65.5% of total ^{125}I .

Decomposition of organic matter with persulfate salt. $\text{K}_2\text{S}_2\text{O}_8$ to a final concentration of 1-50 mg g $^{-1}$, and 1 mg ^{127}I carrier and ^{125}I (500 Bq) labeled organic matter were added to 100 mL lake water sample. The solution was mixed and covered with watch glass for refluxing, and heated on hot plate to 60°C and cultured for 0.5-20 h. After cooling down to room temperature, the decomposed water is treated using solvent extraction using CHCl_3 as described in the following section 2.4. The chemical yield of organic iodine (^{125}I) was calculated by comparing the counts difference between organic ^{125}I spiked and organic ^{125}I remained in aqueous phase after extraction against organic ^{125}I spiked, as shown in Equation 1.

$$\text{Chemical yield of organic iodine} = \frac{{}^{125}I_{sp} \times 65.5\% - {}^{125}I_{aq}}{{}^{125}I_{sp} \times 65.5\%} \quad \text{Equation (1)}$$

Wherein, $^{125}\text{I}_{\text{sp}}$ is the counts of ^{125}I spiked to sample; 65.5% is the fraction of labeled organic ^{125}I in the used ^{125}I tracer solution; $^{125}\text{I}_{\text{aq}}$ is the counts of organic ^{125}I remained in aqueous phase after chloroform extraction, i.e., non-decomposing organic iodine.

2.2.2 Solid samples

Two methods were used to extract iodine from solid samples: combustion and alkaline ashing. In this study, the aerosol samples were analyzed using both methods. Sediment samples were analyzed using the combustion method, and seaweed sample was treated with alkaline ashing method. Prior to analysis, aerosol samples were cut into small pieces (2×2 mm), and the frozen sediment was thaw at room temperature.

Table 2.1 Program temperature of combustion furnace for iodine separation.

Step	Temperature, °C	Status	Duration, min	Combustion gas
1	RT to 160	Heating	30	O ₂ , Air
2	160	Dwell	20	O ₂ , Air
3	160 - 250	Heating	20	O ₂ , Air
4	250	Dwell	10	O ₂ , Air
5	250 - 300	Heating	20	O ₂ , Air
6	300	Dwell	20	O ₂ , Air
7	300 - 350	Heating	20	O ₂ , Air
8	350	Dwell	20	O ₂ , Air
9	350 - 400	Heating	30	O ₂ , Air
10	400	Dwell	30	O ₂ , Air
11	400 - 800	Heating	40	O ₂
12	800	Dwell	30	O ₂
Total			290	

0.2-0.5 g aerosol sample (quartz filter) or 0.5-1.0 g sediment in dry mass were weighted to quartz boat, and 500 Bq of ^{125}I was added to the sample. The sample was combusted in pyrolysis furnace following the temperature protocol in Table 2.1 to release iodine from the matrix. The released iodine was trapped in 0.4 mol L⁻¹NaOH-0.05 mol L⁻¹ KHSO₃ solution. An aliquot of 6 g trap solution was taken to measure ^{125}I using a NaI detector to calculate chemical yield of iodine during combustion. 1.0 mL of trap solution was reserved in a plastic tube for determination of stable iodine (^{127}I) using inductively coupled plasma mass spectrometry (ICP-MS). Iodine in the remaining trap solution was further separated by solvent extraction for measurement of ^{129}I , as described in the following section 2.4. For aerosol samples collected on polypropylene filter paper, except increasing temperature slowly, small sample size (< 0.5 g) and low gas flow of air and

oxygen ($< 0.2 \text{ mL min}^{-1}$) were used to avoid rapid inflammation of air filter that may result in explosion.

Iodine in aerosol samples on polypropylene filters and seaweed was isolated by alkaline ashing. 1.0-3.0 g aerosol filter or 1.0-2.0 g ground seaweed was weighted into porcelain crucible. 10-30 mL of 1 mol L^{-1} NaOH solution, 1 mL of 1 mol L^{-1} KHSO_3 and 500 Bq ^{125}I were added and mixed well with the sample. The sample was placed in an oven for drying completely at 80°C . To prevent cross contamination during alkaline ashing, the crucible with dried sample was capped firmly with aluminum foil that was pierced a hole in diameter of about 1 cm^2 . The samples were put into Muffle furnace for ashing. The temperature was increased to 350°C at ramp rate of 5°C min^{-1} and kept for 2h, then raised to $500\text{-}700^\circ\text{C}$ at the same rate and dwelled for 1-4 h. After cooling down to room temperature, the residue remained in crucible was ground to fine powder using a glass rod and leached with deionized water on hotplate at 70°C for 20 min. The leachate was separated from residue by filtration through a quantitative filter paper (Munktell OOK, Sweden). ^{125}I in the leachate was measured using NaI Gamma detector for calculating chemical yield of iodine in the alkaline ashing procedure. 1.0 mL of the leachate was used to measure ^{127}I using ICP-MS, and the remaining leachate was used to further separate iodine for ^{129}I measurement.

2.3 Speciation analysis of ^{129}I and ^{127}I

2.3.1 Separation of iodide and iodate from water samples

Separation of iodate and iodide from water samples was performed using anion exchange chromatography as previously reported [17, 121]. An anion exchange column of 20-30 cm height and 10 mm diameter was packed with AG 1×4 resin (Cl^- form, 50-100 mesh, Bio-Rad Laboratory, California, USA). To purify and convert resin from Cl^- form to NO_3^- form, the resin column was washed successively with 50 mL of 5% NaClO solution, 30 mL of de-ionized water, 30 mL 0.15 mol L^{-1} KHSO_3 solution, 2 mol L^{-1} NaNO_3 and 50 mL deionized water at a flow rate of 2 mL min^{-1} . 2 drops of 0.5 mol L^{-1} AgNO_3 was added to the effluent to check if chloride in resin was completely replaced by NO_3^- . If white precipitate (AgCl) occurs, the column was washed again with more 3 mol L^{-1} HNO_3 until no white precipitate forms, then rinsed with deionized water until the pH of the effluent was about 6.

Depending on the concentrations of ^{129}I in water samples, 100-600 mL water sample spiked with 500 Bq $^{125}\text{I}^-$ was loaded onto the column at a flow rate of 2 mL min^{-1} , on

which iodate passed through the column due to its low affinity with anion exchange resin, while iodide was absorbed onto the resin. The column was then washed with 30 mL of 0.2 mol L⁻¹ NaNO₃ and 30 mL water. The effluent and the two washes were combined as the iodate fraction. 2.0 mL of this solution was transferred to a vial for ICP-MS measurement of ¹²⁷I, and the remaining solution was used for separation of iodate by solvent extraction. 60 mL of 5% NaClO solution and 30 mL of 3 mol L⁻¹ HNO₃ were sequentially used for eluting iodide from the column at a flow rate of 1 mL min⁻¹. The chemical yield of iodide during chromatographic separation was obtained by measurement of ¹²⁵I in 6.0 mL of the eluate using NaI gamma spectrometry. 1.0 mL of iodide fraction was transferred to a vial for the ICP-MS measurement, and the remaining solution is used for separation of iodide by solvent extraction.

2.3.2 Separation of iodine species in aerosol samples

Iodine in aerosol was extracted sequentially using deionized water and sodium hydroxide solution for water-soluble and NaOH soluble iodine, respectively, followed by alkaline ashing and water leaching to separate insoluble iodine. Inorganic iodine species, iodide and iodate in the water leachate were further separated using anion exchange chromatography, and water-soluble organic iodine was obtained by the difference of total water-soluble iodine and the sum of iodide and iodate.

Extraction of water-soluble iodine and separation of iodate and iodide. 0.2-3.0 g of aerosol filter (corresponding to 60-900 m³ air) was cut to pieces (about 2×2 mm) and put into a beaker with 5-30 mL deionized water. The mixture was agitated on a magnetic stirrer at 600 rpm at room temperature (~20°C) for 15 min-5 h to leach water-soluble iodine. The leachate was vacuum filtered through 0.45 μm membrane (MCE membrane 0.45 UM S-Pak Grid, 47 mm, VWR). The remaining aerosol on filter was rinsed twice with two aliquots of 10 mL deionized water under stirring. The two washes were filtered and combined with the leachate as water-soluble fraction. The remaining aerosol on the filter and the MCE membrane were used for subsequent NaOH leaching.

One-third of the water leachate was used for measurement of total water-soluble iodine isotopes (¹²⁷I and ¹²⁹I), and the remaining two-third for speciation analysis of water-soluble iodine (¹²⁷I and ¹²⁹I). Separation of iodide and iodate from water leachate of aerosols was carried out by anion exchange chromatography method as described in section 2.3.1 with small modification. A small column of 15 cm in height and 7 mm in diameter was packed with strong base anion exchange resin (AG 1×-4, converted to NO₃⁻

form and purified by NaClO rinsing to remove excessive iodine in the resin). 10 mL of 0.2 mol L⁻¹ NaNO₃ and 10 mL deionized water were used to rinse the column sequentially. Iodide absorbed on the column was then eluted using 30 mL 5% NaClO and 10 mL 3 mol L⁻¹ HNO₃ sequentially. 1-10 mL of water leachate, iodate and iodide fractions depending on the iodine concentration in the fractions were taken out for measurement of ¹²⁷I by ICP-MS, and the remaining solution were used to further separate iodine for ¹²⁹I measurement.

Separation of NaOH soluble iodine in aerosol. The remaining aerosol on filter together with the MCE membrane was immersed into 5-40 mL of 0.5 mol L⁻¹ NaOH solution. The suspension was agitated for 30 min-5 h at a certain temperature (20, 45 and 60°C measured by a probe) on a magnetic stirrer, and the beaker was covered by watch glass during leaching. After cooling down to room temperature, the leachate was filtered through a 0.45 µm MCE membrane. The remaining aerosol on the filter was rinsed twice using two aliquots of 10 mL of 0.5 mol L⁻¹ NaOH solution. The two washes were combined with NaOH leachate, which is used for measuring NaOH soluble iodine isotopes. 1 mL of NaOH leachate was reserved for measurement of ¹²⁷I by ICP-MS, and the remaining leachate was used for further separation of iodine for ¹²⁹I measurement. The residue on the filter and MCE membrane for filtration were transferred to a porcelain crucible for alkaline ashing.

Separation of insoluble iodine and total iodine in aerosol filter. The residual aerosol after NaOH leaching was analyzed using alkaline ashing method or combustion method as described in section 2.2.2. 5-10 mL of 1-2 mol L⁻¹ NaOH solution, 0-3 mL of 1 mol L⁻¹ KHSO₃ and 500 Bq ¹²⁵I solution were added and mixed to the aerosol samples. The blended sample was dried at 80 °C, and burnt at 350°C for 2h, then raised to 500-700°C and maintained for 1-4 h.

Decomposition of organic iodine in water and NaOH leachate. As stated in section 2.2.1, 500 Bq ¹²⁵I and 1.0 mg ¹²⁷I carrier were added to the leachates (water and NaOH leachate), then K₂S₂O₈ was added to a final concentration of 30 mg g⁻¹. The mixture was heated at 60°C overnight with watch glass covered for refluxing to decompose organic iodine in the leachate and convert them to inorganic iodine. It was observed that the yellow NaOH leachate turned to colorless after K₂S₂O₈ decomposition.

2.3.3 Separation of iodine species in seaweed

Iodine species in seaweed were extracted using deionized water for water leachable iodine, followed by alkaline ashing for water insoluble iodine.

Extraction of water-soluble iodine and separation of iodate and iodide. 2.0 g ground slurry of seaweed sample was taken into a beaker and 30 mL deionized water was added to the sample. The mixture was stirred using magnetic stirrer at 600 rpm at room temperature (~20°C) for 1 h. The leachate was vacuum filtered through a 0.45 µm MCE membrane. Due to the presence of leached seaweed algin, the leachate is sticky, resulting in a slow filtration process. The remaining residue was rinsed twice with two aliquots of 10 mL deionized water. The two washes were filtered and combined with the leachate as water-soluble fraction. The remaining seaweed residue and the filter paper were used for subsequent alkaline ashing.

After being diluted for 20-fold, 0.4 mL and 2.0 mL of the diluted water leachate were taken for measurements of ^{127}I and ^{129}I , respectively. 10 mL of the diluted solution was further treated with anion exchange chromatography for separation of iodide and iodate as described in section 2.3.1 with a small chromatographic column (15 cm in height and 7 mm in diameter). 1.0 mL of iodate and iodide fractions were taken out for measurement of ^{127}I by ICP-MS, and the remaining solution were used for further separation of iodine by solvent extraction for ^{129}I measurement.

Alkaline ashing of water insoluble iodine in seaweed. The seaweed residue after water leaching was treated by alkaline ashing for separation of water insoluble iodine. 10 mL of 1.0 mol L⁻¹ NaOH solution, 0.5 mL of 1.0 mol L⁻¹ KHSO₃ and 500 Bq ^{125}I solution were added and mixed well with the sample. The same separation procedure as that for total iodine in seaweed (Section 2.2.2) was used for separation of insoluble iodine in seaweed.

2.4 Separation of iodine from water samples and iodine fractions for ^{129}I measurement

The original seawater samples and prepared solutions including all the separated iodine fractions in Section 2.3, were transferred to appropriate separation funnels. 1.0-2.0 mg of ^{127}I carrier and, 500 Bq of ^{125}I tracer (if not added in previous steps) and 1.0-2.0 ml of 1.0 mol L⁻¹ potassium bisulfate (KHSO₃) solution were added to the funnel, and then the pH of the solution was adjusted to 1-2 using 3 mol L⁻¹ HNO₃ to convert all iodine species to iodide. With addition of 20-50 mL chloroform (CHCl₃) and 2-5 mL 1.0 mol L⁻¹ NaNO₂, iodide was oxidized to I₂ and extracted to CHCl₃ phase by appropriate shaking. The CHCl₃ phase (pink color) was transferred to a new separation funnel. The CHCl₃

extraction procedure was repeated to completely extract iodine in the water phase to CHCl₃ phase. All CHCl₃ phases were combined and transferred using 30 mL deionized water to the separation funnel. 0.2 mL 0.05 mol L⁻¹ KHSO₃ solution was added to the funnel to reduce I₂ in chloroform phase to iodide and back-extracted iodine into water phase. This extraction and back extraction were repeated once for further purification. The separated iodine (in iodide form) in a small volume (5-7 ml) was transferred to a centrifuge tube, and precipitated by addition of 1.0 mL of 0.5 mol L⁻¹ AgNO₃ solution to form AgI precipitate. The AgI precipitate was separated using centrifugation at 3000 rpm for 3-5 min, and washed in sequence using 10 mL 3 mol L⁻¹ HNO₃ and two aliquots of 10 mL deionized water to remove possibly formed Ag₂SO₃ and Ag₂SO₄ which are soluble in acidic solution. The precipitate was transferred to a 1.5 mL centrifuge tube. ¹²⁵I in the precipitate was measured using a NaI gamma detector for calculating the chemical yield of iodine. The prepared AgI precipitate in small tube was dried at 70°C, weighed exactly and stored in a desiccator for AMS measurement of ¹²⁹I.

2.5 Measurement

2.5.1 Measurement of ¹²⁵I by NaI well-type gamma spectrometry

For calculation of chemical yield of iodine in the analytical procedure, ¹²⁵I was counted by NaI gamma spectrometry (Cabrera, USA) in energy range of 3.3-58.5 keV (cover X-rays and γ ray of ¹²⁵I). The chemical yield (Y) can be calculated as the following equation.

$$Y = \frac{(\text{counts of sample-blank counts}) \times \text{dilution factor}}{\text{counts of } ^{125}\text{I standard-blank counts}} \times 100\% \quad \text{Equation (2)}$$

2.5.2 Determination of ¹²⁷I by ICP-MS

All aliquots reserved for determination of ¹²⁷I was diluted by a factor of 1-20 and prepared in 1% NH₃·H₂O media (v/v). Cesium (CsNO₃ solution) was added to a final concentration of 2.0 $\mu\text{g L}^{-1}$ as internal standard to normalize ionization efficiency of iodine in ICP-MS measurement. For measurement of ¹²⁷I in ash leachates of aerosol samples, standard addition method was employed by spiking iodine standard solution (NaI, NIST, USA) of 2 $\mu\text{g L}^{-1}$ to the sample solutions. ¹²⁷I in the diluted solution was measured by ICP-MS (Thermo Fisher, X Series II) using Xt cone under normal mode. Prior to analysis, rinsing of the ICP-MS instrument was switched to alkaline medium from acid medium by using water and 1% NH₃·H₂O in sequence, and tuned for maximum sensitivity of iodine and cesium using a quality control solution containing 2.0 $\mu\text{g L}^{-1}$ I⁻ and 2.0 $\mu\text{g L}^{-1}$ Cs⁺ in 1% NH₃·H₂O. The typical operation parameters for measurement of iodine are summarized in

Table 2.2. It is important to note that these parameters need to be optimized each time when the instrument is initialized. The detection limit of the method for iodine in the diluted solution was calculated as 3 times of the standard division of the blank to be $0.02 \mu\text{g L}^{-1}$.

2.5.3 Determination of ^{129}I by AMS

Target preparation. The prepared AgI precipitates were mixed with silver powder in mass ratio of 1:2 or niobium powder in mass ratio of 1:3 using a home-made stain steel or copper stick. Homogeneous mixing between AgI and conductive material (Ag or Nb powder) is crucial for assuring stability of iodine ion current among the runs of AMS measurement. The well-mixed sample was pressed into a copper holder using a set of pressing tool and a pressure machine (Fig. 2.3). The pressed targets were stored in 0.5 mL tube and then put into desiccator until measurement.



Figure 2.3 Picture of pressing tool for target preparation in the SUERC AMS lab, UK. The yellow component (the right most one) is the copper holder.

AMS measurement for ^{129}I . ^{129}I in the targets of most samples was measured by a 5 MV accelerator mass spectrometry (AMS) (NEC, Wisconsin, USA) at Scottish University Environmental Research Center, UK, total ^{129}I and its species in seawater were determined using a 3 MV AMS (HVEE, Amersfoort, Netherland) in Xi'an AMS Center [141, 142]. The main parameters are summarized in Table 2.2 [142, 143]. Fig. 2.3 shows a diagram of the AMS system at the Xi'an AMS Center, consisting of six main components. 50 sample targets were loaded on the carousel of ion source, comprising 5 standards, 5 instrumental blanks (Nb or Ag in this study) and 40 unknowns and procedure blanks. Negative ions of iodine are sputtered out from the holder by Cs^+ beam and extracted to the injector, where the ions are pre-accelerated and ^{129}I and ^{127}I ions are selected. Generally, ionization efficiency in the range of 5-8% can be obtained. The interferences to negative ^{129}I ions, such as molecules as $^{128}\text{TeH}^-$ and $^{127}\text{IH}_2^-$, can be suppressed by

analyzing mass and energy with a 54° electrostatic analyzer and a 90° bouncer magnet in the injector, the isobar $^{129}\text{Xe}^-$ could not be formed in the ion source. The negative ions are injected into the tandem accelerator, where they are firstly accelerated in the positive potential of the terminal. The selected ions with masses of 129 and 127 are injected sequentially into the accelerator system by switching the bouncer voltage [18] at a frequency of 100 Hz. The injection time of ions are 9 ms for mass 129 and 100 μs for mass 127. When reaching the terminal, electrons are stripped off by Ar gas for converting iodine negative ions to multiply charged positive ions, such as I^+ , I^{2+} , I^{3+} , I^{4+} , I^{5+} , I^{6+} , I^{7+} etc. The stripping yield of I^{5+} is measured to be 3.6% to 3.8% in the Xi'an AMS when the voltage was set to 2.5 mV. These are repelled from the positive terminal and a second acceleration takes place by repulsion back to ground potential. After exit of the accelerator tube, $+5$ charge state iodine ions were selected by the 115° magnetic analyzer according to the magnetic rigidity. Stable iodine (^{127}I) is measured as current by Faraday cup immediately after the magnetic analyzer. $^{129}\text{I}^{5+}$ ion from the magnetic analyzer is further separated by a 65° electrostatic analyzer for energy analysis with an energy resolution of $E/\Delta E$ and a 30° magnetic analyzer for mass analysis. $^{129}\text{I}^{5+}$ is finally counted by gas ionization detector. The typical operation parameters of AMS are summarized in Table 2.2.

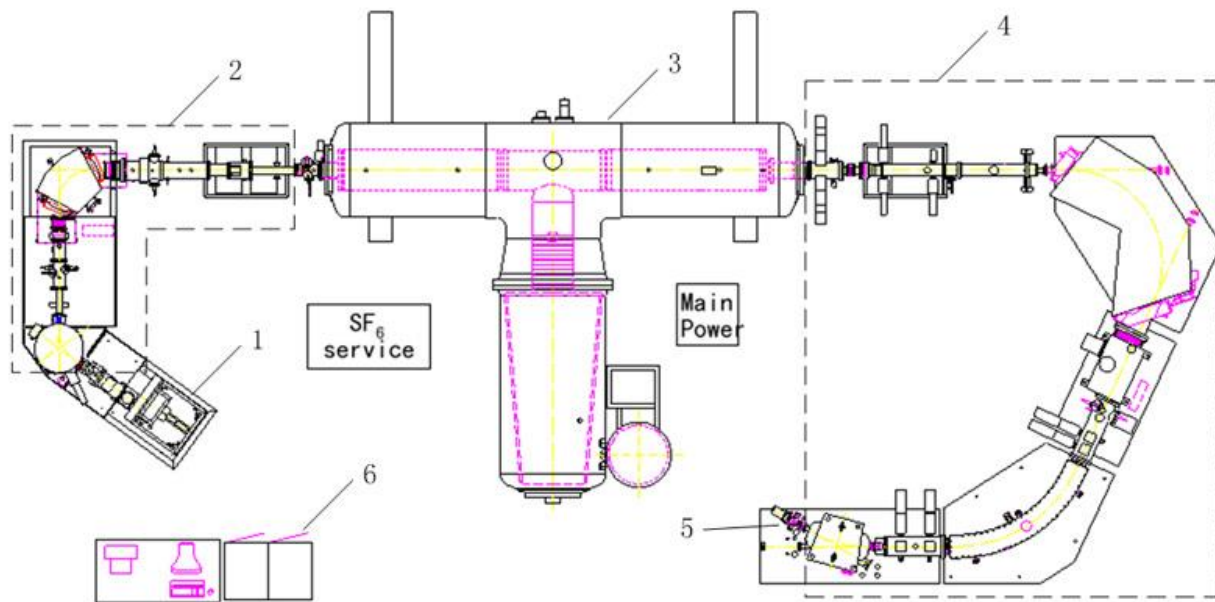


Figure 2.4 Schematic diagram of the Xi'an tandem AMS facility, where 1 is the Cs^+ sputter negative ion source, 2 is the low-energy (35 keV) injector with beam blanking unit and Q-snout, 3 is the 3 MV tandemron with Ar gas stripper and acceleration tube containing combined magnetic and electrostatic suppression, 4 is the high-energy analyzing system with magnetic-electrostatic-magnet analyzers, 5 is the gas ionization chamber detectors and 6 is the control system [106].

Procedure blanks were prepared using the same procedure as the samples, and instrumental blanks were prepared by directly precipitating iodine as AgI in the ^{127}I carrier. The measured $^{129}\text{I}/^{127}\text{I}$ atomic ratios in the instrumental and procedure blanks are $(1.3-3.5)\times 10^{-14}$ and $<5\times 10^{-13}$, respectively. The procedure blank is 1-2 orders of magnitude lower than that observed in the samples analyzed in this work. The measured $^{129}\text{I}/^{127}\text{I}$ ratios were corrected against standards with ratios of 1.138×10^{-10} and 9.952×10^{-12} prepared from the NIST 4949C and ^{127}I carrier. The analytical precisions for the $^{129}\text{I}/^{127}\text{I}$ ratio were obtained to be 1.7-2.0 % in ^{129}I standards and less than 5% in the samples.

2.6 Acquisition of environmental data

Chlorophyll-a concentrations in the central Arctic were acquired from NASA (National Aeronautics & Space Administration, www.nasa.gov).

Backward trajectories computed by means of the NOAA HYSPLIT model [144] were used to trace the transport pathways of the air collected in this work. The mid-point of the aerosol sampling period on a given day was selected as the trajectory arrival time input to HYSPLIT on that day. The global data are given on a latitude-longitude grid (2.5 degrees) at 17 pressure levels (18 sigma levels). The time resolution of the data is 6 h.

Table 2.2 Typical operational parameters of ICP-MS and AMS.

ICP-MS			AMS	
Type	Thermo X Series II		Cs sputter negative ion source	
RF power	1200 W		+5	
Plasma gas flow, L min ⁻¹	13		Argon	
Auxiliary gas flow, L min ⁻¹	1		⁹⁷ Mo ⁴⁺ for ¹²⁹ I ⁵⁺	
Nebulizer gas flow, L min ⁻¹	0.95		NIST 4949B, diluted with iodine carrier (Woodward iodine) Level 1: 1.138 × 10 ⁻¹⁰ Level 2: 9.954 × 10 ⁻¹² (0.9-5) × 10 ⁻¹³	
Expansion pressure, mbar	1.5-2.5		Typical background (¹²⁹ I/ ¹²⁷ I ratio)	
Analysis pressure, mbar	5.3 × 10 ⁻⁸		Detector	
Numbers of replicate runs	3		Faraday cup for ¹²⁷ I	
Isotopes	¹²⁷ I	¹³³ Cs	Gas ionization chamber detectors for ¹²⁹ I	
Standard	NaI (CPI international, USA), 0-100 µg L ⁻¹	CsCl, 2 µg L ⁻¹	Producer HVEE Operator Xi'an AMS center Type 3MV	
Typical background, cps	(2.5-4) × 10 ³	10-100	SUERC AMS laboratory 5 MV	
Typical sensitivity, cps per µg L ⁻¹	(1-2) × 10 ⁴	(5-10) × 10 ⁴	Voltage for ¹²⁹ I, MV 2.5	
Sweeps	700	700	3.5	
Dwell time, ms	25	15	Numbers of runs 6	
Acquisition duration, s	30	30	5-12	
Separation AMU	0.02	0.02	Duration per run, min 5	
			Conductive material in holder Niobium (325 mesh, Alfa Alsa, USA) Holder material Copper	
			Silver (100 mesh, 99.95%, Assure) Aluminum and copper	

3. Results and discussion

This thesis mainly comprises two parts, methodology development and tracing application of total ^{129}I and its speciation in the environment. The $\text{K}_2\text{S}_2\text{O}_8$ oxidation method was further improved for decomposition of organic iodine in various water samples based on the previous work. Methods for speciation analysis of ^{129}I , including pyrolysis and alkaline ashing for separation of total iodine and insoluble iodine, were developed using sequential extraction, anion exchange chromatography and mass spectrometry detection for aerosols collected on quartz filter and polypropylene filter paper (Paper II and V). The influence of aerosol collecting filter type on the analytical methods was discussed.

The second part focuses on environmental tracing applications of ^{129}I and ^{127}I , as well as transformation of iodine species in various environmental systems, including marine water, atmosphere, and seaweed. Level, distribution, sources and conversion of total ^{129}I and ^{127}I and their species in surface and deep seawater from the Central Arctic (Paper III), around Greenland, Danish coast, offshore Fukushima (Paper IV), aerosols from Risø, Denmark (Paper VI) and Tsukuba, Japan (Paper V), as well as seaweed (*Fucus vesiculosus* and *Fucus serratus*) from the Danish coastal areas were summarized and discussed below.

3.1 Methodology development

3.1.1 Persulfate oxidation for decomposition of organic iodine in water samples

Iodine in marine water exists predominantly as dissolved iodate, iodide, and a minute amount of organic iodine [39]. Total ^{129}I is generally separated from water samples by solvent extraction with reduction and oxidation of iodine. While in coastal water, estuary water, lake and river water and precipitation, significant proportion of organic iodine up to 90% of total iodine might occur [55]. Since organic iodine cannot be extracted by organic solvent, total ^{129}I concentration might be underestimated using the conventional solvent extraction without considering decomposition and conversion of organic iodine to inorganic form. Therefore, organic iodine in water samples has to be decomposed prior to solvent extraction of iodine in the samples containing significant amount of organic iodine. For this purpose, persulfate oxidation method ($\text{K}_2\text{S}_2\text{O}_8$) was developed to degrade the organic iodine in the previous study [97]. Nevertheless, this method needs further validation for natural organic iodine. Employing organic ^{125}I as tracer (by labeling organic matter extracted from lake water using radioactive ^{125}I , as described in section 2.2.1), the

crucial parameters affecting the decomposition efficiency of organic iodine in waters, including the pH of initial sample, concentration of $K_2S_2O_8$ used, and decomposition time were investigated and summarized below. The established method was validated using NaOH leachate of sediment with high-content organic iodine.

Influence of $K_2S_2O_8$ concentration. The optimal chemical yield of organic iodine of 95.8% was obtained with 10 mg g^{-1} of $K_2S_2O_8$ compared to that of 72.6% with 1.0 mg g^{-1} $K_2S_2O_8$ (Fig. 3.1). The chemical yield of organic iodine includes the iodine recoveries in two steps: $K_2S_2O_8$ decomposition and solvent extraction, implying an even higher chemical yield to 97.7% in the oxidation decomposition step if considering the extraction yield of 98%. A slightly lower chemical yield was observed when the concentration of $K_2S_2O_8$ was higher than 10 mg g^{-1} , which might be attributed to the high salinity in the decomposed solution, resulting in low recovery of iodine in the solvent extraction step. For the lake water from the Gundsømgle Lake, 10 mg g^{-1} $K_2S_2O_8$ is sufficient to decompose organic iodine. Considering the water samples with much higher organic iodine, it is advisable to use 30 mg g^{-1} $K_2S_2O_8$.

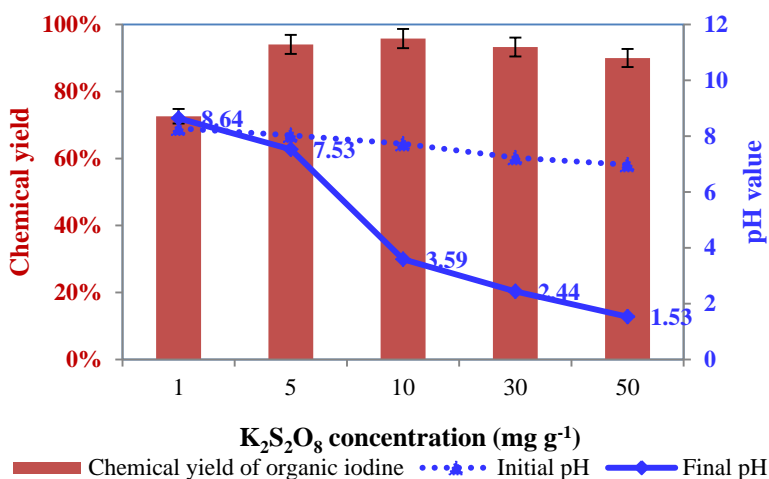


Figure 3.1 Effect of the concentration of $K_2S_2O_8$ on chemical yield of organic iodine (left axis, red) and pH values before and after potassium persulfate degradation (right axis, blue; dot line, initial pH; solid line, final pH). 100 mL of the lake water was treated with $K_2S_2O_8$ to a final concentrations of 1-50 mg g^{-1} at 60°C for 20 h. 1 mg ^{127}I carrier was added for solvent extraction by CHCl_3 .

The initial and final pH values were measured immediately after $K_2S_2O_8$ completely dissolved and 20 hours decomposition, respectively (Fig. 3.1). A slightly decrease trend of the initial pH values was observed with the final concentrations of $K_2S_2O_8$ increasing, indicating the $K_2S_2O_8$ immediately degrades once added to water. After 20 h decomposition, the final pH values decreased dramatically from 8.6 to 1.53 with the

$K_2S_2O_8$ concentrations increased from 1.0 mg g^{-1} to 10 mg g^{-1} . The variation of pH values is a consequence of decomposition of $K_2S_2O_8$, which is also related to the decomposition efficiency of organic iodine. Although iodine is easily lost in acid medium by forming volatile molecular iodine (I_2), the high chemical yield of iodine during the oxidation reaction demonstrates that no visible amount of iodine was lost. This might be explained that organic iodine is oxidized to high valence of iodate by $K_2S_2O_8$, which is stable in acidic media.

The principle of $K_2S_2O_8$ for decomposition of organic iodine in aqueous samples is that persulfate is a strong inorganic oxidant, which degrades in water forming the persulfate radical (HSO_4^\cdot), which is an active oxidizing agent [145]. The persulfate oxidation method has been proved effective to convert organic carbon and organic nitrogen to inorganic ions for determination of total carbon and nitrogen [146, 147]. Ammonium persulfate has been successfully applied in the determination of urinary iodine for removal of interference substance [148]. 1 mL of 1 mol L^{-1} ammonium persulfate was added to 200 μL urinary sample (corresponding to 5 mol/L), which is digested at $90\text{-}95^\circ\text{C}$ for 30 min. The concentration of persulfate used for urinary sample (5 mol/L) is much higher than that for natural water samples in this work (30 mg/L corresponding to 0.1 mol/L) due to the different content of organic matter.

Effect of the initial pH of sample solution. The optimal chemical yield of iodine (93.5%) was obtained when initial pH of sample solution was 7.41, while lower chemical yields (79.5-87.4%) at the other pH conditions (Fig. 3.2) were observed. When adjusting pH to acidic conditions (pH 1 and 4) by adding nitric acid, it is possible iodine was lost because of the formation of volatile I_2 . When the solutions were adjusted to higher pH (10 and 13), the slightly lower chemical yields of iodine might be attributed to the insufficient decomposition of organic iodine by $K_2S_2O_8$. Although initial pH of solution could affect chemical yield of organic iodine, more than 80% of organic iodine was effectively converted to inorganic iodine in the pH range of 1-13. This demonstrates that $K_2S_2O_8$ can be used directly to treat organic iodine in natural waters, and it is better to adjust solution pH to neutral for the acid and alkaline waste samples.

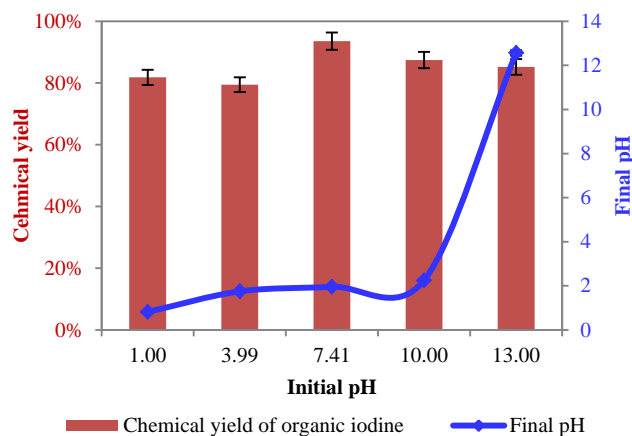


Figure 3.2. Effect of sample initial pH on decomposition efficiency (left red axis) and final pH value (right blue axis). The sample initial pH values were adjusted with HNO₃ or NaOH solutions. 100 mL of the original lake water was treated with K₂S₂O₈ to a final concentrations of 30 mg g⁻¹ at 60°C for 20 h. 1 mg ¹²⁷I carrier was added for solvent extraction by CHCl₃.

Effect of decomposition time. The effect of decomposition time on the chemical yield of organic iodine was investigated at two concentrations of K₂S₂O₈, 10 and 30 mg g⁻¹ (Fig. 3.3). It was observed that more than 90% of organic iodine can be decomposed after 5 h for 10 mg g⁻¹ K₂S₂O₈ and 2 h for 30 mg g⁻¹ K₂S₂O₈. Extending the decomposition time would not impair the chemical yield of iodine. The final pH was closely related to the decomposition time (Fig. 3.3). Only slight decline of final pH values were found within 5 h, which was followed by a large decrease of pH to 2.44 after 20 h of decomposition. This indicates the complete degradation of potassium persulfate requires longer time, but organic iodine could be decomposed to inorganic iodine from the beginning of K₂S₂O₈ degradation. However, in order to ensure sufficient decomposition of organic iodine, long decomposition time is still necessary. Due to no iodine loss observed during the oxidation decomposition, it is recommended that the K₂S₂O₈ oxidation can be carried out overnight. In the cases of fast analytical procedure, organic iodine can be effectively degraded to inorganic iodate in 5 h with addition of 10 mg g⁻¹ K₂S₂O₈, and for only 2 h with addition of 30 mg g⁻¹ K₂S₂O₈.

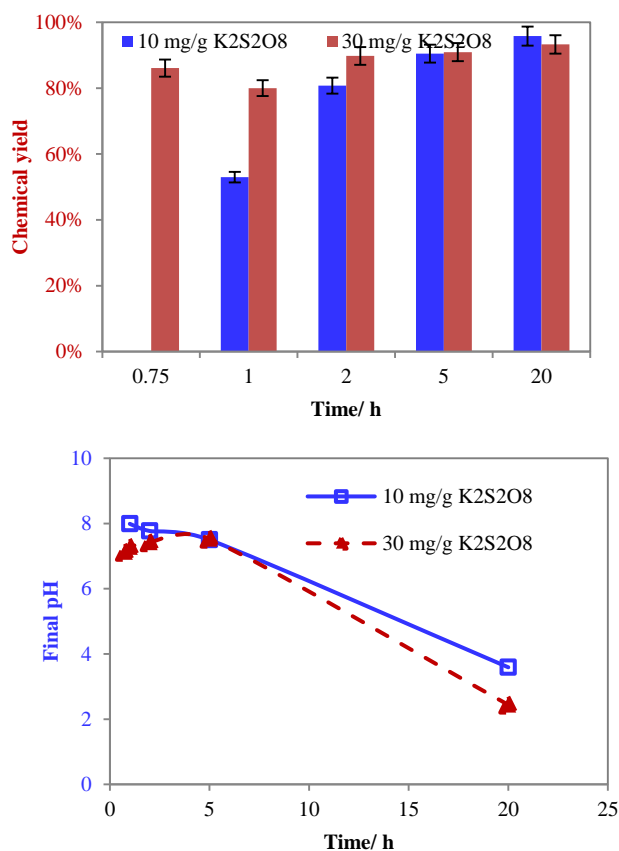


Figure 3.3. Effect of decomposition time on chemical yield of organic iodine (top) and final pH value (bottom). 10 mg g⁻¹ and 30 mg g⁻¹ of K₂S₂O₈ are represented by square in blue and triangle in red, respectively. 100 mL of the original lake water was treated with K₂S₂O₈ to a final concentrations of 10 and 30 mg g⁻¹ at 60°C for 0.75-20 h. 1 mg ¹²⁷I carrier was added for solvent extraction by CHCl₃.

Validation of the decomposition method. As shown above, up to 97.7% of organic iodine can be converted to inorganic iodine by K₂S₂O₈ decomposition. In order to confirm organic iodine in aqueous samples with high content of organic matter can be completely decomposed at the optimal experimental conditions, organic iodine leached from 1.0 g sediment from Rømø, Denmark by 100 mL 0.5 mol L⁻¹ NaOH was used for direct solvent extraction and K₂S₂O₈ decomposition. The content of organic matter in the sediment is about 13% of the total mass roughly estimated from the ignition loss.

The concentration of organic ¹²⁹I in the sediment is $(11.5 \pm 0.9) \times 10^9$ atoms g⁻¹, which is calculated by the difference between the total ¹²⁹I and ¹²⁹I in the residual insoluble iodine after NaOH leaching. Total iodine in the original *sediment and the residual iodine was separated by conventional combustion method* (see section 2.2.2). The results (Table 3.1)

showed that the organic ^{129}I concentration was measured to be 5.7×10^9 atoms g^{-1} without $\text{K}_2\text{S}_2\text{O}_8$ decomposition of the sediment leachate. This indicates only 50% of iodine in the NaOH leachate was extracted by chloroform extraction. After $\text{K}_2\text{S}_2\text{O}_8$ decomposition, a good agreement was obtained between the measured ^{129}I concentration and the calculated value. This result confirms the established method using $\text{K}_2\text{S}_2\text{O}_8$ oxidation could completely decompose organic iodine to inorganic iodine.

Table 3.1. The concentration of organic matter associated ^{129}I ($\times 10^9$ atoms g^{-1}) in the NaOH leachate of sediment with and without $\text{K}_2\text{S}_2\text{O}_8$ oxidation decomposition. The decomposed leachates were further separated by solvent extraction and measured by AMS.

Replicate	^{129}I in the NaOH leachate	Without $\text{K}_2\text{S}_2\text{O}_8$ decomposition		With $\text{K}_2\text{S}_2\text{O}_8$ decomposition	
		^{129}I	Percentage	^{129}I	Percentage
1	11.5 ± 0.9^a	6.2 ± 0.5	54.3%	12.3 ± 1.0	107.0%
2		5.7 ± 0.4	49.7%	12.8 ± 1.0	111.0%
3		5.3 ± 0.4	45.8%	11.8 ± 0.9	102.3%
Average		5.7	49.90%	12.3	106.80%

a. This data were obtained from three replicates.

Recommended procedure for decomposition of organic iodine in natural water samples using $\text{K}_2\text{S}_2\text{O}_8$. Taking 100 mL water samples as an example, the procedure for decomposition of organic iodine using $\text{K}_2\text{S}_2\text{O}_8$ is recommended as the following.

- I. Take 100 mL filtered water samples or solutions to an appropriate size beaker;
- II. Add 30 mg $\text{K}_2\text{S}_2\text{O}_8$ (solid) into the water to a final concentration of 30 mg g^{-1} ;
- III. For determination of total ^{129}I , add 500 Bq ^{125}I tracer and 1-2 mg ^{127}I carrier (in the case that solvent extract is used for separation of iodine for ^{129}I determination);
- IV. Stir the solution with a glass rod until $\text{K}_2\text{S}_2\text{O}_8$ is completely dissolved. Cover the beaker using a watch glass for refluxing;
- V. Put the beaker on a hot plate and heat at 60°C . Stir the solution occasionally in the first few hours, and then keep heating overnight;
- VI. After cooling down, inorganic iodine in the decomposed solution is extracted by solvent extraction for determination of total ^{129}I , or treated by AgI-AgCl co-precipitation (in this case, no ^{127}I carrier should be added before digestion).

It is worthy to note that after $\text{K}_2\text{S}_2\text{O}_8$ decomposition, there may be some $\text{K}_2\text{S}_2\text{O}_8$ remained

in the solution. In the following reduction of iodate using reductant, the residual $K_2S_2O_8$ might consume the added reductant. Hence, more reductant (4 mL 1 mol L⁻¹ $KHSO_3$) is required for the treated 100 mL water compared to the original water sample (0.5-1 mL of 1 mol L⁻¹ $KHSO_3$).

3.1.2 Determination of ¹²⁹I and ¹²⁷I and their species in aerosols

Method for speciation analysis of ¹²⁹I and ¹²⁷I in aerosols was established by coupling sequential extraction with mass spectrometry detection (Paper II and V), allowing to quantitative determination of water-soluble iodine (iodide, iodate), NaOH soluble and residual insoluble iodine for ¹²⁹I and ¹²⁷I in aerosols.

Determination of total ¹²⁹I in aerosols. Atmospheric aerosol can be collected on many different types of filter papers. The most commonly used filter paper materials are quartz fiber, glass fiber, cellulose and polypropylene. In this study, we have analyzed aerosol samples collected on quartz fiber filter and polypropylene filter for determination of ¹²⁹I and its species. The results show that high chemical yield of iodine can be obtained for aerosol on quartz fiber filter using combustion (95.9%) and for polypropylene filter using alkaline ashing with addition of $K_2S_2O_5$ (85.7%) (Table 3.2).

Table 3.2 Chemical yields of iodine using combustion, alkaline ashing and alkaline ashing with $K_2S_2O_5$.

Method	Filter type	Chemical yield, %
Combustion	Quartz	95.9 ± 4.8
Combustion	Polypropylene	65.1 ± 3.2
Alkaline ashing	Polypropylene	62.3 ± 2.5
Alkaline ashing + $K_2S_2O_5$	Polypropylene	85.7 ± 4.3

Selection of method for separation of total ¹²⁹I from aerosol samples is strongly dependent on filter types. ¹²⁹I can be separated from aerosol filter by three methods, NaOH leaching, combustion and alkaline ashing [54, 149, 150]. Due to the complexity of iodine species in aerosols, NaOH leaching cannot ensure to completely extract ¹²⁹I from aerosol, which likely gives rise to underestimate the total ¹²⁹I concentration. Combustion is an excellent method to separate iodine from solid samples, but it is suffered from the influence of organic matter. Rapid combustion of organic matter in a tube furnace could cause eruptive loss of iodine in trap solution, resulting in low chemical yield of iodine (65.1%). Furthermore, the capacity to treat large sample size is greatly limited by the narrow combustion tube and rapid burning of organic substances (< 0.5 g polypropylene filter paper). Alkaline ashing method normally has high capacity for large sample size. While

due to the formation of volatile iodine forms, the chemical yield of iodine is relative low (62.3%) [150]. The addition of a reductant, $K_2S_2O_5$, could effectively avoid the formation of volatile iodine and prevent iodine from loss during ashing (see detail in Paper II).

From the point of sample preparation view, the filter materials for collecting aerosol can be classified into two groups, the inorganic mineral filter (such as quartz and glass fiber) and organic filter paper (such as cellulose and polypropylene). For the first group, combustion method is suitable to achieve high chemical yield of iodine. Alkaline ashing with addition of $K_2S_2O_5$ is applicable to separate iodine in aerosol collected on organic filter papers.

Influence of filter type on stability of iodine species during extraction. Stability of iodine species is pivotal in speciation analysis. However, there are only few experimental investigations on the conditions causing iodine species changing. During leaching for water-soluble iodine species including iodide, iodate and soluble organic iodine, interconversion among dissolved iodine species was observed with increased leaching time (Fig. 3.4). The ratios of iodide to iodate in water leachate decreased from 14.6 within 1 h leaching to 12.4 after 2 h leaching. The declined I/IO_3^- ratio in water leachate might be attributed to oxidation of iodide to iodate during water leaching, which is likely related to photo degradation of polypropylene filter paper (Paper II).

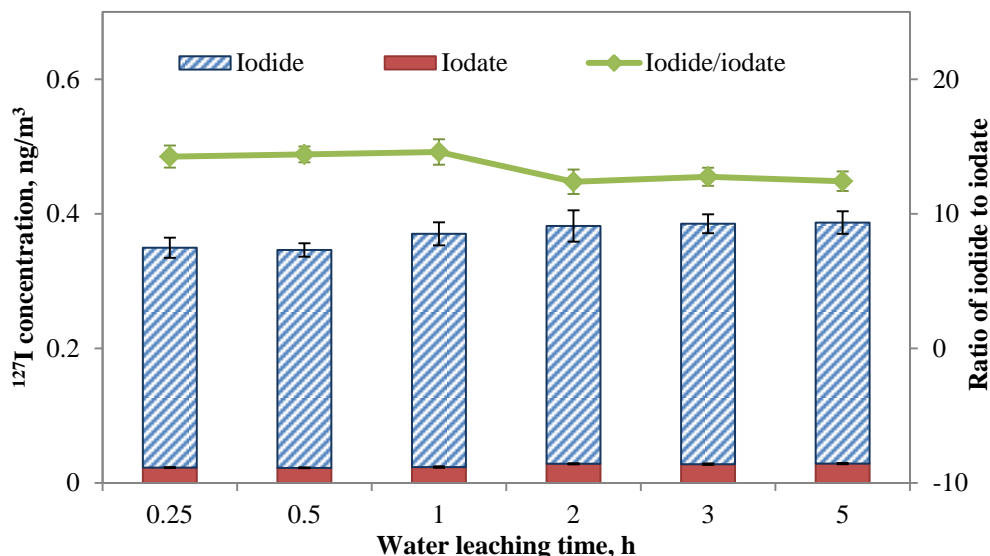


Figure 3.4. Variation of iodine species in water leachate with extracting time.

Oxidation of iodide to iodate was not observed during water leaching for aerosol on quartz fiber filter, for which only iodide was present in water leachate (Paper V). This likely indicates that the stability of iodine species strongly depend on filter materials. Baker et al. (2000) has observed that inorganic iodine concentrations in water leachate of aerosols decrease with extended leaching time when using ultrasonic-assistant extraction; they attributed this to conversion of iodide to organic iodine species on cellulose filter [151]. Xu et al. (2010) also observed significantly decreased recoveries of iodide spiked into cellulose filter from 87% for 5 min leaching to only 18% when extending the leaching time to 1 h, but no variation of iodide recovery when spiked to glass microfiber filter [152]. In consideration of stability of inorganic iodine species, organic filter (polypropylene used in this work and cellulose) shows a stronger influence than inorganic fiber filter (quartz and glass filters). Therefore, leaching time has to be strictly controlled to avoid the transformation of iodine species.

Recommended analytical procedure and analytical performance. In order to develop a reliable method for speciation analysis of ^{129}I and ^{127}I in aerosols collected on polypropylene filter paper, we have optimized the crucial parameters affecting the analytical performance, including the amount of leaching reagent, leaching time for water leaching and NaOH leaching, stability of iodine species during water leaching, NaOH leaching temperature, ashing time, ashing temperature and amount of $\text{K}_2\text{S}_2\text{O}_5$ (Paper II). For the aerosol sample collected in Risø, Denmark, 1 g and 3 g were sufficient for determination of total ^{129}I and ^{127}I species, respectively. The optimal analytical procedure is recommended in Fig. 3.5.

The detection limits of 0.007 ng m^{-3} for ^{127}I and 7.1×10^6 atoms (1.5 fg) for ^{129}I were obtained. The results (see Table 3 in Paper II) show that the sum of all species including water-soluble iodine, NaOH soluble iodine and insoluble iodine is in good agreement with total iodine concentration, as revealed by the ratios of sum to total iodine in the range of 97% to 107% for both ^{127}I and ^{129}I . This confirms the reliability of the presented method for speciation analysis of ^{129}I and ^{127}I in aerosol samples.

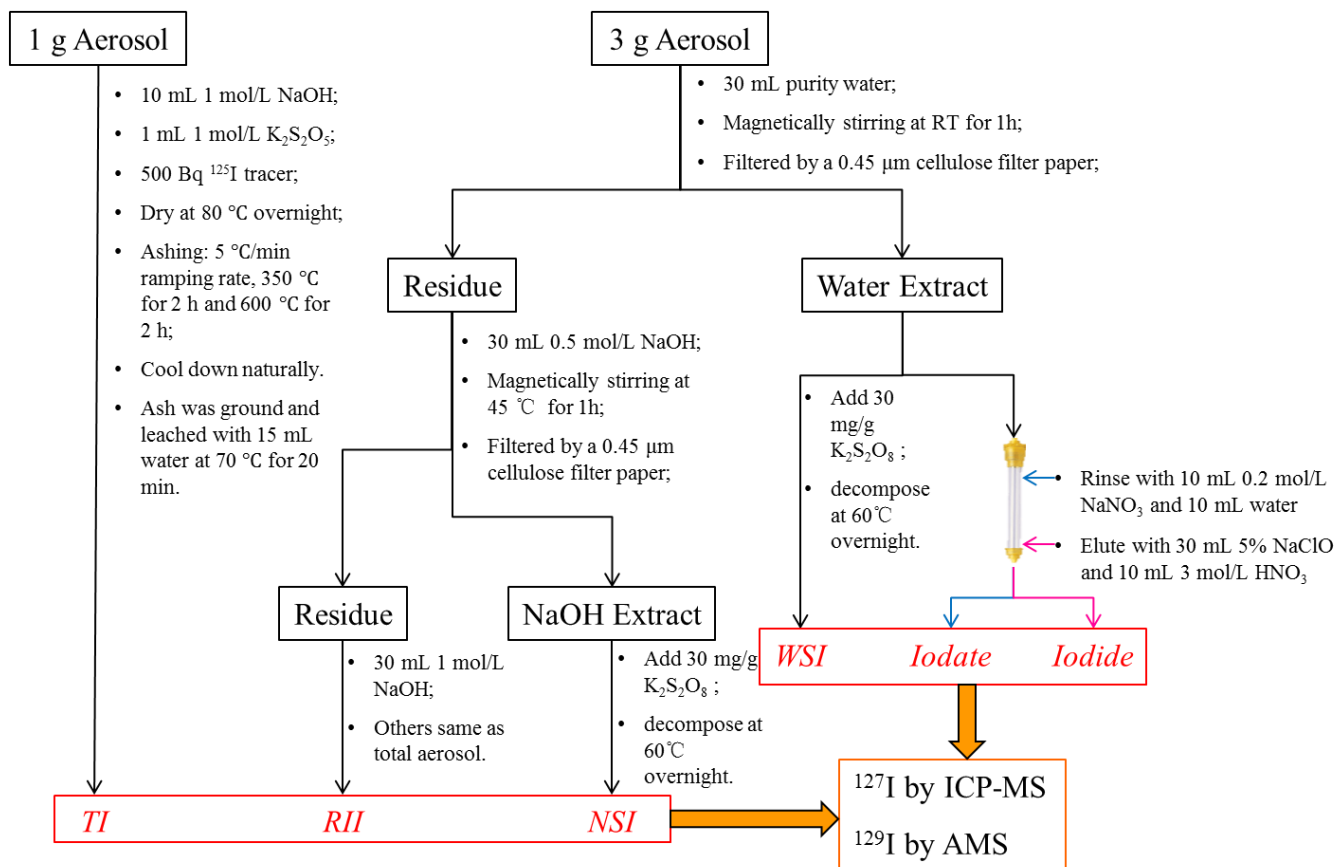


Figure 3.5. Schematic diagram of optimized analytical procedure using sequential extraction, chromatography separation and mass spectrometry techniques for speciation analysis of ^{127}I and ^{129}I in aerosols. TI is for total iodine, WSI for water-soluble iodine, NSI for NaOH soluble iodine, and RII for residual insoluble iodine.

3.2 Environmental tracing application of ^{129}I and ^{127}I species

3.2.1 Speciation of ^{129}I and ^{127}I in marine water

A main part of the thesis has been devoted to the investigations of ^{129}I and ^{127}I , as well as their species in seawater from a variety of oceans and seas, including the central Arctic (Paper III), Greenland and Danish coast, as well as offshore Fukushima (Paper IV).

3.2.1.1 The central Arctic

Depth profile seawater samples (0-800 m) were collected and analyzed for investigations of ^{129}I and its species. The sampling depth covers two layers of the central Arctic, the polar mixed layer (PML, 0-50 m deep and salinity range of 31-34 psu), and warm Atlantic Water Layer (AWL) at depth ranging between 200 and 800 m ($34.5 < \text{Salinity} < 34.8$).

Vertical profiles of total ^{129}I and ^{127}I . The vertical distributions of the concentrations of ^{127}I and ^{129}I , and $^{129}\text{I}/^{127}\text{I}$ atomic ratios are shown in Fig. 3.6. The concentrations of ^{127}I in the PML ranged from $40 \mu\text{g L}^{-1}$ at station 2 over the Mendeleev-Alpha Ridge to $54 \mu\text{g L}^{-1}$ at station 12 in the southeastern Eurasian Basin, with an average level of $48.20 \mu\text{g L}^{-1}$. In the AWL, ^{127}I concentrations were elevated to an average of $56.80 \mu\text{g L}^{-1}$ and relatively constant. In contrast to ^{127}I , a significant decrease of ^{129}I concentrations from a range of $(48.20-72.58) \times 10^8 \text{ atoms L}^{-1}$ in the PML to $(2.89-29.79) \times 10^8 \text{ atoms L}^{-1}$ at 200-500 m and $(5.09-28.79) \times 10^8 \text{ atoms L}^{-1}$ at 700-800 m in the AWL in the water columns of the Eurasian and Makarov Basins. The ^{129}I concentrations in the PML at stations 1 and 2 over the Mendeleev-Alpha Ridge and north of Canada Basin were about 50-fold lower than other stations. The ^{129}I concentration at station 1 in the north Canada Basin increased from $1.36 \times 10^8 \text{ atoms L}^{-1}$ in the PML to $18.24 \times 10^8 \text{ atoms L}^{-1}$ at the depth of 250 m, and then decreased to $6.31 \times 10^8 \text{ atoms L}^{-1}$ at 370 m depth. The $^{129}\text{I}/^{127}\text{I}$ atomic ratios varied from 6×10^{-10} in the Canada Basin to 311×10^{-10} in the southern Eurasian Basin. The vertical distribution pattern of $^{129}\text{I}/^{127}\text{I}$ ratios is similar with ^{129}I concentrations because of the weak variability of ^{127}I .

The measured ^{129}I concentrations of $10^8-10^{10} \text{ atoms L}^{-1}$ in the central Arctic seawater collected in 2011 is 3-5 orders of magnitude higher than the level of pre-nuclear era ($10^5 \text{ atoms L}^{-1}$ for ^{129}I concentration, or ca. 10^{-12} for $^{129}\text{I}/^{127}\text{I}$ ratio) [153], and 1-2 orders of magnitude higher than the global fallout level of the post-nuclear era (ca. 10^{-10} for $^{129}\text{I}/^{127}\text{I}$ ratio) [15, 27]. In the eastern Eurasian Basin (station 12), the concentration of ^{129}I in the PML seawater during mid-1990 measured to be approximately $12 \times 10^8 \text{ atoms L}^{-1}$ [154,

155], was raised by five-fold to about 65×10^8 atoms L^{-1} in late 2000s [156], and by six-fold up to 72.58×10^8 atoms L^{-1} in 2011 in this work. About 4-fold increase in ^{129}I concentrations are found in the AWL seawater from 1995 (5×10^8 atoms L^{-1}) [156] to 2011 (22×10^8 atoms L^{-1}). These dramatically increases in ^{129}I levels in the PML and AWL demonstrate that the high discharge of ^{129}I from the reprocessing plants at Sellafield and La Hague since early 1990s has flowed into the Arctic Ocean with the water current flowing along the European continent and the Arctic marginal seas [24, 154, 155, 157-161]. Not only for the Eurasian and Makarov Basins, the increase of ^{129}I concentration at surface layer (station 1) in the Canada Basin from 0.5×10^8 atoms L^{-1} in 1995 [160] to 1.36×10^8 atoms L^{-1} in 2011 indicates that ^{129}I has intruded the surface layer of Canada Basin with a very slow rate (Paper III).

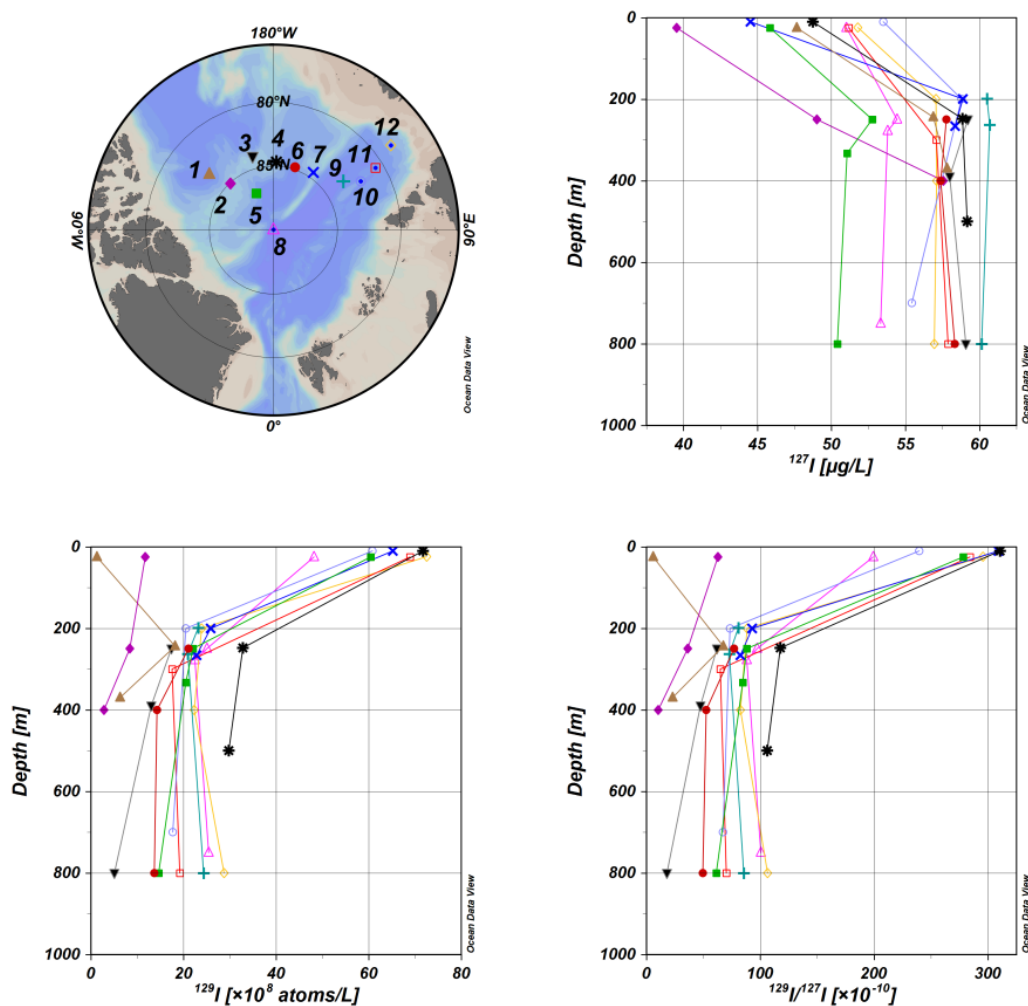


Figure 3.6 Vertical distribution of the concentrations of total ^{127}I and ^{129}I , and the $^{129}I/^{127}I$ ratios in the twelve water depth profiles from the central Arctic.

Vertical profiles of chemical species of ^{129}I and ^{127}I . Distribution of iodate and iodide for both ^{129}I and ^{127}I observed in the twelve water depth profiles showed that iodate is the predominant specie in all depth profiles for both ^{129}I and ^{127}I (Figs. 3.7 and 3.8). Similar to the distribution pattern of total ^{127}I , the concentrations of $^{127}\text{IO}_3^-$ in the PML seawater varied from $22.83 \mu\text{g L}^{-1}$ at station 2 over the Alpha Ridge to $50.70 \mu\text{g L}^{-1}$ at station 12 in the Eurasian Basin, which increased by about 1.2 times ($44.16\text{-}62.96 \mu\text{g L}^{-1}$) in the top of AWL at 200-250 m depth and kept almost constant to 800 m. While a decline trend of $^{127}\text{I}^-$ from the surface to the AWL was observed and distinct from the distributions of both total ^{127}I and $^{127}\text{IO}_3^-$. $^{127}\text{I}^-$ concentrations of $0.71\text{-}11.48 \mu\text{g L}^{-1}$ in the deep layer were 2-8 times lower than those ($9.62\text{-}14.35 \mu\text{g L}^{-1}$) in surface water.

Wide concentration ranges of ^{129}I species were observed in the PML, $(0.82\text{-}50.29) \times 10^8$ atoms L^{-1} for $^{129}\text{IO}_3^-$ and $(2.88\text{-}35.38) \times 10^8$ atoms L^{-1} for $^{129}\text{I}^-$, respectively, in which 27.7%-45.3% of total ^{129}I is in the form of iodide. The depth profiles of $^{129}\text{IO}_3^-$ show the same trend as total ^{129}I . Except the two stations (1 and 2) locating at the Mendeleev-Alpha Ridge and the Canada Basin, the concentrations of $^{129}\text{IO}_3^-$ decreased from $25\text{-}50 \times 10^8$ atoms L^{-1} in the PML to lower than 29×10^8 atoms L^{-1} in the AWL. Same as the total ^{129}I , the maximum of $^{129}\text{IO}_3^-$ appears at the upper AWL (250 m) in the Mendeleev-Alpha Ridge (9×10^8 atoms L^{-1} at station 2) and the Canada Basin (17.8×10^8 atoms L^{-1} at station 1). The vertical distribution of $^{129}\text{I}^-$ concentrations exhibit a decline trend for most of the sampling stations, except the station 1 in the Canada Basin where a $^{129}\text{I}^-$ peak was found at 244 m.

The molecular ratios of iodide to iodate for both ^{129}I and ^{127}I in all PML waters were considerably higher than those in the AWL water, suggesting that higher iodide level was present in the surface layer. $^{129}\text{I}^-/^{129}\text{IO}_3^-$ ratios ranged from 0.05-0.73 were generally higher than $^{127}\text{I}^-/^{127}\text{IO}_3^-$ ratios (0.02-0.62), but no correlation was found between them (see Fig. S-2 in Paper III). This might be attributed to the different sources of ^{129}I and ^{127}I .

Transformation among iodine species. Speciation analysis of ^{129}I and ^{127}I in the central Arctic shed lights on the transformation of iodine species in high latitude and deep ocean (Paper III).

- 1) In the PML of the basin interiors, the extremely weak variation of I^-/IO_3^- ratios for both ^{129}I and ^{127}I suggests oxidation of iodide and reduction of iodate are slow processes.

- 2) In the PML over the ridges, apparently high I^-/IO_3^- ratios for both ^{129}I and ^{127}I demonstrate that reduction of iodate might occur in the central Arctic. This is most likely associated with the input of high nutrient and exuberant biological activities, but less related to photochemical reactions due to the shading overlying thick sea-ice.
- 3) In the AWL, variation of $^{129}I/^{129}IO_3^-$ from 0.28 in the Eurasian Basin to 0.07 in the Canada Basin reveals that iodide is oxidized to iodate in deep-ocean.

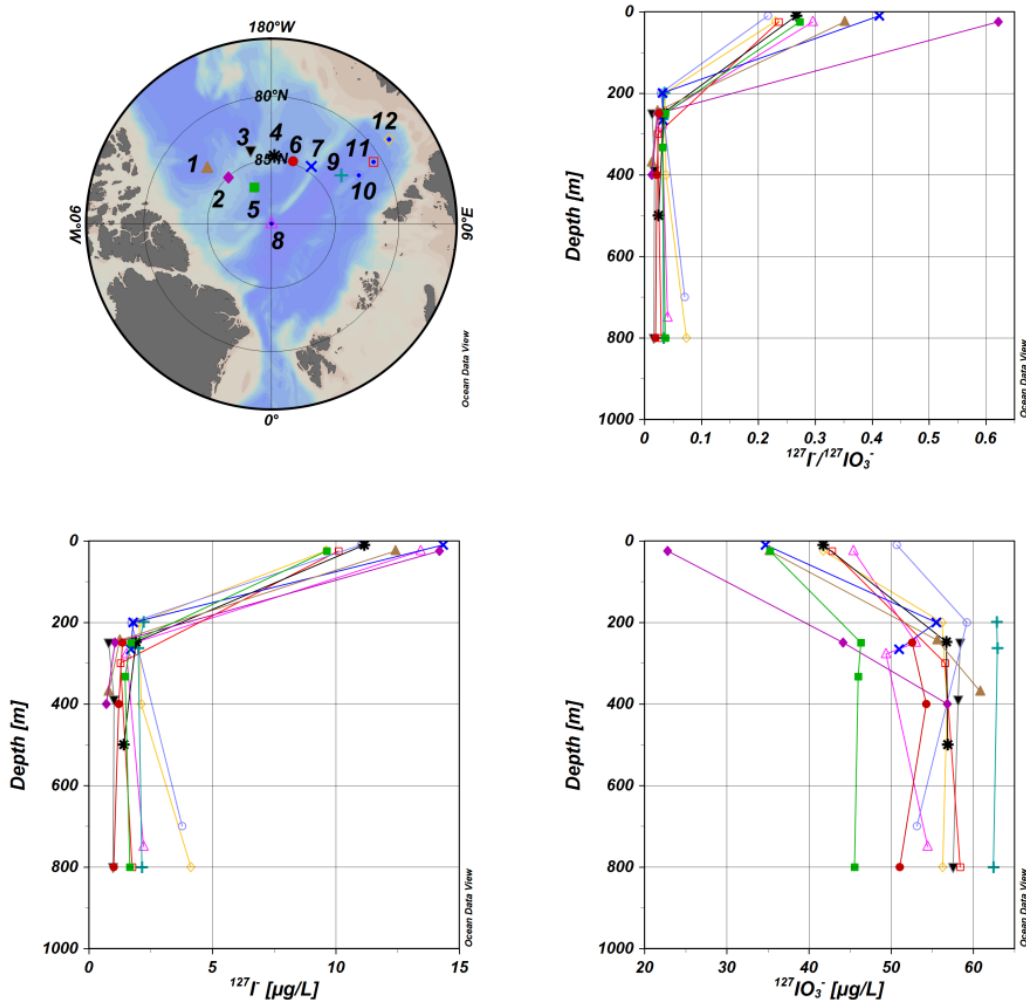


Figure 3.7 Vertical distribution of the concentrations of ^{127}I and $^{127}IO_3^-$, and the $^{127}I/^{127}IO_3^-$ ratios in the twelve water depth profiles from the central Arctic.

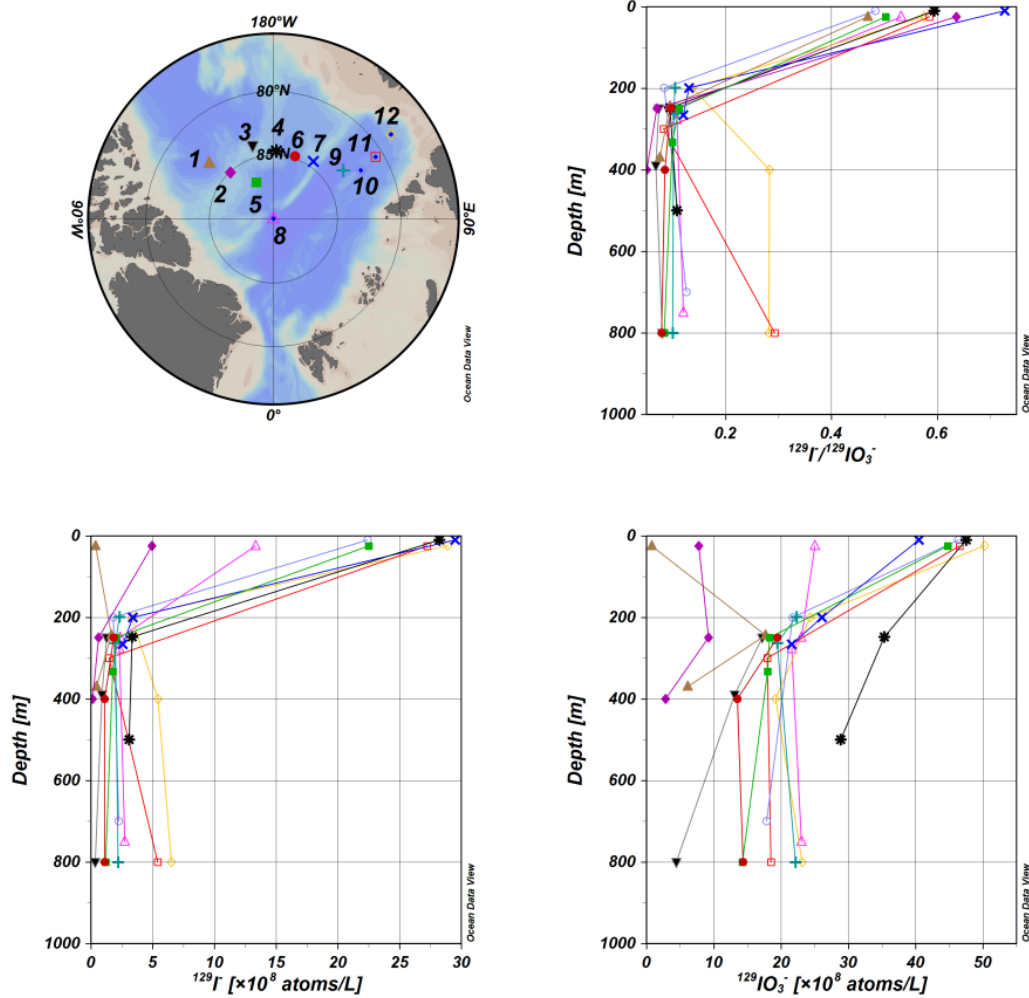


Figure 3.8 Vertical distribution of the concentrations of ^{129}I and $^{129}\text{IO}_3^-$, and the $^{129}\text{I}/^{129}\text{IO}_3^-$ ratios in the twelve water depth profiles from the central Arctic.

3.2.1.2 Greenland coast

Variation of total ^{129}I and ^{127}I , as well as their species in the seventeen seawater samples collected around the Greenland are shown in Figs. 3.9 and 3.10. To facilitate the discussion, samples were classified to four groups as northeast (stations 1-6), southeast (stations 7-11), southwest (stations 12-15) and northwest (stations 16 and 17) of Greenland waters taking the Denmark Strait and Davis Strait as boundaries for east and west coasts, respectively (Fig. 3.11).

Distribution of total ^{129}I and ^{127}I in the Greenland coastal waters. The ^{127}I concentrations showed relatively homogeneous distribution except at a few points in northeast coast and southwest coast of the Greenland with slightly lower ^{127}I concentrations (Fig. 3.9). The concentrations of ^{129}I showed an apparently higher level in northeast coast with maximum value of 27.07×10^8 atoms L^{-1} than those in the west with 16.65×10^8 atoms L^{-1} . The observed highest $^{129}\text{I}/^{127}\text{I}$ ratio in the northeast was 111.40×10^{-10} compared to that of 66.51×10^{-10} in the west coast. Unexpectedly, the southeast Greenland coastal water show lower ^{129}I level than the southwest Greenland coast.

The average $^{129}\text{I}/^{127}\text{I}$ ratio of 71×10^{-10} in the Greenland coast in 2012 is more than one order of magnitude higher than those in North Atlantic Ocean ($(1.82-5.45) \times 10^{-10}$) in 2010 [50], and about two times higher than that in the Irminger Sea in 2010 [162] and falls within the range of the Central Arctic ($(6-311) \times 10^{-10}$) during 2011. In contrast to ten years ago (2001-2002), the current Greenland ^{129}I level has increased about 30 times compared to the simulation data from Orre et al. [163], and is also significantly higher than the Irminger Sea and Labrador Sea in 2001 [163, 164], while still 20 times lower than the concentrations of ^{129}I in the Norwegian coastal current water [158]. At the northwest Greenland coast, the $^{129}\text{I}/^{127}\text{I}$ atomic ratio of $(7-15) \times 10^{-10}$ has been observed in seaweed sample collected in August 1997. Based on the assumption that the $^{129}\text{I}/^{127}\text{I}$ ratio in seaweed is same as that in seawater, it can be calculated that the concentration of ^{129}I in the northwest Greenland seawater would be in a range of $(2-4) \times 10^8$ atoms L^{-1} if taking the ^{127}I concentration of $60 \mu\text{g L}^{-1}$ [122]. This level has increased to $(7.7-18.6) \times 10^8$ atoms L^{-1} in the west Greenland coast by 2012. Proximity to the latitude of 72°N , the ^{129}I concentration has increased by a factor of 2-9 from 1997 to 2012.

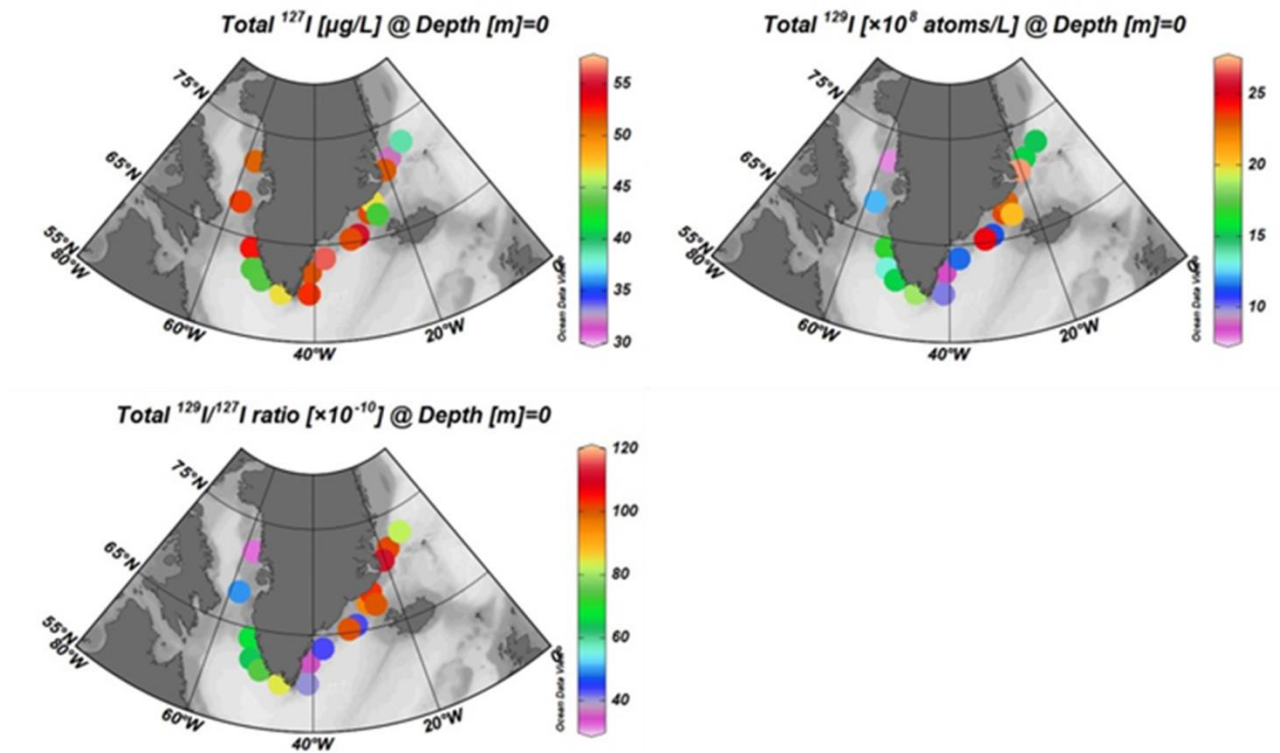


Figure 3.9 Variation of the concentrations of total ^{129}I and ^{127}I , as well as the $^{129}\text{I}/^{127}\text{I}$ ratios in the Greenland coastal seawater.

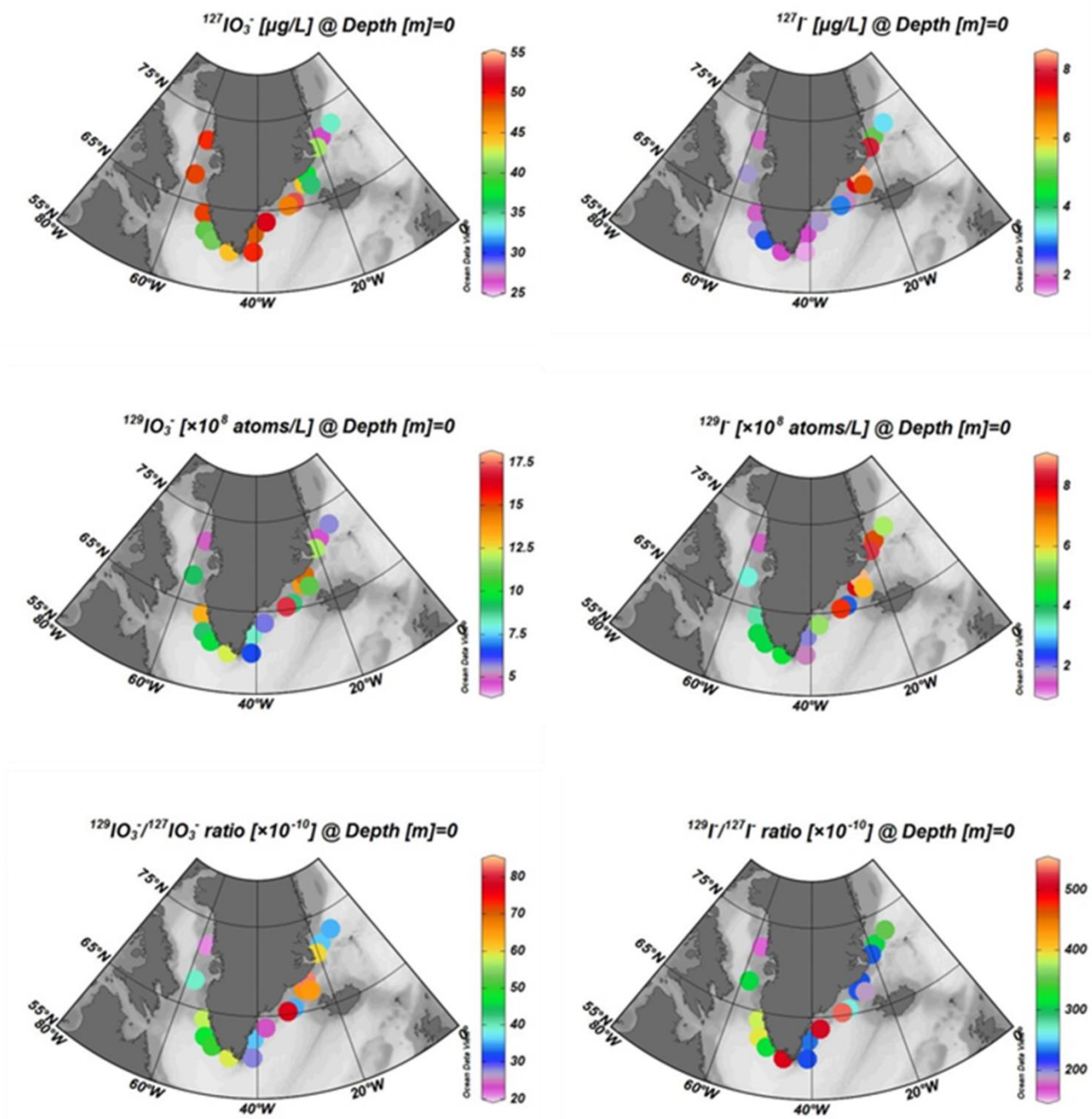


Figure 3.10 Variation of the concentrations of ^{129}I and ^{127}I species, as well as the $^{129}\text{I}/^{127}\text{I}$ ratios for iodide and iodate in the Greenland coastal seawater.

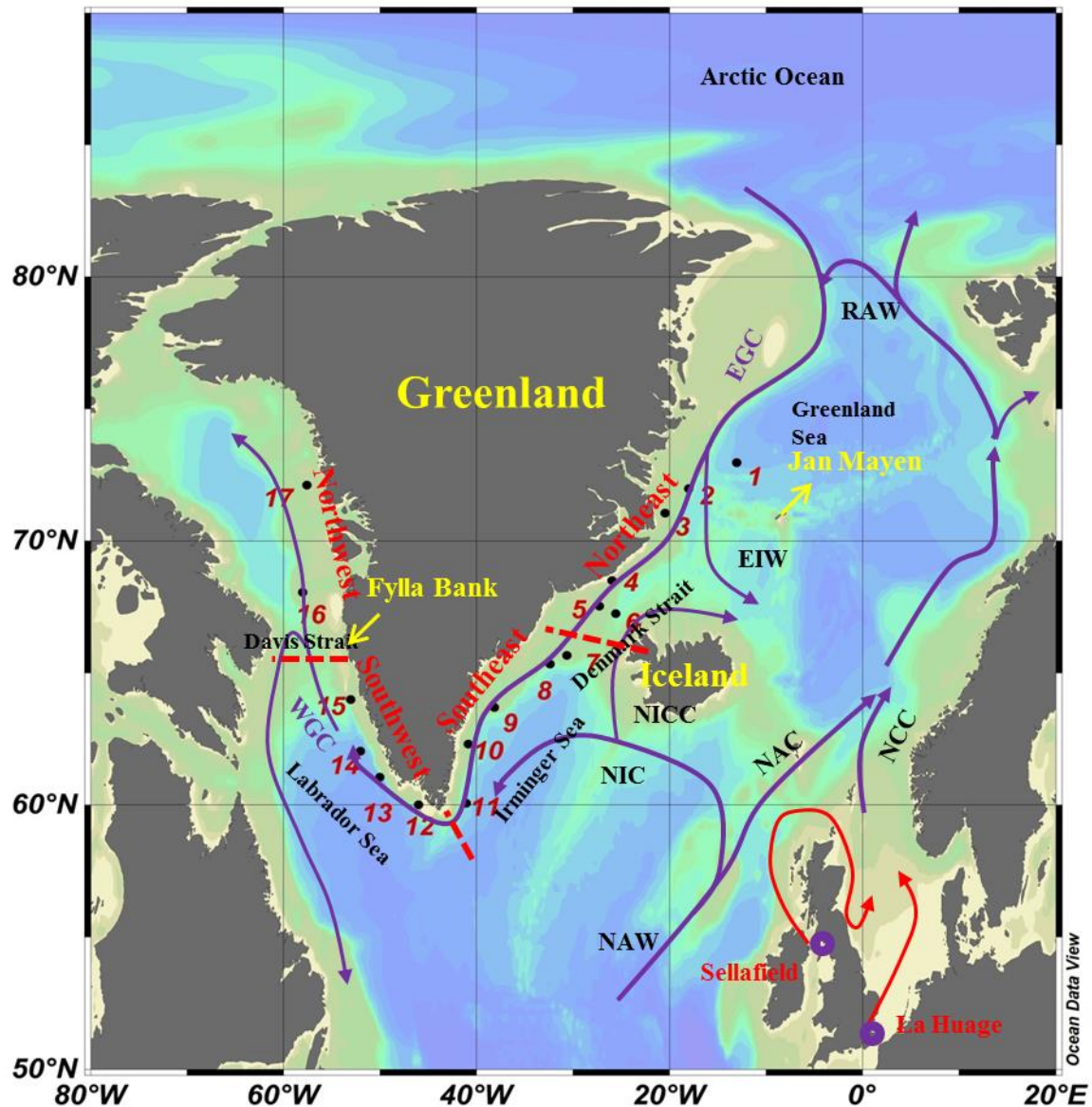


Figure 3.11 Map showing the seventeen sampling sites in the Greenland shelf area, surface water currents and main ^{129}I sources (Sellafield and La Hague) (Compiled from [165-167]). Purple lines are the currents. Red lines show outflow of ^{129}I from Sellafield (UK) and La Hague (France). Red dot lines at the Denmark Strait, the southern tip of Greenland and the Davis Strait are used to separate the four Greenland coastal regions, northeast, southeast, southwest and northwest. Abbreviations are defined as follows: EGC, East Greenland Current; WGC, West Greenland Current; NCC, Norwegian Coastal Current; NAC, North Atlantic Current; NAW, North Atlantic Water; EIW, East Icelandic Water; NICC, North Icelandic Coastal Current; RAW, Return Atlantic Water.

The variation of ^{129}I in the east coast with high level in the north and low value in the south reveals the surface water current flowing southward. East Greenland coastal water is mainly derived from the Arctic Ocean water transported by East Greenland Current

(EGC) (Fig. 3.11). The EGC carries the ^{129}I -rich cold Polar Water (PW) from the Arctic Ocean and the temperate returned North Atlantic Current water (RAW), transports southward through the Fram Strait and Denmark Strait along the east coast of Greenland, and mixes with the North Irminger Current (NIC) water on the west of Irminger Basin [166, 168-170]. Much lower level of $^{129}\text{I}/^{127}\text{I}$ ratios at station 1 (the northernmost location) and station 7 (proximate to the Irminger Sea) reflects the water exchange process between the EGC with Greenland Sea water and the Irminger Sea water, respectively. The highest ^{129}I concentration was found at the Denmark Strait ($65\text{-}71^\circ\text{ N}$) and the lowest in the southeast. This might be related to current convection, for which the ^{129}I -rich intermediate Atlantic water layer (AWL) of the Arctic Ocean ascends to the surface layer in the Denmark Strait and then descend back to deeper layer. This finding is consistent with the previous investigation in the Greenland Sea and Denmark Strait and also supported by the model simulation [9, 163].

In the west Greenland coast, an apparently decreasing trend of the ^{129}I concentrations from south to north was observed. This indicates the surface circulation in the West Greenland is dominated by the northward West Greenland Current (WGC). The significantly low ^{129}I concentrations at the stations 16 and 17 might imply that as the WGC reaches the Fylla Bank (66° N), only a small fraction of WGC passes over the Davis Strait and continues northward, while a significant branch of the WGC turns westward and joins the Labrador Current on the Canadian side [166]. It was reported that the WGC water mass are formed in the western Irminger Basin, where the East Greenland Current and the Irminger Current meet and flow southward side by side [171]. This implies that ^{129}I in the WGC should be a mixing consequence of the ^{129}I -rich EGC with the ^{129}I -poor Irminger water. However, a higher level of ^{129}I in the southwest was observed compared to those in the southeast. This discrepancy might be explained that either 1) the ^{129}I -rich Denmark Strait overflow water [164] upwellings in the southwest Greenland coast and thus contribute high ^{129}I ; or that 2) the EGC might be located beneath the NIC in the southeast Greenland shelf ($< 500\text{ m}$), and rise up to the surface once flowing into the west Greenland shelf. A reported depth profile of ^{129}I (0-3000 m depth) in the Labrador Sea margin (station 23 in the reference [164]) didn't show any upwelling from the ^{129}I -rich Denmark Strait overflow water in deep layer (2000-3000 m). The second conjecture still needs evidence from ^{129}I depth profile data or other hydrological information on the shelf area, but there is no available information so far.

Distribution of ^{129}I and ^{127}I species. Iodate was observed as the predominant specie for both ^{129}I and ^{127}I in all the Greenland waters. The concentrations of $^{127}\text{IO}_3^-$ varied from

26.45 $\mu\text{g L}^{-1}$ at the east Greenland coast close to the latitude of 72° N (station 2) to 53.36 $\mu\text{g L}^{-1}$ at downstream of the Denmark Strait (station 7), accounting for more than 80% of total ^{127}I . The coast water on the northeast Greenland contained lower $^{127}\text{IO}_3^-$ concentrations than southeast and west of Greenland, and the highest $^{127}\text{IO}_3^-$ occurred at southeast Greenland (Fig. 3.10). The concentrations of ^{127}I varied from 4.32 $\mu\text{g L}^{-1}$ at station 1 (73°N, 13 °W) to 11.18 $\mu\text{g L}^{-1}$ at the northeast Greenland proximate to the shore (station 4) (Fig. 3.10).

The concentrations of $^{129}\text{IO}_3^-$ varied from 4.49×10^8 atoms L^{-1} at station 2 on the northeast Greenland to 17.04×10^8 atoms L^{-1} at station 8 at the downstream of the Denmark Strait, accounting for 29-95% of total ^{129}I . The ^{129}I concentrations varied from 1.51×10^8 atoms L^{-1} in the northwest Greenland water (Baffin Bay) to 9.06×10^8 atoms L^{-1} at station 4 in the Denmark Strait, which resulted in high $^{129}\text{I}/^{127}\text{I}$ ratios ((58.18-271.73) $\times 10^{-10}$). ^{129}I showed a decline trend from the east Greenland to the west. The $^{129}\text{I}/^{127}\text{I}$ atomic ratios for iodide were much higher than those for iodate, especially at stations 1 and 2.

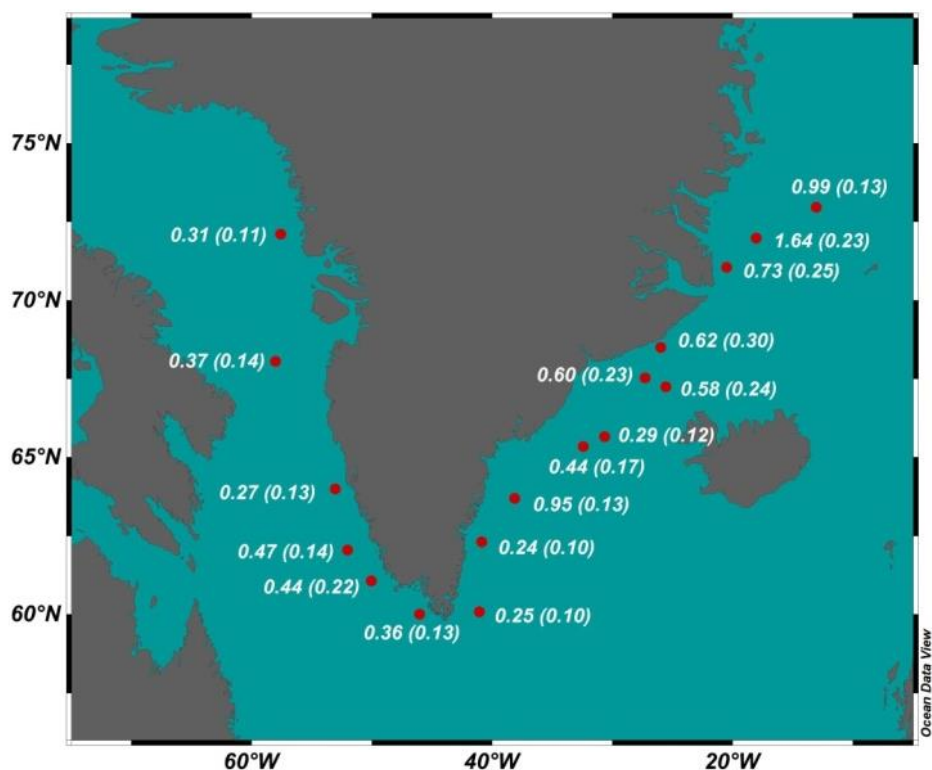


Figure 3.12 Distributions on the molecular ratios of iodide to iodate for ^{129}I and ^{127}I (parenthesis) in Greenland coastal surface water.

The I/IO_3^- molecular ratios north of the Denmark Strait (stations 1-6) were higher than those in the other locations (stations 7-17) by 1.6 for ^{127}I and 2 times for ^{129}I , respectively (Fig. 3.12). The I/IO_3^- ratios for ^{127}I ranged from 0.10 on the southeast Greenland to 0.30 in the east of Denmark Strait. The I/IO_3^- ratios for ^{129}I were below 0.73 in most of waters, while much higher ratios (0.95-1.64) were observed at the stations 1, 2 and 9. The lowest $^{129}I/^{129}IO_3^-$ ratio of 0.24 was found at the southeast Greenland coast and the highest ratio value of 1.64 at station 2 between Jan Mayen and East Greenland, the only location where ^{129}I was the major specie of ^{129}I . The $^{129}I/^{129}IO_3^-$ ratios were much higher than the $^{127}I/^{127}IO_3^-$ ratios by a factor of approximately 2.5 for most of the sampling locations. At the stations 1, 2 and 9, the $^{129}I/^{129}IO_3^-$ ratios were up to 7.77 times higher than the $^{127}I/^{127}IO_3^-$ ratios. Considering all the samples, there was no significant correlation between $^{127}I/^{127}IO_3^-$ and $^{129}I/^{129}IO_3^-$. However, if the three abnormally high I/IO_3^- ratios were excluded (stations 1, 2 and 9), $^{129}I/^{129}IO_3^-$ was significantly positively correlated with $^{127}I/^{127}IO_3^-$ with a correlation efficient of 0.9 (Fig. 3.13).

Distribution of dissolved inorganic iodine species has been reported globally. The variation of iodide to iodate ratios ($^{127}I/^{127}IO_3^-$) of surface waters exhibits a maximum in the tropical and subtropical area, and a decline trend towards the Polar Regions ([50] and references therein). Compared to the southeast and west Greenland with a mean $^{127}I/^{127}IO_3^-$ ratios of 0.14, the northeast Greenland water can be characterized by low $^{127}IO_3^-$ and high ^{127}I concentrations with an average $^{127}I/^{127}IO_3^-$ ratio of 0.23. As stated in the section 3.2.1.1 and in Paper III, the $^{127}I/^{127}IO_3^-$ ratios in the central Arctic varied from 0.20 to 0.57 in the sub-surface waters (10-25 m), which was close to those in the northeast Greenland waters but apparently higher than the other Greenland waters. The elevated ^{127}I concentrations in the surface water of northeast Greenland likely imply the influence of the Polar water with high $^{127}I/^{127}IO_3^-$ ratios. A value of 0.09 for $^{127}I/^{127}IO_3^-$ ratio has been reported by Waite et al. (2006) at an adjacent area (northwest of Iceland) [172], which was 2.5-fold lower than the value in the northeast Greenland but close to those in the southeast and west of Greenland waters. Therefore, ^{127}I species clearly show that the northeast Greenland coastal water mainly origins from the polar water, while the water in southeast and west of the Greenland is the mixed water masses between the polar water and the northern Atlantic water.

On the pathway that ^{129}I was transported from the source points to the Greenland sea, Hou et al. (2007) and He et al. (2013) reported $^{129}I/^{129}IO_3^-$ ratios of 0.10-0.50 and 0.15-2.01 for ^{127}I and ^{129}I respectively in the North Sea, northeast Atlantic Ocean [17, 50]. The I/IO_3^- ratios observed in the Greenland coast, 0.10-0.30 for ^{127}I and 0.24-1.64 for ^{129}I , fell within

the range. However, distinct from ^{127}I species distribution, the $^{129}\text{I}/^{129}\text{IO}_3^-$ ratios of 0.95-1.64 at stations 1, 2 and 9 in the northeast Greenland were markedly higher than the other locations with ratio of 0.24-0.73. This might be attributed to the coastal water with high $^{129}\text{I}/^{129}\text{IO}_3^-$ ratios flowing away from the shore. In consideration of iodine species in the source water, i.e. the Arctic water (see section 3.2.1.1 and Paper III) and the northern Atlantic Ocean [50], no $^{129}\text{I}/^{129}\text{IO}_3^-$ ratios exceed 0.8. This implies the significant fraction of iodide at these stations was produced locally, likely related to contribution of the fresh water from the melting ice during summer time.

The speciation of ^{129}I and ^{127}I off the Greenland seems to support our conjecture that the EGC transports beneath the NIC in the southeast Greenland shelf, and ascends to the surface as the WGC in the southwest Greenland. The low I/IO_3^- ratios for both ^{129}I and ^{127}I at the stations 7, 10 and 11 reflect the surface water originates from the Irminger Sea, while slightly higher I/IO_3^- ratios for both ^{129}I and ^{127}I at stations 12-15 reflect the of the underneath EGC upwelling to the surface layer on the shelf of the southwest Greenland. This speculation is supported by model simulation [173], which has predicted upwelling occurs west of the shelf banks, caused by wind and tidal motions. As mentioned above, further depth profiles of ^{129}I and other hydrological data is favorable for further investigation of the transportation of water current off Greenland.

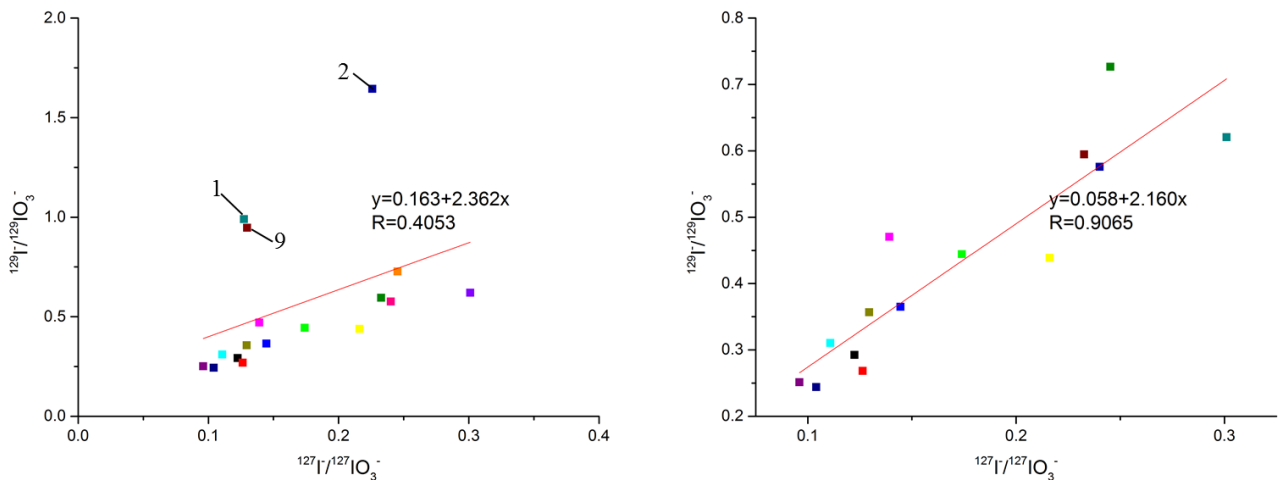


Figure 3.13 Relationship of $^{127}\text{I}/^{127}\text{IO}_3^-$ with $^{129}\text{I}/^{129}\text{IO}_3^-$ in the Greenland coast current. The left was plotted for the sewer samples from all the stations, and the right one was plotted without samples from stations 1, 2 and 9.

Transfer factor of ^{129}I and its species. Transit time and transfer factor are used to evaluate the transportation of ^{129}I from its source points to a given sampling location [122]. Amount of ^{129}I discharged from Sellafield and La Hague to marine environment

has been well documented and used for calculation of the transfer factor from these two point sources to Greenland coast.

If assuming:

- 1) The I/IO_3^- ratio is 0.60 in the original marine discharge waste based on speciation analysis of ^{129}I in the English Channel [17] and this ratio didn't change significantly with time.
- 2) Organic iodine is not considered due to its low content in open sea.
- 3) The transit time has been estimated to be 7-10 years and 9-14 years using ^{137}Cs , ^{99}Tc and ^{129}I in time series seawater and seaweed from La Hague to east and west of Greenland, respectively and two years delay from Sellafield to the Greenland coast [122, 165, 166, 174].

With the ^{129}I amount discharged from the nuclear reprocessing plants and transit time of water from source point to the sampling sites, transfer factor can be calculated as a quotient between observed concentration in water ($ng \cdot m^{-3}$) at the given sampling site and an annual discharge rate ($ton \cdot yr^{-1}$) t years earlier [122]. The results are listed in Table 3.3. The transfer factors varies from 0.63 to $1.45 ng m^{-3} (ton yr^{-1})^{-1}$, which agrees well with $1.2 ng m^{-3} (ton yr^{-1})^{-1}$ calculated by ^{129}I in seaweed in 1997 from reprocessing plant to the northwest Greenland [122]. The transfer factor on the northwest Greenland coast ($0.63 ng \cdot m^{-3} (ton \cdot yr^{-1})^{-1}$) is lower by a factor of 2 than that value reported by Hou et al. (2000). This might be explained that 1) The ^{129}I concentrations in seawater might be overestimated about 20% due to the overestimation of ^{127}I concentration of $60 \mu g L^{-1}$ in seawater ($51 \mu g L^{-1}$ measured in this work), and that 2) annual variation of water current may also contribute the uncertainty.

It is noticeable that transfer factors of iodide are slightly lower than total ^{129}I , while iodate are significantly higher than total ^{129}I and iodide. This probably implies that iodide was oxidized to iodate during transportation. It has been suggested that oxidation of iodide in open sea/ocean is a very tardy process. On time scale of years, the oxidation of iodide to iodate seems visible, which was also reported in previous studies [50].

Table 3.3 The transfer factor of ^{129}I and its species.

Greenland	Transit time, years		Discharge amount, kg			Transfer factor of ^{129}I , $\text{ng}\cdot\text{m}^{-3} (\text{ton}\cdot\text{yr}^{-1})^{-1}$					
	La Hague	Sellafield	Total ^{129}I	$^{129}\text{Iodide}$	$^{129}\text{Iodate}$	Total iodine		Iodide		Iodate	
						Aver	SD	Aver	SD	Aver	SD
Northeast	7	9	303.93	113.97	189.96	1.45	0.34	1.41	0.26	1.92	0.79
Southeast	8	10	326.65	122.50	204.16	0.86	0.42	0.67	0.45	1.62	0.79
Northwest	12	14	337.29	126.48	210.81	0.63	0.20	0.41	0.22	1.18	0.50
Southwest	10	12	276.36	103.64	172.73	1.23	0.18	0.84	0.07	2.28	0.43

3.2.1.3 Danish coast

Total iodine in the Danish coastal seawater. The ^{127}I concentrations in the Danish coastal seawater samples varied from $15.05 \mu\text{g L}^{-1}$ at Bornholm to $57.26 \mu\text{g L}^{-1}$ at Agger Tange, which was positively correlated with the water salinity ranging from 8.4 to 37.1 psu (Table 3.4). A descending trend of the ^{129}I concentrations were observed from 34.94×10^{10} atoms L^{-1} at Agger Tange to 0.55×10^{10} atoms L^{-1} at Bornholm, and the $^{129}\text{I}/^{127}\text{I}$ ratios decreased from 128.72×10^{-8} to 7.74×10^{-8} . About 6000 kg ^{129}I has been discharged from La Hague and Sellafield to the English Channel and the Irish Sea, respectively, which was carried by water current and transported northward along the western coast of European continent. The decrease of the ^{129}I concentrations in the Danish coastal areas apparently reflects the source-dependent ^{129}I signal from the North Sea to the Baltic Sea across the Skagerrak and Kattegat and via the Great belt and the Sound (Fig. 2.1b). However, lower concentrations of ^{129}I and ^{127}I were found at Hvid Sande than those at the downstream location Agger Tange. It is suggested that the collected seawater in Hvid Sande is the outflow water from the Ringkøbing Fjord, where water exchange might frequently happen between the North Sea and the fjord. This conjecture was confirmed by the much lower salinity (14.1‰) than that (37.1 ‰) found at Agger Tange.

It has been reported that the ^{129}I concentrations in seawaters collected in 2000 were observed to be 19.9×10^{10} atoms L^{-1} at Agger Tange, 3.11×10^{10} atoms L^{-1} at Klint and 0.28×10^{10} atoms L^{-1} at Bornholm [175]. Our results suggest that the ^{129}I level in the Danish coasts in 2014 has an overall increase by a factor of 1.5-2.0 compared to those 14 years ago. This temporal variation in ^{129}I concentrations might be ascribed to 1) the magnitude of water mixing between terrestrial runoff water and the water in the North Sea and Baltic Sea was different for the two sampling periods; 2) the amount of ^{129}I discharged from the NRPs has increased. However, the former explanation is unlikely due to the overall elevation in ^{129}I concentrations for the three sampling sites. Considering the transit time of 2 years from La Hague and 4 years from Sellafield to Danish coast [122], the ^{129}I concentrations in the Danish coastal seawater in 2000 reflect the amount of ^{129}I discharged in 1998, when the two nuclear reprocessing plants (NRPs) discharged about 360 kg of ^{129}I to the marine. Therefore, the increased ^{129}I concentrations might indicate that the amount of ^{129}I discharged from the major European NRPs has likely further enhanced in 2012 compared to 1998. However, it should be mentioned that ^{129}I as well as other radionuclides are not continuously and uniformly discharged from the reprocessing plants, and the water samples collected at a time point might only reflect the discharges at

a specific period from the reprocessing plant, not a whole year. The high ^{129}I level observed in the samples collected in 2014 might not represent the ^{129}I discharge in whole year of 2012 from La Hague and 2010 from Sellafield.

Iodine speciation in the Danish coastal seawater. Variations of iodide and iodate for both of ^{129}I and ^{127}I showed similar trends as total iodine (Fig. 3.14). The concentrations of ^{127}I species were found to be 14.26-42.10 $\mu\text{g L}^{-1}$ for $^{127}\text{I}^-$ and 2.12-15.89 $\mu\text{g L}^{-1}$ for $^{127}\text{IO}_3^-$. The ^{129}I concentrations varied from 0.55×10^{10} atoms L^{-1} to 30.29×10^{10} atoms L^{-1} , and $^{129}\text{IO}_3^-$ concentrations from 0.04×10^{10} atoms L^{-1} to 6.23×10^{10} atoms L^{-1} . The $^{129}\text{I}/^{127}\text{I}$ ratios for iodide in seawater from 8.10×10^{-8} to 151.80×10^{-8} were higher than those for iodate of $3.84\text{-}82.73 \times 10^{-8}$ (Table 3.4). It is apparent that in all the analyzed seawater samples, iodide was the predominant form, and gave rise to the ratios of iodide to iodate of 2.1-10.9 for ^{127}I and 3.0-22.1 for ^{129}I (Fig. 3.15). The Γ/IO_3^- ratios for ^{129}I were about 1.7 greater than those for ^{127}I . Such iodine speciation pattern is well consistent with those found in the North Sea, where the Γ/IO_3^- ratios increase from the open sea to the coastal areas, and the Γ/IO_3^- ratios for ^{129}I were higher than those for ^{127}I [17]. The more reductive waters as characterized by the higher Γ/IO_3^- ratios were found at Hvid Sande, Roskilde Fjord and Bornholm with Γ/IO_3^- ratios of 6.7-10.9 for ^{127}I and 14.2-22.1 for ^{129}I , compared to the other three samples sites with lower Γ/IO_3^- ratios less than 3.6 for $^{127}\text{I}/^{127}\text{IO}_3^-$ and 4.9 for $^{129}\text{I}/^{129}\text{IO}_3^-$. These results show that the seawater in the Baltic Sea and the fjord areas is more iodine-reductive than the Skagerrak, Kattegat and the North Sea, as observed in the earlier studies [17, 51, 52]. In addition, the different ratios of Γ/IO_3^- for ^{129}I and ^{127}I also reflected that the equilibrium between ^{129}I and ^{127}I has not been reached.

As stated in section 2.1, the formation of iodide results from many biological mediated and abiotic processes, such as biological activities of algae and bacteria, decomposition of organic matter associated iodine, chemical reactions with reductants in anoxic waters, etc. In the six Danish coastal locations, the highest Γ/IO_3^- for both iodine isotopes was observed at the Roskilde Fjord, and similar high ratio at Hvid Sande (Ringkøbing Fjord) (Fig. 3.15), which is likely dominated by the degradation of iodine-containing organic matter (organic molecular expressed as CHONI), such as debris of dead organisms, by a reaction in the following equation [86].



The two fjords are relatively shallow with depth of 2-5 m in most places, which forms a favorable condition for reduction of iodate at the water-sediment interface to release iodide as a predominant proportion in these waters.

At the Bornholm coast where the surface water originates from the Baltic Sea mainly constituting of fresh water runoff and precipitation, the higher I^-/IO_3^- ratio, might be dominated by abiotic chemical reduction of iodide due to lack of oxygen in this area [176], and subordinately related to the decomposition of organic matter due to the depth of the Baltic Sea (55 m in average).

Biological activity of macroalgae, phytoplankton and bacteria [78, 177, 178] might be the major reason for the conversion of iodate to iodide in the other three locations (Agger Tange, Nyborg and Klint) with I^-/IO_3^- ratio of 2.1-3.2 for ^{127}I and 3.0-4.9 for ^{129}I .

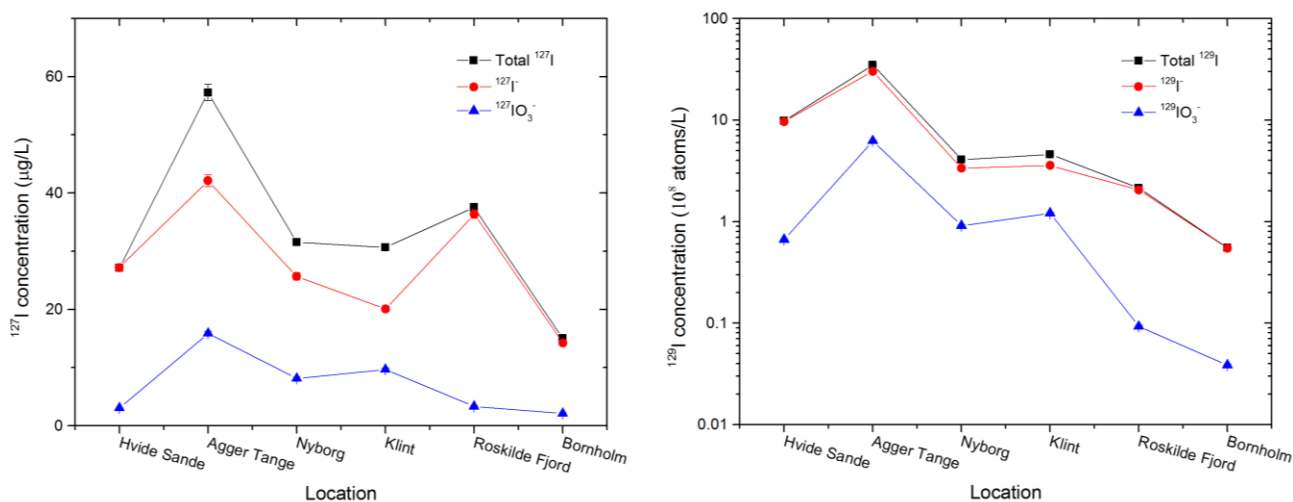


Figure 3.14 Concentrations of iodine isotopes (^{127}I and ^{129}I) and their species (iodide and iodate) in the seawater samples from the Danish coasts in 2014. The samples are ranked according to the water current from the North Sea to the Baltic Sea.

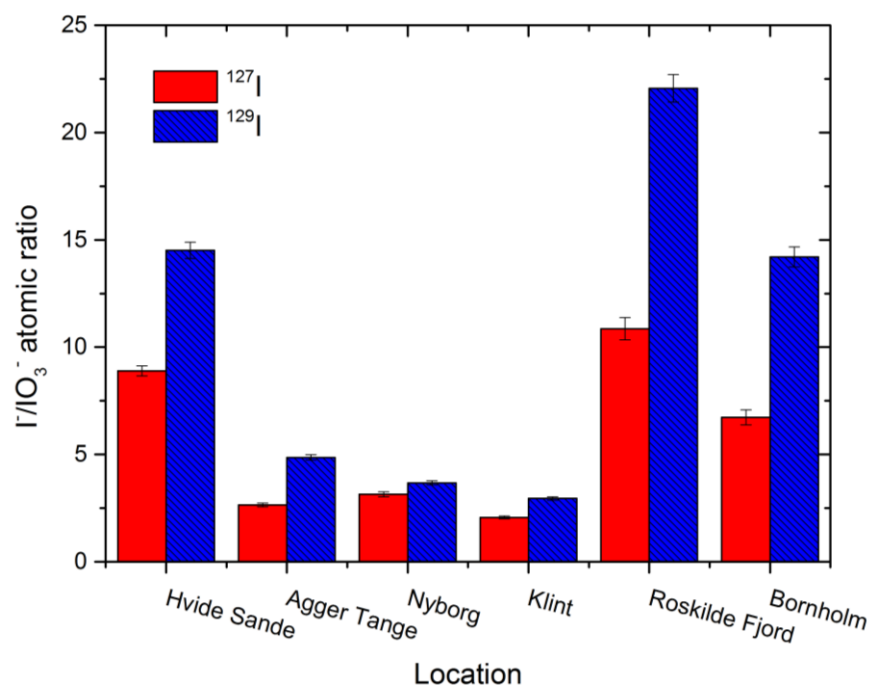


Figure 3.15 The atomic ratios of iodide and iodate for ^{127}I (blue) and ^{129}I (red) in seawater samples from six Danish coastal locations.

Table 3.4 Analytical results of ^{127}I and ^{129}I and the species in seawater and seaweed from Danish coasts during 14-27th October, 2014 ^a.

Location	Salinity , psu	^{127}I concentration, $\mu\text{g L}^{-1}$			^{129}I concentration, $\times 10^{10}$ atoms L^{-1}			$^{129}\text{I}/^{127}\text{I}$ atomic ratio, $\times 10^{-8}$				
		Total iodine	Iodide	Iodate	Total iodine	Iodide	Iodate	Total iodine	Iodide	Iodate		
Hvide Sande	14.1	27.13	± 27.18	\pm			0.67	\pm			45.91	\pm
		0.53	0.47	3.06 ± 0.06	9.81 ± 0.19	9.65 ± 0.18	0.01		76.29 ± 2.07	74.93 ± 1.91	1.27	
Agger Tange	37.1	57.26	± 42.10	± 15.89	± 34.94	± 30.29	± 6.23	± 128.72	± 151.80	± 82.73	\pm	
		1.42	1.02	0.32	0.65	0.52	0.12	4.00	4.50	2.30		
Nyborg	18.3	31.54	± 25.66	\pm			0.91	\pm			23.58	\pm
		0.53	0.63	8.15 ± 0.22	4.08 ± 0.07	3.35 ± 0.06	0.02		27.30 ± 0.68	27.54 ± 0.83	0.76	
Klint	22.5	30.65	± 20.06	\pm			1.21	\pm			26.37	\pm
		0.57	0.45	9.69 ± 0.19	4.59 ± 0.10	3.58 ± 0.07	0.03		31.60 ± 0.92	37.59 ± 1.08	0.76	
Roskilde Fjord	15.2	37.51	± 36.36	\pm			0.09	\pm				
		0.68	0.71	3.35 ± 0.15	2.14 ± 0.06	2.05 ± 0.04	0.00		12.02 ± 0.40	11.89 ± 0.31	5.85 ± 0.29	
Bornholm	8.4	15.05	± 14.26	\pm			0.04	\pm				
		0.26	0.25	2.12 ± 0.10	0.55 ± 0.01	0.55 ± 0.01	0.00		7.74 ± 0.23	8.10 ± 0.22	3.84 ± 0.21	

a. The analytical uncertainties are given in 1σ .

3.2.1.4 Offshore Fukushima

The Fukushima nuclear accident happened on 11th March 2011 and released a large amount of radioactive pollutants to the environment, especially to the local regions. In order to estimate how much ¹²⁹I has been released and evaluate the influence of ¹²⁹I to the adjacent environment, four water depth profiles from the offshore Fukushima were analyzed for measurement of total ¹²⁹I and its species (Paper IV).

Distribution and source of ¹²⁹I in the seawater offshore Fukushima. Depth profiles of ¹²⁹I concentrations in all the sampling locations showed a decline trend from the depth of 10 m to 400 m (see Figs. 1 and 2 in Paper IV). The highest ¹²⁹I concentration was observed to be 62×10^7 atoms L⁻¹ at station 31 (about 40 km away from the FDNPP), which is about 4 times greater than those ($(14-16) \times 10^7$ atoms L⁻¹) in the other three locations (11, 14 and 22 at the depth of 20 m). Low ¹²⁹I concentrations at the depth of 400 m were observed to be $(0.77-1.9) \times 10^7$ atoms L⁻¹ at the stations 14 and 11, about 260 km and 530 km away from the FDNPP, respectively. The ¹²⁷I concentrations in all the seawater samples are quite constant within a range of 54-60 µg L⁻¹. Similar to the distribution of the ¹²⁹I concentrations, the ¹²⁹I/¹²⁷I ratios varied from 22×10^{-10} at the depth of 10 m at the station 31 to 0.26×10^{-10} at the depth of 400 m format the station 14.

The measured ¹²⁹I concentrations as high as 6×10^8 atoms L⁻¹ in the seawater offshore Fukushima are much higher than the global fallout level of about 2×10^7 atoms L⁻¹ in the surface water from the Japan Sea and the Pacific Ocean before the Fukushima accident [179, 180]. However, the ¹²⁹I level in the offshore Fukushima seawater is 1-4 orders of magnitude lower than those observed in the other locations of this study (the central Arctic, the Greenland coast and the Danish coast) (Table 3.5), the latter of which have received a large amount of ¹²⁹I released from Sellafield and La Hague. This implies the Fukushima-derived ¹²⁹I only has a significant influence to the local environment and is almost negligible if compared to the European marine environment and the Arctic Ocean.

Table 3.5 ¹²⁹I concentrations and ¹²⁹I/¹²⁷I ratios in the central Arctic, Greenland and Denmark coastal areas, and offshore Fukushima.

Locations	Depth, m	Sampling date	¹²⁹ I, $\times 10^8$ atoms L ⁻¹	¹²⁹ I/ ¹²⁷ I ratios, $\times 10^{-10}$
Central Arctic	10-50	Aug-Oct, 2011	1.4-72	6-311
	199-800	Aug-Oct, 2011	2.9-29.0	10.6-106.6
Greenland coast	0	Aug-Sep, 2012	17-27	32-110
Denmark coast	0	Oct, 2014	55-3500	774-12872
Offshore Fukushima	10-20	June, 2011	1.4-6.2	5.5-22.0
	90-400	June, 2011	0.08-1.07	0.26-4.15

In combination with the well-documented ^{137}Cs radioactivity in the seawater samples and atmospheric aerosol samples, the sources of ^{129}I in the surface water from offshore Fukushima are suggested to be mainly from the direct liquid discharges from the Fukushima 1FDNPP to the sea, as well as the atmospheric deposition. Both the Fukushima-derived ^{129}I and global fallout contributed ^{129}I to the subsurface water offshore Fukushima.

Inorganic speciation of ^{129}I and ^{127}I in seawater offshore Fukushima. The investigations on species of ^{129}I and ^{127}I showed a distinct distribution pattern between iodide and iodate (See Fig. 3 in Paper IV). For all the analyzed seawater, iodate is the predominant species of ^{127}I with iodide/iodate ratios of 0.07-0.27, which is in good agreement in the surface seawater in open sea, such as the seawater from Greenland coast (0.10-0.25) and the central Arctic (0.22-0.28). In contrast, ^{129}I is predominantly present in the form of iodide with $^{129}\text{I}/^{129}\text{IO}_3^-$ ratios of 2.9-8.7. The decrease of $^{129}\text{I}/^{129}\text{IO}_3^-$ ratios at station 31 from 8.7 at the depth of 10 m to 2.3 at the depth of 120 m might indicate different water mixing processes in the investigated area.

The significant proportion of ^{129}I in the seawater pointed to a possibility that radioactive iodine released by the Fukushima accident was in the form of iodide. This finding is not only applied to distinguish the Fukushima-derived ^{129}I from other ^{129}I sources, but also essential for designing effective ways to decontaminate the radioactive materials from the environment and to prevent further resuspension of the contaminated materials.

Amount of ^{129}I discharged to the sea from the Fukushima nuclear accident. Based on the constant $^{131}\text{I}/^{137}\text{Cs}$ ratio (17.6) in the studied seawater and $^{129}\text{I}/^{131}\text{I}$ atomic ratios (26.6 ± 7.5) from the 1FDNPP, as well as the deposition proportion of Fukushima-released ^{137}Cs in the Ocean and land, ^{129}I released from the Fukushima accident was estimated to 1.2 kg (Paper IV). This released amount of ^{129}I has remarkable contribution to the Japan Sea and further to the Pacific Ocean.

3.2.2 Speciation of ^{129}I and ^{127}I in aerosols

Level and source of ^{129}I and ^{127}I in aerosols from Risø, Denmark and Tsukuba, Japan.

Two time series of aerosol samples from Risø, Denmark and Tsukuba, Japan during Fukushima accident, respectively, were analyzed for total ^{129}I and ^{127}I , as well as their species (Paper V and VI). The $^{129}\text{I}/^{127}\text{I}$ ratios in the aerosols from Denmark in the order of 10^{-7} were one order of magnitude lower than those from Japan in the order of 10^{-6} (Table 3.6) during March-May 2011.

Table 3.6 Concentrations of ^{127}I and ^{129}I and $^{129}\text{I}/^{127}\text{I}$ ratios in the aerosols from Risø, Denmark and Tsukuba, Japan.

Location	Sampling period	^{127}I , ng m^{-3}	^{129}I , $\times 10^5 \text{ atoms m}^{-3}$	$^{129}\text{I}/^{127}\text{I}$ ratios, $\times 10^{-8}$
Risø, Denmark	31 March-2 May, 2011	1.0-2.5	11-73	17.8-85.7
	8-15 December, 2014	2.4	97	86.8
Tsukuba, Japan	15-22 March, 2011	3.7-28.4	2124-5208	175-827

Considering the meteorological parameters (wind direction, wind speed and precipitation), the concentrations of ^{129}I in the aerosols from Risø were closely related to the wind direction. The westerly wind brought higher ^{129}I concentrations into the aerosols than the easterly wind. Back trajectories analysis during our sampling period indicate that the high ^{129}I concentrations in the aerosol originated from the secondary emission of the heavily contaminated seawater in the North Sea that has received a large amount of ^{129}I discharged from Sellafield and La Hague reprocessing plants since 1960s (see Figs. 2 and 3 in Paper VI).

The remarkably elevated ^{129}I level in the Tsukuba aerosols is attributed to the atmospheric release of ^{129}I from the Fukushima nuclear accident. Back trajectories analysis clearly shows that the north wind is prevailing during 15-23 March, 2011 (Fig. 3.16). The sampling site, Tsukuba, locating about 170 km southwest of the Fukushima nuclear power plant, was just right at the downwind area of the FDNPP.

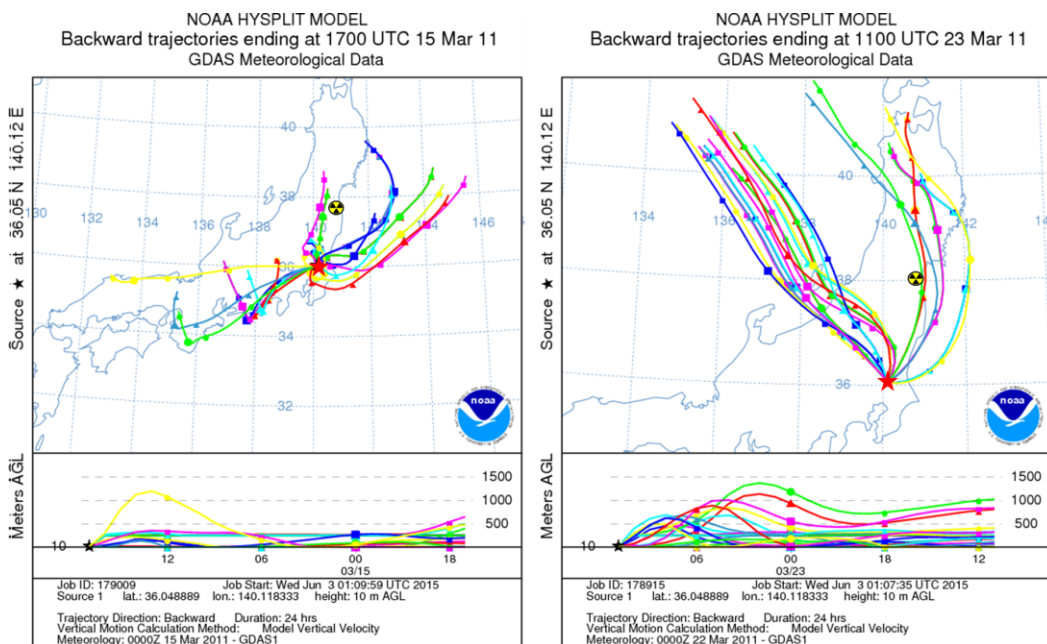


Figure 3.16 Back trajectories at Tsukuba, Japan (red star) during 15-23 March 2011, clearly showing the ^{129}I was transported from the upwind Fukushima Dai-ichi nuclear reprocessing plant (radioactivity label) to the sampling location.

Contribution of the Fukushima-derived ^{129}I to the European atmosphere. The release of radioactive substances from the Fukushima nuclear accident has elevated the ^{129}I level in the local air by two orders of magnitude compared to the pre-accident ^{129}I level [181]. In order to clarify the influence of the Fukushima accident on the ^{129}I level in Europe, time series of the ^{131}I radioactivity measured in our aerosol samples from Denmark was used to reconstruct the contribution of Fukushima-derived ^{129}I [182]. The mean $^{129}\text{I}/^{131}\text{I}$ atomic ratio in the aerosols derived from Fukushima accident was estimated to be 16.0 ± 2.2 (Paper V). Based on these data and assuming the $^{129}\text{I}/^{131}\text{I}$ ratios did not change during long-distance transportation, the concentrations of Fukushima-derived ^{129}I in aerosol in the European atmosphere was reconstructed with a highest concentration of 0.63×10^5 atoms m^{-3} during 30-31 March 2011 (Fig. 3.17). Compared to the measured concentrations of ^{129}I ($11\text{-}97 \times 10^5$ atoms m^{-3}) in the aerosols from Denmark shortly after the Fukushima nuclear accident, the amount of Fukushima-derived ^{129}I accounts for less than 6% of the total ^{129}I in Denmark. It is observed that the Fukushima-derived ^{131}I concentrations declined rapidly, which resulted in a slightly decreased ^{129}I concentration in the European atmosphere (Fig. 3.17). Although the Fukushima accident released a significant amount of ^{129}I to the local atmosphere, its contribution to European atmosphere is almost negligible and considerably overwhelming by the NRPs-derived ^{129}I .

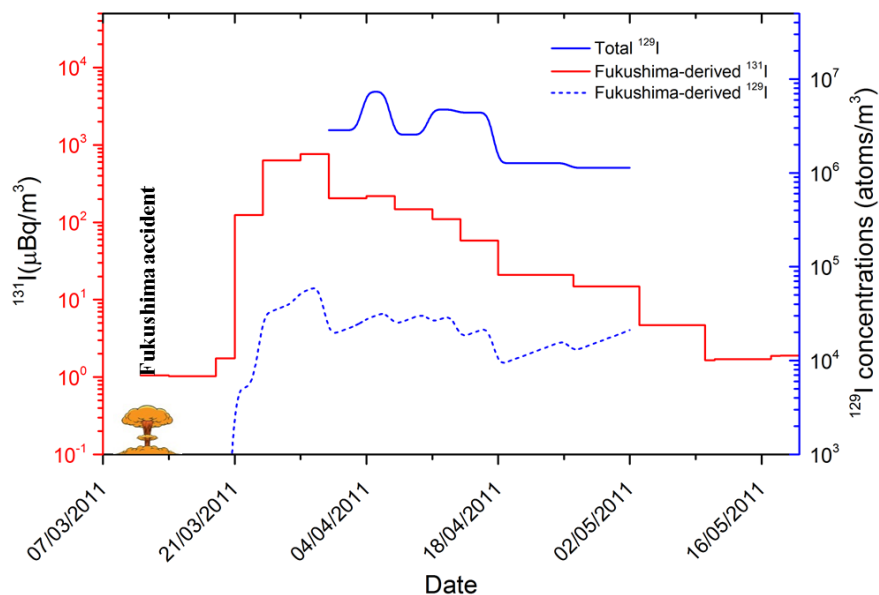


Figure 3.17 ^{131}I radioactivities (red solid line), ^{129}I concentrations (blue solid line) in the aerosols from Risø, Denmark after the Fukushima accident [182]. The Fukushima-derived ^{129}I concentrations (blue dot line) are reconstructed based on the ^{131}I radioactivities and the $^{129}\text{I}/^{131}\text{I}$ atomic ratio of 16.0 ± 2.2 deduced from the Fukushima-sourced aerosol samples [183].

Species of ^{129}I and ^{127}I in aerosols. Interestingly, the distribution patterns of iodine species for ^{129}I in the aerosols collected from the two locations were obviously different (Fig. 3.18 and Fig. 3.19). In the aerosols from Risø, Denmark, water-soluble iodine was the least abundant species accounting for 6-30%. Whereas, 42-60% of ^{129}I was water-soluble iodine in the aerosols from Tsukuba, Japan. The concentrations of the NaOH soluble iodine (NSI) in the aerosols from both the locations were essentially similar counting for 28-42% in Denmark and 32-44% in Japan. A large difference in the percentage of residual insoluble iodine (RII) was observed for two sets of aerosols.

This discrepancy in distribution of ^{129}I species in the aerosols might be attributed to the sources and initial species of ^{129}I . ^{129}I in the aerosols from Denmark mainly originates from atmospheric release of the European nuclear reprocessing plants and re-emission from the heavily contaminated seawater in the North Sea and Kattegat (Paper VI). For the aerosols from Japan, atmospheric release from the FDNPP accident was the major source of ^{129}I (Paper V). Since the aerosols in Tsukuba were collected shortly after the accident and transported a short distance (about 170 km from the FDNPP), the association processes of the Fukushima-released ^{129}I with atmospheric particles, especially in the form of water-soluble iodine specie, were different from those in Denmark. However, there is only scarce knowledge available on the initial iodine species in aerosols. Iodide is found the predominant ^{129}I in the seawater offshore Fukushima, which likely implies the Fukushima released ^{129}I might be mainly in the form of inorganic iodide (Paper IV). The initial ^{129}I species in the aerosols from Risø, Denmark might be mainly in the form of molecular iodine or iodocarbons, which is a consequence of biological activities, especially the iodine metabolism of brown seaweed in the coastal seawater [184].

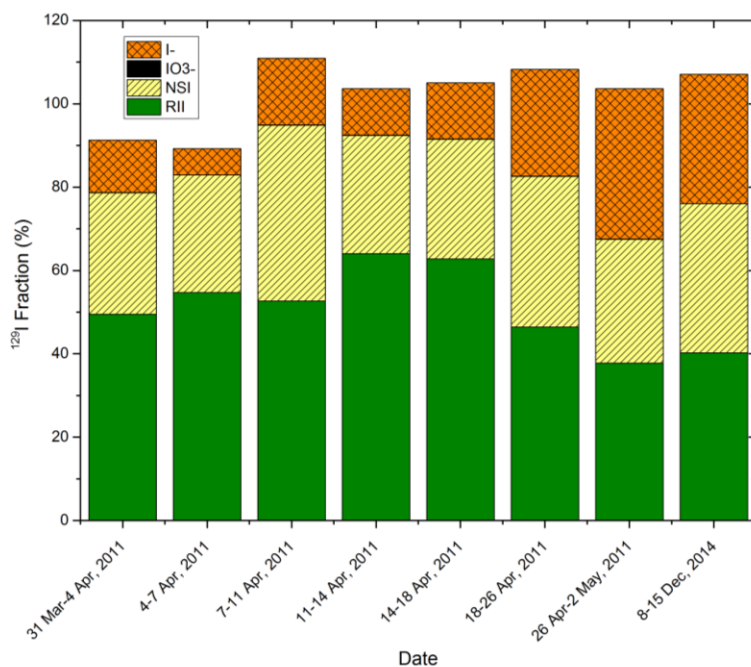


Figure 3.18 Distribution of iodine species (iodide, iodate, NSI for NaOH soluble iodine and RII for residual insoluble iodine) for ^{129}I in aerosol samples from Risø, Denmark.

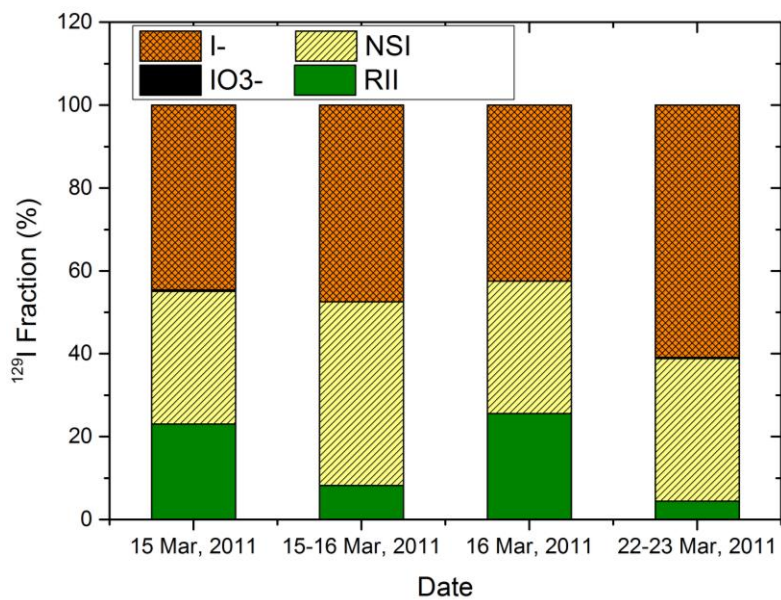


Figure 3.19 Distribution of iodine species (iodide, iodate, NSI for NaOH soluble iodine and RII for residual insoluble iodine) for ^{129}I in aerosol samples from Tsukuba, Japan.

Iodide is the predominant specie of water-soluble iodine in all the studied aerosol samples. Only less than 3% of total iodine exists as iodate and water-soluble organic iodine, which were observed in a few Danish aerosol samples. This is consistent with the ^{129}I species in the four aerosol samples collected soon after the Chernobyl accident at Oak Ridge, Tennessee, and similar to those for natural ^{127}I in the aerosol [185, 186]. However, this is contradictory with those observed in those marine aerosols that enriched in the form of iodate [187]. These results indicate that the dissolved inorganic iodine species might be closely related to the formation processes of aerosols. It is worthy to note that iodide can be found in all the aerosol samples regardless of the geographical locations. Early modelling work predicted that aerosol iodate may be a by-product of the production of higher iodine oxides and is believed to be the only stable iodine species, while iodide becomes negligible due to transformation into gaseous iodine [188, 189]. This work suggested that formation of iodide in aerosol might be related to the reductant in the air, such as SO_3 and disulfites (Paper VI).

NSI in the aerosols is likely organic bound iodine. It has been reported that a significant proportion of aerosol organic matter is humic-like substances (HULIS) [190]. It was observed that the alkaline extractable HULIS accounts for 42-74% of total HULIS in aerosols [191]. Due to the readily association of iodine with HULIS, as observed in soil and sediment [126], the large fraction of NSI is believed to be mainly HULIS bound iodine (Paper II and VI). RII might be associated with inorganic components such as metal oxides and minerals. This might explain the large difference in the RII fractions between the aerosols from Denmark and from Japan. ^{129}I in the European environment has participated in the cycling in various compartments, such as land, terrestrial rivers, and thus incorporated into the oxide and minerals in soil. Suspension of fine soil particles might contribute the insoluble iodine into atmospheric aerosols. For the aerosol from Japan, ^{129}I released from the Fukushima accident was shortly associated to aerosol, therefore might be not effectively bound with minerals.

3.2.3 Speciation of ^{129}I and ^{127}I in seaweed

To explore metabolic activity of iodine in seaweed, species of iodine isotopes in the seaweed and ambient seawater were simultaneously investigated, including iodide and iodate in seawater and water leachable iodine (iodide and iodate) and non-leachable residual iodine in seaweed samples (Table 3.4 and 3.7).

Total iodine in seaweed. Despite the same genus of *Fucus* (brown seaweed), iodine concentrations varied significantly depending on the iodine concentrations in seawater as well as species of *Fucus* (Table 3.7 and Fig. 3.20). In *Fucus vesiculosus*, the iodine concentrations ranged from $47.22 \mu\text{g g}^{-1}$ to $167.95 \mu\text{g g}^{-1}$ in fresh seaweed and $192.20\text{-}549.46 \mu\text{g g}^{-1}$ in dry mass [122], which is nearly one order of magnitude lower than that in *Laminaria digitata* (up to 1% of dry mass) [192]. The ^{129}I concentrations in the seaweed samples collected in the Danish coastal seawater were measured to be $(2.19\text{-}108.61)\times 10^{10}$ atoms g^{-1} in fresh seaweed, corresponding to $(8.90\text{-}355.32)\times 10^{10}$ atoms g^{-1} in dry mass. The $^{129}\text{I}/^{127}\text{I}$ ratios in *Fucus* were observed in a range of $(9.77\text{-}133.92)\times 10^{-8}$ (Table 3.7), which is similar to the $^{129}\text{I}/^{127}\text{I}$ ratios in seawater, proving *Fucus* an good bio-indicator to trace radioactive ^{129}I in the environment. Similar as seawater samples (section 3.2.1.3), the measured $^{129}\text{I}/^{127}\text{I}$ ratios in seaweed samples collected in 2014 increased by a factor of 1.1-2.0 compared to those collected during 1998 and 1999 with $^{129}\text{I}/^{127}\text{I}$ ratios of 4.93×10^{-8} , 9.12×10^{-8} and 37.5×10^{-8} in seaweed collected at Bornholm, Roskilde Fjord and Klint, respectively [122].

The results of ^{129}I and ^{127}I in the seaweed and seawater (Fig. 3.21) show that the $^{129}\text{I}/^{127}\text{I}$ ratios in seaweed are systematically higher than those in seawater by a factor of 1.1-1.3 except for Hvid Sande, where the largest discrepancy by a factor of 1.8 was observed in the $^{129}\text{I}/^{127}\text{I}$ ratios for seaweed and seawater. Such a difference on the $^{129}\text{I}/^{127}\text{I}$ ratios between seaweed and seawater at all the sampling sites can be attributed to their different response rates. $^{129}\text{I}/^{127}\text{I}$ ratio in seawater reflects a transient level of ^{129}I in the sampling location at the time of sampling, while $^{129}\text{I}/^{127}\text{I}$ ratio in seaweed is an integrated level of ^{129}I in a period of seaweed growth related to the metabolic cycle of seaweed. The lower ^{129}I level in seawater likely implies a decrease of ^{129}I released from La Hague and Sellafield when sampling compared to the previous period. As discussed in section 3.2.1.3, the large difference of $^{129}\text{I}/^{127}\text{I}$ ratios in seawater between Hvide Sande and Agger Tang is a consequence of fast water exchange between the North Sea and the Ringkøbing Fjord. However, no significant difference was observed in the $^{129}\text{I}/^{127}\text{I}$ ratios for seaweed from the two locations. Seaweed, therefore, is more representative to monitor long-term

variation of pollutants than seawater. Furthermore, it is promising to explore the metabolism of iodine in seaweed in the natural environment utilizing the discrepancy of $^{129}\text{I}/^{127}\text{I}$ ratios between seawater and seaweed.

Iodine speciation in seaweed. Chemical species of iodine in seaweed were separated to water leachable iodine including iodide, iodate and water-soluble organic iodine (WSOI) and non-water-leachable residual iodine (RI). Because iodide is the only detectable water-soluble iodine specie in seaweed investigated, only iodide and RI were presented in Table 3.7. The concentrations of ^{127}I species were found to be 5.11-17.48 $\mu\text{g g}^{-1}$ for iodide and 43.84-164.65 $\mu\text{g g}^{-1}$ for RI. ^{129}I was predominantly in the RI fraction with the concentrations of 1.96-112.69 $\times 10^{10}$ atoms g^{-1} . The $^{129}\text{I}/^{127}\text{I}$ ratios for iodide and RI in seaweed were not statistically distinct from the total $^{129}\text{I}/^{127}\text{I}$ ratios, which might imply an isotopic equilibrium of iodine in all components of seaweed (Table 3.7). This might also suggested a rapid exchange and metabolic process of iodine in seaweed.

Iodide in *Fucus serratus* accounted for 7.2-16.1% for ^{127}I and 6.8-14.0% for ^{129}I . While *Fucus vesiculosus* collected from Klint showed a higher fraction of water-soluble iodide of 22.7% for ^{127}I and 19.7% for ^{129}I compared to that of *Fucus serratus* collected at other locations (Fig. 3.22). It has been reported that the water leaching rates of iodine in different seaweed vary considerably from 9 % in red algae up to 99% in *Laminaria japonica* (brown seaweed) [71].

Table 3.7 Analytical results of ^{127}I and ^{129}I and their species in seaweed from the Danish coasts during 14-27th October, 2014 ^a.

Location	^{127}I concentration, $\mu\text{g g}^{-1}$ ^b				^{129}I concentration, $\times 10^{10}$ atoms g^{-1}				$^{129}\text{I}/^{127}\text{I}$ atomic ratio, $\times 10^{-8}$		
	Total iodine	Iodide	Residual iodine	I/T	Total iodine	Iodide	Residual iodine	I/T	Total iodine	Iodide	Residual iodine
Hvide Sande	121.05 \pm 6.19	8.72 \pm 0.09	110.03 \pm 5.64	7.2%	76.84 \pm 1.03	5.23 \pm 0.31	65.57 \pm 1.91	6.8%	133.92 \pm 7.08	126.57 \pm 7.54	125.71 \pm 7.42
Agger Tange	167.95 \pm 8.60	17.48 \pm 0.19	164.65 \pm 8.46	10.4%	108.61 \pm 1.46	10.92 \pm 0.62	112.69 \pm 3.15	10.1%	136.43 \pm 7.22	131.78 \pm 7.57	144.39 \pm 8.45
Nyborg	93.91 \pm 4.79	8.21 \pm 0.10	91.23 \pm 4.67	8.7%	14.77 \pm 0.24	1.08 \pm 0.06	15.34 \pm 0.42	7.3%	33.19 \pm 1.78	27.75 \pm 1.60	35.48 \pm 2.06
Klint	64.87 \pm 3.34	13.96 \pm 0.16	53.59 \pm 2.74	21.5%	12.49 \pm 0.20	2.41 \pm 0.14	9.71 \pm 0.30	19.3%	40.63 \pm 2.19	36.34 \pm 2.18	38.23 \pm 2.29
Roskilde Fjord	107.76 \pm 5.52	17.33 \pm 0.18	99.31 \pm 5.08	16.1%	7.07 \pm 0.12	0.99 \pm 0.06	6.08 \pm 0.16	14.0%	13.85 \pm 0.75	12.09 \pm 0.71	12.92 \pm 0.74
Bornholm	47.22 \pm 2.42	5.11 \pm 0.06	43.84 \pm 2.24	10.8%	2.19 \pm 0.06	0.20 \pm 0.02	1.96 \pm 0.08	8.9%	9.77 \pm 0.57	8.06 \pm 0.63	9.43 \pm 0.63

a. The concentrations of iodine are reported in fresh seaweed.

b. Only iodide species in seaweed was presented because it is the only detectable iodine species in water leachate and iodate and soluble organic iodine in water extract of seaweed were not detectable.

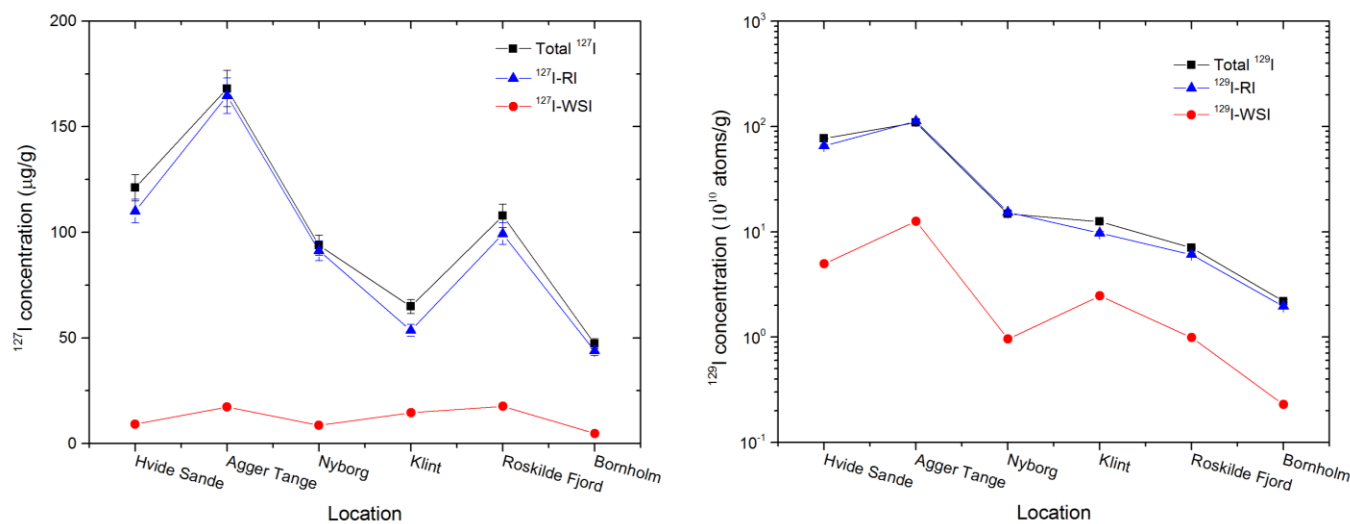


Figure 3.20 Concentrations of iodine isotopes (^{127}I and ^{129}I) and the species (water-soluble iodine, i.e. iodide and residual iodine) in *Fucus serratus* and *vesiculosus* from the Danish coasts in 2014.

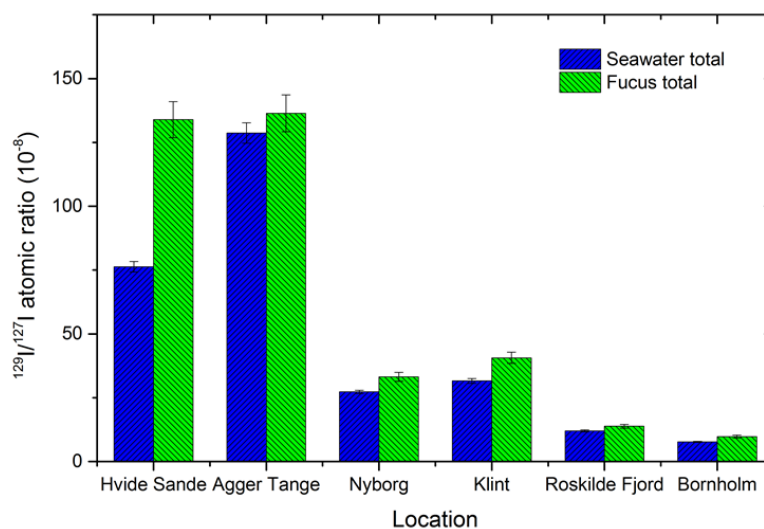


Figure 3.21 $^{129}\text{I}/^{127}\text{I}$ ratios in seawater and seaweed simultaneously collected from the Danish coast in October 2014.

The fact that only iodide was observed in the water leachate of *Fucus serratus* and *vesiculosus* for both ^{129}I and ^{127}I , agree well with the previous reports on chemical species of iodine in seaweed [72, 75, 193-195]. Utilizing sequential extraction coupled to neutron activation analysis, HPLC-ICP-MS, and X-ray absorption spectroscopy (XAS), it was observed that iodide ion is present as the predominant water-soluble inorganic iodine in various seaweed, especially in *Laminaria japonica*, *Kombu*, and *Wakame* [193, 194]. Hou et al. (1997 and 2000) has analyzed ten seaweed species for iodide, iodate and WSOI and suggested less than 5% of water-soluble iodine occurs as iodate, while the distribution of iodide and WSOI were seaweed species-dependent [72, 193]. For *Laminaria digitata*, iodide is the only dominant species of iodine [195]. Although WSOI in forms of 3-iodo-tyrosine (MIT) and 3,5-diiodo-tyrosine (DIT) have been detected by HPLC-ICP-MS, it only accounts for less than 0.5% of total iodine [75]. The result in this work in combination with the previous studies shows that iodide might be ubiquitously present in seaweed and play an important biological role for seaweed, such as acting as an anti-oxidant against oxidative stress (e.g. O_3 , H_2O_2) [195].

More than 80% of iodine in seaweed investigated in this work is non-water-leachable, likely reflecting the associated forms of iodine with biomacromolecules in seaweed. A variety of iodinated compounds have been found in brown seaweed, such as MIT, DIT, phenolics (phloroglucinol, phlorethol, fucol, Fucophlorethol, fuhadol and eckol), fatty acid, terpenes and polysaccharides [70, 72]. With exception of water leachable iodine, most of organic iodine in seaweed (65.5%) were observed to associate with high molecular weight organic matter that participate in metabolism of brown seaweed, especially protein in

Sargassum kjellaniumum [72]. However, the information on biomolecules bound iodine in seaweed is so rare that its biological role is not clear so far.

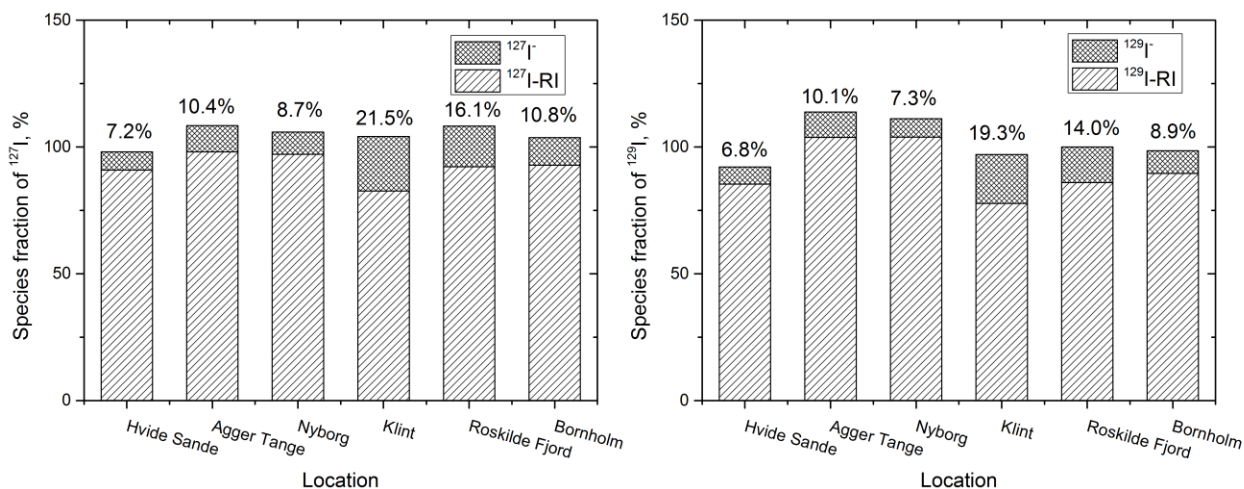


Figure 3.22 Distribution of iodine species (water-soluble iodine and residual iodine) in seaweed for ¹²⁷I (left) and ¹²⁹I (right). Numbers are the percentage of water-soluble iodine in total iodine.

Uptake of ¹²⁹I and ¹²⁷I by brown seaweed from seawater. The degree of element accumulation in organism is generally expressed as concentration factor (CF) that defined as a ratio between concentration per unit mass of organism (wet mass) and concentration per unit mass of sea water (IAEA, 2004). Excluding the two samples from Hvid Sande and Klint because of the influence of fast water exchange between seawater and fjord outflow water and different seaweed species, the average concentration factors (CFs) of iodine in *Fucus serratus* are estimated from the measured values in other locations to be 2955 for ¹²⁷I and 3500 for ¹²⁹I in fresh seaweed (Table 3.8). Lower CFs in *Fucus vesiculosus* were found to be 2116 and 2721 for ¹²⁷I and ¹²⁹I, respectively, indicating that enrichment abilities to iodine vary among seaweed species. The reported CFs of iodine are 1484 L kg⁻¹ in *Fucus vesiculosus* and 2226-3361 L kg⁻¹ in *Fucus serratus* on wet matter basis [196], which are comparable with the values measured in this work. The greater uncertainty is attributed that the seawater iodine concentrations in the literatures was not real measured values, instead an assumed constant value of 60 µg L⁻¹ was used for estimation of concentration factor.

As stated above, the discrepancy of CFs between the two isotopes is attributed to the relatively lagging response of seaweed to the change of ¹²⁹I/¹²⁷I ratios in seawater. Seaweed reflects an integrated iodine level in a period before sampling related to the metabolism cycle of seaweed. However, ¹²⁹I/¹²⁷I ratios in seawater is rapidly variable due

to the different sources of ^{129}I and stable ^{127}I and water masses mixing especially in the coastal areas.

Table 3.8 Concentration factors of ^{129}I and ^{127}I in *Fucus serratus* and *versiculosus*.

Location	Specie	CF- ^{127}I , L kg $^{-1}$	CF- ^{129}I , L kg $^{-1}$
Hvide Sande	<i>Fucus serratus</i>	4462 ± 244	7832 ± 182
Agger Tange	<i>Fucus serratus</i>	2933 ± 166	3108 ± 71
Nyborg	<i>Fucus serratus</i>	2977 ± 160	3620 ± 87
Klint	<i>Fucus versiculosus</i>	2116 ± 115	2721 ± 75
Roskilde Fjord	<i>Fucus serratus</i>	2873 ± 156	3308 ± 107
Bornholm	<i>Fucus serratus</i>	3138 ± 169	3963 ± 148

For the four sampling locations, where no fast water exchange and the same seaweed species, the concentrations of ^{127}I and ^{129}I in the seaweed are highly positively correlated to the total concentrations of ^{127}I and ^{129}I in the seawater. Moreover, similar positive correlations were also observed between the total iodine in seaweed and the concentrations iodate and iodide in seawater (Fig. 3.23a and b). The concentration factors of both ^{129}I and ^{127}I in the seaweed were found to be unchanged with the I^-/IO_3^- ratios of 2-22 in seawater (Fig. 3.23c). These results suggest that iodine enrichment ability of seaweed is strongly dependent on seaweed species, not influenced by the iodine concentration and iodine species in the seawater.

The positive correlations between iodine species (iodide and iodate) in seawater and total iodine concentrations in seaweed for both iodine isotopes are slightly lower but still significant. The results indicate that both iodide and iodate might be assimilated by the *Fucus* species investigated in this work. The mechanism of iodine enrichment in seaweed has continuously attracted interest of researchers in the past decades, in which selection of the iodine species by seaweed for uptaking is one of the key issue, but still remain ambiguous. Laboratory incubation experiments of seaweed slurry or tissue disc traced by radioiodine, such as ^{125}I and ^{131}I suggested that only iodide can be taken up by a brown alga (*Ascophyllum nodosum*) [197-200]. This proposal has been widely accepted and used for establishing mechanism model of iodine in seaweed [199, 201]. However, the investigation in the past decades continuously questioned this statement, and some contrary results have showed that iodate can be also assimilated in the seaweed by intact or culturing living macroalgae (*Hizikia fusiforme*, *Sargassum sagamianum* and *Chondrus ocellatus*), although a lower concentration factor compared to that for iodide was measured [177, 202]. Our investigation in the natural marine environment provides indirect evidence that seaweed (*Fucus serratus* and *versiculosus*) can assimilate both iodide and iodate from seawater. Because the iodide-dominant seawater from the only four sampling locations

could not represent the ordinary marine environment, where iodate is the dominant specie of iodine, further investigations on extensive sampling areas are needed to confirm our observation.

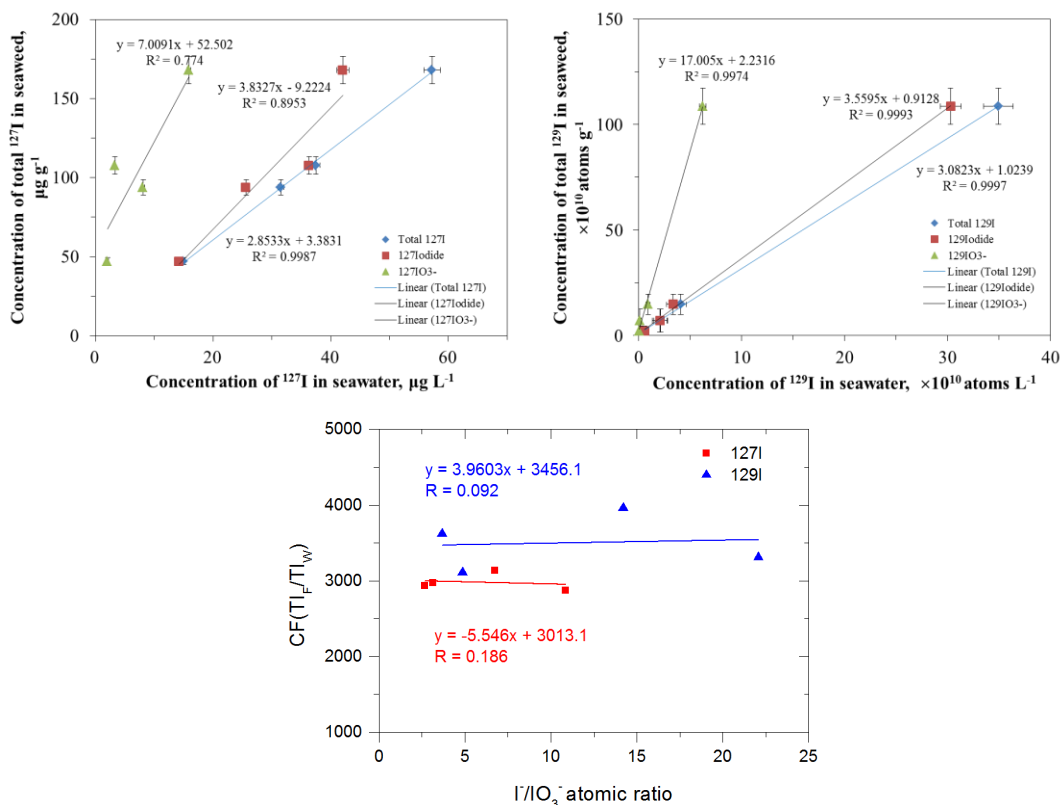


Figure 3.23 Plots of total iodine concentrations in *Fucus serratus* against the concentrations of total iodine and iodine species in seawater for ^{127}I (a) and ^{129}I (b) from the four sampling sites excluding Hvid Sande and Klint (blue dash line) because of fast water exchange between the North Sea and the Rindstedt fjorde and different seaweed specie (*Fucus vesiculosus*). Plot of iodine species in seawater against the concentrations factors of seaweed (c).

Transformation of iodine species and iodine metabolism in seaweed. To explore the metabolism mode of iodine in seaweed, a concept of iodine species related concentration factor (SCF) is introduced and defined as:

$$\text{SCF} = \frac{\text{Concentration of iodine species in } Fucus \text{ (atoms } kg^{-1} \text{ or } mg \text{ } kg^{-1})}{\text{Concentration of total iodine in seawater (atoms } L^{-1} \text{ or } mg \text{ } L^{-1})} \quad \text{Equation (4)}$$

SCFs in *Fucus serratus* collected at the four locations were calculated (Fig. 3.23). It is interesting that the SCFs vary with the I^-/IO_3^- ratios in seawater (Fig. 3.24). The SCFs of labile inorganic form, i.e. iodide, showed a strongly positive correlation with the I^-/IO_3^- ratios in seawater ($r > 0.90$), while a negative correlation of SCFs of water non-leachable iodine in seaweed with the I^-/IO_3^- in seawater were observed. These results in combination with the relatively constant the $^{129}\text{I}/^{127}\text{I}$ ratios among all iodine species in seaweed suggest

that iodine species in seaweed may interconvert, and the response of different iodine species in seaweed to the variation of iodine species in the seawater is different. The water-soluble iodide shows a relatively rapid and direct response to the iodine in seawater. The increased SCFs of iodide in seaweed with the increased Γ/IO_3^- ratios in seawater is likely attributed that water non-leachable iodine in seaweed, presumably in the form of biomacromolecular associated iodine (e.g. protein) [71, 202] is deiodinated and release iodine in the form of iodide under the investigated ambient seawater condition [72, 203]. This might shed a light on the investigation on mechanism of iodine uptake from seawater and accumulation in the cells of seaweed

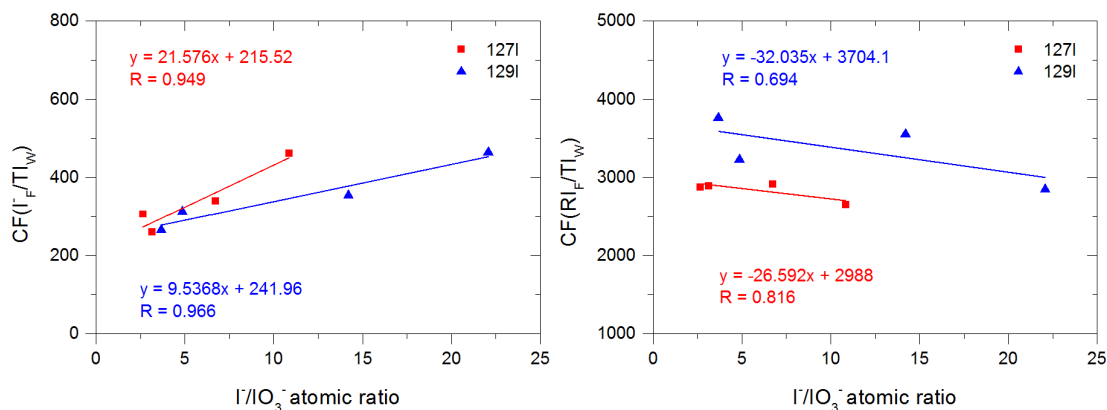


Figure 3.24 Speciation concentrations factors of seaweed iodide to seawater total iodine (Γ_F/TI_W) and seaweed insoluble residual iodine to seawater total iodine (RI_F/TI_W) as functions with iodine species in seawater expressed as ratio of iodide to iodate for ^{127}I (in red) and ^{129}I (in blue).

Over 80% of iodine in *Fucus serratus* and *vesiculosus* exists as water insoluble iodine considered to be bound with biomacromolecular, which is apparently distinct from that reported in *Laminaria digitata* in which most of iodine exists as water-soluble iodide [195]. The proposed mechanism of iodine uptake in *Laminaria digitata* [199, 201] might be therefore not suitable for other genus of brown seaweed. Based on the results in this work, a possible iodine metabolism process is speculated for *Fucus* (Fig. 3.25). Iodide that transferred into seaweed through cell wall might be either accumulated directly or oxidized to I_2 or HIO , which act as intermediates in the specie transformation. Iodate uptake might be related to the reaction with iodide to form intermediates that participate in the subsequent cycling of iodine in seaweed, which need more intensive research works. To the ambient seawater, iodide is released, while molecular iodine is formed under oxidation stress such as ozone and hydrogen peroxide and released to the marine boundary layer [44]. The formation of volatile iodocarbons might be a consequence of breakdown products of biomolecule associated iodine such as carbohydrates, polyphenols and proteins.

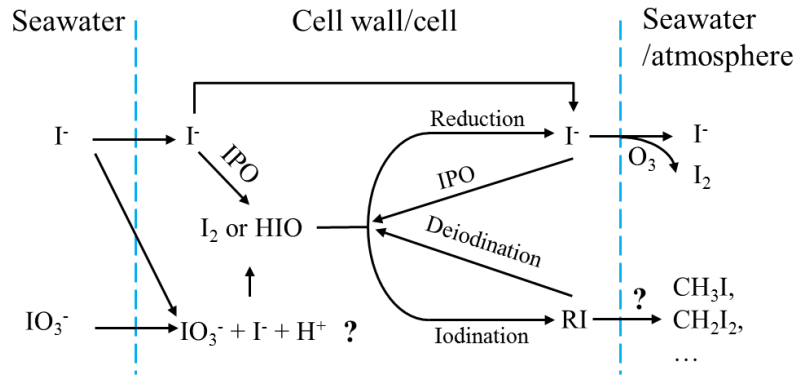


Figure 3.25 A proposed mechanism of iodine uptake and transformation in *Fucus*. RI is water non-leachable residual iodine species presumably as biomolecule associated forms. IPO is iodoperoxidase.

4. Conclusions and perspectives

4.1 Conclusions

Based on the overall work presented in this thesis, the following conclusions on methodology development for speciation analysis of ^{129}I in environmental samples, and environment tracing applications of ^{129}I species in the marine environment and atmosphere can be drawn out.

1. Pretreatment of water samples or leachates of solid sample by the addition of $\text{K}_2\text{S}_2\text{O}_8$ to a final concentration of 30 mg g^{-1} under heating at 60°C overnight can significantly decompose organic iodine (>97.7% of chemical yield) and convert it to inorganic forms. The formation of active oxidant persulfate radical (HSO_4^\cdot) by $\text{K}_2\text{S}_2\text{O}_8$ degradation might play a key function on decomposition of organic iodine.
2. A method for speciation analysis of ^{129}I and ^{127}I in aerosol samples has been established, allowing to quantitatively determine water-soluble iodine (iodide, iodate), NaOH soluble and residual insoluble iodine. The detection limits are 0.007 ng m^{-3} for ^{127}I and 7.1×10^6 atoms (1.5 fg) for ^{129}I . Stability of iodine species during analysis is related to the matrix materials of the aerosol filter. Due to photochemical oxidation of iodide on polypropylene filter, transformation of inorganic iodine species occurs when extending water leaching time. Alkaline ashing with addition of $\text{K}_2\text{S}_2\text{O}_5$ as iodine-protected reagent can significantly reduce the loss of iodine in the ashing step, providing a reliable method for determination of total ^{129}I in aerosol samples, especially a large size of aerosol collected on organic filter materials. For aerosol collected on quartz and glass fiber filter, iodine can be effectively separated by combustion method with high chemical yield (96%).
3. The depth profiles of chemical species of ^{129}I and ^{127}I in the central Arctic provides a potent tool to understand the water circulation and marine iodine recycle. 1) In the polar mixed layer, only a small fraction of the ^{129}I -rich Atlantic water moved to the North Pole along the Eurasian side of the Lomonosov Ridge, but significant fraction of this water current flows into the Makarov Basin. 2) The sharp stratification of ^{129}I concentrations in the depth profiles indicates very limited vertical exchange between the PML and AWL. 3) Reduction of iodate in the polar mixed layer over the ridges and basin margins was significant, which might be related to the relatively high nutrients and active biological activities resulting from influx of the Atlantic water current. 4) Speciation analysis of ^{129}I and ^{127}I in the depth profile seawater confirms that oxidation of iodide back to iodate can occur with conversion rate of about $2 \text{ nmol L}^{-1} \text{ year}^{-1}$ in the Atlantic water layer of the central Arctic. 5) The inventory of ^{129}I in the upper 800 m of the central Arctic is estimated to be 1457 kg by 2011, in which 68% of ^{129}I is in the

Eurasian Basin. Such high amount of ^{129}I implies the central Arctic acts as a secondary source of ^{129}I to the downstream seas and the Arctic atmosphere.

4. The distribution of ^{129}I in the east Greenland seawater show higher ^{129}I level on the north of Denmark Strait and lower level on the southeast, suggesting the East Greenland current originating from the central Arctic transports southwards and mixed with the ^{129}I -poor Irminger current water in the southeast. The ^{129}I concentrations in the west Greenland coast water showed a northwards decreased trend, implying the West Greenland Current is the dominant source of ^{129}I in this water. Iodate was the predominant form in the Greenland waters for both ^{129}I and ^{127}I , and higher ratios of iodide to iodate were observed in northeast Greenland water compared to the southeast and west Greenland waters, which might be attributed to the outflow of the Greenland coastal seawater.
5. The ^{129}I concentrations in the Danish coastal waters in 2014 was elevated by a factor of 1.5-2 compared to those in late 2000s, which implies the amount of ^{129}I discharged from the two European NRPs might be increased around 2012 in comparison to the release during later 2000s. Iodide is the predominant specie for ^{129}I and ^{127}I in these coastal waters, which is consistent with the previous investigations. The formation of iodide in the investigated locations is dominated by different processes, such as degradation of iodine-rich organic matter for the Roskilde Fjord and Hvid Sande, abiotic chemical reduction of iodate for Bornholm, and biological activities for the other three sampling locations.
6. Direct liquid discharge and atmospheric deposition from the FDNPP accident elevated the ^{129}I concentrations up to 6×10^8 atoms L^{-1} in the near-surface water in offshore Fukushima. The total amount of ^{129}I released to sea was estimated to 1.2 kg. Despite much lower than the enormously discharged ^{129}I from the European NRPs, this amount of ^{129}I can remarkably influence the level of ^{129}I in the Pacific Ocean, and thus can be applied to trace the Pacific Ocean currents. ^{129}I in the Fukushima offshore seawater dominantly present as iodide, is completely distinct from ^{127}I species that mainly exists in the form of iodate. This implies the main form of iodine in the liquid waste of FDNPP as well as the atmospheric fallout from the accident might be mainly iodide, which is important for studying the pollution and transferring behavior of radioiodine after the nuclear accident.
7. The $^{129}\text{I}/^{127}\text{I}$ ratios in the aerosol samples collected in Tsukuba, Japan (170 km southwest to the FDNPP) immediately after the Fukushima accident increased to the order of 10^{-6} , about one order of magnitude higher than in Denmark aerosols. Atmospheric release of ^{129}I from the European NRPs and secondary emission from the heavily contaminated seawater in the North Sea and Kattegat are the main sources of

^{129}I in the aerosols from Denmark. Based on the measured Fukushima-derived ^{131}I in the Danish aerosols and the directly Fukushima-influenced $^{131}\text{I}/^{129}\text{I}$ ratio in the Japanese aerosols, the Fukushima-derived ^{129}I immediately after accident contributed only less than 6 % of total ^{129}I to the European atmosphere. This is negligible to the ^{129}I level and inventory in the European environment due to the considerable amount of ^{129}I released from Sellafield and La Hague nuclear fuel reprocessing plants. Iodide is the dominant form (>97%) of the water-soluble iodine in the aerosols. The formation of iodide might be attributed to atmospheric reductants, such as reductive SO_3 and disulfites. The dominant species of iodine in aerosols from Denmark are NSI and RII, accounting for up to 80% of total iodine, NSI might predominantly be organic matters associated iodine, such as HULIS, while RII is likely associated with inorganic components such as metal oxides and minerals.

8. In the brown seaweed (*Fucus serratus* and *Fucus vesiculosus*), iodide was observed the only detectable water-soluble iodine for both ^{129}I and ^{127}I . More than 80% of iodine in seaweed was water non-leachable iodine, likely associated with biomacromolecule. Concentration factors of both ^{129}I and ^{127}I by seaweed were found to be neither relevant to total iodine concentrations in seawater, nor affected by the iodine species in seawater with different I^-/IO_3^- ratios. Nevertheless, the variation of speciation concentration factor in seaweed with iodine species in seawater suggests the response of water-soluble iodine is fast to the seawater, and iodine species interconversion may readily occurs between the soluble and insoluble iodine species in seaweed.

4.2 Perspectives

Speciation analysis of ^{129}I has exhibited its potent applications on water movement tracing in marine environment, geochemical recycling of iodine in the atmosphere and biochemical exchange in the biosphere. Currently, available methods on ^{129}I species are only focused on water, soil and air samples. Although this study has preliminarily exploited the water-soluble ^{129}I and insoluble ^{129}I in seaweed, large unknowns on bimolecular associated ^{129}I species are still unraveled. Further extension of speciation analytical procedure is pivotal to study transfer behaviors of iodine and tracing application.

The existing investigations on species of ^{129}I and ^{127}I mainly focus on the European NRPs-influenced oceans and seas, such as the North Sea, Baltic Sea, the Atlantic Ocean, and the Arctic Ocean, and very few in other areas. The released ^{129}I from the Fukushima nuclear accident provide a unique opportunity to investigate water currents in the Pacific Ocean and its marginal seas. Only sparse data on ^{129}I species in other environmental media, such as soil, vegetation, atmospheric particles have been reported, primarily hindered by the limited available analytical methods and ultra-low level of ^{129}I concentrations in the

environment. With the development of speciation analytical methods, environmental tracing studies is promising to be broaden to these fields. Furthermore, intensive studies on speciation of ^{129}I and ^{127}I also greatly require extensive observations in a vast spatial scope and long time series for various compartments.

Scientific supports

We acknowledge all the scientists and crews in the "Polarstern" to the Arctic in 2011 (ARK-XXVI/3-TransArc) for their great efforts on water sampling in the central Arctic. We thank the Greenland Institute for Natural resources and the National Institute for Aquatic Resources, DTU Aqua for collecting seawater samples from Greenland, Dr. Ken Buesseler (WHOI) and Dr. Harmut Nies (IAEA-EL) for provision of seawater samples from offshore Fukushima, and the National Institute for Environmental Studies for providing the aerosol samples from Tsukuba, Japan. We also thank the Xi'an AMS center (Institute of Earth Environment, China Academy of Sciences, China), the Scottish University Environmental Research Center (Glasgow, UK) and the University of Arizona (Tucson, USA) for their equipment supports on AMS.

All the technicians in the Division of Radioecology, DTU Nutech are sincerely acknowledged for their great support on sampling of seawater, seaweed, lake water, sediment (Claus Bang) and aerosols (Charlotte and Thomas) and for their helps on equipment operation. Financial supports in this work from the Division of Radioecology, DTU Nutech (headed by Sven P. Nielsen) are also sincerely acknowledged.

In addition, we thank the Environmental Protection Agency, Danish Ministry of the Environment, for financial support (Radioactivity AMAP 2011-13, MST-112-00298/00039). This work is partly supported by the projects of Innovation Methodology (No. 2012IM030200) and Fundamental Scientific Research (2015FY110800) from the Ministry of Science and Technology of China.

References

1. Küpper F.C., Feiters MC, Olofsson B, Kaiho T, Yanagida S, Zimmermann MB, Carpenter LJ, Luther GW, Lu Z, Jonsson M (2011) Commemorating Two Centuries of Iodine Research: An Interdisciplinary Overview of Current Research. *Angewandte Chemie* 50:11598-11620
2. John H. Reynolds, *Physics*: Berkeley. (2007)
<http://content.cdlib.org/view?docId=hb1r29n709&doc.view=content&chunk.id=div00061&toc.depth=1&&anchor.id=0> Last access on 4 April 2015
3. Elmore D, Gove HE, Ferraro R, Kilius LR, Lee HW, Chang KH, Beukens RP, Litherland AE, Russo CJ, Purser KH, Murrell MT, Finkel RC (1980) Determination of ^{129}I using tandem accelerator mass spectrometry. *Nature* 286:138
4. Rickard WH, Price KR (1984) Iodine in terrestrial wildlife on the U.S. department of energy's Hanford Site in southcentral Washington. *Environ Monit Assess* 4:379
5. Snyder G, Aldahan A, Aldahan A, Possnert G (2010) Global distribution and long-term fate of anthropogenic ^{129}I in marine and surface water reservoirs. *Geochem Geophys Geosyst* 11:1
6. Edwards RR (1962) Iodine-129: its occurrence in nature and its utility as a tracer. *Science* 137:851
7. Hou X, Dahlgard H, Nielsen SP (2001) Chemical speciation analysis of ^{129}I in seawater and a preliminary investigation to use it as a tracer for geochemical cycle study of stable iodine. *Mar Chem* 74:145
8. Jabbar T, Steier P, Wallner G, Priller A, Kandler N, Kaiser A (2012) Iodine Isotopes (^{127}I and ^{129}I) in Aerosols at High Altitude Alp Stations. *Environ Sci Technol* 46:8637
9. Raisbeck GM, Yiou F (1999) ^{129}I in the oceans: Origins and applications. *Sci Total Environ* 237-238:31
10. Straume T, Anspaugh LR, Marchetti AA, Voigt G, Minenko V, Gu F, Men P, Trofimik S, Tretyakevich S, Drozdovitch V, Shagalova E, Zhukova O, Germenchuk M, Berlovich S (2006) Measurement of I-129 and Cs-137 in soils from Belarus and reconstruction of I-131 deposition from the Chernobyl accident. *Health Phys* 91:7
11. Hou X, Aldahan A, Nielsen SP, Possnert G (2009) Time Series of I-129 and I-127 Speciation in Precipitation from Denmark. *Environ Sci Technol* 43:6522
12. Hou X, Fogh CL, Kucera J, Andersson KG, Dahlgard H, Nielsen SP (2003) Iodine-129 and Caesium-137 in Chernobyl contaminated soil and their chemical fractionation. *Sci Total Environ* 308:97
13. Wershofen H, Aumann DC (1989) Dry deposition velocity of iodine-129 onto grass as obtained by field measurements in the environment of a nuclear fuel reprocessing plant. *J Radioanal Nucl Chem* 137:373
14. Osterc A, Stibilj V (2012) Influence of releases of I-129 from reprocessing plants on the marine environment of the North Adriatic Sea. *Chemosphere* 86:1020
15. Zhang L, Zhou WJ, Hou X, Chen N, Liu Q, He C, Fan Y, Luo M, Wang Z, Fu Y (2011) Level and source of ^{129}I of environmental samples in Xi'an region, China. *Sci Total Environ* 409:3780

16. Hou X, Hansen V, Aldahan A, Possnert G, Lind OC, Lujanienė G (2009) A review on speciation of iodine-129 in the environmental and biological samples. *Anal Chim Acta* 632:181
17. Hou X, Aldahan A, Nielsen SP, Possnert G, Nies H, Hedfors J (2007) Speciation of I-129 and I-127 in seawater and implications for sources and transport pathways in the North Sea. *Environ Sci Technol* 41:5993
18. Schwehr KA, Santschi PH (2003) Sensitive determination of iodine species, including organoiodine, for freshwater and seawater samples using high performance liquid chromatography and spectrophotometric detection. *Anal Chim Acta* 482:59
19. Hu Q, Moran JE (2010) Iodine. In: Atwood DA (ed) *Radionuclides in the Environment*, Wiley, West Sussex, United Kingdom
20. Hou X, Povinec PP, Zhang L, Shi K, Biddulph D, Chang C, Fan Y, Jeřkovský M, Liu Q, Luo M, Steier P, Zhou WJ, Hou Y, Golser R (2013) Iodine-129 in Seawater Offshore Fukushima: Distribution, Inorganic Speciation, Sources, and Budget. *Environ Sci Technol* 47:3091
21. He P, Aldahan A, Possnert G, Hou XL (2013) A summary of global ^{129}I in marine waters. *Nuclear Instruments and Methods in Physics Research Section B: Beam Interactions with Materials and Atoms* 294:537
22. Fabryka-Martin J, Bentley H, Elmore D, Airey PL (1985) Natural iodine-129 as an environmental tracer. *Geochim Cosmochim Acta* 49:337
23. Fehn U, Moran JE, Snyder GT, Muramatsu Y (2005) The initial $^{129}\text{I}/\text{I}$ ratio and the presence of "old" iodine in continental margins. *Nucl Instrum Meth B* 259:496
24. Raisbeck GM, Yiou F, Zhou ZQ, Kilius LR (1995) ^{129}I from nuclear fuel reprocessing facilities at Sellafield (U.K.) and La Hague (France); potential as an oceanographic tracer. *J Mar Syst* 6:561
25. Yiou F, Raisbeck GM, Christensen GC, Holm E (2002) $^{129}\text{I}/^{127}\text{I}$, $^{129}\text{I}/^{137}\text{Cs}$ and $^{129}\text{I}/^{99}\text{Tc}$ in the Norwegian coastal current from 1980 to 1998. *J Environ Radioact* 60:61
26. Rao U, Fehn U (1999) Sources and reservoirs of anthropogenic iodine-129 in western New York. *Geochim Cosmochim Acta* 63:1927
27. Oktay SD, Santschi PH, Moran JE, Sharma P (2001) ^{129}I and ^{127}I transport in the Mississippi River. *Environ Sci Technol* 35:4470
28. Moran JE, Oktay SD, Santschi PH, Schink DR (1999) Atmospheric dispersal of ^{129}I from nuclear fuel reprocessing facilities. *Environ Sci Technol* 33:2536
29. Hou X, Zhou WJ, Chen N, Zhang L, Liu Q, Luo M, Fan Y, Liang W, Fu Y (2010) Determination of Ultralow Level $^{129}\text{I}/^{127}\text{I}$ in Natural Samples by Separation of Microgram Carrier Free Iodine and Accelerator Mass Spectrometry Detection. *Anal Chem* 82:7713
30. Luo M, Hou X, Zhou WJ, He C, Chen N, Liu Q, Zhang L (2013) Speciation and migration of ^{129}I in soil profiles. *J Environ Radioact* 118:30
31. ICRP (1982) Limits for Intakes of Radionuclides by Workers. *Ann ICRP* 8 (1-3) 30
32. Kocher DC (1981-01-01) Radioactive decay data tables. Oak Ridge National Lab DOE/TIC-11026 TRN: 81-015745

33. Kaplan I (1964) Nuclear Physics. Addison-Wesley, New York
34. Leblanc C, Colin C, Cosse A, Delage L, La Barre S, Morin P, Fievet B, Voiseux C, Ambroise Y, Verhaeghe E, Amouroux D, Donard O, Tessier E, Potin P (2006) Iodine transfers in the coastal marine environment: the key role of brown algae and of their vanadium-dependent haloperoxidases. *Biochimie* 88:1773
35. Saiz-Lopez A, Gómez Martín JC, Plane JMC, Saunders RW, Baker AR, Von Glasow R, Carpenter LJ, McFiggans G (2012) Atmospheric chemistry of iodine. *Chem Rev* 112:1773
36. Hu QH, Moran JE, Blackwood V (2009) Geochemical Cycling of Iodine Species in Soils In: Preedy VR, Burrow GN, Watson RR (eds) *The Comprehensive Handbook on Iodine: nutritional, biochemical, pathological and therapeutic aspects*, Elsevier, Amsterdam
37. Hou X, Hou X (2009) Iodine Speciation in Foodstuff, Tissues and Environmental Samples: Iodine species and analytical method In: Watson R, Watson R (eds) *Comprehensive Handbook of Iodine*, Academic Press, Incorporated,
38. Tsunogai S, Sase T (1969) Formation of iodide-iodine in the ocean. *Deep Sea Research and Oceanographic Abstracts* 16:489
39. Wong GTF (1991) The marine geochemistry of iodine. *Rev Aquat Sci* 4:45
40. Wong, Brewer, Spencer (1976) The distribution of particulate iodine in the Atlantic Ocean. *Earth Planet Sci Lett* 32:441-450
41. Wong GTF, Cheng X- (1998) Dissolved organic iodine in marine waters: Determination, occurrence and analytical implications. *Oceanographic Literature Review* 45:1512
42. Campos M, Farrenkopf AM, Jickells TD, Luther GW (1996) A comparison of dissolved iodine cycling at the Bermuda Atlantic Time-Series station and Hawaii Ocean Time-Series Station. *Deep-Sea Research Part II-Topical Studies In Oceanography* 43:455
43. Luther GW, WU JF, Cullen JB (1995) Redox chemistry of iodine in seawater - Frontier molecular orbital theory considerations. *Aqua Chem* 244:135
44. Carpenter LJ (2003) Iodine in the Marine Boundary Layer. *Chem Rev* 103:4953
45. Truesdale VW (1994) Distribution of dissolved iodine in the Irish sea, a temperate shelf sea. *Estuar Coast Shelf Sci* 38:435-446
46. GILFEDDER, B., PETRI, M., BIESTER, H. (2009) Iodine speciation and cycling in fresh waters: a case study from a humic rich headwater lake (Mummelsee). *Journal of Limnology* 68
47. Ullman WJ, Aller RC (1980) Dissolved iodine flux from estuarine sediments and implications for the enrichment of iodine at the sediment water interface. *Geochim Cosmochim Acta* 44:1177
48. Luther III GW, Ferdelman T, Culberson CH, Kostka J, Wu J (1991) Iodine chemistry in the water column of the Chesapeake Bay: Evidence for organic iodine forms. *Estuar Coast Shelf Sci* 32:267
49. Gilfedder BS, Petri M, Biester H (2008) Iodine speciation and cycling in limnic systems: observations from a humic rich headwater lake (Mummelsee). *Biogeosciences Discuss* 5:25

50. He P, Hou X, Aldahan A, Possnert G, Yi P (2013) Iodine isotopes species fingerprinting environmental conditions in surface water along the northeastern Atlantic Ocean. *Scientific Reports* 3: 2685:1
51. Hansen V, Yi P, Hou X, Aldahan A, Roos P, Possnert G (2011) Iodide and iodate (^{129}I and ^{127}I) in surface water of the Baltic Sea, Kattegat and Skagerrak. *Sci Total Environ* 412-413:296
52. Yi P, Aldahan A, Possnert G, Hou X, Hansen V, Wang B (2012) ^{127}I and ^{129}I Species and Transformation in the Baltic Proper, Kattegat, and Skagerrak Basins. *Environ Sci Technol* 46:10948
53. Lehto J, Rätty T, Hou X, Paatero J, Aldahan A, Possnert G, Flinkman J, Kankaanpää H (2012) Speciation of ^{129}I in sea, lake and rain waters. *Sci Total Environ* 419:60
54. Gilfedder BS, Chance R, Dettmann U, Lai SC, Baker AR (2010) Determination of total and non-water soluble iodine in atmospheric aerosols by thermal extraction and spectrometric detection (TESI). *Anal Bioanal Chem* 398:519
55. Gilfedder BS, Lai SC, Petri M, Biester H, Hoffmann T (2008) Iodine speciation in rain, snow and aerosols and possible transfer of organically bound iodine species from aerosol to droplet phases. *Atmos Chem Phys* 8:6069
56. Lai SC, Hoffmann T, Xie ZQ (2008) Iodine speciation in marine aerosols along a 30,000 km round-trip cruise path from Shanghai, China to Prydz Bay, Antarctica. *Geophys Res Lett* GEOPHYS R L GEOPHYS RES LETT GEOPHYS RES LETT 35
57. Steinberg SM, Kimble GM, Schmett GT, Emerson DW, Turner MF, Rudin M (2008) Abiotic reaction of iodate with sphagnum peat and other natural organic matter. *J Radioanal Nucl Chem* 277:185
58. Steinberg SM, Schmett GT, Kimble G, Emerson DW, Turner MF, Rudin M (2008) Immobilization of fission iodine by reaction with insoluble natural organic matter. *J Radioanal Nucl Chem* 277:175
59. Schwehr KA, Santschi PH, Kaplan DI, Yeager CM, Brinkmeyer R (2009) Organo-Iodine Formation in Soils and Aquifer Sediments at Ambient Concentrations. *Environ Sci Technol* 43:7258
60. Yamaguchi N, Nakano M, Takamatsu R, Tanida H (2010) Inorganic iodine incorporation into soil organic matter: evidence from iodine K-edge X-ray absorption near-edge structure. *J Environ Radioact* 101:451
61. Zhang SJ, Schwehr KA, Ho YF, Xu C, Roberts KA, Kaplan DI, Brinkmeyer R, Yeager CM, Santschi PH (2010) A Novel Approach for the Simultaneous Determination of Iodide, Iodate and Organo-Iodide for ^{127}I and ^{129}I in Environmental Samples Using Gas Chromatography Mass Spectrometry. *Environ Sci Technol* 44:9042
62. Kaplan DI, Roberts KA, Schwehr KA, Lilley MS, Brinkmeyer R, Denham ME, Diprete D, Li H, Powell BA, Xu C, Yeager CM, Zhang SJ, Santschi PH (2011) Evaluation of a Radioiodine Plume Increasing in Concentration at the Savannah River Site. *Environ Sci Technol* 45:489

63. Ootosaka S, Schwehr KA, Kaplan DI, Roberts KA, Zhang SJ, Xu C, Li H, Ho Y, Brinkmeyer R, Yeager CM, Santschi PH (2011) Factors controlling mobility of ^{127}I and ^{129}I species in an acidic groundwater plume at the Savannah River Site. *Sci Total Environ* 409:3857
64. Schmitz K, Aumann DC (1995) A study on the association of two iodine isotopes, of natural ^{127}I and of the fission product ^{129}I , with soil components using a sequential extraction procedure. *J Radioanal Nucl Chem* 198:229
65. Strachnov V, Larosa J, Dekner R, Zeisler R, Fajgelj A (1996) Report on the Intercomparison run IAEA-375: Determination of Radionuclides in Soil Sample IAEA-375. International Atomic Energy Agency, Vienna
66. Hansen V, Roos P, Aldahan A, Hou X, Possnert G (2011) Partition of iodine (^{129}I and ^{127}I) isotopes in soils and marine sediments. *J Environ Radioact* 102:1096
67. Qiao J, Hansen V, Hou X, Aldahan A, Possnert G (2012) Speciation analysis of ^{129}I , ^{137}Cs , ^{232}Th , ^{238}U , ^{239}Pu and ^{240}Pu in environmental soil and sediment. *Appl. Radiat. Isot.* 70:1698
68. Xu C, Zhong J, Hatcher PG, Zhang S, Li H, Ho Y, Schwehr KA, Kaplan DI, Roberts KA, Brinkmeyer R, Yeager CM, Santschi PH (2012) Molecular environment of stable iodine and radioiodine (^{129}I) in natural organic matter: Evidence inferred from NMR and binding experiments at environmentally relevant concentrations. *Geochim Cosmochim Acta* 97:166
69. Englund E, Aldahan A, Hou X, Petersen R, Possnert G (2010) Speciation of iodine (I-127 and I-129) in lake sediments. *Nucl Instrum Meth B* 268:1102
70. La Barre S, Potin P, Leblanc C, Delage L (2010) The Halogenated Metabolism of Brown Algae (Phaeophyta), Its Biological Importance and Its Environmental Significance. *Marine Drugs* 8:988
71. Hou X, Chai CF, Qian QF, Yan XJ, Fan X (1997) Determination of chemical species of iodine in some seaweeds .1. *Sci Total Environ* 204:215
72. Hou X, Yan X, Chai C (2000) Chemical Species of Iodine in Some Seaweeds II. Iodine-Bound Biological Macromolecules. *J Radioanal Nucl Chem* 245:461
73. Shah M, Wuilloud RG, Kannamkumaratha SS, Caruso JA (2005) Iodine speciation studies in commercially available seaweed by coupling different chromatographic techniques with UV and ICP-MS detection. *J Anal At Spectrom* 20:176-182
74. Romaris-Hortas V, Moreda-Piñeiro A, Barrera PB (2013) Speciation and bioavailability of Iodine in Edible Seaweed In: Bakirdere S (ed) *Speciation Studies in Soil, Sediment and Environmental Samples*, 1st edn. CRC Press, Boca Raton, Florida, USA
75. Romaris-Hortas V, Bermejo-Barrera P, Moreda-Pineiro J, Moreda-Pineiro A (2012) Speciation of the bio-available iodine and bromine forms in edible seaweed by high performance liquid chromatography hyphenated with inductively coupled plasma-mass spectrometry. *Anal Chim Acta* 745:24
76. Campos M, Sanders R, Jickells T (1999) The dissolved iodate and iodide distribution in the South Atlantic from the Weddell Sea to Brazil. *Mar Chem* 65:167

77. Chance R, Weston K, Baker AR, Hughes C, Malin G, Carpenter L, Meredith MP, Clarke A, Jickells TD, Mann P, Rossetti H (2010) Seasonal and interannual variation of dissolved iodine speciation at a coastal Antarctic site. *Mar Chem* 118:171
78. Moisan TA, Dunstan WM, Udomkit A, Wong GTF (1994) The uptake of iodate by marine phytoplankton. *J Phycol* 30:580
79. Wong GF, Piumsomboon AU, Dunstan WM (2002) The transformation of iodate to iodide in marine phytoplankton cultures. *Mar Ecol Prog Ser* 237:27
80. Amachi S (2008) Microbial Contribution to Global Iodine Cycling: Volatilization, Accumulation, Reduction, Oxidation, and Sorption of Iodine. *Microbes and Environments* 23:269
81. Amachi S, Minami K, Miyasaka I, Fukunaga S (2010) Ability of anaerobic microorganisms to associate with iodine: ^{125}I tracer experiments using laboratory strains and enriched microbial communities from subsurface formation water. *Chemosphere* 79:349
82. Spokes LJ, Liss PS (1996) Photochemically induced redox reactions in seawater, II. Nitrogen and iodine. *Mar Chem* 54:1
83. Zhang J, Whitfield M (1986) Kinetics of inorganic redox reactions in seawater I. The reduction of iodate by bisulfide. *Mar Chem* 19:121
84. Hird FJR, Yates JR (1961) The oxidation of cysteine, glutathione and thioglycollate by iodate, bromate, persulphate and air. *J Sci Food Agric* 12:89
85. Kennedy BM, Hudson B, Hohenberg CM, Podosek FA (1988) $^{129}\text{I}/^{127}\text{I}$ variations among enstatite chondrites. *Geochim Cosmochim Acta* 52:101
86. Aldahan A, Englund E, Possnert G, Cato I, Hou X (2007) Iodine-129 enrichment in sediment of the Baltic Sea. *Appl Geochem* 22:637
87. Truesdale VW, Upstill-Goddard R (2003) Dissolved iodate and total iodine along the British east coast. *Estuar Coast Shelf Sci* 56:261
88. Bluhm K, Croot P, Wuttig K, Lochte K (2010) Transformation of iodate to iodide in marine phytoplankton driven by cell senescence. *Aquat Biol* 11:1
89. Edwards A, Truesdale VW (1997) Regeneration of inorganic iodine species in Loch Etive, a natural leaky incubator. *Estuar Coast Shelf Sci* 45:357
90. Thomas JA, Hager LP (1968) The peroxidation of molecular iodine to iodate by chloroperoxidase. *Biochem Biophys Res Commun* 32:770
91. Jones SD, Truesdale VW (1984) Dissolved iodine species in a British freshwater system. *Limnol Oceanogr* 29:1016
92. Xu C, Miller EJ, Zhang SJ, Li H, Ho Y, Schwehr KA, Kaplan DI, Otosaka S, Roberts KA, Brinkmeyer R, Yeager CM, Santschi PH (2011) Sequestration and Remobilization of Radioiodine (^{129}I) by Soil Organic Matter and Possible Consequences of the Remedial Action at Savannah River Site. *Environ Sci Technol* 45:9975
93. Yamaguchi N, Nakano M, Tanida H, Fujiwara H, Kihou N (2006) Redox reaction of iodine in paddy soil investigated by field observation and the I K-Edge XANES fingerprinting method. *J Environ Radioact* 86:212

94. Hou X, Dahlgard H, Rietz B, Jacobsen U, Nielsen S,P., Aarkrog A (1999) Determination of ^{129}I in seawater and some environmental materials by neutron activation analysis. *Analyst* 124:1109
95. Rao U, Fehn U (1997) The distribution of ^{129}I around West Valley, an inactive nuclear fuel reprocessing facility in Western New York. *Nucl Instrum Meth B* 123:361
96. Reifenhäuser C, Heumann KG (1990) Development of a definitive method for iodine speciation in aquatic systems. *Fresenius J Anal Chem* 336:559
97. Dang H, Hou X, Roos P, Nielsen SP (2013) Release of iodine from organic matter in natural water by $\text{K}_2\text{S}_2\text{O}_8$ oxidation for ^{129}I determination. *Anal Methods* 5:449
98. Fehn U, Tullai S, Teng RTD, Elmore D, Kubik PW (1987) Determination of ^{129}I in heavy residues of two crude oils. *Nucl Instrum Meth B* 29:380
99. Tullai S, Tubbs LE, Fehn U (1987) Iodine extraction from petroleum for analysis of $^{129}\text{I}/^{127}\text{I}$ ratios by AMS. *Nucl Instrum Meth B* 29:383
100. Park SD, Kim JS, Han SH, Ha YK, Song KS, Jee KY (2009) The measurement of ^{129}I for the cement and the paraffin solidified low and intermediate level wastes (LILWs), spent resin or evaporated bottom from the pressurized water reactor (PWR) nuclear power plants. *Appl.Radial.Isot.* 67:1676
101. Parry SJ, Bennett BA, Benzing R, Lally AE, Birch CP, Fulker MJ (1995) The determination of ^{129}I in milk and vegetation using neutron activation analysis. *Sci Total Environ* 173-174:351
102. Grogan KP, DeVol TA (2011) Online Detection of Radioactive Iodine in Aqueous Systems through the Use of Scintillating Anion Exchange Resin. *Anal Chem* 83:2582
103. Studier MH, Postmus CJ, Mech J, Walters RR, Sloth EN (1962) The use of ^{129}I as an isotopic tracer and its determination along with normal ^{127}I by neutron activation-The isolation of iodine from a variety of materials. *J Inorgan Nucl Chem* 24:755
104. Aumann DC, Buheitel F, Hauschild J, ROBENS E, Wershofen H (1987) Chemical and nuclear interferences in neutron activation of ^{129}I and ^{127}I in environmental samples. *J Radioanal Nucl Chem* 109:261
105. Muramatsu Y, Uchida S, Sumiya M, Ohmomo Y (1985) Iodine separation procedure for the determination of iodine-129 and iodine-127 in soil by neutron activation analysis. *J Radioanal Nucl Chem* 94:329
106. Zhou WJ, Hou X, Chen N, Zhang LY, Liu Q, He CH, Luo MY, Liang WG, Fan YK, Wang ZW, Fu YC, Li HB (2010) Preliminary study of radioisotope ^{129}I application in China using Xi'an accelerator mass spectrometer. *ICNS News* 25:8
107. Sahoo SK, Muramatsu Y, Yoshida S, Matsuzaki H, Ruehm W (2009) Determination of I-129 and I-127 Concentration in Soil Samples from the Chernobyl 30-km Zone by AMS and ICP-MS. *J Radiat Res* 50:325
108. Quintana EE, Thyssen SM (2000) Determination of ^{129}I in Conifer Samples Around Nuclear Facilities in Argentina. *J Radioanal Nucl Chem* 245:545

109. Rao U, Fehn U, Muramatsu Y, McNeil H, Sharma P, Elmore D (2002) Tracing the history of nuclear releases: Determination of ^{129}I in tree rings. *Environ Sci Technol* 36:1271
110. Brown CF, Geiszler KN, Vickerman TS (2005) Extraction and quantitative analysis of iodine in solid and solution matrixes. *Anal Chem* 77:7062
111. Nishiizumi K, Elmore D, Honda M, Arnold JR, Gove HE (1983) Measurements of ^{129}I in meteorites and lunar rock by tandem accelerator mass spectrometry. *Nature* 305:611
112. Zhao P, Hu Q, Rose TP, Nimz GJ, Zavarin M (2008) Distribution of ^{99}Tc and ^{129}I in the vicinity of underground nuclear tests at the Nevada Test Site. *J Radioanal Nucl Chem* 276:755
113. Gómez-Guzmán JM, López-Gutiérrez JM, Pinto-Gómez AR, Holm E, García-León M (2010) Analysis of ^{129}I in lichens by accelerator mass spectrometry through a microwave-based sample preparation method. *Nucl Instrum Meth B* 268:1171
114. Roman D, Fabryka-Martin J (1988) Iodine-129 and chlorine-36 in uranium ores 1. Preparation of samples for analysis by AMS. *Chem. Geol.* 72:1
115. Ashton L, Warwick P, Giddings D (1999) The measurement of ^{36}Cl and ^{129}I in concrete wastes. *Analyst* 124:627
116. Martin JE, Marcinowski F, Cook S (1990) Optimization of Neutron Activation Analyses of ^{129}I in Low-level Radioactive Waste Samples. *Appl Radial Isot* 31:727
117. Zhang L, Hou X, Zhou WJ, Chen N, Liu Q, Luo M, Fan Y, Fu Y (2013) Performance of Accelerator Mass Spectrometry for ^{129}I using AgI–AgCl carrier-free coprecipitation. *Nuclear Instruments and Methods in Physics Research Section B: Beam Interactions with Materials and Atoms* 294:276
118. Moreda-Piñeiro A, Romaris-Hortas V, Bermejo-Barrera P (2011) A review on iodine speciation for environmental, biological and nutrition fields. *J Anal At Spectrom* 26:2107
119. Shimamoto YS, Itai T, Takahashi Y (2010) Soil column experiments for iodate and iodide using K-edge XANES and HPLC-ICP-MS. *J Geochem Explor* 107:117
120. Izmer AV, Boulyga SF, Zoriy MV, Becker JS (2004) Improvement of the detection limit for determination of ^{129}I in sediments by quadrupole inductively coupled plasma mass spectrometer with collision cell. *J Anal At Spectrom* 19:1278
121. Hou X, Dahlgaard H, Rietz B, Jacobsen U, Nielsen SP, Aarkrog A (1999) Determination of Chemical Species of Iodine in Seawater by Radiochemical Neutron Activation Analysis Combined with Ion-Exchange Preseparation. *Anal. Chem.* 71:2745
122. Hou X, Dahlgaard H, Nielsen SP (2000) Iodine-129 Time Series in Danish, Norwegian and Northwest Greenland Coast and the Baltic Sea by Seaweed. *Estuar Coast Shelf Sci* 51:571
123. Bio-Rad Laboratories (2000) AG® 1, AG MP-1 and AG 2 Strong Anion Exchange Resin: Instruction Manual. Bio-Rad Laboratories
124. Luo M, Hou X, He C, Liu Q, Fan Y (2013) Speciation Analysis of ^{129}I in Seawater by Carrier-Free AgI–AgCl Coprecipitation and Accelerator Mass Spectrometric Measurement. *Anal Chem* 85:3715

125. Hou X, Aldahan A, Possnert G, Lujanienė G, Lehto J, Skipperud L, Lind OC, Salbu B (2009) Speciation analysis of radionuclides in the environment - NSK-B SPECIATION project report 2009.
126. Xu C, Zhang SJ, Ho Y, Miller EJ, Roberts KA, Li H, Schwehr KA, Otosaka S, Kaplan DI, Brinkmeyer R, Yeager CM, Santschi PH (2011) Is soil natural organic matter a sink or source for mobile radioiodine (^{129}I) at the Savannah River Site? *Geochim Cosmochim Acta* 75:5716
127. Michel R, Daraoui A, Gorny M, Jakob D, Sachse R, Tosch L, Nies H, Goroncy I, Herrmann J, Synal HA, Stocker M, Alfimov V (2012) Iodine-129 and iodine-127 in European seawaters and in precipitation from Northern Germany. *Sci Total Environ* 419:151
128. Huang R, Hou X, Hoffmann T (2010) Extensive Evaluation of a Diffusion Denuder Technique for the Quantification of Atmospheric Stable and Radioactive Molecular Iodine. *Environ Sci Technol* 44:5061
129. Huang R, Hoffmann T (2009) Development of a Coupled Diffusion Denuder System Combined with Gas Chromatography/Mass Spectrometry for the Separation and Quantification of Molecular Iodine and the Activated Iodine Compounds Iodine Monochloride and Hypoiodous Acid in the Marine Atmosphere. *Anal Chem* 81:1777
130. Raisbeck G (2001) ^{129}I and $^{129}\text{I}/^{127}\text{I}$ ratio determination in environmental biological samples by RNAA, AMS and direct γ -X spectrometry measurements. *J Radioanal Nucl* 249:133
131. Kim YJ, Kim CS, Kang SH, Lee DM, Kim CK (2005) Determination of ^{129}I using liquid scintillation counting. In: Chatupnik S, Schönhofer F, Noakes J (eds) *Advances in Liquid Scintillation Spectrometry*, the Arizona Board of Regents on behalf of the University of Arizona LSC,
132. Goles RW, Fukuda RC, Cole MW, Brauer FP (1981) Detection of iodine-129 by laser induced fluorescence spectrometry. *Anal Chem* 53:776
133. Stoffels JJ (1982) Measurement of iodine-129 at the femtogram level by negative surface ionization mass spectrometry. *Radiochemical and Radioanalytical Letters* 55:99
134. Zhang S, Schwehr KA, Ho Y-, Xu C, Roberts KA, Kaplan DI, Brinkmeyer R, Yeager CM, Santschi PH (2010) A Novel Approach for the Simultaneous Determination of Iodide, Iodate and Organo-Iodide for ^{127}I and ^{129}I in Environmental Samples Using Gas Chromatography Mass Spectrometry. *Environ Sci Technol* 44:9042
135. Izmer AV, Boulyga SF, Becker JS (2003) Determination of $^{129}\text{I}/^{127}\text{I}$ isotope ratios in liquid solutions and environmental soil samples by ICP-MS with hexapole collision cell. *J Anal At Spectrom* 18:1339
136. Fujiwara H, Kawabata K, Suzuki J, Shikino O (2011) Determination of ^{129}I in soil samples by DRC-ICP-MS. *J Anal At Spectrom* 26:2528
137. Kilius LR, Rucklidge JC, Litherland AE (1987) Accelerator mass spectrometry of ^{129}I at isotrace. *Nucl Instrum Meth B* 29:72
138. Kilius LR, Litherland AE, Rucklidge JC, Baba N (1992) Accelerator mass-spectrometric measurements of heavy long-lived isotopes. *International journal of radiation applications and instrumentation Part A, Applied radiation and isotopes* 43:279

139. Schauer U (2012) The expedition of the research vessel "Polarstern" to the Arctic in 2011 (ARK-XXVI/3 - TransArc). Alfred Wegener Institute for Polar and Marine Research 649:1
140. Buesseler KO, Jayne SR, Fisher NS, Rypina II, Baumann H, Baumann Z, Breier CF, Douglass EM, George J, Macdonald AM, Miyamoto H, Nishikawa J, Pike SM, Yoshida S (2012) Fukushima-derived radionuclides in the ocean and biota off Japan. *Proc Natl Acad Sci U S A* 109:5984
141. Xu S, Freeman SPHT, Hou X, Watanabe A, Yamaguchi K, Zhang L (2013) Iodine Isotopes in Precipitation: Temporal Responses to ¹²⁹I Emissions from the Fukushima Nuclear Accident. *Environmental Science and Technology* 47:2010851-10859
142. Zhou WJ, Zhao X, Lu X, Liu L, Wu Z, Cheng P, Zhao W, Huang C (2008) The 3MV multi-element AMS in Xi'an, China: unique features and preliminary tests. *Radiocarbon* 48
143. Freeman, Bishop, Bryant, Cook, Fallick, Harkness, Metcalfe, Scott, Scott, Summerfield (2004) A new environmental sciences AMS laboratory in Scotland. *Nucl Instrum Meth B* 223-224:31
144. HYSPLIT (HYbrid SingleParticle Lagrangian Integrated Trajectory) Model, access via NOAA ARL READY Website, <http://www.arl.noaa.gov/ready/hysplit4.html> (2003) 8 May 2015
145. Kolthoff IM, Miller IK (1951) The chemistry of persulfate .1. The kinetics and mechanism of the decomposition of the persulfate ion in aqueous medium. *J Am Chem Soc* 73:3055-3059
146. Peyton GR (1993) The free-radical chemistry of persulfate-based total organic carbon analyzers. *Mar Chem* 41:91-103
147. Hagedorn F, Schleppe P (2000) Determination of total dissolved nitrogen by persulfate oxidation. *J Plant Nutrit & Soil Sci* 163:81-82
148. Pino S, Fang SL, Braverman LE (1996) Ammonium persulfate: a safe alternative oxidizing reagent for measuring urinary iodine. *Clin Chem* 42:239
149. Jabbar T, Steier P, Wallner G, Kandler N, Katzlberger C (2011) AMS analysis of iodine-129 in aerosols from Austria. *Nucl Instrum Meth B* 269:3183
150. Li D, Zhang L, Wang X, Liu L (2003) Ashing and microwave digestion of aerosol samples with a polypropylene fibrous filter matrix. *Anal Chim Acta* 482:129
151. Baker AR, Thompson D, Campos MLAM, Parry SJ, Jickells TD (2000) Iodine concentration and availability in atmospheric aerosol. *Atmos Environ* 34:4331
152. Xu S, XIE Z, Liu W, Yand H, Li B (2010) Extraction and Determination of Total Bromine, Iodine, and Their Species in Atmospheric Aerosol. *Chinese Journal of Analytical Chemistry* 38:219
153. Raisbeck GM, Yiou F, Zhou ZQ, Kilius LR, Dahlgaard H, Raisbeck GM, Yiou F, Zhou ZQ, Kilius LR, Dahlgaard H (1993) Anthropogenic ¹²⁹I in the Kara Sea. *Environmental radioactivity in the Arctic and Antarctic. Proceedings* :125-128
154. Buraglio N, Aldahan A, Possnert (1999) Distribution and inventory of ¹²⁹I in the central Arctic Ocean. *Geophys Res Lett (USA)* 26:1011

155. Cooper LW, Beasley T, Aagaard K, Kelley JM, Larsen IL, Grebmeier JM (1999) Distributions of nuclear fuel-reprocessing tracers in the Arctic Ocean: Indications of Russian river influence. *J Mar Res* 57:715-738
156. Smith JN, McLaughlin FA, Smethie WM, Moran SB, Lepore K (2011) Iodine-129, ¹³⁷Cs, and CFC-11 tracer transit time distributions in the Arctic Ocean. *Journal of Geophysical Research: Oceans* 116:- C04024
157. Smith JN, Ellis KM, Kilius LR (1998) ¹²⁹I and ¹³⁷Cs tracer measurements in the Arctic Ocean. *Deep-sea research Part 1 Oceanographic research papers* 45:959
158. Alfimov V, Aldahan A, Possnert G, Winsor P (2004) Anthropogenic iodine-129 in seawater along a transect from the Norwegian coastal current to the North Pole. *Mar Pollut Bull* 49:1097
159. Josefsson D (1998) Anthropogenic Radionuclides in the Arctic Ocean. PhD thesis.
160. Smith JN, Ellis KM, Boyd T (1999) Circulation features in the central Arctic Ocean revealed by nuclear fuel reprocessing tracers from Scientific Ice Expeditions 1995 and 1996. *J Geophys Res* 104:29663
161. Cooper LW, Hong GH, Beasley TM, Grebmeier JM (2001) Iodine-129 Concentrations in Marginal Seas of the North Pacific and Pacific-influenced Waters of the Arctic Ocean. *Mar Pollut Bull* 42:1347
162. Gómez-Guzmán JM, Villa M, Le Moigne F, López-Gutiérrez JM, García-León M (2013) AMS measurements of ¹²⁹I in seawater around Iceland and the Irminger Sea. *Nucl Instrum Meth B* 294:547-551
163. Orre S, Smith JN, Alfimov V, Bentsen M (2010) Simulating transport of ¹²⁹I and idealized tracers in the northern North Atlantic Ocean. *Environ Fluid Mech* 10:213
164. Smith JN, Jones, Moran, Smethic J, Kieser (2005) Iodine-129/CFC 11 transit times for Denmark Strait overflow water in the Labrador and Irminger Seas. *J Geophys Res* 110
165. Aarkrog, Dahlgaard, Hallstadius, Hansen, Holm (1983) Radiocaesium from Sellafield effluents in Greenland waters. *Nature* 304:49-51
166. Dahlgaard H (1994) Sources of ¹³⁷Cs, ⁹⁰Sr and ⁹⁹Tc in the East Greenland Current. *J Environ Radioact* 25:37
167. Rudels B, Fahrbach E, Meincke J, Budeus G, Eriksson P (2002) The East Greenland Current and its contribution to the Denmark Strait overflow. *ICES J Mar Sci* 59:1133
168. Rudels B (2012) Arctic Ocean circulation and variability - advection and external forcing encounter constraints and local processes. *Ocean Science Discussions* 8:261
169. Rudels B, Bjork G, Nilsson J, Winsor P, Lake I, Nohr C (2005) The interaction between waters from the Arctic Ocean and the Nordic Seas north of Fram Strait and along the East Greenland Current: results from the Arctic Ocean-02 Oden expedition. *J Mar Syst* 55:1
170. Aarkrog A, Dahlgaard H, Nielsen SP (1999) Marine radioactivity in the Arctic: a retrospect of environmental studies in Greenland waters with emphasis on transport of ⁹⁰Sr and ¹³⁷Cs with the East Greenland Current. *Sci Total Environ* 237–238:143

171. Hvid Ribergaard M, Anker Pedersen S, Ådlandsvik B, Kliem N (2004) Modelling the ocean circulation on the West Greenland shelf with special emphasis on northern shrimp recruitment. *Cont Shelf Res* 24:1505
172. Waite TJ, Truesdale VW, Olafsson J (2006) The distribution of dissolved inorganic iodine in the seas around Iceland. *Mar Chem* 101:54-67
173. Pedersen SA, Ribergaard MH, Simonsen CS (2005) Micro- and mesozooplankton in Southwest Greenland waters in relation to environmental factors. *J Mar Syst* 56:85
174. Kershaw P, Baxter A (1995) The transfer of reprocessing wastes from north-west Europe to the Arctic. *Deep-sea research Part 2, Topical studies in oceanography* 42:1413
175. Hou X, Dahlgaard H, Nielsen SP, Kucera J (2002) Level and origin of Iodine-129 in the Baltic Sea. *J Environ Radioact* 61:331
176. Truesdale VW, Nausch G, Baker A (2001) The distribution of iodine in the Baltic Sea during summer. *Mar Chem* 74:87
177. Truesdale VW (2008) The biogeochemical effect of seaweeds upon close-to natural concentrations of dissolved iodate and iodide in seawater – Preliminary study with *Laminaria digitata* and *Fucus serratus*. *Estuar Coast Shelf Sci* 78:155
178. Amachi S, Mishima Y, Shinoyama H, Muramatsu Y, Fujii T (2005) Active transport and accumulation of iodide by newly isolated marine bacteria. *Appl Environ Microbiol* 71:741
179. Suzuki T, Minakawa M, Amano H, Togawa O (2010) The vertical profiles of iodine-129 in the Pacific Ocean and the Japan Sea before the routine operation of a new nuclear fuel reprocessing plant. *Nucl Instrum Meth B* 268:1229
180. Povinec PP, Lee S, Kwong LL, Oregioni B, Jull AJT, Kieser WE, Morgenstern U, Top Z (2010) Tritium, radiocarbon, ^{90}Sr and ^{129}I in the Pacific and Indian Oceans. *Nucl Instrum Meth B* 268:1214
181. Tsukada H, Ishida J, Narita O (1991) Particle-size distributions of atmospheric ^{129}I and ^{127}I aerosols. *Atmospheric Environment. Part A. General Topics* 25:905
182. Nielsen SP, Anderson KP, Miller A (2011) December 2011 Radioactivity in the Risø District January-June 2011. *Risø Report Risø-R-1800(EN)*
183. Xu S, Zhang L, Freeman SPHT, Hou X, Shibata Y, Sanderson D, Cresswell A, Doi T, Tanaka A (2015) Speciation of Radiocesium and Radioiodine in Aerosols from Tsukuba after the Fukushima Nuclear Accident. *Environ Sci Technol* 49:1017
184. Ball SM, Hollingsworth AM, Humbles J, Leblanc C, Potin P, McFiggans G (2010) Spectroscopic studies of molecular iodine emitted into the gas phase by seaweed. *Atmos Chem Phys* 10:6237
185. Bondietti EA, Brantley JN (1986) Characteristics of Chernobyl radioactivity in Tennessee. *Nature* 322:313
186. Baker AR (2004) Inorganic iodine speciation in tropical Atlantic aerosol. *Geophys Res Lett* 31:- L23S02

187. Xu S, Xie Z, Li B, Liu W, Sun L, Kang H, Yang H, Zhang P (2010) Iodine speciation in marine aerosols along a 15000-km round-trip cruise path from Shanghai, China, to the Arctic Ocean. *Environ Chem* 7:406
188. Vogt R, Sander R, von Glasow R, Crutzen P (1999) Iodine Chemistry and its Role in Halogen Activation and Ozone Loss in the Marine Boundary Layer: A Model Study. *J Atmos Chem* 32:375
189. McFiggans G, Plane JMC, Allan BJ, Carpenter LJ, Coe H, O'Dowd C (2000) A modeling study of iodine chemistry in the marine boundary layer. *Journal of Geophysical Research: Atmospheres* 105:14371
190. Zheng G, He K, Duan F, Cheng Y, Ma Y (2013) Measurement of humic-like substances in aerosols: A review. *Environmental Pollution* 181:301
191. Feczko T, Puxbaum H, Kasper-Giebl A, Handler M, Limbeck A, Gelencsér A, Pio C, Preunkert S, Legrand M (2007) Determination of water and alkaline extractable atmospheric humic-like substances with the TU Vienna HULIS analyzer in samples from six background sites in Europe. *J Geophys Res - Atmos* 112:1
192. Gall EA, Küpper FC, Bernard K (2005) A survey of iodine content in *Laminaria digitata*. *Bot Mar* 47:30
193. Hou X (1997) Study on iodine and its chemical species in biological and environmental systems by nuclear techniques. *Institut of High Energy Physics China Academy of Science* :1
194. Han X, Cao L, Cheng H, Liu J, Xu Z (2012) Determination of iodine species in seaweed and seawater samples using ion-pair reversed phase high performance liquid chromatography coupled with inductively coupled plasma mass spectrometry. *Anal Methods* 4:3471
195. Küpper F.C., Carpenter LJ, McFiggans GB, Palmer CJ, Waite TJ, Boneberg E, Woitsch S, Weiller M, Abela R, Grolimund D, Potin P, Butler A, Luther, George W., 3rd, Kroneck PMH, Meyer-Klaucke W, Feiters MC (2008) Iodide accumulation provides kelp with an inorganic antioxidant impacting atmospheric chemistry. *PNAS* 105:6954
196. Fréchou C, Calmet D (2003) Variations of iodine-129 activities in various seaweed collected on the French channel coast. *Czech J Phys* 53:A83
197. Baily NA, Kelly S (1955) Iodine Exchange in *Ascophyllum*. *Biological Bulletin*
198. Kelly S, Baily NA (1951) The Uptake of Radioactive Iodine by *Ascophyllum*. *Biol Bull* 100:188
199. Küpper FC, Schweigert N, Ar Gall E, Legendre JM, Vilter H, Kloareg B (1998) Iodine uptake in *Laminariales* involves extracellular, haloperoxidase-mediated oxidation of iodide. *Planta* 207:163
200. Klemperer HG (1957) The accumulation of iodide by *Fucus ceranoides*. *Biochem J* 67:381
201. Verhaeghe EF, Fraysse A, Guerquin-Kern J, Wu T, Deves G, Mioskowski C, Leblanc C, Ortega R, Ambroise Y, Potin P (2008) Microchemical imaging of iodine distribution in the brown alga *Laminaria digitata* suggests a new mechanism for its accumulation. *J Biolog Inorg Chem* 13:257-269

202. Hirano S, Ishii T, Nakamura R, Matsuba M, Koyanagi T (1983) Chemical forms of radioactive iodine in seawater and its effects upon marine organisms. *Radioisotopes* 32:319
203. Romarís-Hortas V, Bianga J, Moreda-Piñeiro A, Bermejo-Barrera P, Szpunar J (2014) Speciation of iodine-containing proteins in Nori seaweed by gel electrophoresis laser ablation ICP–MS. *Talanta* 127:175

Paper I

Speciation analysis of ^{129}I and its applications in environmental research

By L. Y. Zhang¹ and X. L. Hou^{1,2,*}

¹ Center for Nuclear Technologies, Technical University of Denmark, Risø Campus, Roskilde 4000, Denmark

² Xi'an AMS Center, SKLLQG, Institute of Earth Environment, CAS, Xi'an 710075, China

(Received November 28, 2013; accepted in revised form April 4, 2013)

(Published online July 29, 2013)

^{129}I / Speciation analysis / Environmental tracer /
Geochemical cycle of iodine

Summary. ^{129}I , a long-lived radionuclide, is important in view of geological repository of nuclear waste, and environmental tracing applications related to diverse natural processes of iodine. The environmental behaviors and bioavailability of ^{129}I are highly related to its species. A number of methods have been reported for speciation analysis of ^{129}I in a variety of environmental samples. These methods have been applied in many researches, including conversion processes of iodine species in marine and terrestrial systems, migration and retention of iodine in soil and sediment, geochemical cycling of iodine, as well as studies on atmospheric chemistry of iodine. This article aims to review these methods and their applications in environmental research.

1. Introduction

^{129}I ($T_{1/2} = 1.57 \times 10^7$ yr) in the current environment originates mainly from human nuclear activity (more than 6000 kg) and to a minor extent from natural process (about 250 kg) [1, 2]. Regarding the anthropogenic sources, more than 95% of ^{129}I was released from reprocessing plants of spent nuclear fuel [2]. Atmospheric nuclear weapons testing during 1940's–1980's only contributes about 3% of ^{129}I [3], and 1.3–6 kg from the Chernobyl accident in 1986 and 1.2 kg from the Fukushima accident in 2011 [4, 5] constitute a minor contribution. Besides these sources, radioactive waste dumping and repository, for example approximate 13 600 kg of ^{129}I in Yucca Mountain repository and Hanford reservation (USA) [3], in which ^{129}I was captured and stored in the untreated spent fuel, is a potentially important source of ^{129}I to the environment in the future.

Releases of large amount of anthropogenic ^{129}I into the environment have resulted in an elevation of its level by 2–6 orders of magnitude compared to the pre-nuclear era. Due to the long half-life of ^{129}I , high volatility of iodine, accumulation of iodine in human thyroid and lower sensitivity of radiometric methods for ^{129}I measurement, early

researches on ^{129}I (before 1980s) mainly focused on environmental hazard of anthropogenic ^{129}I released from nuclear facilities, accidents, as well as nuclear weapons testing. With the development of high sensitive measurement methods, especially accelerator mass spectrometry (AMS), increased applications of ^{129}I in environmental tracing have been implemented to provide knowledge on geochemical cycling of stable iodine [6, 7], transport and exchange of water masses in ocean [2, 8–11], atmospheric behavior and process of iodine [12], and volcano fluid migration [13]. Furthermore, natural ^{129}I has been used as geochronometer on timescale of 2 to 80 million years, for dating brines incorporated in salt domes [14–16], pore water of sediment and hydrocarbons [17] and groundwater [18].

As a mobile radionuclide, ^{129}I is one of the important radionuclides in nuclear waste disposal. The migration behavior of ^{129}I in the environment is determined by its species, while many parameters, such as pH, redox potential (E_h) and medium components are important factors affecting its speciation. In order to understand the migration of radioiodine in radioactive waste repositories on long-term scale, to remediate radioactive contamination in the environment and nuclear facilities, as well as to estimate the transfer of radioiodine among environmental media and from environment to humans, speciation analysis of ^{129}I in environmental samples has to be implemented. This can also provide insight into various environmental processes of stable iodine species, such as the geochemistry cycle and atmospheric chemistry of stable iodine. A critical review on speciation analysis of ^{129}I has been published in 2009 [19], since then some new methods have been developed and applications of ^{129}I speciation analysis have quickly increased in the past years. This article aims to review the present progress on analytical methods and their applications; some perspectives on the potential applications of speciation analysis of ^{129}I are highlighted.

1.1 Level and distribution of ^{129}I in the environment

^{129}I distributes unevenly in the environment, the $^{129}\text{I}/^{127}\text{I}$ atomic ratios range from 10^{-12} in samples of pre-nuclear era up to 10^{-4} in the highly contaminated samples, depending on its sources (Fig. 1) [20]. Atmospheric nuclear weapons

*Author for correspondence (E-mail: xiho@dtu.dk).

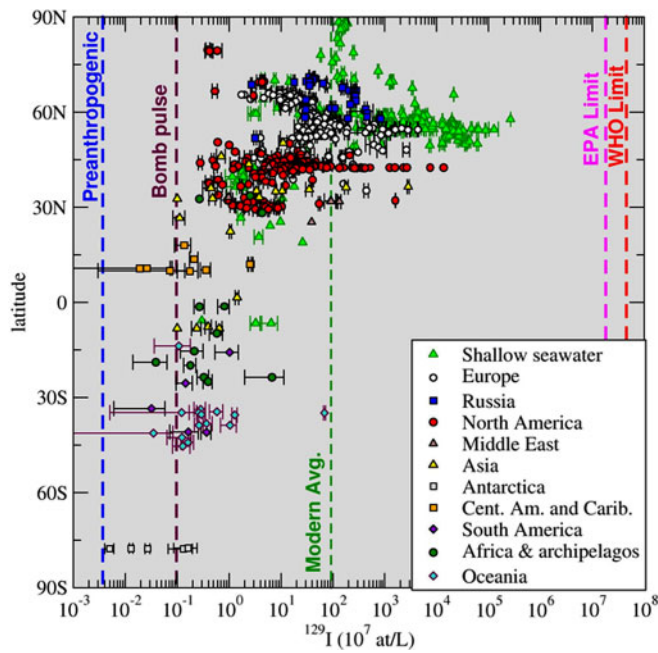


Fig. 1. Global distribution of $^{129}\text{I}/^{127}\text{I}$ ratios in shallow seawater, rivers and lakes (adopted from [20] with copyright permission from AGU).

testing has elevated the $^{129}\text{I}/^{127}\text{I}$ atomic ratio from 10^{-12} to $10^{-11} \sim 10^{-9}$, and the huge contribution of the reprocessing plants and nuclear accident further raised the $^{129}\text{I}/^{127}\text{I}$ ratios to $10^{-9} \sim 10^{-6}$. According to the source and distribution, ^{129}I in the environment can be sorted into three categories.

1.1.1 Natural ^{129}I level of pre-nuclear era

In the samples of pre-nuclear era, such as deep sediment and soil, ^{129}I originates from the natural processes. When the naturally generated ^{129}I reaches equilibrium with ^{127}I , it leads to a steady-state $^{129}\text{I}/^{127}\text{I}$ isotope ratio (Table 1) [14, 15, 17, 21–25]. A value of 1.5×10^{-12} is regarded as the initial ratio of $^{129}\text{I}/^{127}\text{I}$ in marine system based on the measurement of marine sediment and seaweed collected before 1940 [25]. In terrestrial system, since ^{127}I concentration (*i.e.*

about $2 \mu\text{g g}^{-1}$ in most of soil) is 1–2 orders of magnitude lower compared to that in marine system, a higher natural $^{129}\text{I}/^{127}\text{I}$ ratio with 20×10^{-12} was observed in deep soil at Loess Plateau, China [24]. After isolating from surface environment, the $^{129}\text{I}/^{127}\text{I}$ ratio in the sample decreases with the radioactive decay of ^{129}I , which forms the basis of geological dating using ^{129}I .

1.1.2 The present environmental background level of ^{129}I from global fallout

The environmental background level refers to ^{129}I concentrations or $^{129}\text{I}/^{127}\text{I}$ ratios in background areas without direct contamination from nuclear facilities, ^{129}I in such environment only originates from global fallout of weapons testing and long distance dispersion of releases from reprocessing plants. The environmental background level of ^{129}I varies spatially and temporally in relation to the sources, and differs vastly with sample types because of different enrichment factors of iodine. In the present environment, background $^{129}\text{I}/^{127}\text{I}$ ratios range from 10^{-11} to 10^{-8} in the northern hemisphere [20, 26], which are higher than those in the southern hemisphere and the equator area. This is because most of nuclear weapons testing and other nuclear activities, including nuclear fuel reprocessing, have been carried out in the middle latitude of the north hemisphere [27].

1.1.3 Elevated environmental level in contaminated areas directly influenced by nuclear activities

In highly contaminated areas, such as vicinity of nuclear reprocessing plants, nuclear weapons testing and nuclear accident sites, as well as radioactive waste repository sites, $^{129}\text{I}/^{127}\text{I}$ ratios of $10^{-8} \sim 10^{-4}$ in the environment have been reported [28–30].

1.2 Chemical species of ^{129}I and ^{127}I

Once anthropogenic ^{129}I is discharged to environment, like stable ^{127}I , it forms diverse species through complicated

Table 1. Natural level of ^{129}I in samples of pre-nuclear age.

Sample	Location	Year of collection	$^{129}\text{I}/^{127}\text{I}$ ratio ($\times 10^{-12}$)	Age (Ma)	Refs.
Pore waters	Blake Ridge in the Atlantic Ocean		0.17	50	[17]
Springs	Clear Lake area, California		0.03–1.78	40–80	[15]
Pore waters	Peru Margin		0.14–0.99	9–54	[25]
Fore arc fluids	North Island of New Zealand		0.05–1.5	0–75	[25]
Crater lake fluids	Copahue, Argentina		0.70		[21]
Crater lake fluids	White Island, New Zealand		0.28		[21]
Volcanic fluids	Central America		0.50–0.80	15–25	[22]
Algae	Novaya Zemlya	1931	3.69		[25]
Algae	White Sea	1938	1.35		[25]
Algae	Hokkaido	1883	1.40		[25]
Algae	Miyagi	1904	1.87		[25]
Algae	Hokkaido	1883	0.55		[25]
Deep sea water	Gulf of Mexico	1990	1.40		[25]
Deep sea water	Nankai(deep water)	2000	1.49		[25]
Groundwater	Great Artesian Basin, Australia		0.4–7.1		[14]
Loess (63.5 m depth)	Loess Plateau, China		20		[24]

Table 2. Major species of iodine in the environment.

Ecosystem	Main species of iodine	Examples	Refs.
Hydrosphere	Inorganic ions	I^- , IO_3^-	[31]
	Water soluble organic iodine	Humic substance associated iodine	[33]
Atmosphere	Particle associated iodine, <i>i.e.</i> aerosol	I^- , IO_3^- , organic iodine	[32]
	Gaseous organic iodine	CH_3I , CH_2I_2 , $\text{CH}_3\text{CH}_2\text{I}$, CH_2ICl	
	Molecular iodine	I_2	[36]
	Radical/activated iodine	IO , OIO , HOI	[37]
Geosphere (soil and sediment)	Inorganic ions	I^- , IO_3^-	
	Organic matter (humic substances)	Humic acid, fulvic acid and humin	[34, 35]
	Sequentially extracted species	Water soluble, exchangeable, carbonate, organic bound, oxides and residue	[30, 38]
Biosphere (seaweed, tissues)	Inorganic ions	I^- , IO_3^-	[39–41]
	Low molecular weight organic iodine	Triiodothyronine (T3), Tetraiodothyronine (T4), I-amino-acid	
	Biological macromolecules bound iodine	Algin, fucoidan, protein, polyphenol, pigment	

chemical and physical processes and reactions with the surrounding media. In general, iodine exists in inorganic and organic forms in the environment (Table 2). In water, soil, sediment, and aerosol samples, I^- and IO_3^- are the major inorganic species [31, 32], while humic substances associated iodine is the major organic form of iodine in soil, sediment and natural water [33–35]. In atmosphere, molecular iodine (I_2), HI, HIO, as well as some short-lived radicals of iodine (OIO, IO, *etc.*) occur as inorganic form [36, 37]. Plenty of volatile organic iodine compounds occur in the atmosphere, mainly as alkyl iodide, *e.g.* CH_3I , CH_2I_2 , *etc.* Meanwhile, some iodine in the air also exists in particle (aerosol) associate form [32]. Sequential extraction is often used for fractionation of iodine in soil and sediment to separate iodine into water soluble, exchangeable, carbonate, organic bound, oxides and residue fractions [30, 38]. This information is important to elucidate various transfer processes of iodine in the geosphere. In the biosystem, a few work on ^{127}I speciation of biomaterials were reported [39–41]; however, speciation study of ^{129}I in biomaterials has not yet been reported.

2. Recent progress in analytical methods of ^{129}I and its speciation

2.1 Determination of total ^{129}I

Due to the extremely low concentration of ^{129}I in environmental samples ($< 10^{-16}$ g/g), its determination involves great effort on sample pretreatment, pre-concentration and purification, as well as sensitive measurement. Fig. 2 shows a schematic procedure for determination of ^{129}I in three types of samples. The performance of the pre-treatment and separation methods is strongly related to matrix type, sample size, and iodine concentration (Table 3).

Although water samples were generally treated by either direct solvent extraction or precipitation with carrier, organic matter associated iodine present in water always leads to underestimation of ^{129}I concentration since organic iodine can

not be separated by solvent extraction or precipitation. In order to convert organic iodine to inorganic form, ultraviolet (UV) irradiation [42], combustion [43, 44] and alkaline digestion [33] have been used. However, these methods are either tedious and time consuming (> 24 h) or lack the ability to treat a large volume of sample. A simple and highly effective way to decompose organic iodine has been recently reported [45]. In this method, a strong oxidant, potassium persulfate ($\text{K}_2\text{S}_2\text{O}_8$) was utilized in a concentration of 30 mg L^{-1} to decompose organic matter at 60° for 20 h, resulting in a decomposition of more than 95% of organic iodine in more than 500 mL water. It is generally quite hard to isolate iodine from organic liquid, *e.g.* crude oil. A reducing reagent sodium biphenyl ($\text{C}_{12}\text{H}_{10}\text{Na}$) has been utilized to release iodine by breaking covalent halogen bonds, resulting in 60–90% chemical yield of iodine [46, 47].

Oxidizing combustion [48, 49], alkaline leaching, alkaline ashing/fusion, microwave assisted acid digestion and acid distillation have been reported to separate iodine from a variety of solid samples, as summarized in review article [50]. Vanadium oxide (V_2O_5) as a catalyst has been used to improve the combustion efficiency, especially for the materials containing high organic matter [51]. A commercial furnace equipped with four combustion tubes (Raddec Pyrolyser) has been modified and applied to separate iodine with high efficiency [52]. Alkaline fusion/ashing followed by water leaching has been a choice for separating iodine from solid samples due to its low-cost, while compared to combustion method, it is time-consuming and gives relatively lower recovery of iodine [53–55]. Formation of silica acid in the acidification of leachate of fused soil, sediment and rock, makes the following treatment, such as solvent extraction, difficult to handle. Acid digestion has been rarely used because of its major disadvantages consisting of incomplete decomposition of sample matrices, application of high risk HClO_4 , relatively time consuming process, and difficulty to treat large-sized samples (> 5 g) [56–58]. Microwave assisted acid digestion is apparently an alternative method to improve the efficiency of acid digestion for sep-

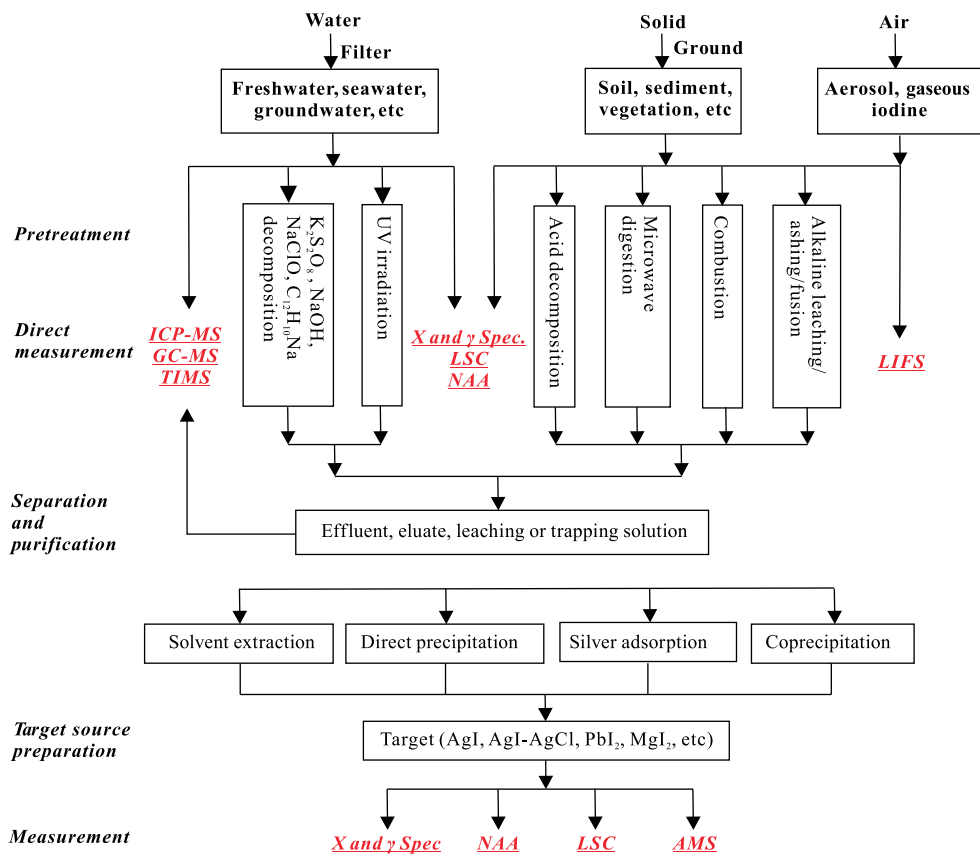


Fig. 2. Schematic diagram of analytical procedures for ^{129}I in environmental samples. LIFS: Laser Induced Fluorescence Spectrometry; X and γ Spec.: X and γ ray Spectrometry; LSC: Liquid Scintillation Counting; NAA: Neutron Activated Analysis; ICP-MS: Inductively Coupled Plasma Mass Spectrometry; GC-MS: Gas Chromatography Mass Spectrometry; TIMS: Thermal Ionization Mass Spectrometry; AMS: Accelerator Mass Spectrometry.

Table 3. Comparison of sample pretreatment and iodine separation methods for ^{129}I measurement in environmental samples.

Sample type	Method	Mass/volume	Chemical yield	Time consuming	Refs.
Pretreatment methods					
Fresh water	UV radiation with HNO_3 and H_2O_2	< 50 mL	NA	> 3 h	[42]
Fresh water	NaOH digestion with assistant of ethanol and ultrasonication	—	NA	> 24 h	[33]
Lake water	$\text{K}_2\text{S}_2\text{O}_8$	> 500 mL	95%	24 h	[45]
Crude oil	Sodium biphenyl ($\text{C}_{12}\text{H}_{10}\text{Na}$)	> 100 mL	60–90%	48 h	[46, 47]
Seawater, freshwater	Anion exchange chromatography–column method	—	80–98%	2–4 mL/min	[61, 78]
Leachate, milk	Anion exchange chromatography–batch method	1–20 L	50–87%	12 h	[79]
Soil, sediment, thyroid, halite, lignite, solid waste	Oxidizing combustion, trapping iodine with $\text{NaOH}/\text{NaHSO}_3$ solution	< 0.1–500 g	> 95%	3–5 h	[48, 49]
Vegetation, soil, meteorites, lunar rock, solid waste	NaOH and Na_2O_2 ashing/fusion, plus hot water leaching	< 1–500 g	50–90%	1–5 h	[53–55]
Uranium ores, solid waste	Acid digestion using HF or HNO_3	< 500 g	43–83%	< 5 h	[56–58]
Glass, rock, lichen	Microwave assistant digestion using TMAH or HNO_3	0.5–1 g	90%	< 1 h	[59, 60]
Separation methods					
Seawater, freshwater, leachate	Solvent extraction using CCl_4 or CH_2Cl_2	< 2 L	40–100%	30 min	[93]
Leachate	Direct precipitation using AgNO_3 (2 mg carrier)	50 mL	70–95%	< 10 min	[62]
Seawater	Silver adsorption (carrier free)	< 100 mL	< 30%	24–48 h	[63, 64]
Water, leachate	AgI – AgCl coprecipitation (carrier free)	< 50 mL	70–80%	< 15 min	[24]

aration of iodine [59, 60]. However, the low capacity and cross contamination of samples using the same digestion containers are the major shortages, which highly restrict its application in ^{129}I determination.

Solvent extraction and precipitation/coprecipitation have been reported to separate iodine from leachate, trap solution, eluate, as well as environmental water samples. Solvent extraction using CCl_4 or CHCl_3 is the most commonly used method to extract iodine from aqueous solution based on

the high solubility of I_2 in these organic solvents. Chemical yield of iodine is related with sample volume, iodine concentration and salt content [61]. This method is easy to operate, but environmentally unfriendly and difficult to operate on board during expedition. Moreover, addition of carrier to sample with low iodine concentration is not favored when analyzing the samples with ultra-low $^{129}\text{I}/^{127}\text{I}$ ratios [24], such as pre-nuclear geological samples. Direct precipitation of iodine as AgI is an alternative method for iodine sepa-

ration, which requires sufficient amount of iodine present in the solution to form AgI precipitate, usually more than 0.5 mg of iodine, leading normally to a recovery of 70–95% for iodine [62]. Notably, anions, such as Cl^- , Br^- , SO_4^{2-} , SO_3^{2-} , S^{2-} interfere with the separation of iodine and are co-precipitated with iodide, therefore need to be removed before measurement.

Silver metal absorption [63, 64] and coprecipitation of AgI with Ag_2O [65] have been reported to separate carrier free iodine from water. However, low recovery of less than 30% for iodine and low capacity of less than 100 mL are the main drawbacks. Based on coprecipitation of AgI with AgCl, a new method for separation of trace amount of carrier free iodine has been reported recently [24]. In this method, all iodine species are firstly converted to iodide, which could be implemented by a procedure of decomposition of organic iodine followed by reduction of high valence states of iodine to iodide using sulfite at $\text{pH} < 2$. Chloride was then added into the prepared solution (leachate, trap solution or eluate), and AgNO_3 was added to co-precipitate iodine as AgI-AgCl. The precipitate was washed with HNO_3 and deionized water to remove Ag_2SO_3 and Ag_2SO_4 in the precipitate. An overall recovery up to 70–80% could be obtained [24]. If high concentration of chloride is present in samples, no more chloride was added, and $\text{NH}_3 \cdot \text{H}_2\text{O}$ in appropriate concentrations are used to wash the excessive AgCl out to a small mass of precipitate. This method has been applied in speciation analysis of ^{129}I in loess profile [66].

For environmental water samples of large volume, iodine is normally pre-concentrated and separated using anion exchange chromatography. In this method, all species of iodine are first converted to iodide, the treated sample is loaded on to an anion exchange chromatographic column; iodide absorbed on the column is eluted using 2.0 mol/L NaNO_3 , and further separated using solvent extraction after addition of iodine carrier, or directly co-precipitated with chloride as AgI-AgCl.

Gamma and X-ray spectrometry, liquid scintillation counting (LSC), neutron activation analysis (NAA), gas chromatography mass spectrometry (GC-MS), inductively coupled plasma mass spectrometry (ICP-MS) and accelerator mass spectrometry (AMS) can be used for measurement of ^{129}I [43, 52, 67–74]. These methods have been presented, compared and reviewed elsewhere [19, 50]. Of these methods, AMS is the most sensitive measurement technique, and the only method for analysis of samples with $^{129}\text{I}/^{127}\text{I}$ atomic ratios lower than 10^{-10} .

2.2 Speciation analysis of ^{129}I

A number of methods have been established for speciation analysis of stable iodine, including high performance liquid chromatography hyphenated with inductively coupled plasma mass spectrometry (HPLC-ICP-MS) and gas chromatography mass spectrometry (GC-MS) [75, 76]. Direct detection techniques including XANES and EXAFS [77] have also shown potential for speciation analysis of iodine in samples with high level of iodine. However, an extremely low concentration of ^{129}I in the environment makes the application of these techniques impossible. Therefore, speciation analysis of ^{129}I has to be implemented by first separation of

different species of iodine in the samples followed by determination of ^{129}I in each fraction. An overview of methods for ^{129}I speciation analysis in environmental samples have been published in 2009 [19]. A remarkable progress on speciation analysis of ^{129}I has been achieved in the past few years, and is reviewed below.

Anion exchange chromatography for water and other liquid samples, sequential extraction for soil and sediment and multiple stages filtration for atmospheric samples are the major approaches for speciation analysis of ^{129}I . Some modifications on these methods have been made aiming to improve chemical yield of iodine and purity of separated iodine species, as well as to eliminate cross contamination of different species of iodine. In water samples, iodine occurs as iodide (I^-), iodate (IO_3^-) and soluble organic iodine (SOI). Anion exchange chromatography has been used to separate these species from aqueous solution by column and batch methods [61, 78, 79], which is based on the high affinity of iodide on the strong basic anion exchange resin, wherein the affinity of iodate is very low. The content of organic iodine can be obtained by the difference between total iodine and total inorganic iodine [33, 78]. Salinity influences capacity of the resin for iodide retention due to competitive adsorption of other anions, such as Cl^- and Br^- , with iodide on functional group of resin. To avoid loss of iodine during loading, a long column or less volume of water is used when analyzing high salinity water samples. For seawater with salinity of 35, less than 400 mL water can be treated with an anion exchange (e.g. AG 1- $\times 4$, 50–100 mesh) column of 10 mm $\varnothing \times 200$ mm without measurable loss of iodide during loading. In open sea water, organic iodine is normally minor, while in fresh water and coastal seawater it might account up to 90% of total iodine [31]. In this case, non-anion organic iodine may flow through the column along with iodate, and some anion organic iodine retained on the column or eluted to iodide fraction, resulting in overestimation of concentrations of stable iodate and iodide ($^{127}\text{IO}_3^-$ and $^{127}\text{I}^-$). To solve this problem, $^{127}\text{I}^-$ and $^{127}\text{IO}_3^-$ can be measured by HPLC-ICP-MS, while organic ^{129}I can be removed during solvent extraction separation because organic iodine does not follow the inorganic iodine in the cycle of extraction and back extraction of iodine (Fig. 3).

For speciation analysis of ^{129}I in soil and sediment, conventional sequential extraction procedure has to be modified considering the volatility of iodine in acidic solution and presence of oxidants. For example, H_2O_2 - HNO_3 solution under heating is often used to decompose organic matter for separation of organic associated elements. In this medium, the released iodine will be converted to I_2 , resulting in complete loss of iodine through volatilization of gaseous I_2 from the solution. Thus, NaOH or TMAH solution has been utilized in the modified procedure to extract organic matter from soil and sediment [66]. Recently, a method to separate iodine associated humic acid and fulvic acid has been reported [34], which is implemented by extracting both forms of organic iodine with 5% tetramethylammonium hydroxide (TMAH) and then separating humic acid from the leachate by precipitation under acidic conditions. Another procedure has also been applied to extract ^{129}I associated with different types of humic substances by successive extraction using alkaline, glycerol and citric acid-alkaline system (Table 4) [80]. In this procedure, water extractable colloid,

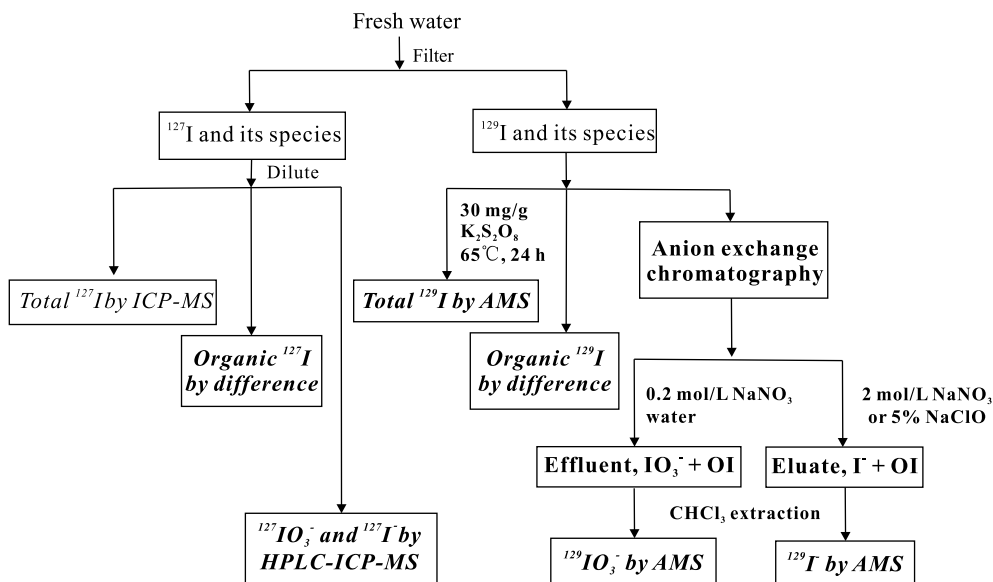


Fig. 3. Diagram of analytical procedure for speciation analysis of ^{129}I in water.

ten fulvic acids and eight humic acids were obtained. In general, the sequential extraction procedure is carried out manually, which does not reflect the real situation in nature. An automatically dynamic solvent extraction system using soil column has been reported for speciation analysis of plutonium and americium in soil and sediment [81], which is also potentially useful for extraction of ^{129}I species in soil and sediment. In seaweed, iodine is present in the form of both inorganic ions and biological macromolecules. Hou *et al.* [39] proposed a procedure for speciation analysis of stable iodine in seaweed, by separating water soluble iodide, iodate, and various biological macromolecules, including algin, fucoidan, protein, polyphenol, and pigment from fresh seaweed [41]. However, speciation analysis of ^{129}I in vegetation has not yet been reported. This situation might be changed by modifying the methods for speciation analysis of ^{127}I in vegetation, combining sensitive determination methods of ^{129}I .

Chemical species of iodine in air are much more complicated. In general, iodine exists in three categories, *i.e.* particulate associated iodine (in forms of iodide, iodate, organic iodine), inorganic gaseous iodine (I_2 , HI, HIO, *etc.*), and organic gaseous iodine (CH_3I , $\text{CH}_3\text{CH}_2\text{I}$, CH_2IBr , *etc.*). Although anthropogenic ^{129}I can provide a unique approach in atmospheric research, analytical method for speciation analysis of atmospheric ^{129}I is still limited [82, 83]. So far, iodine species in air are often sampled by an air sampler equipped with sequentially connected filters and cartridges driven by a vacuum pump, a glass fiber filter for aerosol, followed by a charcoal cartridge for gaseous iodine with collection efficiency of approximately 94% [84, 85]. Efforts on determination of specific species of ^{129}I in atmosphere have also been made by selectively collecting I_2 from air using a denuder coated with α -cyclodextrin. A collection efficiency of 95% for I_2 has been obtained [36]. This method has been utilized for analysis of $^{129}\text{I}_2$ in air by modifying the system to improve the sampling capacity and extending the sampling time. Field investigation of $^{129}\text{I}_2$ concentration in air based on this method is expected in combination with highly sensitive AMS measurement of ^{129}I .

Besides anion exchange chromatography, another two practical analytical methods have been proposed for separating iodine species from water. Hou *et al.* [86] have reported a simple procedure to separate iodide from water samples using solvent extraction and selective oxidation of iodide to I_2 using NaClO. In the conventional solvent extraction procedure, the sample has to be acidified to $\text{pH} < 2$ for oxidizing iodide to I_2 using NaNO_2 or H_2O_2 , or reducing iodate to I_2 using $\text{NH}_2\text{OH}\cdot\text{HCl}$. However, iodide and iodate can react with each other at $\text{pH} < 2$ to form I_2 , which makes the separation of iodine species impossible. NaClO is a strong oxidant and has been widely used to oxidize iodine to high oxidation state (IO_3^- or IO_4^-). By controlling the amount and concentration of NaClO added to the water sample and pH value at 4–8, iodide can be quantitatively oxidized to I_2 and extracted into the organic phase, while iodate and organic iodine remain in water phase. This approach has been successfully applied for speciation analysis of ^{129}I in both seawater and fresh water. The separation of iodide and total inorganic iodine just takes less than one hour per sample ($< 1\text{ L}$), which significantly improves the separation efficiency, and is useful for in situ separation as well as emergency analysis of short-lived radioiodine. However, this method is only suitable for water with high iodine concentration or with addition of ^{127}I carrier, because the recovery of iodine in solvent extraction process is very low for normal environmental water samples in which iodine concentration is low.

A rapid method using single step coprecipitation has been reported for selective precipitation of iodide from seawater for speciation analysis of ^{129}I [86, 87]. This method takes the feature of different solubility products of AgI ($K_{\text{sp}} = 8.52 \times 10^{-17}$), AgIO_3 ($K_{\text{sp}} = 3.17 \times 10^{-8}$) and AgCl ($K_{\text{sp}} = 1.77 \times 10^{-10}$) to selectively precipitate iodide from seawater while leaving iodate in the solution. By controlling pH of the seawater, the amount of NaHSO_3 and Ag^+ added to the seawater, iodide can be quantitatively precipitated as AgI , while only less than 3% iodate is co-precipitated. Salinity does not affect the precipitation of iodide, but the amount of iodate (as AgIO_3) cross-over to AgI - AgCl co-precipitate increases with the decreased salinity, therefore this method

Table 4. Procedure for speciation analysis of iodine (^{129}I or ^{127}I) in solid samples.

Sample type	Fraction	Subfraction	Extraction procedure	Refs.
Soil and sediment for both ^{129}I and ^{127}I	Water soluble		Water, RT ^a , 1 h, sample pH.	[19, 30, 34, 38]
	Exchangeable		1 M $\text{NH}_4\text{Ac-HAc}$, 20 °C, 2 h, sample pH; or 1.0 M NaAc in 25% HAc (v/v), 20 °C, 1 h, pH 4.	
	Carbonate Metal oxides		1 M $\text{NH}_4\text{Ac-HAc}$, 20 °C, 2 h, pH 5. 0.04 M $\text{NH}_2\text{OH}\cdot\text{HCl}$ and 0.01 M NaHSO_3 in 25% HAc (v/v), 80–100 °C, 6 h, pH 3.	
	Residue	Humic substance Humin and minerals	Combustion, 650 °C, 3 h or NaOH fusion, 550 °C, 8 h. 5% TMAH, RT, 4 h, pH 14. Combustion, 650 °C, 3 h or NaOH fusion, 550 °C, 8 h.	
Soil for both ^{129}I and ^{127}I	Fulvic acids (FA) and humic acids (HA)	FA1	Step 1: 1 M HCl, RT, 1 h, pH 1–2. Centrifuge, FA1 in supernatant; Step 2: Load FA1 onto 15 mL XAD-8 resin, back-eluted with 0.1 M NaOH and water, then acidify to pH 1.0 and add HF to a final concentration of 0.3 M HF. Step 3: Adjust pH to 7 with 1 M NaOH, 0.1 M NaOH, N_2 atmosphere, RT, overnight; 6 M HCl, RT, 12 h, pH 1. Centrifuge, FA2 in supernatant; FA2 is processed in by the same method as FA1 (step 2) Step 4: Combine FA1 and FA2 fractions and purify with a third XAD-8 column. Then pass through a H^+ -saturated cation exchange resins to remove the cation. Step 5: 0.1 M KOH under N_2 purging, KCl attaining a concentration of 0.3 M K^+ . 6 M HCl, centrifuge, HA1 in supernatant; 0.1 M HCl/0.3 M HF, stir overnight; wash with Milli-Q water.	[80]
		FA2	Step 6: repeat steps 1–5 for another four times. Dry the soil residue, 1 : 1 (v/v) glycerol in de-gassed Milli-Q water, 20 h; repeat this step for HA7.	
		HA1	0.5 M citric acid, N_2 atmosphere, 20 h; NaOH. Water, 3 days; spiral-wound 1 kDa SOC 1812 cartridge; an Amicon 8400 stirred-cell ultrafiltration unit with a 1 kDa regenerated cellulose filter at 275 kPa.	
		FA 3–10 and HA 2–5 HA 6,7		
		HA 8		
		Water extractable colloid		
Seaweed for ^{127}I	Water soluble	Soluble organic	Water, RT, 3 h. 40 mg/mL Bi^{3+} , 8 mg/mL S^{2-} ; $\text{N}_2\text{H}_4\cdot\text{H}_2\text{SO}_4$, 40 mg/mL Bi^{3+} , 8 mg/mL S^{2-} . Precipitate after adding 40 mg/mL Bi^{3+} , 8 mg/mL S^{2-} . Precipitate after adding $\text{N}_2\text{H}_4\cdot\text{H}_2\text{SO}_4$, 40 mg/mL Bi^{3+} , 8 mg/mL S^{2-} . Residue.	[39]
		I^- IO_3^-		
Seaweed for ^{127}I	Biological macromolecules	Algin	Boiling deionized water; ethanol to 30%.	[41]
		Fuoidan	Boiling deionized water; ethanol to 70%.	
		Protein	Acetone for three times; 1% CaCl_2 and 0.5% caffeine; tris-HCl (pH 8.0) containing 0.1% SDB and 0.05% NaN_3 , 48 h; $(\text{NH}_4)_2\text{SO}_4$. Ethanol, PVPP column chromatography. Acetone, RT, 2 h; water.	
		Polyphenol Pigment		

a: RT refers to room temperature.

is not suitable for the speciation separation of iodine in fresh water and low salinity water. Since a large amount of chloride is also precipitated, which has to be removed from AgI precipitate prior to AMS measurement, this can be implemented by washing the co-precipitate with diluted $\text{NH}_3\cdot\text{H}_2\text{O}$ because AgI is not soluble in diluted $\text{NH}_3\cdot\text{H}_2\text{O}$, while AgCl is highly dissolved in $\text{NH}_3\cdot\text{H}_2\text{O}$, even in 5% $\text{NH}_3\cdot\text{H}_2\text{O}$. The concentration of $^{129}\text{IO}_3^-$ can be obtained by the difference of $^{129}\text{I}^-$ and total inorganic ^{129}I , which is obtained using the same method but converting all inorganic iodine to iodide before addition of Ag^+ . This procedure is rapid, simple, and suitable for in situ separation, especially on board ship during expedition.

GC-MS, conventionally employed for speciation analysis of ^{127}I , has been modified and used for ^{129}I in high-level up to a concentration of 2.3×10^8 molecule m^{-3} of $^{129}\text{I}_2$ in air [72]. Zhang *et al.* [43] reported a method for determination of iodide, iodate and organic iodine in groundwater using chemical separation and derivation of iodine combined with GC-MS measurement, in which total iodine was separated by combustion method to convert all iodine to gaseous I_2 that was trapped into water. ^{129}I concentrations in the trap solution (for total iodine) and original water (for total inorganic iodine) were measured by first reducing all inorganic iodine to iodide, followed by derivation of iodide to 4-iodo-*N,N*-

Table 5. List of available ^{129}I standard materials.^a

Standard code	Matrix/material	Sampling location/type	^{129}I concentration Bq g ^{-1b}	$^{129}\text{I}/^{127}\text{I}$ ratio at/at	Value type ^c	Refs.
NIST SRM 4949C	0.01 M NaOH		3451 ± 22	NA	CV	
NIST SRM 3231 (High Level)	0.5% TMAH	Level I	NA	$(0.981 \pm 0.012) \times 10^{-6}$	CV	
		Level II	NA	$(0.982 \pm 0.012) \times 10^{-8}$	CV	
NIST SRM 3230 (Low Level)	0.01 mol/L NaOH	Level I	NA	$(4.920 \pm 0.062) \times 10^{-10}$	CV	
	0.006 mol/L Na ₂ SO ₃	Level II	NA	$(0.985 \pm 0.012) \times 10^{-12}$	CV	
		Blank	NA	$(16 \pm 5) \times 10^{-15}$	CV	
IAEA 418	Mediterranean sea water	Mediterranean Sea	$(3.2 \pm 1.3) \times 10^{-7}$ Bq L ⁻¹	NA	CV	
NIST SRM 4357	Ocean Sediment	Irish Sea	$(6-12) \times 10^{-6}$	NA	IV	
NIST SRM 4359	Seaweed Radionuclide	Irish coast and White Sea	$(14.8-15.1) \times 10^{-6}$	NA	IV	[95]
IAEA 375	Soil (0–20 cm)	Brjansk, Russia	$(1.3-2.1) \times 10^{-6}$	1.27×10^{-7}	IV&LV	[96, 97]
IAEA 414	Mixed Fish	Irish Sea and North Sea	$(8-12) \times 10^{-6}$	NA	IV	[98]
IAEA 437	Soft tissues of mussels (<i>Mytilus galloprovincialis</i>)	Mediterranean Sea	$(0.8 \pm 0.1) \times 10^{-6}$	NA	LV	[99]
NIST SRM 2709	Soil	San Joaquin	$(4.9 \pm 1.3) \times 10^{-9}$	1.8×10^{-10}	LV	[100]
IAEA 446	Seaweed	Baltic Sea	$(130 \pm 20) \times 10^{-6}$	NA		

a: Data are from certificates of the standard issued by National Institute of Standard and Technology (NIST, www.nist.gov) and International Atomic Energy Agency (IAEA, www.iaea.org), as well as literatures cited in the table.

b: The values in italics are given as range of values.

c: Certified value (CV); Information value (IV); Literature value (LV).

NA: Not available.

dimethylaniline and measured by GC-MS. ^{129}I concentration in iodide form was measured by GC-MS after direct derivation of iodide. The concentration of ^{129}I in iodate was calculated by the difference of total inorganic and iodide forms. Organic ^{129}I concentration was calculated as the difference between the total ^{129}I and total inorganic ^{129}I (iodide-129 plus iodate-129). The detection limits of the method for iodide-129 and iodate-129 were 10.3 ng $^{129}\text{I}/\text{L}$ [43]. Due to the high detection limit, this method can be only used for analysis of high-level waste samples.

Laser induced fluorescence spectroscopy (LIFS) has potential to directly measure gaseous molecular iodine (I_2). In this method, $^{129}\text{I}_2$ and $^{127}\text{I}_2$ are excited by laser to emit fluorescence signals of different wavelengths, the intensities of the signals corresponding to I_2 concentration for ^{129}I and ^{127}I , respectively. A detection limit of this method of 8.6×10^{-13} g m⁻³ or 4.0×10^9 atoms m⁻³ for $^{129}\text{I}_2$ has been reported [70], which is one order of magnitude higher than that of GC-MS [72]. This technique is supposed to be used to on-line monitor $^{129}\text{I}_2$ that is released during dissolution of spent nuclear fuel from a reprocessing plant [88, 89]. However, so far the technique is still at laboratory level, and its application in the measurement of $^{129}\text{I}_2$ in real samples has not yet been reported.

2.3 Carrier, chemical yield tracer and standards

To improve the chemical yield of ^{129}I in chemical separation and to obtain sufficient amount of iodine for measurement of ^{129}I , stable iodine (^{127}I) is normally added as carrier. However, the carrier might contain some levels of ^{129}I impurity, which introduces extra ^{129}I to the sample, resulting in high analytical uncertainty. Therefore, ^{129}I level ($^{129}\text{I}/^{127}\text{I}$ ratio) in carrier should be as low as possible. An iodine reagent produced by Woodward Inc. (USA) has been widely used as iodine carrier in ^{129}I analysis due to its low $^{129}\text{I}/^{127}\text{I}$ ratio down to 2×10^{-14} [90]. However, elevated $^{129}\text{I}/^{127}\text{I}$ ratios (to 10^{-13}) in this reagent have also been observed, which might be attributed to a contamination of the reagent by anthropogenic ^{129}I from the air during the storage in laboratory

where high ^{129}I level exists in atmosphere, such as in the European laboratories [19]. Therefore, it is necessary to assay ^{129}I level in the iodine reagent prior to use.

As a key issue in chemical separation, chemical yield of ^{129}I is important for the determination of ^{129}I , which is often monitored by gravimetric method [91] and radioisotopic tracers ^{131}I or ^{125}I [56, 92–94]. Gravimetric method can only be used when highly excessive amount of stable iodine carrier is added to the samples prior to separation. The obvious disadvantage of this method is that only a final yield can be measured after iodine is separated, purified, and converted to precipitate form, e.g. AgI. Yields of iodine in each step and iodine in the solution are not measurable. These drawbacks can be overcome by use of radioisotopes of iodine as yield tracer. Due to the suitable half-lives and gamma rays emission that can be easily measured by gamma spectrometry, ^{131}I ($T_{1/2} = 8.02$ days) or ^{125}I ($T_{1/2} = 59.4$ days) has been applied as yield tracer by addition to the solution and equilibrated with iodine isotopes (^{129}I and ^{127}I) in the original samples through redox reactions. However, it has been reported that ^{131}I tracer normally contains some amount of ^{129}I , because ^{129}I can be produced during the production of ^{131}I by neutron-induced fission of ^{235}U and neutron activation of Te isotopes [94], consequently ^{131}I is not suitable as a chemical yield tracer of ^{129}I , especially for the determination of low-level ^{129}I . ^{125}I is therefore recommended. It is worthy to mention that the species of ^{125}I in tracer solution should be checked when it is used as a tracer for speciation analysis of ^{129}I .

Table 5 lists the commercially available ^{129}I standard materials, as well as the certified reference materials with reported ^{129}I values. A series of ^{129}I standards solutions with $^{129}\text{I}/^{127}\text{I}$ ratios ranging from 10^{-6} to 10^{-12} are commercially available from the National Institute of Standard Technology, USA (NIST), which can be used as calibration standard for ^{129}I measurement. ^{129}I standard solution with high $^{129}\text{I}/^{127}\text{I}$ ratio up to 10^{-4} is also available from NIST, which can be used for the analysis of sample with high ^{129}I concentration using radiometric methods. The early standards of ^{129}I were often prepared from this standard solution by sequential dilution using ^{127}I carrier for AMS and RNAA

measurement of ^{129}I . A certified reference material of natural seawater for ^{129}I , IAEA-418, has been issued by the IAEA and is commercially available. A few standard reference materials of soil, sediment, fish and seaweed with information values of ^{129}I concentration and/or $^{129}\text{I}/^{127}\text{I}$ ratio or reported ^{129}I level in literatures are also commercially available [95–100]. Although these standards include seawater, sediment, seaweed, soil, and biological tissue, they still can not satisfy the analytical requirement for a large number of complex environmental and geological samples. In addition, no standard reference material is provided with ^{129}I speciation information is available.

3. Applications of ^{129}I speciation in environmental research

Once anthropogenic ^{129}I is released to the environment, it disperses from the source, incorporates in various environmental media and participates in various environmental processes. Major pathways of these processes include the emission of gaseous organic and inorganic iodine compounds into the atmosphere from nuclear facilities and from the oceans where anthropogenic ^{129}I was discharged to, conversion of iodine species in the atmosphere, deposition of iodine species from the atmosphere to the lands, uptake and accumulation of iodine in living organisms, and adsorption and association of iodine to the components of soil and sediment [101]. Accurate assessment of these processes necessitates consideration of the speciation of iodine [102].

In this article, recent applications of ^{129}I speciation in various environmental processes are reviewed. In hydrosphere, speciation analysis of ^{129}I and ^{127}I has been applied to study conversion mechanism of iodine species in European seas [2, 10] and in groundwater at Savannah River Site (SRS) [103]. In soil and sediment, the main factors controlling migration and retention of iodine can be also investigated by speciation analysis of ^{129}I . Transfer of atmospheric iodine could be elucidated by wet and dry deposition of ^{129}I , in which ^{129}I was used as an atmospheric tracer for air masses movement. The feasibility of utilizing ^{129}I to trace organic carbon cycling has been proposed by speciation analysis of ^{129}I in estuary water. Although no application of ^{129}I speciation analysis on the biosystem has been reported, great potential exists for studies on elaboration of metabolism mechanism of iodine in organisms.

3.1 Conversion of iodine species in water system

Iodine species can be used to investigate the environmental behavior and geochemical cycle of iodine. Despite the factors affecting transformation of iodine species in water systems are known, such as pH, E_h , dissolved oxygen concentration, concentration of reductant (e.g. Fe^{2+} , H_2S), biological activity and light, the conversion mechanism of iodine is still not well understood. Reduction of iodate to iodide, for instance, is a thermodynamically unfavorable process, while iodide is often measured in coastal and surface water in the ocean. Many investigations have been carried out to explore the iodide formation in the ocean by speciation analysis of stable iodine [104, 105]; however, it is difficult to identify the newly produced forms from the previously

existing species, consequently offering no explanation of the conversion pathways and processes. Anthropogenic ^{129}I discharged from reprocessing plants at La Hague (France) has been successfully applied as tracer to study mechanism of iodine species conversion in the English Channel, North Sea and Baltic Sea [2, 78, 106, 107]. The chemical speciation analysis of ^{129}I and ^{127}I in surface water of the North Sea showed a significant increase of I^-/IO_3^- ratio for both ^{129}I and ^{127}I in the water at the Dutch coast and German Bight compared to those in the English Channel, demonstrating a fast iodate reduction to iodide at the Dutch coast. Nevertheless, the oxidation of iodide to iodate in the open sea presented a slow process based on the relatively stable I^-/IO_3^- ratio [2]. Baltic Sea shows a distinct pattern of iodine species. $^{129}\text{IO}_3^-/^{127}\text{IO}_3^-$ ratio in Baltic seawater was much higher than $^{129}\text{I}^-/^{127}\text{I}^-$ ratio, but close to the level in the Kattegat. This was attributed to the fact that both ^{127}I and ^{129}I in iodate in the Baltic Sea water originated from the Kattegat [78, 107]. Most of iodate in the Kattegat seawater was reduced to iodide when transported to the Baltic Sea, considering that iodine mainly occurs as iodide in the anoxic water of the Baltic Sea. As a consequence, $^{129}\text{I}^-/^{127}\text{I}^-$ ratio in the Baltic Sea is much lower than that in the Kattegat and the North Sea. The water in the Kattegat is a mixture of high ^{129}I water from the North Sea and low ^{129}I water from the Baltic Sea [106, 107].

It has been proposed that many processes are related to the conversion of iodine species in seawater, such as biological process involving microorganism and seaweed [32, 108], chemical process involving reductive substance indicated by low E_h value in the water like Baltic Sea water [2], as well as photochemical process [37]. A high ratio of iodide/iodate in the surface water compared with the deep water observed in the Arctic Sea showed that the biological process might be the main reason causing the reduction of iodate, where the E_h of seawater from the deep sea and surface are the same (unpublished data). Furthermore, a significantly high correlation between the iodide/iodate ratio and concentration of chlorophyll in seawater was observed in the Arctic seawater, which also confirmed that the reduction of iodate to iodide in the Arctic Sea is a biologically controlled process. Although many investigations have proposed that the biological process might be the major process for the conversion of iodine species in seawater, but it is still not clear how iodate was transformed to iodide through organisms.

Besides studies on ocean system, ^{129}I speciation also has a potential application to explore the origin of iodine in terrestrial water system. Unfortunately, only few data was available for ^{129}I speciation in lake water [109].

In addition to natural systems, the speciation analysis of iodine showed significant implication for remediation and protection of groundwater in some specific areas. Investigations on speciation of ^{129}I and ^{127}I in groundwater at Savannah River Site (SRS) have been conducted. At this site, ^{129}I had been released to the environment as waste during operation of a spent nuclear fuel reprocessing plant between 1955 and 1988, which contaminated surrounding groundwater. Results showed that equilibrium of ^{129}I with stable ^{127}I was reached with $^{129}\text{I}/^{127}\text{I}$ ratios of 0.03 for I^- , IO_3^- and organic iodine within decadal time. The fast conversion among iodine species in groundwater system at SRS was

proposed to be related to the significantly changed chemistry of down-gradient groundwater affected by the strongly acidic waste. Iodine transportation in SRS groundwater from upstream to downstream was highly pH-dependent through transforming iodine species from iodide to iodate or organic iodine [110, 111], which confirmed again the fast conversion among the three iodine species. Compared to fresh water, the relatively high fraction of iodate (27.3%) and organic iodine (23.9%) were also regulated by chemical and biological factors, other than pH and E_h , in the studied system [43]. From the point of environmental remediation at SRS, by injecting base solution, ^{129}I could be converted to iodate form, which is easily adsorbed on soil and sediment [111].

3.2 Migration and retention of iodine in soil and sediment

Migration and bioavailability of iodine are of high concern not only because iodine is a micronutrient to humans and radioiodine (^{131}I and ^{129}I) is high hazard to thyroid, but also due to the implication for disposal of radioactive waste. Iodine species in soil and sediment is the main factor controlling the processes of retention, mobilization and transportation of iodine in the environment. Fractionation analysis of ^{129}I in loess profile of Chinese loess plateau [66] has showed similar $^{129}\text{I}/^{127}\text{I}$ ratios in organic and leachable phases, implying that organic associated iodine might be also mobile. Even though the organic associated and leachable iodine constitutes for 80–90% of the total iodine for both ^{129}I and stable iodine and are more labile than those in oxides and residue phases, rapid decrease of $^{129}\text{I}/^{127}\text{I}$ ratios with depth indicated downwards transportation of iodine is a slow process for all fractions. In the loess profile, ^{129}I mainly originated from global fallout; the leachable ^{129}I including water soluble, exchangeable and carbonate iodine, accounts for 12–19% of total ^{129}I , while higher percentage of water soluble ^{129}I might occur in soil with specific source of ^{129}I . Speciation analysis of ^{129}I and ^{127}I in soil contaminated by a small reprocessing plant release has shown that 2.5–4% of ^{127}I and 38–49% of ^{129}I were in water soluble form [112]. In Chernobyl accident contaminated soil, different concentration but still as high as 10–20% of ^{129}I was in water soluble and exchangeable form [30]. These results indicated that a large portion of ^{129}I compared to ^{127}I occurs as readily mobile iodine that can be taken up and accumulated by plants, and subsequently transferred to humans. Different soil-to-vegetation transfer factors as indicator of bioavailability of natural ^{127}I (0.006–0.27) and anthropogenic ^{129}I (0.01–1.05) have been reported [26, 113]. In contrast to ^{127}I , large fraction of water soluble ^{129}I and transfer factors of ^{129}I represent higher risks of radioactive iodine.

It has been proposed that the presence of organic matter facilitates the retention of iodine in soil and sediment. Mobility of iodine species follows the order of $\text{I}^- > \text{IO}_3^- >$ organic iodine; and for organic iodine, LMW $>$ HMW $>$ particulate organic iodine (LMW, low molecular weight; HMW, high molecular weight) [43, 110, 111, 114]. High level of organic iodine has been observed in the lake sediment collected in central Sweden accounting for 47–95% and 57–82% for ^{129}I and ^{127}I , respectively [38]. For relatively readily mobile inorganic

iodine ions in soil and sediment, I^- and IO_3^- , incubation experiments have shown that 72–77% of the newly introduced $^{129}\text{I}^-$ or $^{129}\text{IO}_3^-$ was irreversibly sequestered into the organic rich riparian soil [114], and they can be retarded presumably by forming covalent bonds with surface organic carbon binding sites [43]. When iodine occurs in highly mobile organic species, such as the organic-colloidal form and organic ^{129}I with low molecular weight, retention of iodine by soil organic matter might be moderated, and remobilization of ^{129}I associated organics and oxides in the soil might happen during soil erosion and storm run-off [35, 80].

It is well known that most of the iodine in soil and sediment combines with humic substances, including humic, fulvic acid and humin, which significantly influence iodine mobility [35, 115]. Investigation on organic iodine in different soils and sediments showed diverse distribution patterns in humic, fulvic acid and humin, which are related to the surrounding circumstances. It has been observed that in soil samples 37–50% of iodine isotopes (both ^{129}I and ^{127}I) are associated with humic acid, about 10% with fulvic acid, and 3–15% with humin and residues. In lake sediment, different distributions of iodine species (^{129}I and ^{127}I) were observed for oxic and anoxic sediments. In an oxic lake sediment, it was observed that 31%, 10% and 21% of ^{129}I and 21%, 8% and 43% of ^{127}I were associated with humic acid, fulvic acid and humin, respectively; while in an anoxic sediment 5%, 44% and 12% of ^{129}I and 30%, 16%, and 42% of ^{127}I were associated with humic acid, fulvic acid and humin, respectively. The fraction distribution of iodine isotopes in the oxic sediment is similar to that in soil, but different from that in anoxic sediment, indicating that association of iodine with soil and sediment is circumstance dependent. This result is useful to assess iodine retention and transfer in the environment, especially at dumping sites of radioactive waste.

3.3 Dispersion of iodine in atmosphere

Atmospheric chemistry of iodine is important for geochemical cycle of iodine, primary particle formation, and depletion of ozone in the stratosphere [116]. Iodine emission from oceanic and terrestrial systems are major sources of iodine in the atmosphere [117], while due to the complicated atmospheric iodine chemistry, the processes are still not well understood related to the speciation conversion, interaction among iodine species and with atmospheric components, and transport pathway. Atmospheric ^{129}I originating from gaseous releases and re-emission of ^{129}I from the seas to where ^{129}I has been discharged from the spent nuclear fuel reprocessing plants can take part in all atmospheric processes, such as speciation transformation, association to aerosol and capture in precipitation, as well as final deposition to earth surface. Few studies have been conducted using ^{129}I species as atmospheric tracer to elucidate these chemical and physical processes.

Wet deposition is the dominant pathway to transfer iodine from atmosphere to land and ocean. The concentration of ^{129}I in precipitation over Europe ranges between 10^8 and 10^{10} atoms L^{-1} with significant spatial and temporal variations [118–120]. Compared to the ^{129}I concentration in USA with a range of $(0.07\text{--}0.67) \times 10^8$ atoms L^{-1} [121], European atmosphere with 2–3 orders of magnitude higher ^{129}I

has been strongly influenced by the ^{129}I discharges from the two European nuclear reprocessing facilities. This deduced annual wet deposition of about $60\text{ g }^{129}\text{I}$ in Sweden and Denmark, which accounts for less than 1% and 0.05% of the total annual gaseous and liquid discharges from the Sellafield and La Hague Facilities, respectively [122]. Large variation of ^{129}I concentration in precipitation in Europe has been attributed to different sources of moisture and precipitation rate. For instance, in northern Europe, Norway and Germany receive the rain influenced directly by the North Sea with strong ^{129}I contamination, while the precipitation in Italy and Spain is mainly from the West Atlantic Ocean containing much less ^{129}I [118]. According to the correlation between ^{129}I and the source of air masses, it should be feasible to utilize ^{129}I to trace the sources and pathway of air masses.

By speciation analysis of ^{129}I and ^{127}I in a time series of precipitation collected from Risø, Denmark during 2001–2006 [123], it has been observed that the concentrations of total ^{129}I in precipitation were $(2.8\text{--}56.3) \times 10^8\text{ atoms L}^{-1}$, which was in the same range as those in Norway $((16\text{--}41) \times 10^8\text{ atoms L}^{-1}$, in 2003) and Sweden $((10\text{--}57) \times 10^8\text{ atoms L}^{-1}$, during 2001 to 2002). 50–99% of ^{129}I in the precipitate was in the form of iodide, while iodate was the major species of ^{127}I , accounting for 43–93% of total ^{127}I . By comparing seasonal variation of ^{129}I concentrations and $^{129}\text{I}/^{127}\text{I}$ ratios with the discharge history of ^{129}I from the reprocessing plants to marine and atmosphere, it was concluded that ^{129}I in the northern Europe mainly originated from the re-emission of ^{129}I from the sea, especially the near-shore area of the North Sea and the Norwegian Sea. This conclusion has also been confirmed by speciation analysis of ^{129}I and ^{127}I in atmosphere in Foehr, Germany [124], where 15% of ^{127}I and 18% of ^{129}I were associated with particles ($> 0.1\text{ }\mu\text{m}$), 45% of ^{127}I and 43% of ^{129}I in inorganic gaseous form and about 40% for both ^{127}I and ^{129}I in organic gaseous form. The $^{129}\text{I}/^{127}\text{I}$ ratios in these iodine species were significantly different, following the order: particle-bound iodine $(8.4 \times 10^{-7}) >$ organic iodine $(3.1 \times 10^{-7}) >$ inorganic fraction (1.2×10^{-7}) . Distribution of iodine species in the atmosphere also indicated that ^{129}I at Foehr was dominated by local source, while global aerosol was just of minor importance [124].

^{129}I concentration in aerosol collected at Seville, Spain in 2001 has been reported to be $(1.8\text{--}19.3) \times 10^4\text{ atoms m}^{-3}$, which showed a less influence by emissions from reprocessing plants than that in north Europe [125]. Although 2–3 orders of magnitude higher ^{129}I concentrations of $(40\text{--}930) \times 10^4\text{ atoms m}^{-3}$ [126] in aerosol collected at Vienna, Austria in the same year were observed compared to that in the southern Europe (Spain), the influence of air emission of ^{129}I from reprocessing plant was also not evident. Even in northern Europe, for instance Sweden, only liquid discharge of ^{129}I from the reprocessing plants to the seas is a dominant impact, instead of gaseous source [127]. The previous works only focus on the horizontal transportation of atmospheric ^{129}I , vertical dispersion of ^{129}I in different altitudes has not yet been well investigated. A recent investigation showed an influence of altitude on the concentrations of ^{129}I and $^{129}\text{I}/^{127}\text{I}$ ratios [128], about one order of magnitude lower ^{129}I concentrations (10^4 atoms m^{-3}) at

high altitude areas (Sonnblick and Zugspitze, eastern Alps, about 3000 m ASL) was observed in contrast to about 10^5 atoms m^{-3} in lower altitude station (Vienna, Austria, 202 m ASL). This might be attributed to the source term of ^{129}I at different altitude, because less ^{129}I from reprocessing air emission and re-emission from seawater can be injected to high altitude atmosphere. Furthermore, clouds scavenging and precipitation are possible ways to reduce ^{129}I concentration in the high altitude. Temporal variation of ^{129}I at Sonnblick and Zugspitze was related to the sources of air masses. Highest ^{129}I concentrations were observed to be $(7.6 \pm 0.3) \times 10^4\text{ atoms m}^{-3}$ during 23rd February to 1st March at Sonnblick, and $(7.5 \pm 0.8) \times 10^4\text{ atoms m}^{-3}$ during 1st–7th May at Sonnblick. Using back trajectory analysis, the sources of ^{129}I at both sites were elucidated. Sonnblick and Zugspitze were influenced mainly by air masses from southeast Europe and northwest Europe, respectively, which contacted with surface of Mediterranean Sea and Baltic Sea separately before they arrived at the two locations. This indicated that even at high altitude, atmospheric ^{129}I to some extent originated from the air from the sea surface.

In recent years, it has been proposed that emission of molecular iodine (I_2) from seaweed to the atmosphere might be an important pathway of iodine from marine system to atmosphere [129]. The $^{127}\text{I}_2$ concentrations have been reported to be $0.03\text{--}1.05\text{ ng m}^{-3}$ at the west coast of Ireland during August 2002 and $0.29\text{--}1.23\text{ ng m}^{-3}$ at Mweenish Bay, Ireland during August and September 2007. High emission of I_2 from the seas is important for the formation of primary nuclei as precursor, as well as for the depletion of ozone in stratosphere [72, 130]. For $^{129}\text{I}_2$, a concentration of $2.33 \times 10^8\text{ molecule m}^{-3}$ has been measured in Mainz, Germany using GC-MS by collecting a large volume of air in a few weeks [72]. Although $^{129}\text{I}_2$ is an ideal tracer for investigation of iodine cycle in atmosphere, the state of art of techniques for measurement of $^{129}\text{I}_2$ is not satisfactory, either unavailable sampling or low sensitive detection that hinder this application. It is therefore expected that better understanding of $^{129}\text{I}_2$ emission from marine system and mechanism of molecular iodine formation can be conducted by advanced sampling and high sensitive AMS measurement techniques.

Besides molecular iodine, a number of gaseous organic iodine compounds, as well as inorganic forms of iodine and radicals of iodine were also observed in atmosphere [102]. The life-time of these organic forms in the atmosphere ranges from several days (CH_3I , $\text{CH}_3\text{CH}_2\text{I}$) to several minutes (CH_2I_2) [32], determining the residence time and reaction rate of iodine in atmosphere. A recent work suggested that the marine phytoplankton is the predominant source of organic iodine by analysis of gaseous organic iodine in marine boundary layer of southern Atlantic Ocean comparing with chlorophyll-a on the ocean surface [32]. However, no ^{129}I in individual volatile organic compounds has been reported, which is mainly attributed to the extremely low concentration of gaseous ^{129}I and lack of appropriate separation and preconcentration techniques.

Many efforts have been made to investigate the marine geochemical cycle of iodine, while the iodine cycle in terrestrial systems was still poorly understood due to its com-

plex environmental chemistry and low natural abundance. It has been suggested that iodine in the terrestrial environment mainly originates from ocean by long distance transportation as gaseous iodine and particle-associated species, but a recent investigation showed that emission of iodine to atmosphere from terrestrial vegetation and soil is in a magnitude similar to the oceanic source strength [131]. Based on the different source terms of ^{129}I and ^{127}I in the environment, speciation analysis of ^{129}I and ^{127}I in the terrestrial system might provide useful information to further understand this process. The major challenges are separation and concentration of iodine species from air to be able to measure ^{129}I species in the environment.

3.4 Dissoluble organic iodine as an analog tracing cycling of dissoluble organic carbon

As stated above, a large proportion of iodine associates with organic matter in natural water systems. It has been observed that organic ^{129}I accounts for approximately 40 to 75% of the total ^{129}I in fresh and coastal marine waters. The $^{129}\text{I}/^{127}\text{I}$ ratios in dissolved organic iodine (DOI) as a function of salinity showed similar variation with values of $\delta^{13}\text{C}$ and $\delta^{14}\text{N}$ in dissolved organic matter in the upper estuary, while $^{129}\text{I}/^{127}\text{I}$ ratios in iodide and iodate did not show this feature [33]. Therefore, DOI has the potential to be a proxy indicator of terrestrial dissolved organic carbon (tDOC) in coastal areas. Besides, ^{129}I level has been elevated by more than two orders of magnitude by anthropogenic releases since 1940s. Dissolved organic ^{129}I was also proposed as a geochronometer for short-term processes (about 50 years) to date the tDOC [33].

3.5 Biogeochemical cycle of iodine

In order to understand biogeochemical cycle of iodine and estimation of radiation risk of radioactive iodine to human and to the ecosystem, it is crucial to investigate biological and environmental behaviors of iodine [101]. Iodine is highly concentrated in marine plants, especially brown seaweed. The mechanism of iodine uptake and enrichment in seaweed from seawater is proposed to be one of facilitated diffusions, involving oxidation of the charged iodide to the hydrophobic compounds HIO and elementary iodine by a haloperoxidase in the cell wall, requiring low levels of hydrogen peroxide [108]. However, after passing through the cell wall, iodine retention and its associated forms in cells is still not clear. Information on biological macromolecule bound iodine, such as protein, polyphenol, polysaccharide, small organic molecular associated iodine such as amino acids, T3 and T4, and inorganic iodine ions can help us to understand the mechanism of iodine uptake and release in marine and terrestrial organism, such as seaweed and terrestrial vegetation [39]. However, few works on speciation analysis of ^{129}I in biological samples have been reported due to the difficulties in separation of different ^{129}I bound biological macromolecules. Hou *et al.* [39, 41] have reported a biochemical method for separation of inorganic iodine species and macromolecule associated iodine in seaweed. This method might be utilized for ^{129}I speciation analysis with some modifications for investigating the biogeochemical cycles of iodine.

3.6 ^{129}I and its speciation in the Fukushima accident

The Fukushima accident in 2011 has released some amount of ^{129}I to the atmosphere and ocean. A dispersion model has suggested that 42% of ^{129}I was attached to aerosol, and the remaining 58% of ^{129}I in gaseous forms [132]. This distribution of ^{129}I was deduced from a measurement of ^{129}I deposited in soil in vicinity of Savannah River Plant [133]. However, ^{131}I measured in atmosphere dispersed from Fukushima accident to European countries presents a different distribution of species. The measured data of ^{131}I in many European stations showed that 10–30% of ^{131}I in atmosphere was associated to aerosols, and more than 70% of ^{131}I was in gaseous forms [134]. The difference between the two sets of data may be ascribed to the different source of ^{129}I . More recently, speciation analysis of ^{129}I and ^{127}I in seawater offshore Fukushima has shown that most of ^{129}I (> 60–90%) in seawater is in iodide form, while iodate is the dominant species of ^{127}I . It has been estimated that a total 1.2 kg of ^{129}I has been released to the environment, in which 0.35 kg of ^{129}I was directly discharged to the sea, and 0.68 kg of ^{129}I released to the atmosphere was deposited in the Ocean [5]. The migration of ^{129}I released from Fukushima accident is still not clear so far, further investigation on ^{129}I and its speciation will be of benefit to precise estimation of radioactive risk of radioiodine released during nuclear accident.

4. Conclusions and prospects

Analytical techniques of ^{129}I speciation have been advanced in recent years, including denuder sampling for molecular iodine (I_2), selective coprecipitation separation of carrier free ^{129}I , and GC-MS measurement of ^{129}I species. They will promote the application of ^{129}I speciation in environmental processes in the near future. Some standard materials of ^{129}I are commercially available but still limited and could not satisfy the requirement of quality insurance for numerous types of environmental samples; moreover, no standard material is available for ^{129}I species.

Applications of ^{129}I as environmental tracer have been expanded from measurement of total ^{129}I to speciation analysis of ^{129}I . ^{129}I speciation analysis has been applied in the fields of hydrosphere, geosphere and atmosphere to elucidate geochemical cycling of iodine, transfer and retention of iodine in various reservoirs, as well as conversion mechanism of iodine species. The major progress and potential applications include:

1. In marine system, the source, distribution, transport pathways and species of ^{129}I and ^{127}I in the English Channel, North Sea, Baltic Proper, Kattegat and Skagerrak Basins have been investigated, providing further knowledge on conversion process, mechanism and rate of iodine species, as well as iodine circulation in the ocean.
2. In geosphere, mobility and retention of iodine in soil and sediment were investigated by ^{129}I speciation analysis, using the modified sequential extraction procedure. Iodine in soil and sediment mainly associates with organic matter, mainly humic substances. Different distribution of iodine in humic substances (humic acid, fulvic acid and humin) of soil, oxic and anoxic sediments indicated

that association of iodine with organic matter is related to their redox conditions. Immobilization of iodine in organic matter may be temporal if iodine is present in organic-colloidal form or low molecular weight organic iodine. These studies have significant implications on environmental remediation, especially at highly radioiodine contaminated sites, and assessment of immobilization and remigration of iodine in soil and sediment.

- ^{129}I has been applied to trace the source and pathways of air masses. With applications of ^{129}I speciation analysis in atmosphere, it is expected that complicated atmospheric chemistry of iodine can be studied, for instance, explaining the probable reactions and transportation of iodine in atmosphere.
- Due to the importance of low dose radioiodine exposure to human and enrichment of iodine in ecosystem, it is expected that ^{129}I speciation in organisms and biological macromolecules will have a potential application to investigate biogeochemical cycling and biological behaviors of iodine in the future.
- Analysis of ^{129}I and its speciation in the Fukushima accident can provide valuable information to retrospect the release of radioactive iodine in the nuclear accident and to predict the effect of this accident.

The current applications of ^{129}I speciation are still limited and mainly focus on inorganic ^{129}I species in marine water, soil and sediment. No application of speciation of ^{129}I in biological materials has been reported. With development of speciation analysis techniques for ^{129}I in bio-materials, it is expected that the application of ^{129}I speciation can improve our understanding on the complicated biological processes of iodine in the environment.

Acknowledgment. This work was partly supported by Innovation Methodology project from the Ministry of Science and Technology of China (2012IM030200).

References

- Fabryka-Martin, J.: Natural iodine-129 as a ground-water tracer. Master Thesis, Department of Hydrology and Water Resources, The University of Arizona (1984).
- Hou, X. L., Aldahan, A., Nielsen, S. P., Possnert, G., Nies, H., Hedfors, J.: Speciation of I-129 and I-127 in seawater and implications for sources and transport pathways in the North Sea. *Environ. Sci. Technol.* **41**, 5993–5999 (2007).
- Hu, Q. H., Moran, J. E., Blackwood, V.: Geochemical cycling of iodine species in soils. In: *The Comprehensive Handbook on Iodine: Nutritional, Biochemical, Pathological and Therapeutic Aspects*. Elsevier, Amsterdam (2009), pp. 93–105.
- Yiou, F., Raisbeck, G. M., Zhou, Z. Q., Kilius, L. R.: ^{129}I from nuclear fuel reprocessing, potential as an oceanographic tracer. *Nucl. Instrum. Methods B* **92**, 436–439 (1994).
- Hou, X., Povinec, P. P., Zhang, L., Shi, K., Biddulph, D., Chang, C. C., Fan, Y. K., Golsner, R., Hou, Y. K., Jeskovsky, M., Jull, A. J. T., Liu, Q., Luo, M. Y., Steier, P., Zhou, W. J.: Iodine-129 in seawater offshore Fukushima: distribution, inorganic speciation, sources, and budget. *Environ. Sci. Technol.* **47**, 3091–3098 (2013).
- Muramatsu, Y., Yoshida, S., Fehn, U., Amachi, S., Ohmomo, Y.: Studies with natural and anthropogenic iodine isotopes: iodine distribution and cycling in the global environment. *J. Environ. Radioact.* **74**, 221–232 (2004).
- Snyder, G. T., Fehn, U.: Global distribution of ^{129}I in rivers and lakes: implications for iodine cycling in surface reservoirs. *Nucl. Instrum. Methods B* **223–224**, 579–586 (2004).
- Raisbeck, G. M., Yiou, F.: ^{129}I in the oceans: Origins and applications. *Sci. Total Environ.* **237–238**, 31–41 (1999).
- Povinec, P. P., Breier, R., Coppola, L., Groening, M., Jeandel, C., Jull, A. J. T., Kieser, W. E., Lee, S. H., Liang, W. K. L., Morgenstern, U., Park, Y. H.: Tracing of water masses using a multi isotope approach in the southern Indian Ocean. *Earth Planet. Sci. Lett.* **302**, 14–26 (2011).
- Yi, P., Aldahan, A., Possnert, G., Hou, X. L., Hansen, V., Wang, B.: ^{127}I and ^{129}I species and transformation in the Baltic proper, Kattegat, and Skagerrak basins. *Environ. Sci. Technol.* **46**, 10948–10956 (2012).
- Jacobsen, G. E., Hotchkis, M. A. C., Fink, D., Child, D. P., Tuniz, C., Sacchi, E., Levins, D. M., Povinec, P. P., Mulsow, S.: AMS measurement of ^{129}I , ^{36}Cl and ^{14}C in underground waters from Mururoa and Fangataufa atolls. *Nucl. Instrum. Methods B* **172**, 666–671 (2000).
- López-Gutiérrez, J. M., Santos, F. J., García-León, M., Schnabel, C., Synal, H. A., Ernst, T., Szidat, S.: Levels and temporal variability of ^{129}I concentrations and $^{129}\text{I}/^{127}\text{I}$ isotopic ratios in atmospheric samples from southern Spain. *Nucl. Instrum. Methods B* **223–224**, 495–500 (2004).
- Fehn, U.: Tracing crustal fluids: Applications of natural ^{129}I and ^{36}Cl . *Ann. Rev. Earth Planet. Sci.* **40**, 45–67 (2012).
- Fabryka-Martin, J., Bentley, H., Elmore, D., Airey, P. L.: Natural iodine-129 as an environmental tracer. *Geochim. Cosmochim. Acta* **49**, 337–347 (1985).
- Fehn, U., Peters, E. K., Tullai-Fitzpatrick, S., Kubik, P. W., Sharma, P., Teng, R. T. D., Gove, H. E., Elmore, D.: ^{129}I and ^{36}Cl concentrations in waters of the eastern Clear Lake area, California: Residence times and source ages of hydrothermal fluids. *Geochim. Cosmochim. Acta* **56**, 2069–2079 (1992).
- Moran, J. E., Teng, R. T. D., Rao, U., Fehn, U.: Detection of iodide in geologic materials by high-performance liquid chromatography. *J. Chromatography* **706**, 215–220 (1995).
- Fehn, U., Snyder, G., Egeberg, P. K.: Dating of pore waters with ^{129}I : relevance for the origin of marine gas hydrates. *Science* **289**, 2332–2335 (2000).
- Fabrykamartin, J., Whittemore, D. O., Davis, S. N., Kubik, P. W., Sharma, P.: Geochemistry of halogens in the milk river aquifer, Alberta, Canada. *Appl. Geochem.* **6**, 447–464 (1991).
- Hou, X. L., Hansen, V., Aldahan, A., Possnert, G., Lind, O. C., Lujanienė, G.: A review on speciation of iodine-129 in the environmental and biological samples. *Anal. Chim. Acta* **632**, 181–196 (2009).
- Snyder, G., Aldahan, A., Aldahan, A., Possnert, G.: Global distribution and long-term fate of anthropogenic ^{129}I in marine and surface water reservoirs. *Geochem. Geophys. Geosyst.* **11**, 1–19 (2010).
- Fehn, U., Snyder, G. T., Varekamp, J. C.: Detection of recycled marine sediment components in crater lake fluids using ^{129}I . *J. Volcanol. Geotherm. Res.* **115**, 451–460 (2002).
- Snyder, G. T., Fehn, U.: Origin of iodine in volcanic fluids – ^{129}I results from the Central American Volcanic Arc. *Geochim. Cosmochim. Acta* **66**, 3827–3838 (2002).
- Moran, J. E., Fehn, U., Hanor, J. S.: Determination of source ages and migration patterns of brines from the, U. S. Gulf Coast basin using ^{129}I . *Geochim. Cosmochim. Acta* **59**, 5055–5069 (1995).
- Hou, X. L., Zhou, W. J., Chen, N., Zhang, L. Y., Liu, Q., Luo, M., Fan, Y. K., Liang, W. G., Fu, Y. C.: Determination of ultralow level $^{129}\text{I}/^{127}\text{I}$ in natural samples by separation of microgram carrier free iodine and accelerator mass spectrometry detection. *Anal. Chem.* **82**, 7713–7721 (2010).
- Fehn, U., Moran, J. E., Snyder, G. T., Muramatsu, Y.: The initial $^{129}\text{I}/\text{I}$ ratio and the presence of 'old' iodine in continental margins. *Nucl. Instrum. Methods B* **259**, 496–502 (2007).
- Zhang, L. Y., Zhou, W. J., Hou, X. L., Chen, N., Liu, Q., He, C., Fan, Y. K., Luo, M. Y., Wang, Z. W., Fu, Y. C.: Level and source of ^{129}I of environmental samples in Xi'an region, China. *Sci. Total Environ.* **409**, 3780–3788 (2011).
- Fehn, U., Snyder, G.: ^{129}I in the Southern Hemisphere: Global redistribution of an anthropogenic isotope. *Nucl. Instrum. Methods B* **172**, 366–371 (2000).
- Bowl, C., Howe, J. R.: The origin of ^{125}I and ^{129}I in sheep thyroids from birmingham, UK. *J. Environ. Radioact.* **27**, 117–123 (1995).

29. Fréchet, C., Calmet, D., Bertho, X., Gaudry, A.: $^{129}\text{I}/^{127}\text{I}$ ratio measurements in bovine thyroids from the North Cotentin area (France). *Sci. Total Environ.* **293**, 59–67 (2002).
30. Hou, X. L., Fogh, C. L., Kucera, J., Andersson, K. G., Dahlgard, H., Nielsen, S. P.: Iodine-129 and Caesium-137 in Chernobyl contaminated soil and their chemical fractionation. *Sci. Total Environ.* **308**, 97–109 (2003).
31. Wong, G. T. F.: The marine geochemistry of iodine. *Rev. Aquat. Sci.* **4**, 45–73 (1991).
32. Lai, S. C., Williams, J., Arnold, S. R., Atlas, E. L., Gebhardt, S., Hoffmann, T.: Iodine containing species in the remote marine boundary layer: A link to oceanic phytoplankton. *Geophys. Res. Lett.* **38**, L20801 (2011).
33. Schwehr, K. A., Santschi, P. H., Elmore, D.: The dissolved organic iodine species of the isotopic ratio of I-129/I-127: A novel tool for tracing terrestrial organic carbon in the estuarine surface waters of Galveston Bay, Texas. *Limnol. Oceanogr. Meth.* **3**, 326–337 (2005).
34. Hansen, V., Roos, P., Aldahan, A., Hou, X. L., Possnert, G.: Partition of iodine (^{129}I and ^{127}I) isotopes in soils and marine sediments. *J. Environ. Radioact.* **102**, 1096–1104 (2011).
35. Xu, C., Zhang, S. J., Ho, Y., Miller, E. J., Roberts, K. A., Li, H., Schwehr, K. A., Otsuka, S., Kaplan, D. I., Brinkmeyer, R., Yeager, C. M., Santschi, P. H.: Is soil natural organic matter a sink or source for mobile radioiodine (^{129}I) at the Savannah River Site? *Geochim. Cosmochim. Acta* **75**, 5716–5735 (2011).
36. Huang, R., Hoffmann, T.: Development of a coupled diffusion denuder system combined with gas chromatography/mass spectrometry for the separation and quantification of molecular iodine and the activated iodine compounds iodine monochloride and hypoiodous acid in the marine atmosphere. *Anal. Chem.* **81**, 1777–1783 (2009).
37. O'Dowd, C. D., Jimenez, J. L., Bahreini, R., Flagan, R. C., Seinfeld, J. H., Hämeri, K., Pirjola, L., Kulmala, M., Jennings, S. G., Hoffmann, T.: Marine aerosol formation from biogenic iodine emissions. *Nature* **417**, 632–636 (2002).
38. Englund, E., Aldahan, A., Hou, X. L., Petersen, R., Possnert, G.: Speciation of iodine (I-127 and I-129) in lake sediments. *Nucl. Instrum. Methods B* **268**, 1102–1105 (2010).
39. Hou, X. L., Chai, C. F., Qian, Q. F., Yan, X. J., Fan, X.: Determination of chemical species of iodine in some seaweeds. 1. *Sci. Total Environ.* **204**, 215–221 (1997).
40. Hou, X. L., Chen, C., Ding, W., Chai, C.: Study on chemical species of iodine in human liver. *Biol. Trace Elem. Res.* **69**, 69–76 (1999).
41. Hou, X. L., Yan, X., Chai, C.: Chemical species of iodine in some seaweeds II. Iodine-bound biological macromolecules. *J. Radioanal. Nucl. Chem.* **245**, 461–467 (2000).
42. Reifenhäuser, C., Heumann, K. G.: Development of a definitive method for iodine speciation in aquatic systems. *Fresenius J. Anal. Chem.* **336**, 559–563 (1990).
43. Zhang, S. J., Schwehr, K. A., Ho, Y. F., Xu, C., Roberts, K. A., Kaplan, D. I., Brinkmeyer, R., Yeager, C. M., Santschi, P. H.: A novel approach for the simultaneous determination of iodide, iodate and organo-iodide for ^{127}I and ^{129}I in environmental samples using gas chromatography mass spectrometry. *Environ. Sci. Technol.* **44**, 9042–9048 (2010).
44. Krupp, G., Aumann, D. C.: Iodine-129 in rainfall over Germany. *J. Environ. Radioact.* **46**, 287–299 (1999).
45. Dang, H. J.: Release of iodine from organic matter in natural water by $\text{K}_2\text{S}_2\text{O}_8$ oxidation for ^{129}I determination. *Anal. Methods* **5**, 449–456 (2013).
46. Tullai, S., Tubbs, L. E., Fehn, U.: Iodine extraction from petroleum for analysis of $^{129}\text{I}/^{127}\text{I}$ ratios by AMS. *Nucl. Instrum. Methods B* **29**, 383–386 (1987).
47. Fehn, U., Tullai, S., Teng, R. T. D., Elmore, D., Kubik, P. W.: Determination of ^{129}I in heavy residues of two crude oils. *Nucl. Instrum. Methods B* **29**, 380–382 (1987).
48. Studier, M. H., Postmus, C. J., Mech, J., Walters, R. R., Sloth, E. N.: The use of ^{129}I as an isotopic tracer and its determination along with normal ^{127}I by neutron activation – The isolation of iodine from a variety of materials. *J. Inorg. Nucl. Chem.* **24**, 755–761 (1962).
49. Aumann, D. C., Buheitel, F., Hauschild, J., ROBENS, E., Wershofen, H.: Chemical and nuclear interferences in neutron activation of ^{129}I and ^{127}I in environmental samples. *J. Radioanal. Nucl. Chem.* **109**, 261–274 (1987).
50. Fan, Y. K., Hou, X. L., Zhou, W. J.: Progress on ^{129}I analysis and its application in environmental and geological researches. *Desalination*, **321**, 32–46 (2013).
51. Sahoo, S. K., Muramatsu, Y., Yoshida, S., Matsuzaki, H., Ruehm, W.: Determination of I-129 and I-127 concentration in soil samples from the Chernobyl 30-km zone by AMS and ICP-MS. *J. Radiat. Res.* **50**, 325–332 (2009).
52. Zhou, W. J., Hou, X. L., Chen, N., Zhang, L. Y., Liu, Q., He, C. H., Luo, M. Y., Liang, W. G., Fan, Y. K., Wang, Z. W., Fu, Y. C., Li, H. B.: Preliminary study of radioisotope ^{129}I application in China using Xi'an accelerator mass spectrometer. *ICNS News* **25**, 8–23 (2010).
53. Rao, U., Fehn, U., Muramatsu, Y., McNeil, H., Sharma, P., Elmore, D.: Tracing the history of nuclear releases: Determination of ^{129}I in tree rings. *Environ. Sci. Technol.* **36**, 1271–1275 (2002).
54. Nishiizumi, K., Elmore, D., Honda, M., Arnold, J. R., Gove, H. E.: Measurements of ^{129}I in meteorites and lunar rock by tandem accelerator mass spectrometry. *Nature* **305**, 611–612 (1983).
55. Bunzl, K., Kracke, W.: Determination of iodine-129 in large soil samples after alkaline wet disintegration. *Fresenius J. Anal. Chem.* **343**, 505–508 (1992).
56. Roman, D., Fabryka-Martin, J.: Iodine-129 and Chlorine-36 in uranium ores. 1. Preparation of samples for analysis by AMS. *Chem. Geol.* **72**, 1–6 (1988).
57. Ashton, L., Warwick, P., Giddings, D.: The measurement of ^{36}Cl and ^{129}I in concrete wastes. *Analyst* **124**, 627–632 (1999).
58. Martin, J. E., Marcinowski, F., Cook, S.: optimization of neutron activation analyses of ^{129}I in low-level radioactive waste samples. *Appl. Radial. Isot.* **31**, 727–131 (1990).
59. Zhao, P., Hu, Q., Rose, T. P., Nimz, G. J., Zavarin, M.: Distribution of ^{99}Tc and ^{129}I in the vicinity of underground nuclear tests at the Nevada Test Site. *J. Radioanal. Nucl. Chem.* **276**, 755–761 (2008).
60. Gómez-Guzmán, J. M., Enamorado-Báez, S. M., Pinto-Gómez, A. R., Abril-Hernández, J. M.: Microwave-based digestion method for extraction of ^{127}I and ^{129}I from solid material for measurements by AMS and ICP-MS. *Int. J. Mass Spectrom.* **303**, 103–108 (2011).
61. Hou, X. L., Dahlgard, H., Rietz, B., Jacobsen, U., Nielsen, S. P., Aarkrog, A.: Determination of chemical species of iodine in seawater by radiochemical neutron activation analysis combined with ion-exchange pre-separation. *Anal. Chem.* **71**, 2745–2750 (1999).
62. Englund, E., Aldahan, A., Possnert, G., Alfimov, V.: A routine preparation method for AMS measurement of ^{129}I in solid material. *Nucl. Instrum. Methods B* **259**, 365–369 (2007).
63. You, F., Diel, K., Martin, F., Raisbeck, G.: Preparation of microgram quantities of carrier-free iodine for AMS analysis. *Nucl. Instrum. Methods B* **172**, 395–398 (2000).
64. Fitoussi, C., Raisbeck, G. M., Hubert, P.: A wine tour around the world traced with ^{129}I , potential as a forensic tool. *Nucl. Instrum. Methods B* **268**, 1265–1268 (2010).
65. Fitoussi, C., Raisbeck, G. M.: Chemical procedure for extracting ^{129}I , ^{60}Fe and ^{26}Al from marine sediments: Prospects for detection of a ~ 2.8 My old supernova. *Nucl. Instrum. Methods B* **259**, 351–358 (2007).
66. Luo, M., Hou, X., Zhou, W., He, C., Chen, N., Liu, Q., Zhang, L. Y.: Speciation and migration of ^{129}I in soil profiles. *J. Environ. Radioact.* **118**, 30–39 (2013).
67. Muramatsu, Y., Uchida, S., Sumiya, M., Ohmomo, Y.: Iodine separation procedure for the determination of iodine-129 and iodine-127 in soil by neutron activation analysis. *J. Radioanal. Nucl. Chem.* **94**, 329–338 (1985).
68. Fréchet, C., Calmet, D., Bouisset, P., Piccot, D., Gaudry, A., You, F., Raisbeck, G.: I-129 and I-129/I-127 ratio determination in environmental biological samples by RNAA, AMS and direct gamma-X spectrometry measurements. *J. Radioanal. Nucl. Chem.* **249**, 133–138 (2001).
69. Verrezen, F., Hurtgen, C.: The measurement of Tc-99 and I-129 in waste-water from pressurized nuclear-power reactors. *Appl. Radiat. Isot.* **43**, 61–68 (1992).

70. Goles, R. W., Fukuda, R. C., Cole, M. W., Brauer, F. P.: Detection of iodine-129 by laser induced fluorescence spectrometry. *Anal. Chem.* **53**, 776–778 (1981).
71. Chao, J. H., Tseng, C. L., Lee, C. J., Hsia, C. C., Teng, S. P.: Analysis of I-129 in radwastes by neutron activation. *Appl. Radial. Isot.* **51**, 137–143 (1999).
72. Huang, R., Hou, X. L., Hoffmann, T.: Extensive evaluation of a diffusion denuder technique for the quantification of atmospheric stable and radioactive molecular iodine. *Environ. Sci. Technol.* **44**, 5061–5066 (2010).
73. Izmer, A. V., Boulyga, S. F., Zoriy, M. V., Becker, J. S.: Improvement of the detection limit for determination of ¹²⁹I in sediments by quadrupole inductively coupled plasma mass spectrometer with collision cell. *J. Anal. At. Spectrom.* **19**, 1278–1280 (2004).
74. Fujiwara, H., Kawabata, K., Suzuki, J., Shikino, O.: Determination of ¹²⁹I in soil samples by DRC-ICP-MS. *J. Anal. At. Spectrom.* **26**, 2528–2533 (2011).
75. Moreda-Piñeiro, A., Romaris-Hortas, V., Bermejo-Barrera, P.: A review on iodine speciation for environmental, biological and nutrition fields. *J. Anal. At. Spectrom.* **26**, 2107–2152 (2011).
76. Li, H. B., Xu, X. R., Chen, F.: Determination of iodine in seawater: methods and applications. In: *The Comprehensive Handbook on Iodine: Nutritional, Biochemical, Pathological and Therapeutic Aspects*. Elsevier, Amsterdam (2009), pp. 3–13.
77. Shimamoto, Y. S., Itai, T., Takahashi, Y.: Soil column experiments for iodate and iodide using K-edge XANES and HPLC-ICP-MS. *J. Geochem. Explor.* **107**, 117–123 (2010).
78. Hou, X. L., Dahlgaard, H., Nielsen, S. P.: Chemical speciation analysis of ¹²⁹I in seawater and a preliminary investigation to use it as a tracer for geochemical cycle study of stable iodine. *Mar. Chem.* **74**, 145–155 (2001).
79. Park, S. D., Kim, J. S., Han, S. H., Ha, Y. K., Song, K. S., Jee, K. Y.: The measurement of ¹²⁹I for the cement and the paraffin solidified low and intermediate level wastes (LILWs), spent resin or evaporated bottom from the pressurized water reactor (PWR) nuclear power plants. *Appl. Radial. Isot.* **67**, 1676–1682 (2009).
80. Xu, C., Miller, E. J., Zhang, S. J., Li, H., Ho, Y., Schwehr, K. A., Kaplan, D. I., Ootosaka, S., Roberts, K. A., Brinkmeyer, R., Yeayer, C. M., Santschi, P. H.: Sequestration and remobilization of radioiodine (¹²⁹I) by soil organic matter and possible consequences of the remedial action at savannah river site. *Environ. Sci. Technol.* **45**, 9975–9983 (2011).
81. Petersen, R., Hou, X. L., Hansen, E. H.: Evaluation of the read-sorption of plutonium and americium in dynamic fractionations of environmental solid samples. *J. Environ. Radioact.* **99**, 1165–1174 (2008).
82. Kundel, M., Huang, R., Thorenz, U. R., Bosle, J., Mann, M. J. D., Ries, M., Hoffmann, T., Huang, R. J., Ries, M.: Application of time-of-flight aerosol mass spectrometry for the online measurement of gaseous molecular iodine. *Anal. Chem.* **84**, 1439–1445 (2011).
83. Bruchertseifer, H., Cripps, R., Guentay, S., Jaekel, B.: Analysis of iodine species in aqueous solutions. *Anal. Bioanal. Chem.* **375**, 1107–1110 (2003).
84. Pacific Northwest National Laboratory: Environmental Monitoring Plan United States Department of Energy Richland Operations Office Pacific Northwest National Laboratory. DOE/RL-91-50, US Department of Energy (2008).
85. Koarashi, J., Akiyama, K., Asano, T., Kobayashi, H.: A practical method for monitoring ¹²⁹I concentration in airborne release. *J. Radioanal. Nucl. Chem.* **267**, 155–159 (2006).
86. Hou, X. L., Aldahan, A., Possnert, G., Lujanienė, G., Lehto, J., Skipperud, L., Lind, O. C., Salbu, B.: Speciation analysis of radionuclides in the environment – NSK-B SPECIATION Project Report 2009, Nordic Nuclear Safety Research, NKS-205 (2009).
87. Luo, M. Y., Hou, X. L., He, C. H., Liu, Q., Fan, Y. K.: Speciation analysis of ¹²⁹I in seawater by carrier free AgI-AgCl coprecipitation and AMS measurement. **85**, 3715–3722 (2013).
88. Zaspá, Y. P., Kireev, S. V., Protsenko, E. D., Veselov, V. K., Isupov, V. K.: Laser fluorescence-absorption analysis of iodine-129 and nitrogen dioxide impurities in a special atmosphere. *J. Appl. Spectrosc.* **56**, 88–92 (1992).
89. Kireev, S. V., Shnyrev, S. L.: Laser excited fluorescence of molecular iodine ¹²⁷I and ¹²⁹I isotopes in the 632–637 nm spectral region. *Laser Phys.* **21**, 1775–1783 (2011).
90. Roberts, M. L., Caffee, M. W., Proctor, I. D.: ¹²⁹I interlaboratory comparison. *Nucl. Instrum. Methods B* **123**, 367–370 (1997).
91. Keogh, S. M., Aldahan, A., Possnert, G., Finegan, P., León Vitró, L., Mitchell, P. I.: Trends in the spatial and temporal distribution of ¹²⁹I and ⁹⁹Tc in coastal waters surrounding Ireland using *Fucus vesiculosus* as a bio-indicator. *J. Environ. Radioact.* **95**, 23–38 (2007).
92. Parry, S. J., Bennett, B. A., Benzing, R., Lally, A. E., Birch, C. P., Fulker, M. J.: The determination of ¹²⁹I in milk and vegetation using neutron activation analysis. *Sci. Total Environ.* **173–174**, 351–360 (1995).
93. Chao, J. H., Tseng, C. L., Chou, F. I.: Determination of ¹²⁹I in ¹³¹I-pharmaceuticals produced in THOR. *Appl. Radial. Isot.* **49**, 1587–1590 (1998).
94. Hou, X. L., Dahlgaard, H., Rietz, B., Jacobsen, U., Nielsen, S., P., Aarkrog, A.: Determination of ¹²⁹I in seawater and some environmental materials by neutron activation analysis. *Analyst* **124**, 1109–1114 (1999).
95. Outola, I., Filliben, J., Inn, K. G., La Rosa, J., McMahon, C. A., Peck, G. A., Twining, J., Tims, S. G., Fifield, L. K., Smedley, P., Anton, M. P., Gasco, C., Povinec, P., Pham, M. K., Raaum, A., Wei, H. J. H. J., Krijger, G. C., Bouisset, P., Litherland, A. E., Kiessner, W. E., Betti, M., Aldave de las Heras, L., Hong, G. H., Holm, E., Skipperud, L., Harms, A. V., Arinc, A., Youngman, M., Arnold, D., Wershofen, H., Sill, D. S., Bohrer, S., Dahlgaard, H., Croudance, I. W., Warwick, P. E., Ikäheimonen, T. K., Klemola, S., Vakulovsky, S. M., Sanchez-Cabeza, J. A.: Characterization of the NIST seaweed standard reference material. *Appl. Radial. Isot.* **64**, 1242–1247 (2005).
96. Jiang, S., Chang, Z., Zhao, M., Zhao, Y., Zhao, X. L., Kieser, W. E.: New measurement of ¹²⁹I in IAEA-375 reference material. *J. Radioanal. Nucl. Chem.* **264**, 549–553 (2005).
97. Marchetti, A. A., Gu, F., Robl, R., Straume, T.: Determination of total iodine and sample preparation for AMS measurement of ¹²⁹I in environmental matrices. *Nucl. Instrum. Methods B* **123**, 352–355 (1997).
98. Pham, M. K., Sanchez-Cabeza, J., Povinec, P. P., Arnold, D., Benmansour, M., Bojanowski, R., *et al.*: Certified reference material for radionuclides in fish flesh sample IAEA-414 (mixed fish from the Irish Sea and North Sea). *Appl. Radiat. Isot.* **64**, 1253–1259 (2006).
99. Pham, M. K., Betti, M., Povinec, P. P., Benmansour, M., Bojanowski, R., Bouisset, P., Calvo, E. C., Ham, G. J., Holm, E., Hult, M., Ilchann, C., Kloster, M., Kanisch, G., Köhler, M., La Rosa, J., Legarda, F., Llauradó, M., Nourredine, A., Oh, J. S., Pellicciari, M., Rieth, U., Rodrigue, Y. B. A. M., Sanchez-Cabeza, J. A., Satake, H., Schikowski, J., Takeishi, M., Thébault, H., Varga, Z.: A new reference material for radionuclides in the mussel sample from the Mediterranean Sea (IAEA-437). *J. Radioanal. Nucl. Chem.* **283**, 851–859 (2010).
100. Schmidt, A., Schnabel, C., Handl, J., Jakob, D., Michel, R., Synal, H. A., Lopez, J. M., Sulter, M.: On the analysis of iodine-129 and iodine-127 in environmental materials by accelerator mass spectrometry and ion chromatography. *Sci. Total Environ.* **223**, 131–156 (1998).
101. Amachi, S.: Microbial contribution to global iodine cycling: volatilization, accumulation, reduction, oxidation, and sorption of iodine. *Microb. Environ.* **23**, 269–276 (2008).
102. Hu, Q. H., Moran, J. E., Gan, J. Y.: Sorption, degradation, and transport of methyl iodide and other iodine species in geologic media. *Appl. Geochem.* **27**, 774–781 (2012).
103. Zhang, S. J., Du, J., Xu, C., Schwehr, K. A., Ho, Y., Li, H.-P., Roberts, K. A., Kaplan, D. I., Brinkmeyer, R., Yeager, C. M., Chang, H. S., Santschi, P. H.: Concentration-dependent mobility, retardation, and speciation of iodine in surface sediment from the Savannah River site. *Environ. Sci. Technol.* **45**, 5543–5549 (2011).
104. Wong, G. T. F., Cheng, X.: Dissolved inorganic and organic iodine in the Chesapeake Bay and adjacent Atlantic waters: Speciation changes through an estuarine system. *Mar. Chem.* **111**, 221–232 (2008).

105. Schwehr, K. A., Santschi, P. H.: Sensitive determination of iodine species, including organo-iodine, for freshwater and seawater samples using high performance liquid chromatography and spectrophotometric detection. *Anal. Chim. Acta* **482**, 59–71 (2003).
106. Yi, P., Aldahan, A., Hansen, V., Possnert, G., Hou, X. L.: Iodine isotopes (^{129}I and ^{127}I) in the Baltic Proper, Kattegat, and Skagerrak Basins. *Environ. Sci. Technol.* **43**, 903–909 (2011).
107. Hansen, V., Yi, P., Hou, X. L., Aldahan, A., Roos, P., Possnert, G.: Iodide and iodate (^{129}I and ^{127}I) in surface water of the Baltic Sea, Kattegat and Skagerrak. *Sci. Total Environ.* **412–413**, 296–303 (2011).
108. Küpper, F. C., Carpenter, L. J., McFiggans, G. B., Palmer, C. J., Waite, T. J., Boneberg, E. M., Woitsch, S., Weiller, M., Abela, R., Grolimund, D., Potin, P., Butler, A., Luther, G. W., Kroneck, P. M. H., Meyer-Klaucke, W., Feiters, M. C.: Iodide accumulation provides kelp with an inorganic antioxidant impacting atmospheric chemistry. *Proc. Nat. Acad. Sci. (PNAS)* **105**, 6954–6958 (2008).
109. Lehto, J., Rätty, T., Hou, X. L., Paatero, J., Aldahan, A., Possnert, G., Flinkman, J., Kankaapää, H.: Speciation of ^{129}I in sea, lake and rain waters. *Sci. Total Environ.* **419**, 60–67 (2012).
110. Kaplan, D. I., Roberts, K. A., Schwehr, K. A., Lilley, M. S., Brinkmeyer, R., Denham, M. E., Diprete, D., Li, H. P., Powell, B. A., Xu, C., Yeager, C. M., Zhang, S. J., Santschi, P. H.: Evaluation of a radioiodine plume increasing in concentration at the Savannah River site. *Environ. Sci. Technol.* **45**, 489–495 (2011).
111. Otsaka, S., Schwehr, K. A., Kaplan, D. I., Roberts, K. A., Zhang, S. J., Xu, C., Li, H. P., Ho, Y. F., Brinkmeyer, R., Yeager, C. M., Santschi, P. H.: Factors controlling mobility of ^{127}I and ^{129}I species in an acidic groundwater plume at the Savannah River Site. *Sci. Total Environ.* **409**, 3857–3865 (2011).
112. Schmitz, K., Aumann, D. C.: A study on the association of two iodine isotopes, of natural ^{127}I and of the fission product ^{129}I , with soil components using a sequential extraction procedure. *J. Radioanal. Nucl. Chem.* **198**, 229–236 (1995).
113. Deitermann, W. I., Hauschild, J., Robens-Palavinskas, E., Aumann, D. C.: Soil-to-vegetation transfer of natural ^{127}I , and of ^{129}I from global fallout, as revealed by field measurements on permanent pastures. *J. Environ. Radioact.* **10**, 79–88 (1989).
114. Xu, C., Zhong, J., Hatcher, P. G., Zhang, S. J., Li, H., Ho, Y., Schwehr, K., Kaplan, D., Roberts, K. A., Kimberly, A., Brinkmeyer, R., Yeager, C. M., Santschi, P. H.: Molecular environment of stable iodine and radioiodine (^{129}I) in natural organic matter: Evidence inferred from NMR and binding experiments at environmentally relevant concentrations. *Geochim. Cosmochim. Acta* **97**, 166–182 (2012).
115. Yamaguchi, N., Nakano, M., Takamatsu, R., Tanida, H.: Inorganic iodine incorporation into soil organic matter: evidence from iodine K-edge X-ray absorption near-edge structure. *J. Environ. Radioact.* **101**, 451–457 (2010).
116. Carpenter, L. J.: Iodine in the marine boundary layer. *Chem. Rev.* **103**, 4953–4962 (2003).
117. Baker, A. R., Tunnicliffe, C., Jickells, T. D.: Iodine speciation and deposition fluxes from the marine atmosphere. *J. Geophys. Res.* **106**, 28743–28749 (2001).
118. Buraglio, N., Aldahan, A., Possnert, G., Vintersved, I.: ^{129}I from the nuclear reprocessing facilities traced in precipitation and runoff in northern Europe. *Environ. Sci. Technol.* **35**, 1579–1586 (2001).
119. Persson, S., Aldahan, A., Possnert, G., Alfimov, V., Hou, X. L.: ^{129}I Variability in precipitation over Europe. *Nucl. Instrum. Methods B* **259**, 508–512 (2007).
120. Keogh, S. M., Aldahan, A., Possnert, G., León Vitró, L., Mitchell, P. I., Smith, K. J., *et al.*: Anthropogenic ^{129}I in precipitation and surface waters in Ireland. *Nucl. Instrum. Methods B* **268**, 1232–1235 (2010).
121. Moran, J. E., Oktay, S. D., Santschi, P. H., Schink, D. R.: Atmospheric dispersal of ^{129}I from nuclear fuel reprocessing facilities. *Environ. Sci. Technol.* **33**, 2536–2542 (1999).
122. Aldahan, A., Persson, S., Possnert, G., Hou, X. L.: Distribution of ^{127}I and ^{129}I in precipitation at high European latitudes. *Geophys. Res. Lett.* **36** (2009).
123. Hou, X. L., Aldahan, A., Nielsen, S. P., Possnert, G.: Time series of I-129 and I-127 speciation in precipitation from Denmark. *Environ. Sci. Technol.* **43**, 6522–6528 (2009).
124. Michel, R., Daraoui, A., Gorny, M., Jakob, D., Sachse, R., Tosch, L., Nies, H., Goroncy, I., Herrmann, J., Snyal, H. A., Stocker, M., Alfimov, V.: Iodine-129 and iodine-127 in European seawaters and in precipitation from Northern Germany. *Sci. Total Environ.* **419**, 151–169 (2012).
125. Santos, F. J., López-Gutiérrez, J. M., García-León, M., Suter, M., Snyal, H. A.: Determination of $^{129}\text{I}/^{127}\text{I}$ in aerosol samples in Seville (Spain). *J. Environ. Radioact.* **84**, 103–109 (2005).
126. Jabbar, T., Steier, P., Wallner, G., Kandler, N., Kätzberger, C.: AMS analysis of iodine-129 in aerosols from Austria. *Nucl. Instrum. Methods B* **269**, 3183–3187 (2011).
127. Englund, E., Aldahan, A., Hou, X. L., Possnert, G., Soderstrom, C.: Iodine (I-129 and I-127) in aerosols from northern Europe. *Nucl. Instrum. Methods B* **268**, 1139–1141 (2010).
128. Jabbar, T., Steier, P., Wallner, G., Priller, A., Kandler, N., Kaiser, A.: Iodine isotopes (^{127}I and ^{129}I) in aerosols at high altitude Alp stations. *Environ. Sci. Technol.* **46**, 8637–8644 (2012).
129. Saiz-Lopez, A., Gómez Martín, J. C., Plane, J. M. C., Saunders, R. W., Baker, A. R., Von Glasow, R., Carpenter, L. J., McFiggans, G.: Atmospheric chemistry of iodine. *Chem. Rev.* **112**, 1773–1804 (2012).
130. Saiz-Lopez, A., Plane, J. M. C.: Novel iodine chemistry in the marine boundary layer. *Geophys. Res. Lett.* **31**, L04112, 1–4 (2004).
131. Sive, B. C., Varner, R. K., Mao, H., Talbot, R., Blake, D. R., Wingen, O. W.: A large terrestrial source of methyl iodide. *Geophys. Res. Lett.* **34**, (2007).
132. Reithmeier, H., Lazarev, V., Rühm, W., Nolte, E.: Anthropogenic ^{129}I in the atmosphere: Overview over major sources, transport processes and deposition pattern. *Sci. Total Environ.* **408**, 5052–5064 (2010).
133. Kantelo, M. V., Tiffany, B., Anderson, T. J.: Iodine-129 distribution in the terrestrial environment surrounding a nuclear fuel reprocessing plant after 25 years of operation. Environmental migration of long-lived radionuclides, Proceedings of an International Atomic Energy Agency conference, Knoxville (USA), 27–31 July 1981, IAEA, Vienna (Austria), pp. 495–500.
134. Masson, O., Baeza, A., Bieringer, J., Brudecki, K., Bucci, S., Cappai, M., Carvalho, F. P., Connan, O., Cosma, C., Dalheimer, A., Didier, D., Depuydt, G., De Geer, L. E., De Vismes, A., Gini, L., Groppi, F., Gudnason, K., Gurriaran, R., Hainz, D., Halldorsson, O., Hammond, D., Hanley, O., Holey, K., Homoki, Zs., Ioannidou, A., Isajenko, K., Jankovick, M., Kätzberger, C., Ketunen, M., Kierepko, R., Kontro, R., Kwakman, P. J. M., Lecomte, M., Leon Vintro, L., Leppänen, A.-P., Lind, B., Lujaniene, G., McGinnity, P., Mc Mahon, C., Mala, H., Manenti, S., Manolopoulos, M., Mattila, A., Mauring, A., Mietelski, J. W., Möller, B. S., Nielsen, P., Nikolick, J., Overwater, R. M. W., Palsson, S. E., Papastefanou, C., Penev, I., Pham, M. K., Povinec, P. P., Ramebäck, H., Reis, M. C., Ringer, W., Rodriguez, A., Rulf, P., Saey, P. R. J., Samsonov, V., Schlosser, C., Sgorbati, G., Silobritiene, B. V., Söderström, C., Sogni, R., Solier, L., Sonck, M., Steinhäuser, G., Steinkopff, T., Steinmann, P., Stoulos, S., Sykora, I., Todorovic, D., Tooloutalae, N., Tositti, L., Tschiersch, J., Ugron, A., Vagena, E., Vargas, A., Wershofen, H. and Zhukova, O.: Tracking of airborne radionuclides from the damaged Fukushima Dai-Ichi nuclear reactors by European networks. *Environ. Sci. Technol.* **45**, 7670–7677 (2011).

Paper II

Speciation Analysis of ^{129}I and ^{127}I in Aerosols Using Sequential Extraction and Mass Spectrometry Detection

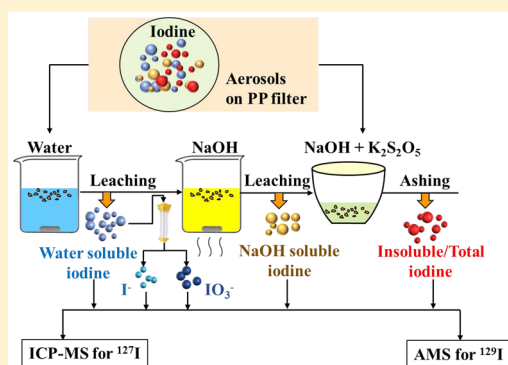
Luyuan Zhang,[†] Xiaolin Hou,^{*,†,‡} and Sheng Xu[§]

[†]Center for Nuclear Technologies, Technical University of Denmark, Risø Campus, Roskilde 4000, Denmark

[‡]Xi'an AMS Center, SKLLQG, Institute of Earth Environment, CAS, Xi'an 710075, China

[§]Scottish Universities Environmental Research Center, East Kilbride G75 0QF, United Kingdom

ABSTRACT: A new analytical method has been developed for speciation analysis of ^{127}I and ^{129}I in aerosols collected on polypropylene (PP) filter paper. Iodide, iodate, NaOH soluble iodine, and insoluble iodine were separated from aerosols using sequential extraction, chromatography separation, and alkaline ashing and measured using inductive coupled plasma mass spectrometry (ICP-MS) for ^{127}I and accelerator mass spectrometry (AMS) for ^{129}I . Parameters affecting the leaching efficiency and stability of iodine species, such as leaching time and temperature, amount of alkaline reagent for ashing, ashing temperature and time, and iodine protective agent, were investigated and optimized. It was observed that long time water leaching would change inorganic iodine species due to photochemical oxidation of iodide on the PP filter surface. NaOH leaching can only extract less than 60% of iodine from the studied aerosol filters even under heating, implying that total ^{129}I in aerosol might be underestimated by NaOH leaching. The addition of a reductive agent significantly reduced the loss of iodine during alkaline ashing from more than 35% to 4%, efficiently improving the separation efficiency of iodine in aerosols. Speciation analysis of ^{129}I and ^{127}I in aerosol samples collected at Risø, Denmark using the developed method shows that the measured values of total ^{129}I and ^{127}I are in good agreement with the sum of all iodine species for each isotope, confirming the reliability of the proposed method. Similar distribution patterns between ^{129}I and ^{127}I species show that iodine is enriched in NaOH leachable and insoluble species and depleted in water-soluble species, as observed in all aerosol samples.



Atmospheric chemistry of iodine plays a key role in the formation of primary nuclei of air particles^{1,2} and ozone depletion^{3,4} linking to Earth's radiation budget and climate regulation.⁵ Transformation and interaction of iodine species in gaseous phases and aerosol particles consist of the complicated but important processes of iodine chemistry in the atmosphere. Speciation analysis of iodine in aerosol provides direct and critical information for understanding these chemical processes of iodine in the atmosphere, including its origination, transfer pathway, and interconversion.

A number of investigations on speciation analysis of stable iodine in aerosol have been carried out in order to study the atmospheric process of iodine related to particles.^{6–8} However, due to the difficulties in identification of iodine sources in aerosols by measurement of the only stable ^{127}I , the atmospheric chemical process of iodine is still not well understood. ^{129}I , a long-lived radioisotope of iodine (half-life 1.57×10^7 years), was released to the environment mainly from nuclear reprocessing plants (NRPs) with small fractions from nuclear weapons testing and nuclear accidents,^{9,10} providing a unique tracer with specific point source function for investigation of atmospheric chemistry of iodine. Because of the ultralow level of ^{129}I in the atmosphere ($<10^7$ atoms/ m^3),^{11–14} speciation analysis of ^{129}I in aerosols is still a

challenge, and no method on this issue has been reported so far.

For speciation analysis of stable iodine in aerosol,^{15–17} iodine is often extracted using water under ultrasonic assistance and subsequently quantified as iodide and iodate and water-soluble organic iodine using chromatography (ion chromatography and high performance liquid chromatography) in combination with ICP-MS quantification.^{16,17} However, it was observed that ultrasonification might change the original species of iodine in aerosol by reactions of inorganic iodine ions with cellulose filter paper and forming new organic iodine species.⁶ This is confirmed by a significant decrease in chemical yield of iodide under ultrasonic extraction from 87% for 5 min to 18% for 60 min.¹⁸ In contrast, efficient extraction of soluble iodine from an aerosol filter, especially for a hydrophobic filter (e.g., polypropylene filter), is also critical in obtaining a reliable result of iodine species in aerosol. However, these issues were not well addressed in the previous investigations.

Most of the studies on speciation analysis of iodine in aerosol only focused on the water-soluble fraction,^{15,17} without

Received: April 24, 2015

Accepted: June 5, 2015

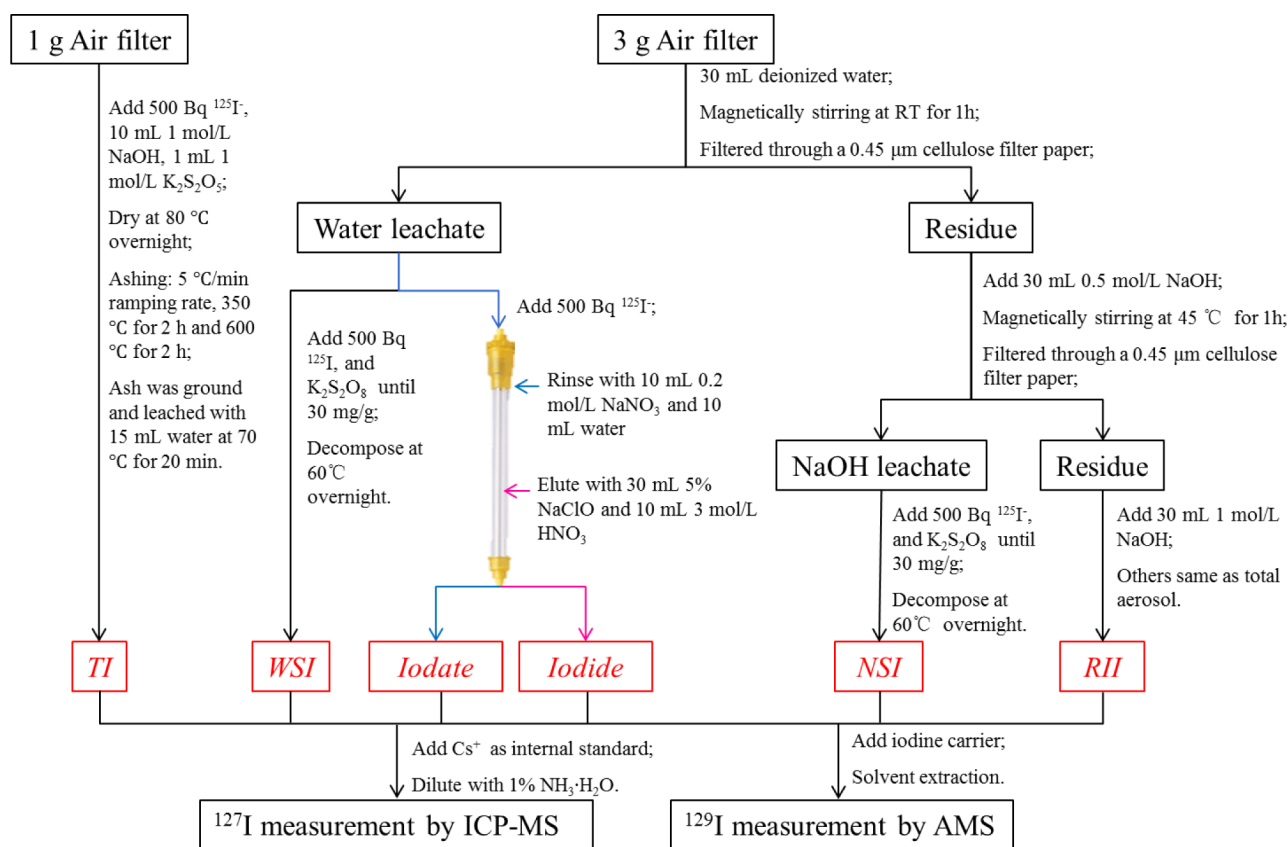


Figure 1. Schematic diagram of analytical procedure for determination of ^{127}I and ^{129}I species in aerosols. TI for total iodine, WSI for water-soluble iodine, NSI for NaOH soluble iodine, and RII for residual insoluble iodine.

sufficient information on iodine species in the water insoluble fraction, which might account for a major proportion^{19,20} and is important for the atmospheric chemistry of iodine. Alkaline leaching using NaOH- Na_2SO_3 , microwave-assisted acid digestion, pyrolysis, and alkaline ashing have been used for the extraction of total iodine from aerosol samples.^{14,18,19,21,22} Among these methods, acid digestion with pressure or microwave assistance might cause iodine loss, due to the formation of volatile molecular iodine and hydrogen iodide, which are chemically active and easily react with the materials of the canister, such as Teflon. Meanwhile, the limited volume of the digestion canister is incapable of treating an adequate amount of the filter for speciation analysis of ^{129}I . So far, almost all the reports on the determination of total ^{129}I in aerosols employed alkaline leaching at room temperature for 1–2 days,^{12,13,22} but no data confirms a complete extraction of total iodine from aerosol by this method. Only few works on determination of total and water insoluble ^{127}I in aerosol were implemented using instrumental neutron activation analysis (INAA),²⁰ which do not need to decompose the sample. Pyrolysis was proposed to separate total or insoluble iodine from aerosol on quartz and a cellulose filter.¹⁹ However, our preliminary experiment shows that it is not well suited for filters of organic materials (e.g., polypropylene) because of rapid burning of organic materials at high temperatures, causing a low iodine recovery (<60%). Alkaline ashing is a cost-efficient method for decomposition of a large size sample for separation of iodine, but low chemical yield of iodine (ca. 60%) for aerosol on polypropylene filter was reported.²¹

This work aims to develop an effective method for speciation analysis of ^{129}I and ^{127}I in aerosol samples, including iodide,

iodate, and organic iodine in the water-soluble fraction, as well as alkaline soluble iodine and insoluble iodine. The parameters for water leaching, stability of iodine species during leaching, reagents, and parameters for separation of total and insoluble iodine on a PP aerosol filter are investigated to obtain reliable results of iodine species (^{129}I and ^{127}I) in aerosol samples.

EXPERIMENTAL SECTION

Chemical Reagents and Standards. The ^{127}I carrier (solid I_2 crystal with low ^{129}I level) was obtained from Woodward Company (Colorado, USA), which was dissolved in a 0.4 mol/L NaOH-0.05 mol/L $\text{Na}_2\text{S}_2\text{O}_5$ solution. The ^{129}I standard solution (NIST-SRM-4949c) was purchased from the National Institute of Standard Technology (Gaithersburg, MD, USA). ^{125}I in the form of iodide was purchased from PerkinElmer Corporate (Waltham, USA). All other chemical reagents are of analytical grade and prepared using deionized water (18.2 M Ω ·cm).

Aerosol Sampling. The aerosol samples were collected on a polypropylene filter (Type G-3, PTI, Germany). Six sheets of filter paper of 44 × 55 cm² (corresponding to ca. 80 g for each) were equipped on an in-house aerosol collector (air flux ca. 2000 m³/h), and the filters were changed 1–2 times per week. The collected aerosols on filters were put into plastic bags and stored in the dark until analysis. Two aerosol samples collected at Risø, Denmark (55°41.77'N, 12°05.39'E) in 2011 were analyzed in this work.

Separation of Iodine Species from Aerosol. Iodine in aerosol was extracted sequentially using deionized water and sodium hydroxide solution for water-soluble and NaOH soluble

iodine, followed by alkaline ashing and water leaching of ash for insoluble iodine. Iodide and iodate in the water leachate were further separated using anion exchange chromatography, and water-soluble organic iodine was obtained by the difference of total water-soluble iodine and the sum of iodide and iodate. Figure 1 schematically shows the diagram of the separation procedure for speciation analysis of iodine isotopes (^{129}I and ^{127}I).

Extraction of Water-Soluble Iodine and Separation of Iodate and Iodide. An aerosol filter of 0.2–3.0 g (corresponding to 60–900 m³ air) was cut to pieces (about 2 × 2 mm) and put into a beaker with 5–30 mL of deionized water. The mixture was stirred using a magnetic stirrer at 600 rpm at room temperature (~20 °C) for 15 min–5 h to leach water-soluble iodine. The leachate was vacuum filtered through a 0.45 μm membrane (MCE membrane 0.45 UM S-Pak Grid, 47 mm, VWR). The remaining aerosol on the filter was rinsed twice with two aliquots of 10 mL deionized water under stirring. The two washes were filtered and combined with the leachate as the water-soluble fraction. The remaining aerosol on the filter and the MCE membrane were used for subsequent NaOH leaching.

One-third of the water leachate was used for measurement of total water-soluble iodine isotopes (^{127}I and ^{129}I) and the remaining two-thirds for speciation analysis of water-soluble iodine (^{127}I and ^{129}I). An anion exchange chromatography method modified from Hou et al.^{23,24} was used for the separation of iodate and iodide from water leachate of aerosol. A column of 15 cm in height and 7 mm in diameter was packed with strong base anion exchange resin (AG 1 × -4, NO₃⁻ form, 50–100 mesh, Bio-Rad, California, USA). The water leachate spiked with 500 Bq of $^{125}\text{I}^-$ as a chemical yield tracer was loaded to the column, on which iodate passed through the column due to its low affinity with anion exchange resin, while iodide was strongly adsorbed onto the resin. A total of 10 mL of 0.2 mol/L NaNO₃ and 10 mL of deionized water were used to rinse the column sequentially. The washes were combined with the effluent for determination of iodate. Iodide absorbed on the column was then eluted using 30 mL of 5% NaClO and 10 mL of 3 mol/L HNO₃ sequentially. The chemical yield of iodide during chromatographic separation was obtained by measurement of ^{125}I in the eluate using NaI gamma spectrometry (Canberra Inc., Connecticut, USA). A total of 1–10 mL of water leachate, iodate, and iodide fractions depending on the iodine concentration in the fractions were taken out for measurement of ^{127}I by ICP-MS, and the remaining solution was used to further separate iodine for the ^{129}I measurement.

Separation of NaOH Soluble Iodine in Aerosol. The remaining aerosol on the filter together with the MCE membrane was immersed into 5–40 mL of a 0.5 mol/L NaOH solution. The suspension was stirred for 30 min–5 h at a certain temperature (20, 45, and 60 °C measured using a probe), and the solution was covered by watch glass for refluxing. After cooling down to room temperature, the leachate was vacuum filtered through a 0.45 μm MCE membrane. The remaining aerosol on the filter was rinsed twice using two aliquots of 10 mL of 0.5 mol/L NaOH solution. The two washes were combined with NaOH leachate, which is used for measuring NaOH soluble iodine isotopes. A total of 1 mL of NaOH leachate was reserved for measurement of ^{127}I by ICP-MS, and the remaining leachate was used for further separation of iodine for ^{129}I measurement. The residue on the filter and

MCE membrane for filtration were transferred into a porcelain crucible for alkaline ashing.

Separation of Insoluble Iodine and Total Iodine in Aerosol Filter. The residual aerosol after NaOH leaching or 1.0 g of original aerosol sample in small pieces (about 2 × 2 mm) was weighted into a porcelain crucible. A total of 5–10 mL of 1–2 mol/L NaOH solution, 0–3 mL of 1 mol/L K₂S₂O₈, and 500 Bq $^{125}\text{I}^-$ solution were added and mixed. The blended sample was dried at 80 °C, and the completely dried sample was covered with aluminum foil with a 1 cm² hole pierced on it and put into a furnace. The temperature of the furnace was raised to 350 °C at a ramp rate of 5 °C/min and kept for 2 h, then raised to 500–700 °C at the same rate, at which it dwelled for 1–4 h.

After cooling down to room temperature, the ash in the crucible was ground to powder using a glass rod and leached with deionized water on a hot plate at 70 °C for 20 min. The leachate was separated from residue by filtration through a quantitative filter paper (Munktell OOK, Sweden). ^{125}I in the leachate was measured using a NaI Gamma detector (Canberra, Connecticut, USA) for calculating the chemical yield of iodine in the alkaline ashing procedure. A total of 1 mL of the leachate was used to measure ^{127}I using ICP-MS, and the remaining leachate was used to further separate iodine for ^{129}I measurement.

Decomposition of Organic Iodine in Water and NaOH Leachate. A total of 500 Bq $^{125}\text{I}^-$ and 1.0 mg of ^{127}I carrier were added to the leachates (water and NaOH leachate), then K₂S₂O₈ was added to a final concentration of 30 mg/g. The mixture was heated at 60 °C overnight with a watch glass cover for refluxing to decompose organic iodine in the leachate and convert them to inorganic iodine.²⁵ It was observed that the yellow NaOH leachate turned colorless after K₂S₂O₈ decomposition.

Separation of Iodine in Each Fraction for ^{129}I Measurement. The prepared solutions including separated iodide and iodate fractions, decomposed water and NaOH leachates, water leachate from ashes of original aerosol filter, and residue filter after water and NaOH leaching were transferred to appropriate separation funnels. A total of 1.0 mg of ^{127}I carrier, 500 Bq of $^{125}\text{I}^-$ tracer (if not added in previous steps), and 1.0 mL of 1.0 mol/L KHSO₃ solution were added, and then the solution was adjusted to pH 1–2 using HNO₃ to convert all iodine species to iodide. With the addition of an appropriate amount of 1 mol/L NaNO₂, iodide was oxidized to I₂ and extracted by CHCl₃. Iodine in the chloroform phase was transferred to a new separation funnel and back-extracted using KHSO₃ solution. The CHCl₃ extraction and back extraction were repeated once for further purification. The separated iodine (in iodide) in a small volume (5–7 mL) was transferred to a centrifuge tube and precipitated as AgI by the addition of 1.0 mL of 0.5 mol/L AgNO₃ solution. ^{125}I in the precipitate was measured using a NaI gamma detector for calculating the chemical yield of iodine. The AgI precipitate was separated using centrifugation and dried at 70 °C for AMS measurement of ^{129}I .

Determination of ^{127}I by ICP-MS and ^{129}I by AMS. ^{127}I in all separated solutions was measured using ICP-MS (Thermo Fisher, X Series II) as described elsewhere.²⁴

^{129}I in the prepared AgI precipitates was measured by a 5 MV accelerator mass spectrometer (NEC, Wisconsin, USA) at Scottish Universities Environmental Research Center, U. K., as described in detail elsewhere.²⁶ Procedure blanks were prepared

Table 1. Influence of Experimental Parameters on Leaching Efficiency of Iodine

category	experimental parameters						water/NaOH soluble ^{127}I , ng/ m^3
	group number	mass of aerosol filter, g	leachant volume, mL	leaching time, h	leaching temperature, $^{\circ}\text{C}$		
amount of leaching water	1-1	0.2	5	0.5	RT	0.261 \pm 0.010	
	1-2	0.2	10	0.5	RT	0.306 \pm 0.013	
	1-3	0.2	15	0.5	RT	0.289 \pm 0.014	
water leaching time	2-1	1.0	20	0.25	RT	0.356 \pm 0.009	
	2-2	1.0	20	0.5	RT	0.360 \pm 0.010	
	2-3	1.0	20	1	RT	0.392 \pm 0.017	
	2-4	1.0	20	2	RT	0.382 \pm 0.012	
	2-5	1.0	20	3	RT	0.388 \pm 0.009	
	2-6	1.0	20	5	RT	0.387 \pm 0.017	
NaOH leaching temperature	3-1	1.0	40	4	20	0.564 \pm 0.013	
	3-2	1.0	40	4	45	0.663 \pm 0.011	
	3-3	1.0	40	4	60	0.646 \pm 0.014	
NaOH leaching time	4-1	0.2	20	0.5	45	0.549 \pm 0.034	
	4-2	0.2	20	1	45	0.661 \pm 0.021	
	4-3	0.2	20	2	45	0.659 \pm 0.026	
	4-4	0.2	20	3	45	0.658 \pm 0.031	

using a blank filter (without aerosol) and the same procedure as samples. The measured $^{129}\text{I}/^{127}\text{I}$ atomic ratios in the procedure blanks are $\sim 5 \times 10^{-13}$, 1–3 orders of magnitude lower than that observed in the aerosol samples in this work.

RESULTS AND DISCUSSION

Water-Soluble Iodine. Volume of Water and Leaching Time. The results (Table 1, group 1) show that the amount of iodine leached using 5 mL of deionized water was about 14% lower than those using 10 or 15 mL, and the latter two leached a similar amount of iodine. The relatively lower leaching efficiency of iodine using 5 mL of water might be attributed to insufficient immersion of the aerosol filter in water. An excessive amount of water will cause dilution of iodine in the leachate, resulting in undetectable ^{127}I species in the leachate by ICP-MS. Given the volume of PP aerosol filter pieces, it is recommended to use 10 mL of deionized water for less than 1 g filter and a mass ratio of water to filter of 10 for more than 1 g filter.

The amount of water leached iodine increased with the leaching time extending from 15 min to 1 h and kept constant afterward until 5 h (Table 1, group 2). A long leaching time could guarantee complete leaching of iodine and better repeatability. However, the extended leaching time will reduce sample throughput and likely increase the risk of iodine species transformation.

Stability of Iodine Species during Leaching. Maintaining the species unchanged during the separation process is critical for obtaining reliable results in speciation analysis. A synchronous increase in the concentrations of iodide and iodate was observed with extending the leaching time from 15 min to 1 h, which was followed by a slightly decreased iodide concentration and increased iodate concentration but a constant sum of iodide and iodate after 2 h (Figure 2). The iodide/iodate molecular ratios decreased from 14.4 ± 0.2 within 1 h to 12.6 ± 0.2 for over 2 h leaching. This might be attributed to oxidation of iodide to iodate in the water leachate for long time leaching (≥ 2 h). However, such variation of iodine species in water leachate was not observed for the aerosols collected on the quartz filter even for a leaching time up to 24 h.²⁷

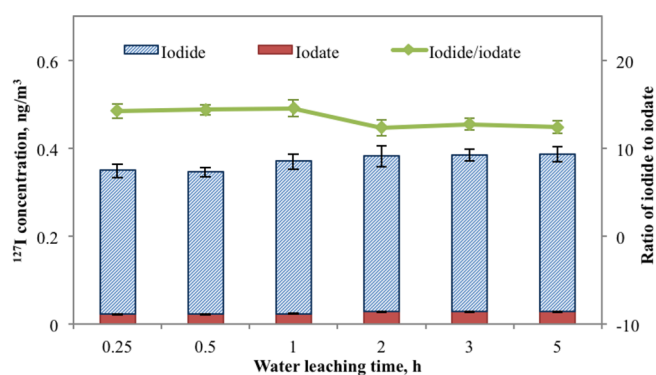


Figure 2. Variation of iodine species in water extracts with extracting time (see experimental conditions in group 2, Table 1).

Baker et al.⁶ have observed that inorganic iodine concentrations in water leachate of aerosols using ultrasonic-assistant extraction decrease with extended leaching time and attributed this to conversion of iodide to organic iodine species on a cellulose filter.⁶ Xu et al.¹⁸ also observed significantly decreased recoveries of iodide spiked to aerosols on a cellulose filter from 87% to only 18% when leached time was extended from 5 min to 1 h but no variation of iodide recovery when spiked to glass microfiber filter.¹⁸ The stability of iodide during water leaching of aerosols is therefore likely related to the filter type. In the view of stability of inorganic iodine species, the organic filter (PP used in this work and cellulose) shows a stronger influence than the inorganic fiber air filter (quartz and glass filters), and thus leaching time has to be strictly controlled to avoid the transformation of iodine species.

It has been reported that the PP polymer is liable to degradation when exposed to heat and UV radiation,²⁸ which is primarily a peroxide- and alkyl radical-mediated chain oxidation process, forming oxidative products, e.g., free radicals (Reactions 1–4):²⁹

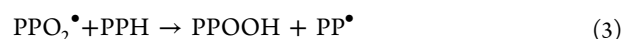
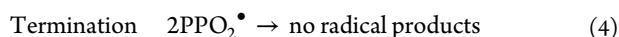


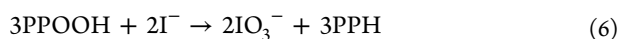
Table 2. Influences of Various Parameters on Separation of Iodine from Aerosol Filter by Alkaline Ashing

category	group number	experimental parameters						iodine in ash, %	iodine in leachate, %
		amount of aerosol filter, g	NaOH conc., mol/L	NaOH volume, mL	temperature, °C	ashing time, h	1.0 mol/L K ₂ S ₂ O ₅ , mL		
concentration of NaOH	5-1	1.0	1	10	600	2	0	59.8 ± 0.7	
	5-2	1.0	2	10	600	2	0	55.8 ± 4.6	
amount of NaOH	6-1	0.5	2	5	600	2	0	62.3 ± 0.6	
	6-2	0.5	2	7	600	2	0	64.4 ± 1.6	
	6-3	0.5	2	10	600	2	0	70.7 ± 3.5	
ashing temperature	7-1	0.5	2	5	500	2	0	53.7 ± 3.9	
	7-2	0.5	2	5	550	2	0	43.9 ± 4.0	
	7-3	0.5	2	5	600	2	0	62.3 ± 2.5	
	7-4	0.5	2	5	650	2	0	48.0 ± 6.1	
	7-5	0.5	2	5	700	2	0	43.1 ± 4.0	
ashing time	8-1	1.0	1	10	600	1	1	92.8 ± 2.8	59.1 ± 4.5
	8-2	1.0	1	10	600	2	1	96.1 ± 4.2	90.0 ± 3.8
	8-3	1.0	1	10	600	3	1	91.5 ± 3.6	85.7 ± 0.1
	8-4	1.0	1	10	600	4	1	89.3 ± 5.3	79.1 ± 10.3
effect of K ₂ S ₂ O ₅	9-1	1.0	1	10	600	2	0	65.0 ± 1.5	50.4 ± 2.1
	9-2	1.0	1	10	600	3	0.1	85.8 ± 4.3	80.2 ± 4.0
	9-3	1.0	1	10	600	3	0.2	86.3 ± 3.4	72.5 ± 3.7
	9-4	1.0	1	10	600	3	0.3	91.1 ± 4.6	79.5 ± 4.0
	9-5	1.0	1	10	600	3	0.5	92.5 ± 5.4	77.1 ± 3.9
	9-6	1.0	1	10	600	3	0.7	95.7 ± 3.6	85.7 ± 4.3
	9-7	1.0	1	10	600	3	1	90.3 ± 4.2	82.1 ± 1.5
	9-8	1.0	1	10	600	3	2	86.2 ± 4.1	75.7 ± 6.0
	9-9	1.0	1	10	600	3	3	87.6 ± 5.4	63.5 ± 9.7



where PPH is polypropylene, PP[•] is free radical of polypropylene, PPO₂[•] is peroxide radical, and PPOOH is hydroperoxide.

In the microenvironment of the PP surface, the strongly oxidative peroxides most likely convert iodide to iodate, as demonstrated in the Reactions 5 and 6.



Since the degradation is a thermally induced slow activation process, and time and temperature dependent, it results in oxidation of iodide after some time. In order to reduce transformation of iodine species in aerosol on a PP filter, the water leaching time is controlled within 1 h.

NaOH Soluble Iodine. Amount of NaOH and Leaching Time. This procedure was the same as the water leaching experiment; 10 mL of 0.5 mol/L NaOH solution was used for 1 g aerosol filter sample to get sufficient contact between leaching solution and aerosol filter. The effect of leaching time on the leaching efficiency of iodine using 0.5 mol/L NaOH (see Table 1, group 4) shows that the amount of leached iodine increased when leaching time extended from 0.5 to 1 h, and then remained constant when further extending leaching time to 3 h. This indicates that a complete liberation of iodine with 0.5 mol/L NaOH solution can be achieved in 1 h.

Leaching Temperature. The amount of iodine leached using 0.5 mol/L NaOH (Table 1, group 3) increased with the temperature rising from room temperature to 45 °C, but remained constant when the temperature further increased to 60 °C. Considering the evaporation loss of leaching solution at high temperature and partial dissolution of the cellulose membrane used for filtration of the leachate in warm NaOH

solution, the leaching temperature at 45 °C was used for NaOH leaching of aerosol filter.

Extraction of iodine from an aerosol filter using 0.5 mol/L NaOH at room temperature have been often used for determination of total ¹²⁹I.^{12,13,22} Based on the above results, ¹²⁹I concentrations in aerosols might be underestimated when leaching at room temperature even without consideration of NaOH insoluble iodine in aerosol.

Species of NaOH Soluble Iodine. No iodine species in the NaOH leachate was identified because NaOH solution might change the species of iodine during leaching. NaOH leaching is often used to remove organic substances in fractionation analysis of soil and sediment.^{30,31} This is based on the high solubility of major organic substances in soil and sediment, such as humic substances. The major organic substances in aerosol include lipidic, saccharides, proteinaceous materials, and humic-like substances (HULIS).³²⁻³⁴ Most of these organic compounds have hydrophilic functional groups (e.g., carboxylic acid, amino acid, aliphatic alcohol) in low molecular weight and thus are water-soluble. HULIS found ubiquitous in aerosol are termed so because of their similarity with terrestrial/aquatic humic substances.³⁵ It was observed that the alkaline extractable HULIS accounts for 42–74% (expressed as carbon mass) of total HULIS in aerosols.³⁴ Because iodine is readily associated with HULIS, especially active iodine species (e.g., I₂ and HOI), as observed in soil and sediment,³⁶ the NaOH soluble iodine species might be mainly HULIS bound iodine.

Separation of Total and Insoluble Iodine in Aerosols on PP Filter. Pyrolysis using a tube furnace is most commonly applied for extraction of total and insoluble iodine from solid samples such as soil, sediment, and aerosol on a filter due to its high efficiency.^{10,19,37} However, the conventionally used tube furnace has a maximum capacity of 0.5 g PP aerosol filter that is insufficient for speciation analysis of ¹²⁹I. In addition, the rapid

Table 3. Analytical Results of ^{127}I and ^{129}I Species in Aerosols Collected from Risø, Denmark in 2011

sample ID	total iodine	water-soluble iodine	iodate	iodide	NaOH soluble iodine	residual insoluble iodine	sum of iodine species	sum/total, %
^{127}I concentration, ng/m ³								
AE015	2.027 ± 0.104	0.221 ± 0.011	ND	0.237 ± 0.012	0.638 ± 0.036	1.308 ± 0.087	2.168 ± 0.095	107.0
AE017	1.041 ± 0.055	0.316 ± 0.019	0.033 ± 0.024	0.283 ± 0.014	0.377 ± 0.027	0.343 ± 0.018	1.036 ± 0.037	99.5
^{129}I concentration, × 10 ⁵ atoms/m ³								
AE015	43.81 ± 1.28	5.55 ± 0.27	ND	5.91 ± 0.74	12.58 ± 0.46	27.51 ± 1.28	45.64 ± 1.39	104.2
AE017	11.31 ± 0.43	3.34 ± 0.11	ND	3.68 ± 0.24	3.36 ± 0.25	4.27 ± 0.74	10.97 ± 0.78	97.0
$^{129}\text{I}/^{127}\text{I}$ atomic ratio, × 10 ⁻⁸								
AE015	45.60 ± 2.70	52.85 ± 3.66	ND	52.50 ± 7.16	41.58 ± 2.79	44.36 ± 3.61		
AE017	22.92 ± 1.48	22.30 ± 1.55	ND	30.43 ± 2.38	18.81 ± 1.93	26.28 ± 4.73		

burning of PP filter produces large amount of gas, suddenly increases the pressure in the combustion tube, and causes a risk of extrusive loss of iodine during insufficient combustion, even an explosion. Ashing is an alternative method to release iodine from an aerosol filter without limitation on sample size, but it has to be implemented in an alkali medium to prevent the loss of iodine through forming volatile species of iodine during ashing at high temperatures. Effects of the amount of NaOH, ashing temperature and time, and protection reagent on the extraction efficiency of iodine were investigated by spiking an ^{125}I tracer on the PP filter (Table 2).

Effect of Amount of NaOH. The analytical results (Table 2, group 5) show that although the leaching rate of iodine on the aerosol filter using 10 mL of 1.0 mol/L NaOH (59.8%) for a 1.0 g PP aerosol filter is slightly higher than that using 10 mL of 2.0 mol/L NaOH solution (55.8%); the difference is not statistically significant. For a 0.5 g PP filter, when the volume of 2.0 mol/L NaOH solution added to filter increased from 5 to 10 mL (corresponding to NaOH/filter mass ratios of 20–40 mmol/g), the leaching rate of iodine slightly increased from 62.3% to 70.7% (Table 2, group 6). The recovery of iodine in the ash leachate is related to two aspects: the loss of iodine during the ashing process and the leaching efficiency of iodine from the ash. In aerosols as well as other environmental samples, iodine may exist as inorganic iodide and iodate, organic associated iodine, and mineral and oxide associated iodine. These forms of iodine will be converted to molecular iodine or other volatile iodine species when the temperature increases in the atmosphere of oxygen. The addition of alkali such as NaOH to the sample provides an alkaline medium, which prevents the formation of volatile species of iodine (e.g., disproportionated reaction with I_2); however, it also impairs the combustion of iodinated organic compounds. To get an overall better recovery of iodine in the ashing and leaching steps, the amount of NaOH added has to be compromised. With the consideration of the effect of high salt content in the leachate on the ICP-MS measurement of ^{127}I , 10 mL of 1 mol/L NaOH solution is added to 1.0 g of PP aerosol filter, i.e. an NaOH/filter mass ratio of 10 mmol/g.

Ashing Temperature. The experiments on influence of ashing temperature (Table 2, groups 7 and 8) show that the recoveries of iodine in the leachate increased from 43.9% at 550 °C to 62.3% at 600 °C, and then decreased to 43.1% with a temperature increasing to 700 °C. The optimal ashing temperature is 600 °C for separation of iodine from aerosols on a PP filter. The lower recovery of iodine at higher temperatures might be attributed to an increased loss of iodine because of the formation of volatile iodine species and limited protection function of NaOH at high temperatures. However,

the low recovery of iodine at lower temperatures might mainly result from the insufficient combustion of organic substances and retardation of iodine in the resulting carbon. Even at optimal temperatures, the unsatisfactory iodine recovery in the leachate might result from both the loss of iodine during ashing due to defective protection of the NaOH medium and association of iodine with insufficient combusted carbon.

Protection of Iodine from Loss during Ashing. The loss of iodine during ashing might be caused by the oxidation of iodine to volatile I_2 at high temperatures. In order to prevent oxidation loss of iodine during ashing, a reductant, potassium metabisulfite ($\text{K}_2\text{S}_2\text{O}_5$) was added to the aerosol filter, and the results (Table 2, group 9) show a significant improvement on iodine recovery, which increased from 65% in the absence of $\text{K}_2\text{S}_2\text{O}_5$ to 96% with the addition of a suitable amount of $\text{K}_2\text{S}_2\text{O}_5$. Such a protection function of the reductant was also reported in analyzing protein samples for iodine.³⁸ The loss of iodine decreased with increased $\text{K}_2\text{S}_2\text{O}_5$ amount and reached as low as 4% of iodine loss when 0.7–1.0 mmol $\text{K}_2\text{S}_2\text{O}_5$ was added to 1 g of PP filter. Further addition of $\text{K}_2\text{S}_2\text{O}_5$ decreased the recovery of iodine in both ashing and leaching steps, especially the latter one. This is probably ascribed to incomplete combustion of the PP filter in the addition of excessive amount of $\text{K}_2\text{S}_2\text{O}_5$. The protection mechanism of $\text{K}_2\text{S}_2\text{O}_5$ for iodine during ashing might be explained by the fact that volatile iodine species (e.g., I_2) formed by oxidation of iodine species on a filter during ashing can be rapidly reduced to stable iodide by $\text{K}_2\text{S}_2\text{O}_5$, while the rate of disproportionation reaction of I_2 in a NaOH medium is relatively slower, resulting in partial loss of the formed volatile iodine species.

Ashing Time. The experiment (Table 2, group 8) shows that although a high recovery of iodine of 93% was obtained for 1 h of ashing, the iodine recovery in leachate is of only 59%, indicating insufficient ashing of the sample. A total of 2–3 h ashing produced a good recovery of iodine in the ashing step, but the best recovery of iodine (>90%) was obtained for 2 h ashing in both ashing and leaching steps. Further extending ashing time to more than 4 h slightly reduced the iodine recovery in both ashing and leaching steps.

Based on all these experiments, the optimal parameters for ashing 1 g of PP filter are 10 mL of 1 mol/L NaOH and 1 mmol of $\text{K}_2\text{S}_2\text{O}_5$ added as protection reagents and ashing at 600 °C for 2 h.

Analytical Performance. Detection Limit of the Method. Procedure blanks were prepared through the entire analytical procedure the same as the samples, and the resulted ^{127}I concentration and $^{129}\text{I}/^{127}\text{I}$ ratio are 4.3 ± 0.7 ng/g filter and less than 5×10^{-13} , respectively. The detection limit of ^{127}I was calculated as 3 times blank standard deviation (σ_0) for a certain

amount of measurements, i.e. $DL = 3\sigma_0$, is 2.1 ng/g filter ($n = 5$). Based on the typical parameters of aerosol sampling, 14 520 cm^2 (corresponding to about 480 g) of aerosol filter used for sampling at an air flow rate of 2000 m^3/h for 72 h, i.e. 300 m^3/g filter; a corresponding detection limit of 0.007 ng/m^3 air can be obtained. This is sufficiently low for measurement of iodine in the atmosphere, where its concentrations are usually in range of 0.1–25 ng/m^3 .⁷

For ^{129}I , the detection limit estimated as 3 times the $^{129}\text{I}/^{127}\text{I}$ ratio of the procedure blank was 1.5×10^{-12} , corresponding to ^{129}I of 7.1×10^6 atoms (1.5 fg) considering 1.0 mg of ^{127}I carrier was used for target preparation. The $^{129}\text{I}/^{127}\text{I}$ ratios of $(5-76) \times 10^{-8}$ were measured in precipitation at the same sampling location in Denmark.⁴⁰ For the aerosols with a similar $^{129}\text{I}/^{127}\text{I}$ ratio as precipitation ($(5-76) \times 10^{-8}$) and 1 ng/m^3 of ^{127}I , and assuming the least abundant species accounts for 5% of total ^{129}I , at least 600 m^3 of air (corresponding to 2.0 g aerosol filter) is needed for speciation analysis of ^{129}I . For the background areas with $^{129}\text{I}/^{127}\text{I}$ atomic ratios of $(1-10) \times 10^{-9}$, such as those in Asia and America,^{37,41} more than 30 000 m^3 of air volume (corresponding to 100 g filter) is needed for speciation analysis of ^{129}I .

Speciation Analysis of ^{129}I and ^{127}I in Aerosol in Denmark. Two aerosol samples collected at Risø, Denmark in 2011 were analyzed using the established method for speciation analysis of ^{129}I and ^{127}I . The results (Table 3) show that the sum of all the species including water-soluble iodine, NaOH soluble iodine, and insoluble iodine is in good agreement with total iodine concentrations, as revealed by the ratios of sum to total iodine in the range of 97% to 107% for both ^{127}I and ^{129}I . This confirms the reliability of the presented method for speciation analysis of ^{129}I and ^{127}I in aerosol samples.

The total ^{127}I concentrations in the aerosol samples vary from 1.04 ng/m^3 to 2.03 ng/m^3 . These values fall within the typical range of iodine concentrations in aerosol from coastal areas (0.3–21 ng/m^3).⁷ The total ^{129}I concentrations in the aerosol samples vary from 11.3×10^5 atoms/ m^3 to 43.8×10^5 atoms/ m^3 , which is consistent with the reported ^{129}I concentrations in the European aerosol samples of 0.07–79 $\times 10^5$ atoms/ m^3 .^{11,12,39} The measured $^{129}\text{I}/^{127}\text{I}$ atomic ratios range from 22.9×10^{-8} to 45.6×10^{-8} , which is comparable with those in precipitation ($5.04-76.5 \times 10^{-8}$) collected at the same location during 2001–2006.⁴⁰ The variation of ^{129}I concentrations and $^{129}\text{I}/^{127}\text{I}$ ratios in the aerosols might be attributed to different sampling dates and meteorological conditions. A similar large variation was also observed in the precipitation samples.⁴⁰

Water-soluble, NaOH soluble, and insoluble iodine account for 11–30%, 32–36%, and 33–65% of total ^{127}I in the aerosols, respectively. A similar distribution of ^{129}I in the three fractions was observed, corresponding to 13–30%, 29–30%, and 38–63%, respectively. This pattern differs from the Fukushima-derived ^{129}I in aerosol collected in Japan, with 42–61% in water leachate, 32–44% in NaOH leachate, and only 4–23% insoluble ^{129}I .²⁷ This large discrepancy might be ascribed to the different sources of ^{129}I (nuclear reprocessing plants and Fukushima nuclear accident, respectively). However, the influence of filter matrix used for aerosol sampling cannot be ruled out either. Iodine in aerosol particles may be strongly bounded to the organic matrix of the filter during sampling and storage, such as the PP filter used in this work compared to the

quartz filter used for aerosol sampling of Fukushima-derived ^{129}I in Japan.²⁷

Almost all reported total ^{129}I data in aerosols were obtained by extraction using 0.5 mol/L NaOH and 0.025 mol/L NaHSO_3 with the assistance of an ultrasonic bath.^{12,13,22} However, the large fraction of insoluble ^{129}I and ^{127}I up to 60% of total iodine in aerosols observed in this work and our previous work²⁷ might imply an underestimation of ^{129}I concentrations when only NaOH leaching method is used. A method of alkaline ashing with the assistance of $\text{K}_2\text{S}_2\text{O}_5$ presented in this work or combustion might have to be applied for reliable determination of total ^{129}I and ^{127}I in aerosol samples.

Iodide is the predominant species of water-soluble iodine for both ^{129}I and ^{127}I in the aerosol samples. The sum of iodate and water-soluble organic iodine calculated by the difference between water-soluble iodine and iodide is less than 3% of total iodine and 10% of water-soluble iodine. This distribution pattern is distinct from that reported by Gilfeder et al.¹⁷ They observed that 83–97% of water-soluble iodine was present as soluble organically bound iodine in the aerosols collected with cellulose nitrate filter paper. The great inconsistency might be attributed to the different sampling areas, and different sources and formation processes of aerosols. The different methods for leaching water-soluble iodine should not be ignored either. A milder magnetic stirring method was utilized in this work compared to the ultrasonification leaching for 20 min in their work; the latter might increase the risk of transformation of inorganic iodide to organic iodine.⁶

CONCLUSIONS

Based on the experiment and discussion above, the following can be concluded:

The established analytical method allows for quantitative determination of water-soluble iodine (iodide, iodate) and NaOH soluble and residual insoluble iodine for ^{129}I and ^{127}I in aerosols, with detection limits of 0.007 ng/m^3 for ^{127}I and 7.1×10^6 atoms (1.5 fg) for ^{129}I . The reliability of the proposed method is confirmed by the good agreement between the sum of all iodine species and total iodine. Transformation of inorganic iodine species occurs during water leaching over 1 h, which is suggested to be attributed to photochemical oxidation of iodide on the organic aerosol filter.

Conventional NaOH extraction both at room temperature and 45–60 °C would lead to underestimate the concentrations of total ^{129}I in aerosols. Alkaline ashing with the addition of $\text{K}_2\text{S}_2\text{O}_5$ as a protection reagent can significantly reduce the loss of iodine in the ashing step, providing a reliable method for determination of total ^{129}I in aerosol samples, especially large size samples and aerosol collected on filters of organic materials. The speciation analysis of ^{129}I and ^{127}I in the aerosol samples collected at Risø, Denmark shows that ^{129}I in water-soluble, NaOH soluble and insoluble species account for 13–30%, 29–30%, and 38–63%, respectively, indicating the commonly used NaOH leaching method for total ^{129}I determination in aerosol might underestimate the ^{129}I level.

AUTHOR INFORMATION

Corresponding Author

*Phone: +45 2132 5129. E-mail: xiho@dtu.dk.

Notes

The authors declare no competing financial interest.

ACKNOWLEDGMENTS

L. Z. is grateful for the supports from all the colleagues in the Division of Radioecology (headed by Sven P. Nielsen), Center for Nuclear Technologies, Technical University of Denmark for her Ph.D. project. This work is partly supported through the project of Innovation Methodology (no. 2012IM030200) from the Ministry of Science and Technology of China.

REFERENCES

- (1) O'Dowd, C. D.; Jimenez, J. L.; Bahreini, R.; Flagan, R. C.; Seinfeld, J. H.; Hämeri, K.; Pirjola, L.; Kulmala, M.; Jennings, S. G.; Hoffmann, T. *Nature* **2002**, *417*, 632–636.
- (2) McFiggans, G. *Nature* **2005**, *433*, E13–E13.
- (3) Vogt, R.; Sander, R.; Von Glasow, R.; Crutzen, P. J. *Atmos. Chem. Phys.* **1999**, *32*, 375–395.
- (4) Solomon, S.; Garcia, R. R.; Ravishankara, A. R. *J. Geophys. Res.: Atmos.* **1994**, *99*, 20491–20499.
- (5) Slingo, A. *Nature* **1990**, *343*, 49–51.
- (6) Baker, A. R.; Thompson, D.; Campos, M. L. A. M.; Parry, S. J.; Jickells, T. D. *Atmos. Environ.* **2000**, *34*, 4331–4336.
- (7) Saiz-Lopez, A.; Gómez Martín, J. C.; Plane, J. M. C.; Saunders, R. W.; Baker, A. R.; Von Glasow, R.; Carpenter, L. J.; McFiggans, G. *Chem. Rev.* **2012**, *112*, 1773–1804.
- (8) Moreda-Piñeiro, A.; Romaris-Hortas, V.; Bermejo-Barrera, P. J. *Anal. At. Spectrom.* **2011**, *26*, 2107–2152.
- (9) Raisbeck, G. M.; Yiou, F.; Zhou, Z. Q.; Kilius, L. R. *J. Mar. Syst.* **1995**, *6*, S61–S70.
- (10) Hou, X.; Hansen, V.; Aldahan, A.; Possnert, G.; Lind, O. C.; Lujanienė, G. *Anal. Chim. Acta* **2009**, *632*, 181–196.
- (11) Jabbar, T.; Steier, P.; Wallner, G.; Priller, A.; Kandler, N.; Kaiser, A. *Environ. Sci. Technol.* **2012**, *46*, 8637–8644.
- (12) Englund, E.; Aldahan, A.; Hou, X.; Possnert, G.; Soderstrom, C. *Nucl. Instrum. Methods Phys. Res., Sect. B* **2010**, *268*, 1139–1141.
- (13) Santos, F. J.; López-Gutiérrez, J. M.; Chamizo, E.; García-León, M.; Sinal, H. A. *Nucl. Instrum. Methods Phys. Res., Sect. B* **2006**, *249*, 772–775.
- (14) López-Gutiérrez, J. M.; García-León, M.; Schnabel, C.; Schmidt, A.; Michel, R.; Sinal, H. A.; Suter, M. *Appl. Radial. Isot.* **1999**, *51*, 315–322.
- (15) Baker, A. R.; Tunnicliffe, C.; Jickells, T. D. *J. Geophys. Res.* **2001**, *106*, 28743–28749.
- (16) Baker, A. R. *Environ. Chem.* **2005**, *2*, 295–298.
- (17) Gilfedder, B. S.; Lai, S. C.; Petri, M.; Biester, H.; Hoffmann, T. *Atmos. Chem. Phys.* **2008**, *8*, 6069–6084.
- (18) Xu, S.; Xie, Z.; Liu, W.; Yang, H.; Li, B. *Chin. J. Anal. Chem.* **2010**, *38*, 219–224.
- (19) Gilfedder, B. S.; Chance, R.; Dettmann, U.; Lai, S. C.; Baker, A. R. *Anal. Bioanal. Chem.* **2010**, *398*, 519–526.
- (20) Tsukada, H.; Ishida, J.; Narita, O. *Atmos. Environ. Part A Gen. Topics* **1991**, *25*, 905–908.
- (21) Li, D.; Zhang, L.; Wang, X.; Liu, L. *Anal. Chim. Acta* **2003**, *482*, 129–135.
- (22) Jabbar, T.; Steier, P.; Wallner, G.; Kandler, N.; Katzberger, C. *Nucl. Instrum. Methods Phys. Res., Sect. B* **2011**, *269*, 3183–3187.
- (23) Hou, X.; Dahlgaard, H.; Rietz, B.; Jacobsen, U.; Nielsen, S. P.; Aarkrog, A. *Anal. Chem.* **1999**, *71*, 2745–2750.
- (24) Hou, X.; Aldahan, A.; Nielsen, S. P.; Possnert, G.; Nies, H.; Hedfors, J. *Environ. Sci. Technol.* **2007**, *41*, S993–S999.
- (25) Dang, H.; Hou, X.; Roos, P.; Nielsen, S. P. *Anal. Methods* **2013**, *5*, 449–456.
- (26) Xu, S.; Freeman, S. P. H. T.; Hou, X.; Watanabe, A.; Yamaguchi, K.; Zhang, L. *Environ. Sci. Technol.* **2013**, *47*, 2010851–10859.
- (27) Xu, S.; Zhang, L.; Freeman, S. P. H. T.; Hou, X.; Shibata, Y.; Sanderson, D.; Cresswell, A.; Doi, T.; Tanaka, A. *Environ. Sci. Technol.* **2015**, *49*, 1017–1024.
- (28) Wikipedia. <http://en.wikipedia.org/wiki/Polypropylene>.
- (29) Makipirtti, S.; Bergholm, H. European Patent Office. 1995.8.16, EP0667406 (A1), 1–43.
- (30) Hou, X.; Fogh, C. L.; Kucera, J.; Andersson, K. G.; Dahlgaard, H.; Nielsen, S. P. *Sci. Total Environ.* **2003**, *308*, 97–109.
- (31) Englund, E.; Aldahan, A.; Hou, X.; Petersen, R.; Possnert, G. *Nucl. Instrum. Methods Phys. Res., Sect. B* **2010**, *268*, 1102–1105.
- (32) O'Dowd, C. D.; Facchini, M. C.; Cavalli, F.; Ceburnis, D.; Mircea, M.; Decesari, S.; Fuzzi, S.; Yoon, Y. J.; Putaud, J. *Nature* **2004**, *431*, 676–680.
- (33) Duarte, A. d. C.; Duarte, R. M. B. O. In *Biophysico-Chemical Processes Involving Natural Nonliving Organic Matter in Environmental Systems*; Senesi, N.; Xing, B.; Huang, P. M., Eds.; Wiley: Hoboken, NJ, 2009; pp 451–485.
- (34) Feczko, T.; Puxbaum, H.; Kasper-Giebl, A.; Handler, M.; Limbeck, A.; Gelencsér, A.; Pio, C.; Preunkert, S.; Legrand, M. *J. Geophys. Res.: Atmos.* **2007**, *112*, D23S10.
- (35) Zheng, G.; He, K.; Duan, F.; Cheng, Y.; Ma, Y. *Environ. Pollut.* **2013**, *181*, 301–314.
- (36) Xu, C.; Miller, E. J.; Zhang, S. J.; Li, H.; Ho, Y.; Schwehr, K. A.; Kaplan, D. I.; Otsuka, S.; Roberts, K. A.; Brinkmeyer, R.; Yeager, C. M.; Santschi, P. H. *Environ. Sci. Technol.* **2011**, *45*, 9975–9983.
- (37) Zhang, L.; Zhou, W. J.; Hou, X.; Chen, N.; Liu, Q.; He, C.; Fan, Y.; Luo, M.; Wang, Z.; Fu, Y. *Sci. Total Environ.* **2011**, *409*, 3780–3788.
- (38) Andersson, S.; Forsman, U. *J. Chromatogr. B Biomed. Sci. Appl.* **1997**, *692*, 53–59.
- (39) Michel, R.; Daraoui, A.; Gorny, M.; Jakob, D.; Sachse, R.; Tosch, L.; Nies, H.; Goroncy, I.; Herrmann, J.; Sinal, H. A.; Stocker, M.; Alifimov, V. *Sci. Total Environ.* **2012**, *419*, 151–169.
- (40) Hou, X.; Aldahan, A.; Nielsen, S. P.; Possnert, G. *Environ. Sci. Technol.* **2009**, *43*, 6522–6528.
- (41) Oktay, S. D.; Santschi, P. H.; Moran, J. E.; Sharma, P. *Environ. Sci. Technol.* **2001**, *35*, 4470–4476.

Paper III

Depth Profile of Chemical Species of ^{129}I and ^{127}I and Implication for Water Circulation and Marine Environmental Chemistry in the Central Arctic

Luyuan Zhang¹, Xiaolin Hou^{1,2*}, Justin P. Gwynn³, Michael Karcher^{4,5}, Weijian Zhou², Yukun Fan², Qi Liu²

1) Center for Nuclear Technologies, Technical University of Denmark, Risø Campus, Roskilde 4000, Denmark

2) Xi'an AMS Center, State Key Laboratory of Loess and Quaternary Geology, Shanxi Key Laboratory of Accelerator Mass Spectrometry Technology and Application, Institute of Earth Environment, Chinese Academy of Sciences, Xi'an 710075, China

3) Norwegian Radiation Protection Authority, The Fram Centre, Tromsø 9296, Norway

4) O.A.Sys - Ocean Atmosphere Systems GmbH, Hamburg 22767, Germany

5) Alfred Wegener Institute for Polar and Marine Research, Bremerhaven 27515, Germany

Abstract

Speciation and cycling of iodine in high latitude and deep-ocean are not well investigated. Depth profile seawater samples collected from the central Arctic were analyzed for total ^{129}I and ^{127}I , as well as their iodide and iodate species. The sharp stratification of ^{129}I concentrations in the depth profiles indicates very limited vertical exchange between the polar mixed layer and the Atlantic water layer. In the polar mixed layer, the highest ^{129}I concentration (72×10^8 atoms/L) was observed in the marginal area compared to the interior of the Eurasian Basin, and a similar high ^{129}I concentration was found in the Makarov Basin, which significantly declined in the Canada basin. These results indicate the ^{129}I -enriched water from the Eurasian Basin moved to the Makarov Basin and from marginal side to basin interior, and only small fraction of ^{129}I -enriched water moved to the Canada Basin, where it mixed with ^{129}I -depleted Pacific water. Iodate is the predominant species for both ^{129}I and ^{127}I in all water columns. The molecular ratios of iodide to iodate are 0.22-0.62 for ^{127}I and 0.47-0.73 for ^{129}I in the polar mixed layer, whereas these ratios in the Atlantic water layer decreased dramatically to 0.02-0.07 for ^{127}I and 0.07-0.28 for ^{129}I . The observations in this work shed new lights on transformation of iodine species in high latitude and deep-ocean. The results show that reduction of iodate and oxidation of iodide in the polar mixed layer of the basin interior are rather slow. In contrast, relatively fast reduction of iodate to iodide in the polar mixed layer over the ridges and basin margins was found, which might be attributed to the relatively high nutrients and higher biological activities. In the Atlantic water layer of the Arctic Ocean, oxidation of iodide back to iodate occurred with conversion rate of about $2 \text{ nmol L}^{-1} \text{ year}^{-1}$. ^{129}I

*Corresponding author.

E-mail address: xiho@dtu.dk

inventory in top 800 m of the Arctic Ocean is estimated to be about 1460 kg by 2011, which was increased 4-6 times compared to that before 2000.

Keywords: ^{129}I , speciation analysis of iodine, the Arctic Ocean, tracing study, current circulation

1. Introduction

The element iodine plays an essential role on human health as a constituent of thyroid hormone, and lack of dietary iodine will cause goiter. Ocean is considered as the major reservoir of iodine with a concentration of approximately 60 $\mu\text{g/L}$, and a source of terrestrial iodine through atmosphere transportation (Wong. 1991). Geochemical cycling of iodine in the environment is strongly dependent on iodine species that exhibit distinct environmental behaviors (Hu et al. 2012; Wong. 1991). In seawater, iodine mainly exists as iodate, iodide and dissolved organic iodine (Elderfield and Truesdale. 1980; Truesdale. 1994a; Wong and Cheng. 2001; Wong and Cheng. 2008). The dissolved inorganic iodine species are the predominant forms of iodine especially in open seas. The distribution of iodide and iodate differs in geophysical locations due to differences in the plankton community composition, physicochemical characteristics and climate conditions (He et al. 2013). It has been extensively studied for the formation of iodide in the oxygenated seawater, conversion mechanism and rate among iodine species and fluxes of iodine between oceans and atmosphere in tropical and temperate seas (Chance et al. 2010; Luther et al. 1995; Tian and Nicolas. 1995; Tsunogai and Sase. 1969; Wong and Cheng. 2001). Only few studies have focused on the distribution of iodine species in high latitude regions (Bluhm et al. 2011; Campos et al. 1999; Tsunogai and Henmi. 1971; Waite et al. 2006). However, there is no information on how iodine species are distributed and whether transformation among iodine species behavior differently in the harsh environment of the Arctic up to now.

Due to the difficulties for distinguishing the origin of newly produced and converted iodine species, the conversion process of iodine species is still unclear. ^{129}I is one of isotopes of iodine with long half-life of 1.57×10^7 years. As an important fission product with high fission yield (0.7%), ^{129}I in the environment presumably originates from marine discharges from two nuclear reprocessing plants at Sellafield (UK) and La Hague (France) (Hou et al. 2007; Raisbeck et al. 1995). Speciation analysis of radioactive ^{129}I provides an ideal approach on iodine cycling in various water systems (He et al. 2014; Hou et al. 2001; Hou et al. 2007; Hou et al. 2009; Lehto et al. 2012; Yi et al. 2012). Iodine is a conservative element that remains in seawater and can travel over long distances from the point of injection without removal from the water body to the seabed. ^{129}I has been applied as an oceanographic tracer in recent years and successfully employed in the Atlantic, Pacific, Arctic and Indian Oceans, as well as the Nordic seas, Baltic Sea, etc (Alfimov et al. 2004; Edmonds et al. 2001; Michel et al.

2012; Povinec et al. 2010; Raisbeck and Yiou. 1999; Smith et al. 1998). Despite its significance on geochemical cycling of iodine, nevertheless, studies on speciation analysis of ^{129}I in the environment is very limited, and less was applied to explore conversion of iodine species in water systems. Hou et al. firstly investigated ^{129}I and ^{127}I chemical species in the North Sea, and suggests that interconversion between iodate and iodide is a sluggish process in open sea (Hou et al. 2007). Yi et al. reported the distribution of iodide and iodate for both ^{129}I and ^{127}I in the Baltic Proper, Kattegat, and Skagerrak Basins, which suggested that effective reduction of iodate occurs in the waters of the Baltic Proper (Yi et al. 2012). Furthermore, ^{129}I speciation in the North Atlantic Ocean shows a relation with its sources, environmental conditions and water residence time (He et al. 2013). However, none of these studies on speciation of ^{129}I and ^{127}I in the polar marine environment has been reported.

In this study, we analyzed 12 water depth profiles collected from the Arctic Ocean during Polarstern expedition ARK-XXVI/3 on August-October 2011 for total of ^{129}I and ^{127}I , as well as their inorganic species, iodide and iodate, in order to depict a picture on the distribution of ^{129}I and ^{127}I species in the high latitude ocean as well as in deep ocean, and more importantly, to improve our understanding on water circulation and marine environmental chemistry in the central Arctic.

2. Materials and analytical methods

The seawater samples were collected by CTD rosette from the central Arctic Ocean during the Polarstern expedition ARK-XXVI/3 conducted by the Alfred Wegener Institute (AWI) in a period of 22 August - 22 September 2011. 12 water columns down to 800 m depth were sampled in the southeastern Eurasian Basin (EB), Makarov Basin (MB), and northern Canada Basin (CB) (Fig. 1). Hydrographic data, including salinity, potential temperature and dissolved oxygen concentrations are shown in Table S-1. All water samples were filtered through a 0.45 μm filter after collection, and 1 L subsample was sealed in polyethylene bottle and stored in dark until laboratory analysis in Technical University of Denmark.

The sample preparation method used for iodine speciation was modified from our previous procedure (Hou et al. 2007). In brief, anion exchange chromatography method was used to separate iodide and iodate species from seawater. After addition of an appropriate amount of ^{127}I carrier (Woodward Company, USA) and ^{125}I tracer (PerkinElmer, Waltham, USA), ^{129}I in the original seawater sample and fractions of iodide and iodate were first reduced to iodide form using KHSO_3 in acidic media. Iodine was then oxidized by NaNO_2 to I_2 and extracted to chloroform phase. I_2 in the CHCl_3 phase was reduced to iodide and back-extracted into water phase. This extraction and back extraction were repeated once for further purification. Iodide in the final solution was precipitated as AgI . After mixing with niobium powder (325 mesh, Alfa Aesar, Karlsruhe, Germany), the AgI targets were measured for ^{129}I by AMS (3MV,

HVEE, Netherland) at Xi'an AMS Center, China (Zhou et al. 2010). Procedure blank was prepared using the same procedure as samples, and measured to be less than 5×10^{-13} for $^{129}\text{I}/^{127}\text{I}$ ratio, which is two orders of magnitude lower than samples. Overall analytical uncertainty for ^{129}I is less than 5% and 10% for samples with $^{129}\text{I}/^{127}\text{I}$ atomic ratio of 1.0×10^{-10} and 1.0×10^{-11} , respectively. Concentrations of ^{127}I in seawater, iodide and iodate fractions were determined by ICP-MS (Thermo Fisher, X Series II) using Xt cone under normal mode (Hou et al. 2007). The detailed method is presented in [the supporting information](#).

3. Result

Level and distribution of total ^{127}I and ^{129}I . The concentrations of ^{129}I and ^{127}I in 12 water depth profiles are shown in [Table 1](#). An apparent depletion of ^{127}I by approximately 15% was observed in the polar mixed layer (PML, 0-50 m deep) compared to those in the Atlantic water layer (AWL, 200-800 m,) ([Fig. 3 and Table 1](#)). ^{127}I concentrations in the PML ranged from 39.6-53.5 $\mu\text{g/L}$ and showed a positively dependent on the salinity ($R^2=0.44$ and $p=0.03$, [Fig. S-1](#)). While in the AWL, ^{127}I concentrations elevated to an average of 56.80 $\mu\text{g/L}$ and kept relatively constant (55-60 $\mu\text{g/L}$). The relative lower ^{127}I concentration in the PML might be attributed to the dilution of seawater by relative fresh sea ice containing less ^{127}I , this is supported by the relative lower and variable salinity in the PML (31-34 psu) compared to a relative constant salinity in the AWL (34.5-34.8 psu).

The concentrations of ^{129}I in the Arctic seawater show a large variation range of $1.4\text{-}72.6 \times 10^8$ atoms/L ([Fig. 2](#)). A similar trend for $^{129}\text{I}/^{127}\text{I}$ atomic ratios of up to 2 orders of magnitude difference is also observed ([Fig. 3](#)), where the lowest $^{129}\text{I}/^{127}\text{I}$ ratio of 6.03×10^{-10} in the CB and the highest value of 310×10^{-10} in the EB occurred ([Table 2](#)). In the PML, the highest ^{129}I concentrations of $(61.8\text{-}72.6) \times 10^8$ occurred in the EB (sampling point No. 9, 10, 11, 12), which slightly decreased to $(60.5\text{-}71.8) \times 10^8$ atoms/L in the MB, and then significantly decreased to $(1.4\text{-}11.8) \times 10^8$ atoms/L in the CB. In the EB, the ^{129}I concentrations slightly declined from the basin margin (station 12) to the interior (stations 9-11) ([Table 1, 2 and Fig. 2, 3](#)). The depth profiles of ^{129}I in the 12 sampling stations ([Fig. 3](#)) show that ^{129}I concentrations dramatically decreased with the increased depth in the top 200 m (the PML) except station 1 in CB, but slightly decreased in 200-800 m (the AWL). The typical depth distributions of ^{129}I in Eurasian, Makarov and Canada Basins (at the sampling stations 1, 5 and 12) are illustrated in [Fig. 4 and S-2](#). Within AWL, relative high ^{129}I concentrations were observed in EB and Lomonosov Ridge compared to in the MB, the lowest concentration in the CB and Mendeleev-Alpha Ridge. Meanwhile slightly higher values in the stations closed to the ridge than those in the basin interiors ([Fig. 3](#)).

Distribution of ^{127}I and ^{129}I species. The results of speciation analysis of inorganic

iodine species, iodate and iodide (Table 1, 2 and Fig. 4, S-2) show that iodate (expressed as IO_3^-) is the predominant specie in all depth profiles for both ^{129}I and ^{127}I . Except $^{127}\text{I}^-$ that enriched in the surface layer and depleted in deep layer, depth profile of ^{129}I species ($^{129}\text{I}^-$ and $^{129}\text{IO}_3^-$) and $^{127}\text{IO}_3^-$ follow the patterns of total ^{129}I and ^{127}I , respectively. The average $^{127}\text{I}^-$ concentration of 11.77 $\mu\text{g/L}$ in the PML is approximately 7 times higher than that in the AWL (1.61 $\mu\text{g/L}$ in average). The distribution features for $^{127}\text{IO}_3^-$ and $^{127}\text{I}^-$ are well consistent with those in the Pacific Ocean and the northwestern Mediterranean Sea (Huang et al. 2005; Tian and Nicolas. 1995). Wide concentration ranges of ^{129}I species presented in the PML, $(0.82-50.29) \times 10^8$ atoms/L for $^{129}\text{IO}_3^-$ and $(2.88-35.38) \times 10^8$ atoms/L for $^{129}\text{I}^-$, in which 27.7 - 45.3% of total ^{129}I were $^{129}\text{I}^-$. Relative higher $^{129}\text{I}^-/^{129}\text{IO}_3^-$ molecular ratios compared to $^{127}\text{I}^-/^{127}\text{IO}_3^-$ ratios in all water columns and a remarkable difference between the PML and the AWL (Fig. 5 and 6) were observed. There is no significant gradient in I/IO_3^- ratios in the PML ranging in 0.22-0.62 for ^{127}I and 0.48-0.73 for ^{129}I , but it seems they were higher over the Alpha and Lomonosov Ridges and basin margin (stations 2 and 6) than those in the interior of basins in the PML. The of $^{127}\text{I}^-/^{127}\text{IO}_3^-$ molecular ratios in the AWL were relative constant and keep much low values of 0.02-0.07, while $^{129}\text{I}^-/^{129}\text{IO}_3^-$ ratios shows a remarkable decrease trend from the highest value of 0.28 in the EB to the lowest value of 0.07 in the CB.

4. Discussion

Sources of ^{129}I in the central Arctic.

The observed ^{129}I level in the Arctic ($(6-310) \times 10^{-10}$ for $^{129}\text{I}/^{127}\text{I}$ ratios) is 1-2 orders of magnitude higher than the background environmental level of the post-nuclear era (ca. 1×10^{-10} for $^{129}\text{I}/^{127}\text{I}$ ratios) (Oktay et al. 2001; Zhang et al. 2011). At the eastern EB (station 12), the concentration of ^{129}I in the PML measured to be approximately 12×10^8 atoms/L in mid-1990 (Buraglio et al. 1999; Cooper et al. 1999), has raised by six-fold to about 65×10^8 atoms/L in late 2000s (Smith et al. 2011), and up to 72.58×10^8 atoms/L in 2011 in this work. About 4-fold increase in ^{129}I concentrations are found in the AWL from 1995 (5×10^8 atoms/L) to 2011 (22×10^8 atoms/L) (Smith et al. 2011). Scientific explorations in the Arctic since 1980s indicated that the Arctic Ocean becomes one of major reservoirs of ^{129}I (Alfimov et al. 2006; Josefsson. 1998; Smith et al. 1998). The source of ^{129}I in the Arctic Ocean has been extensively established, including the nuclear weapon testing, Chernobyl nuclear accident and the nuclear reprocessing plants (especially Sellafield in United Kingdom and La Hague in France) (Alfimov et al. 2004; Beasley et al. 1998; Cooper et al. 1999; Josefsson. 1998; Smith et al. 1998). Of these, the two European NRPs, Sellafield in UK and La Hague in France, are the dominant source of ^{129}I , from which about 6000 kg ^{129}I has been discharged into the English Channel and the Irish Sea by 2009. A large fraction of the marine discharged ^{129}I was transported to the North Sea and then further moved northwards by the North Atlantic

Current and Norwegian Coastal Current, finally entered into the Arctic Ocean through the Barents Sea and Fram Strait (Alfimov et al. 2004; Hou et al. 2007; Smith et al. 1998). Besides this source, the Fukushima nuclear accident took place in March 2011, six months before this Polarstern expedition, is probably a new contributor of ^{129}I to the Arctic Ocean. A large amount of radioiodine was released to the environment (Xu et al. 2015), which has been transported by the prevailing westerly wind cross the Pacific Ocean and further. Fukushima-derived ^{131}I of $810 \mu\text{Bq}/\text{m}^3$ in aerosol samples has been observed in Svalbard, the high arctic area (Paatero et al. 2012). Based on the reported Fukushima derived $^{129}\text{I}/^{131}\text{I}$ atomic ratio of 16.0 (Xu et al. 2015) and an average ^{127}I concentration of $1 \mu\text{g}/\text{m}^3$, corresponding to a Fukushima derived $^{129}\text{I}/^{127}\text{I}$ atomic ratio of 1.7×10^{-11} in the Arctic atmosphere. Compared with the measured $^{129}\text{I}/^{127}\text{I}$ atomic ratio of $(6-310) \times 10^{-10}$ in the seawater of the PML in the central Arctic, the ^{129}I signal from the Fukushima nuclear accident is negligible and greatly overwhelming by the reprocessing signal.

^{129}I traced water circulation pathway in the central Arctic.

In the PML, the ^{129}I concentrations highest in the EB (sampling point No. 9, 10, 11, 12) and slightly lower in the MB dramatically decreased in the CB by a factor of more than 5. This clearly shows the transport pathway of the water mass in the central Arctic. Reprocessing-derived ^{129}I enter to the Arctic mainly through the Barents Sea and Kara Sea through the North Sea and Norwegian coast (Alfimov et al. 2004; Beasley et al. 1998; Smith et al. 1998). In the EB, the slightly declined ^{129}I concentrations from the basin margin (station 12) to interior (stations 9-11) (Table 1, Fig. 2 and 3) indicate that a fraction of Norwegian coast current and Norwegian Atlantic current carrying reprocessing-derived ^{129}I was transported to the Laptev Sea and further gradually into the EB interior (Stations 12, 11, 10, and 9). The remarkably declined ^{129}I at station 8 indicates that only a small fraction of this water moved to the station 8 along the Eurasian side of the Lomonosov Ridge, and most of water carried high ^{129}I moves to the MB, causing similar high ^{129}I concentrations in the PML in the MB (station 4, 6 and 7). The relative higher ^{129}I concentration at station 4 (71.8×10^8 atoms/L) compared to station 7 (65.4×10^8 atoms/L) and station 5 (60.5×10^8 atoms/L) indicate that the ^{129}I enrich water from the EB first moved to the station 7 in the MB and then moved towards station 5 with dispersion to station 7. From marginal side of the MB, only small fraction of ^{129}I -enriched water moved to the CB, where it mixed with ^{129}I depleted Pacific water, resulting in a much lower ^{129}I concentration in the PML in the CB. The lowest ^{129}I concentration at station 1 might be attributed to that it located in the relative center part of CB, and the water circulation mainly along the Mendeleev-Alpha Ridge and marginal area.

The sharp stratification of ^{129}I concentrations in the depth profiles indicates very limited vertical exchange between the PML and AWL. This agrees with the oceanographic

studies, which suggest that a thick advective layer of intermediate density (i.e. halocline) inhibits the interaction between the two layers (Rudels et al. 1996). The small variation of ^{129}I and ^{127}I in the AWL in the Eurasian and Makarov Basins suggests a sufficient vertical mixture/exchange of water in these areas. Within the AWL, the feature of relative high ^{129}I concentrations in EB and Lomonosov Ridge compared to the MB and the lowest concentration in the CB and Mendeleev-Alpha Ridge (Fig. 3) reflects the pathways of water currents and water circulation in the three major basins in the Arctic Ocean (Smith et al. 1998).

Unlike to other station, the lowest ^{129}I concentration in the Sampling station 1 in the CB was observed in the PML, and a peak value of ^{129}I concentrations in the depth profiles occurs at upper AWL (244 m depth), which is comparable with the values observed in MB and Mendeleev-Alpha Ridge in the same layer. This feature clearly indicates the formation pathway of the intermediate water in the east side of the CB through the MB margin. While the water in the PML in the CB should mainly from the Pacific ocean through the Bering Strait, which carrying much less ^{129}I mainly weapons fall out derived ^{129}I (Cooper et al. 2001). This finding agrees well with the previous report on transportation of ^{129}I in the Arctic Ocean (Karcher et al. 2012; Smith et al. 2011; Smith et al. 1998), and also supported by the oceanographic evidence on water mixing between the Pacific water mass and Atlantic water mass (Rudels. 2012).

In the PML of the northern CB, despite the presence of the front between Atlantic water and Pacific water locating over the Mendeleev-Alpha Ridge (Rudels et al. 2004), ^{129}I concentration increased at surface layer (station 1) from 0.5×10^8 atoms/L in 1995 (Smith et al. 1999) to 1.36×10^8 atoms/L in 2011, indicating that ^{129}I has intruded to the surface layer of CB with a very slow rate. This process might be implemented through two possible ways: 1) lateral mixing between the Atlantic and Pacific water masses; 2) vertical exchange of the ^{129}I contained AWL water with the surface water. Whatever, the slow increase of ^{129}I in the CB implies that this mixing process is rather limited.

^{127}I and ^{129}I speciation traced marine environmental chemistry in the central Arctic.

Except along the Lomonosov and Mendeleev-Alpha ridges (stations 2 and 6), ^{127}I in the PML is mainly present in iodate with ratios of iodide to iodate of 0.22-0.35, generally below 0.30 (Fig.5). This agrees well with the reported values in the Arctic Ocean (with ratios of 0.23) in 2008 (He et al. 2013), and comparable with those in the open area of the North Sea (ratios of <0.30) in 2005 (Hou et al. 2007) (Table S-2). A high iodide level with $^{127}\text{I}/^{127}\text{IO}_3^-$ ratios of 0.41-0.62 was observed along the ridges (Fig. 5). There is no other iodine speciation information available over the ridges so far. High level of iodide is generally observed in inshore surface water ($^{127}\text{I}/^{127}\text{IO}_3^-$ ratios > 0.6) (Hou et al. 2007), where is considered to have higher biological activities. Similar to ^{127}I , the major species of ^{129}I was iodide in the PML, with $^{129}\text{I}/^{129}\text{IO}_3^-$ ratios

0.47-0.60 excluding the samples collected over the ridges. These $^{129}\text{I}/^{129}\text{IO}_3^-$ ratios falls within the range in the off-shore of the English Channel, but much lower than those found in the coastal area of the North Sea (Hou et al. 2007). A higher ^{129}I iodide level with $^{129}\text{I}/^{129}\text{IO}_3^-$ ratios of 0.64-0.73 was observed along the ridges. Insignificant change of iodine species for ^{129}I and ^{127}I was observed in the PML water in the central Arctic except the water over the ridges (Fig. 5 and 6). The resident time of the PML water in the Arctic was estimated to be about 5 years (Becker and Bjork. 1996), and transit time from the EB to the MB to be 1-3 years (Smith et al. 2011). The speciation results in this work suggest that the species transformation of iodine, including oxidation of iodide and reduction of iodate in the PML of the basin interior in the central Arctic Ocean is tardy.

The concurrent elevation of iodide/iodate ratios for ^{129}I and ^{127}I observed over the ridges might suggest a fast reduction of iodate to iodide in local area. Although reduction of iodate to iodide is regarded as a thermodynamically unfavorable reaction, it can be observed widely in oxygenated seawater (Bluhm et al. 2011; Tsunogai and Sase. 1969; Waite et al. 2006; Wong and Cheng. 1998). Factors controlling reduction of iodate to iodide in oxygenated seawater have not fully understood so far. Multi-processes, including photochemically induced reduction in presence of organic matter, reactions with reductants (bisulfides and thiols such as glutathione), decomposition of sinking organism debris especially in water-sediment interface, phytoplankton growth and cell senescence, have been demonstrated to related to the reduction of iodate to iodine in seawater (Aldahan et al. 2007; Bluhm et al. 2011; Chance et al. 2010; Hird and Yates. 1961; Spokes and Liss. 1996; Zhang and Whitfield. 1986). Despite photochemical reaction as an inducement, the central Arctic covered by thick sea-ice sheet hardly receives direct solar radiation even in summer time. Compared to other seas, no significant decrease in iodide proportion to total iodine was observed in the Arctic interior, which indicates photochemical process might not be key to induce iodate reduction in high latitude area. Reductive chemicals are normally present in anoxic seawaters, which could not be the case in the Arctic. Biological activity, therefore, might play an important role on reduction of iodate to iodide. The inflows of the Atlantic water along the continental margin and ridges (Fig. 1) can import heat and nutrients as showed by the higher concentrations of nitrate and phosphate (Fig. S-3), which promotes the primary production, such as phytoplankton and microalgae in the basin margin and ridge areas. This is confirmed by the enriched chlorophyll a concentrations over the ridges and basin margin but depleted in the basin interior in the central Arctic (Fig. S-4). Additionally, a significant negative correlation of salinity with ^{127}I in the PML ($R^2=0.47$ and $p=0.02$, Fig. S-1) might indicate formation of iodide is linked to the intrusion of freshwater, such as sea-ice melting that also provides nutrients to the mixed layer and facilitates phytoplankton bloom. It is therefore suggested that reduction of iodate to iodide in water over the ridges and basin

margin results from the biological activities. Since only two water samples were analyzed in these areas, more intensive studies are still needed for further confirmation. For the deep Arctic water, iodate for both ^{129}I and ^{127}I is the predominate species with a relative constantly low $^{127}\text{I}/^{127}\text{IO}_3^-$ ratios (0.02-0.07) in the AWL (Fig. 3 and S-2). This agrees well with those found in deep layer of the Pacific Ocean ($^{127}\text{I}/^{127}\text{IO}_3^-$ ratios of less than 0.08) (Huang et al. 2005; Tsunogai and Henmi. 1971). Unlike ^{127}I , $^{129}\text{I}/^{129}\text{IO}_3^-$ ratios in the AWL exhibit a marked declining trend from the EB (0.28) to the CB (0.07). Data on ^{129}I speciation in water depth profiles are rather scarce. Yi et al. have reported high $^{129}\text{I}/^{129}\text{IO}_3^-$ values of 0.4 - 44.9 in water columns from Skagerrak, Kattegat and the Baltic Sea (Yi et al. 2012) (Table S-2). In their work, effective reduction of iodate in the waters of the Baltic Proper is suggested the reason of high ratios of inorganic ^{129}I species, attributing to the decomposition of organic matter and photochemically induced reactions.

Currently, it is believed that iodide oxidation must happen in the deep-ocean, where almost all of the iodine is in the form of iodate (Truesdale. 1994b; Truesdale. 2008). However, no direct evidence has shown the oxidation of iodide to iodate at depth of oceans. $^{129}\text{I}/^{129}\text{IO}_3^-$ ratios are significantly declined from the EB to the CB in the AWL, but $^{127}\text{I}/^{127}\text{IO}_3^-$ ratios in this layer didn't show dramatical change. This might indicates that ^{129}I was oxidized to $^{129}\text{IO}_3^-$ in the AWL during water mixing and current movement. Transit time of the AWL water current from the EB to the Canada was estimated to be about 7-10 years (Smith et al. 2011). If taking 0.28 and 0.07 as the representative $^{129}\text{I}/^{129}\text{IO}_3^-$ ratios in the two basins, 21.7% and 6.5% of ^{129}I should be iodide in these two basins respectively. An oxidation rate of iodide to iodate can be estimated to be 1.5-2.1% per year. Based on a ^{127}I concentration of 15 $\mu\text{g/L}$ (120 nmol/L) as observed in the surface layer, the calculated oxidation rate is 1.8-2.5 $\text{nmol L}^{-1} \text{ year}^{-1}$ in the AWL. This oxidation rate is comparable with those reported in the deep water of the Southern Ocean with value of 3-6 $\text{nmol L}^{-1} \text{ year}^{-1}$ (Bluhm et al. 2011), but one order of magnitude lower than that in the deep waters of a Scottish Loch with an oxidation rate of $30 \pm 10 \text{ nmol L}^{-1} \text{ year}^{-1}$ (Edwards and Truesdale. 1997). This suggests that the oxidation of iodide back to iodate is quite slow in the deep polar water. Since the residence time of the AWL water in the Arctic Ocean is about 35 years (Becker and Bjork. 1996), iodide in the downwelling water from the continental shelves can be sufficiently oxidized to iodate to reach equilibrium between iodide and iodate.

Chemical oxidation of iodide is thermodynamically favored in oxygenated water through dissolved oxygen (Table S-1) (Wong. 1980), which might be predominantly responsible to the dominated iodate species in the AWL water in the central Arctic. Biologically catalyzed iodide oxidation has also been proposed as another process of the iodate production in seawater (Campos et al. 1996), among various biological species, the fungus *Caldariomyces fumago* and marine proteobacteria have been confirmed to oxidizes iodide to iodate via the chloroperoxidase enzyme and

extracellular enzyme (Amachi et al. 2005; Thomas and Hager. 1968).

Although both ^{127}I and ^{129}I showed a similar higher iodide concentration in the PML compared to those in the AWL, there is no significant correlation between $^{127}\text{I}/^{127}\text{IO}_3^-$ ratios with $^{129}\text{I}/^{129}\text{IO}_3^-$ in both layers (Fig. S-5). This might be attributed to the different sources of ^{127}I and ^{129}I , and a slow process to reach isotope equilibrium.

Inventory of ^{129}I in the central Arctic Ocean.

Along with the increased discharges of anthropogenic ^{129}I from Sellafield and La Hague, quantity of ^{129}I retained in the Arctic Ocean has elevated significantly. In order to estimate ^{129}I inventory in the central Arctic with a total area of $1.64 \times 10^6 \text{ km}^2$, it is divided to three parts, the Eurasian, Canada and Makarov Basins, on the basis of typical ^{129}I vertical profiles (Fig. 3). Depth distribution of ^{129}I was established by performing curve fitting using the least-squares method based on the present and reported data with time correction (Smith et al. 2011), and the inventory of ^{129}I was calculated by integrating these fitting functions at depth range of 0-800 m (See details in the supporting information, Table S-3 and Fig. S-5).

Inventory of ^{129}I resided in top 800 m of the central Arctic is estimated to be 1457 kg by 2011 (Table 3), which accounts for 25.6% of total marine discharge of the two European NRPs (5693 kg by 2009), almost equivalent to the total discharge from Sellafield and La Hague before 1994 (1426 kg). Due to large variation of ^{129}I in the Arctic Ocean, especially over the ridge and in the basin interior, uncertainty of ^{129}I inventory is as large as 24% for this estimation. Buraglio et al. have estimated a total inventory of 2.7×10^{27} atoms of ^{129}I (equivalent to 578.6 kg) in the central Arctic Ocean in 1996 based on the assumptions with a depth of about 4100 m and a surface area of about $6.6 \times 10^6 \text{ km}^2$ (Buraglio et al. 1999). This corresponds to approximately 230 kg in the top 800 m. Another estimation of the ^{129}I inventory in the upper 1000 m of the central Arctic was 440 kg in 2001, corresponding to 350 kg in the top 800 m (Alfimov et al. 2004). It is apparent that the inventory of ^{129}I within a depth of 800 m in the central Arctic by 2011 has increased at least by a factor of 6 and 4 compared to those by 1996 and 2001, respectively. The high inventory of ^{129}I estimated in this work compared to the previous ones results from the remarkably increased discharges of ^{129}I from the two European reprocessing plants since 1990. If considering the average transit time of ^{129}I from Sellafield and La Hague to the central Arctic Ocean is 10 years, 4-6 times higher inventory of ^{129}I in 2011 estimated in this work compared to those in 1996 and 2001 is well consistent with the about 4 times increased total ^{129}I discharges from two European reprocessing plants by 2001 (3583 kg) compared to those by 1990 (847 kg).

The EB and MB converged most of ^{129}I in the central Arctic, accounting for 67.8% and 22.2% respectively. More than half of ^{129}I was found in the Atlantic Layer (835 kg). Only 10% of ^{129}I entered into the CB, of which only 1% was detained in upper 200 m. It takes 10-15 years for ^{129}I to reach the central Arctic from Sellafield and La Hague

(Orre et al. 2010; Smith et al. 2011). Water residence time in polar mixed layer and Atlantic water layer are about 5 years and 35 years, respectively (Becker and Bjork. 1996). This implies, during the four decades discharges since 1966, the amount of ^{129}I transported to the PML has been renewed for several times (>5 times), whereas ^{129}I in the AWL water was just exchanged 1-2 times in the Arctic Ocean. Consequently, the AWL of the Arctic Ocean acts as not only a major reservoir but also a buffer that postpone reprocessing discharged ^{129}I into the downstream Nordic Seas and further to the North Atlantic Ocean along the Greenland continental slope. The constantly high discharge of ^{129}I from two European reprocessing plants in the past 10-15 years has not arrived to the Arctic, which will continue to elevate the inventory of ^{129}I in following ten years.

5. Conclusion

Vertical distribution of ^{129}I in the Eurasian and Makarov Basins shows a different pattern from those in the CB, which is strongly associated with water mixing between the ^{129}I -rich Atlantic-originated water and the ^{129}I -poor Pacific-originated water. Speciation analysis of ^{129}I and ^{127}I in the water samples indicates iodide level in the PML is significantly higher than those in the AWL. Elevated iodide levels found in the PML water sampled over the Lomonosov and Mendeleev-Alpha Ridges indicate reduction of iodate occurs with a strong relationship with abundant nutrients and active biological activities. A weak variation of Γ/IO_3^- between ^{129}I and ^{127}I reveals conversion of iodine species is rather slow in the PML. Oxidation of iodide back to iodate in deep ocean has been clearly demonstrated by the change of $^{129}\text{I}/^{129}\text{IO}_3^-$ in the AWL. This provides a direct proof for the regeneration of iodate in marine systems.

The ^{129}I inventory in the upper Arctic Ocean is estimated to be 1457 kg, 4-6 times higher than that before 2000s, makes the Arctic Ocean an important reservoir and a major source of ^{129}I to the downstream and atmosphere.

Supporting Information

Supporting information described the details of methods for chemical speciation separation and instrumental measurement for ^{129}I , ^{127}I . The calculation of ^{129}I inventory in the Arctic Ocean was also presented in detail. It includes three tables and six figures.

Acknowledgement

All scientists and crews in the "Polarstern" to the Arctic in 2011 (ARK-XXVI/3-TransArc) are sincerely grateful for their great efforts on water sampling. This work is partly supported by the projects of Innovation Methodology (no.2012IM030200) and Fundamental Scientific Research (2015FY110800) from the Ministry of Science and Technology of China.

Reference

- Aldahan A, Englund E, Possnert G, Cato I, Hou X. Iodine-129 enrichment in sediment of the Baltic Sea. *Appl Geochem* 2007;22:637-47.
- Alfimov V, Aldahan A, Possnert G, Winsor P. Anthropogenic iodine-129 in seawater along a transect from the Norwegian coastal current to the North Pole. *Mar Pollut Bull* 2004;49:1097-104.
- Alfimov V, Possnert G, Aldahan A. Anthropogenic iodine-129 in the Arctic Ocean and Nordic Seas: Numerical modeling and prognoses. *Mar Pollut Bull* 2006;52:380-5.
- Amachi S, Mishima Y, Shinoyama H, Muramatsu Y, Fujii T. Active transport and accumulation of iodide by newly isolated marine bacteria. *Appl Environ Microbiol* 2005;71:741-5.
- Beasley T, Cooper LW, Grebmeier JM, Aagaard K, Kelley JM, Kilius LR. $^{237}\text{Np}/^{129}\text{I}$ atom ratios in the Arctic Ocean - Has ^{237}Np from Western European and Russian fuel reprocessing facilities entered the Arctic Ocean?. *J Environ Radioact* 1998;39:255-77.
- Becker P, Bjork G. Residence times in the upper Arctic Ocean. *Journal of Geophysical Research C: Oceans* 1996;101:28377-96.
- Bluhm K, Croot PL, Huhn O, Rohardt G, Lochte K. Distribution of iodide and iodate in the Atlantic sector of the southern ocean during austral summer. *Deep Sea Research Part II: Topical Studies in Oceanography* 2011;58:2733-48.
- Buraglio N, Aldahan A, Possnert. Distribution and inventory of ^{129}I in the central Arctic Ocean. *Geophys Res Lett (USA)* 1999;26:1011-4.
- Campos M, Farrenkopf AM, Jickells TD, Luther GW. A comparison of dissolved iodine cycling at the Bermuda Atlantic Time-Series station and Hawaii Ocean Time-Series Station. *Deep-Sea Research Part II-Topical Studies In Oceanography* 1996;43:455-66.
- Campos M, Sanders R, Jickells T. The dissolved iodate and iodide distribution in the South Atlantic from the Weddell Sea to Brazil. *Mar Chem* 1999;65:167-75.
- Chance R, Weston K, Baker AR, Hughes C, Malin G, Carpenter L et al. Seasonal and interannual variation of dissolved iodine speciation at a coastal Antarctic site. *Mar Chem* 2010;118:171-81.
- Cooper LW, Beasley T, Aagaard K, Kelley JM, Larsen IL, Grebmeier JM. Distributions of nuclear fuel-reprocessing tracers in the Arctic Ocean: Indications of Russian river influence. *J Mar Res* 1999;57:715-38.
- Cooper LW, Hong GH, Beasley TM, Grebmeier JM. Iodine-129 Concentrations in Marginal Seas of the North Pacific and Pacific-influenced Waters of the Arctic Ocean. *Mar Pollut Bull* 2001;42:1347-56.
- Edmonds, Zhou, Raisbeck, Yiou F, Kilius, Edmond. Distribution and behavior of anthropogenic ^{129}I in water masses ventilating the North Atlantic Ocean. *J Geophys Res* 2001;106:6881-94.
- Edwards A, Truesdale VW. Regeneration of inorganic iodine species in Loch Etive, a natural leaky incubator. *ESTUARINE COASTAL AND SHELF SCIENCE* 1997;45:357-66.
- Elderfield H, Truesdale VW. On the biophilic nature of iodine in seawater. *Earth Planet Sci Lett* 1980;50:105-14.

- He P, Hou X, Aldahan A, Possnert G, Yi P. Iodine isotopes species fingerprinting environmental conditions in surface water along the northeastern Atlantic Ocean. *Scientific Reports* 2013;3:In press.
- He P, Aldahan A, Possnert G, Hou X. Temporal Variation of Iodine Isotopes in the North Sea. *Environmental Science and Technology* (Washington) 2014;48:1419-25.
- Hird FJR, Yates JR. The oxidation of cysteine, glutathione and thioglycollate by iodate, bromate, persulphate and air. *J Sci Food Agric* 1961;12:89-95.
- Hou X, Aldahan A, Nielsen SP, Possnert G. Time Series of I-129 and I-127 Speciation in Precipitation from Denmark. *Environ Sci Technol* 2009;43:6522-8.
- Hou X, Aldahan A, Nielsen SP, Possnert G, Nies H, Hedfors J. Speciation of I-129 and I-127 in seawater and implications for sources and transport pathways in the North Sea. *Environ Sci Technol* 2007;41:5993-9.
- Hou X, Dahlgaard H, Nielsen SP. Chemical speciation analysis of ¹²⁹I in seawater and a preliminary investigation to use it as a tracer for geochemical cycle study of stable iodine. *Mar Chem* 2001;74:145-55.
- Hu QH, Moran JE, Gan JY. Sorption, degradation, and transport of methyl iodide and other iodine species in geologic media. *Appl Geochem* 2012;27:774-81.
- Huang Z, Ito K, Morita I, Yokota K, Fukushima K, Timerbaev AR et al. Sensitive monitoring of iodine species in sea water using capillary electrophoresis: vertical profiles of dissolved iodine in the Pacific Ocean. *JOURNAL OF ENVIRONMENTAL MONITORING* 2005;7:804-8.
- Josefsson D. Anthropogenic Radionuclides in the Arctic Ocean. PhD thesis 1998.
- Karcher M, Smith JN, Kauker F, Gerdes R, Smethie WM. Recent changes in Arctic Ocean circulation revealed by iodine-129 observations and modeling. *JOURNAL OF GEOPHYSICAL RESEARCH-OCEANS* 2012;117.
- Kattner G, Ludwiczowski K. Inorganic nutrients measured on water bottle samples during POLARSTERN cruise ARK-XXVI/3 (TransArc). Alfred Wegener Institute, Helmholtz Center for Polar and Marine Research, Bremerhaven 2014;doi:10.1594/PANGAEA.832164.
- Lehto J, Rätty T, Hou X, Paatero J, Aldahan A, Possnert G et al. Speciation of ¹²⁹I in sea, lake and rain waters. *Sci Total Environ* 2012;419:60-7.
- Luther GW, WU JF, Cullen JB. Redox chemistry of iodine in seawater - Frontier molecular orbital theory considerations. *AQUATIC CHEMISTRY* 1995;244:135-55.
- Michel R, Daraoui A, Gorny M, Jakob D, Sachse R, Tosch L et al. Iodine-129 and iodine-127 in European seawaters and in precipitation from Northern Germany. *Sci Total Environ* 2012;419:151-69.
- Oktay SD, Santschi PH, Moran JE, Sharma P. ¹²⁹I and ¹²⁷I transport in the Mississippi River. *Environ Sci Technol* 2001;35:4470-6.
- Orre S, Smith JN, Alfimov V, Bentsen M. Simulating transport of ¹²⁹I and idealized tracers in the northern North Atlantic Ocean. *Environ Fluid Mech* 2010;10:213-33.
- Paatero J, Vira J, Siitari-Kauppi M, Hatakka J, Holmen K, Viisanen Y. Airborne fission products in the high Arctic after the Fukushima nuclear accident. *J Environ Radioact* 2012;114:41-7.

- Povinec PP, Lee S-, Kwong LL, Oregioni B, Jull AJT, Kieser WE et al. Tritium, radiocarbon, ⁹⁰Sr and ¹²⁹I in the Pacific and Indian Oceans. *Nucl Instrum Meth B* 2010;268:1214-8.
- Raisbeck GM, Yiou F. ¹²⁹I in the oceans: Origins and applications. *Sci Total Environ* 1999;237-238:31-41.
- Raisbeck GM, Yiou F, Zhou ZQ, Kilius LR. ¹²⁹I from nuclear fuel reprocessing facilities at Sellafield (U.K.) and La Hague (France); potential as an oceanographic tracer. *J Mar Syst* 1995;6:561-70.
- Rudels B. Arctic Ocean circulation and variability - advection and external forcing encounter constraints and local processes. *Ocean Science Discussions* 2012;8:261-86.
- Rudels B, Anderson LG, Jones EP. Formation and evolution of the surface mixed layer and halocline of the Arctic Ocean. *Journal of Geophysical Research: Oceans* 1996;101:8807-21.
- Rudels B, Jones EP, Schauer U, Eriksson P. Atlantic sources of the Arctic Ocean surface and halocline waters. *Polar Res* 2004;23:181-208.
- Smith JN, McLaughlin FA, Smethie WM, Moran SB, Lepore K. Iodine-129, ¹³⁷Cs, and CFC-11 tracer transit time distributions in the Arctic Ocean. *Journal of Geophysical Research: Oceans* 2011;116:- C04024.
- Smith JN, Ellis KM, Boyd T. Circulation features in the central Arctic Ocean revealed by nuclear fuel reprocessing tracers from Scientific Ice Expeditions 1995 and 1996. *J Geophys Res* 1999;104:29663-77.
- Smith JN, Ellis KM, Kilius LR. ¹²⁹I and ¹³⁷Cs tracer measurements in the Arctic Ocean. Deep-sea research Part 1 Oceanographic research papers 1998;45:959-84.
- Spokes LJ, Liss PS. Photochemically induced redox reactions in seawater, II. Nitrogen and iodine. *Mar Chem* 1996;54:1-10.
- Thomas JA, Hager LP. The peroxidation of molecular iodine to iodate by chloroperoxidase. *Biochem Biophys Res Commun* 1968;32:770-5.
- Tian RC, Nicolas E. IODINE SPECIATION IN THE NORTHWESTERN MEDITERRANEAN-SEA - METHOD AND VERTICAL PROFILE. *Mar Chem* 1995;48:151-6.
- Truesdale VW. DISTRIBUTION OF DISSOLVED IODINE IN THE IRISH SEA, A TEMPERATE SHELF SEA. *ESTUARINE COASTAL AND SHELF SCIENCE* 1994a;38:435-46.
- Truesdale VW. A reassessment of redfield correlations between dissolved iodine and nutrients in oceanic waters and a strategy for further investigations of iodine. *Mar Chem* 1994b;48:43-56.
- Truesdale VW. The biogeochemical effect of seaweeds upon close-to natural concentrations of dissolved iodate and iodide in seawater – Preliminary study with *Laminaria digitata* and *Fucus serratus*. *Estuar Coast Shelf Sci* 2008;78:155-65.
- Tsunogai S, Henmi T. Iodine in the surface water of the ocean. *J Oceanogr Soc Jpn* 1971;27:67-72.
- Tsunogai S, Sase T. Formation of iodide-iodine in the ocean. *Deep Sea Research and Oceanographic Abstracts* 1969;16:489-96.
- Waite TJ, Truesdale VW, Olafsson J. The distribution of dissolved inorganic iodine in the seas around Iceland. *Mar Chem* 2006;101:54-67.

- Wong GTF, Cheng XH. Dissolved organic iodine in marine waters: Role in the estuarine geochemistry of iodine. *Journal of Environmental Monitoring* 2001;3:257-63.
- Wong GTF, Cheng X-. Dissolved organic iodine in marine waters: Determination, occurrence and analytical implications. *Oceanographic Literature Review* 1998;45:1512-3.
- Wong GTF. The marine geochemistry of iodine. *Rev Aquat Sci* 1991;4:45-73.
- Wong GTF. The stability of dissolved inorganic species of iodine in seawater. *Mar Chem* 1980;9:13-24.
- Wong GTF, Cheng X. Dissolved inorganic and organic iodine in the Chesapeake Bay and adjacent Atlantic waters: Speciation changes through an estuarine system. *Mar Chem* 2008;111:221-32.
- Xu S, Zhang L, Freeman SPHT, Hou X, Shibata Y, Sanderson D et al. Speciation of Radiocesium and Radioiodine in Aerosols from Tsukuba after the Fukushima Nuclear Accident. *Environ Sci Technol* 2015;49:1017-24.
- Yi P, Aldahan A, Possnert G, Hou X, Hansen V, Wang B. 127I and 129I Species and Transformation in the Baltic Proper, Kattegat, and Skagerrak Basins. *Environ Sci Technol* 2012;46:10948-56.
- Zhang J, Whitfield M. Kinetics of Inorganic Redox Reactions In Seawater I. The Reduction of Iodate By Bisulfide. *Mar Chem* 1986;19:121-38.
- Zhang L, Zhou WJ, Hou X, Chen N, Liu Q, He C et al. Level and source of 129I of environmental samples in Xi'an region, China. *Sci Total Environ* 2011;409:3780-8.
- Zhou WJ, Hou X, Chen N, Zhang LY, Liu Q, He CH et al. Preliminary study of radioisotope 129I application in China using Xi'an accelerator mass spectrometer. *ICNS News* 2010;25:8-23.

Table 1. Analytical results of ^{127}I and ^{129}I and their species in depth profile seawater from the central Arctic.

Station	Description	Depth [m]	^{127}I Conc, ppb						^{129}I Conc, $\times 10^8$ atoms/L					
			Total iodine		I^-		IO_3^-		Total iodine		I^-		IO_3^-	
			Mean	SD	Mean	SD	Mean	SD	Mean	SD	Mean	SD	Mean	SD
1	Canada Basin	25	47.67	1.27	12.42	0.90	35.25	1.40	1.36	0.09	0.39	0.10	0.82	0.09
		244	56.90	1.51	1.26	0.09	55.63	2.20	18.24	1.05	1.68	0.24	17.72	1.58
		370	57.83	1.54	0.81	0.06	60.84	2.29	6.31	0.37	0.47	0.12	6.18	0.58
2		25	39.55	1.05	14.20	1.03	22.83	0.90	11.79	0.70	4.97	0.57	7.80	0.68
		250	49.03	1.30	1.07	0.08	44.16	1.72	8.47	0.53	0.64	0.12	9.26	0.81
		400	57.58	1.53	0.71	0.05	56.87	2.27	2.89	0.18	0.15	0.10	2.88	0.27
3	Mendeleev -Alpha Ridge	250	59.22	1.57	0.81	0.06	58.41	2.34	17.45	1.01	1.28	0.18	17.21	1.51
		390	57.99	1.54	1.02	0.07	58.17	2.22	13.07	0.76	0.90	0.15	13.16	1.15
		800	59.09	1.57	0.99	0.07	57.54	2.37	5.09	0.31	0.36	0.10	4.47	0.41
4		10	48.75	1.30	11.16	0.80	41.78	1.68	71.78	4.10	28.26	3.02	47.53	4.23
		248	58.87	1.56	1.91	0.14	56.72	2.33	32.83	1.88	3.36	0.39	35.38	3.46
		500	59.17	1.57	1.42	0.10	56.89	2.31	29.79	1.71	3.12	0.37	28.91	2.58
5	Makarov Basin	25	45.85	1.22	9.64	0.69	35.27	1.37	60.47	3.48	22.52	2.39	44.80	3.85
		250	52.76	1.40	1.71	0.13	46.32	1.81	22.09	1.27	2.06	0.25	18.32	1.59
		333	51.07	1.36	1.48	0.11	45.99	1.79	20.52	1.18	1.78	0.23	18.03	1.56
6		800	50.40	1.35	1.67	0.12	45.56	1.78	14.68	0.85	1.20	0.18	14.31	1.27
		250	57.78	1.53	1.36	0.10	52.56	2.09	21.10	1.22	1.87	0.24	19.45	1.68
		400	57.39	1.52	1.21	0.09	54.28	2.21	14.33	0.83	1.14	0.17	13.54	1.23
7	Lomonosov Ridge	800	58.35	1.55	1.01	0.07	51.07	2.07	13.72	0.79	1.13	0.17	14.40	1.43
		10	44.53	1.18	14.35	1.04	34.73	1.39	65.24	3.74	29.52	3.11	40.53	3.61
		200	58.89	1.56	1.80	0.13	55.52	2.24	25.91	1.49	3.42	0.40	26.08	2.45
8		266	58.36	1.56	1.70	0.12	50.98	2.05	22.86	1.32	2.59	0.31	21.62	1.91
		25	51.01	1.37	13.45	0.95	45.45	1.80	48.20	2.75	13.35	1.46	25.08	2.21
		250	54.44	1.45	1.88	0.13	53.03	2.10	25.11	1.44	2.39	0.32	23.05	2.07
9		278	53.81	1.43	1.53	0.11	49.40	1.94	22.49	1.29	2.32	0.32	21.61	1.95
		750	53.34	1.42	2.22	0.16	54.47	2.16	25.44	1.48	2.77	0.37	23.06	1.99
		199	60.51	1.61	2.22	0.16	62.85	2.52	23.23	1.36	2.31	0.28	22.30	1.99
10	Eurasian Basin	263	60.70	1.62	2.00	0.15	62.96	2.53	21.00	1.21	1.99	0.25	19.46	1.70
		800	60.15	1.59	2.15	0.16	62.43	2.52	24.42	1.40	2.21	0.27	22.17	1.96
		10	53.51	1.42	11.02	0.79	50.70	2.01	60.83	3.47	22.42	2.37	46.39	4.30
11		200	58.79	1.58	1.73	0.13	59.21	2.44	20.52	1.20	1.83	0.23	21.77	2.21
		700	55.43	1.48	3.79	0.27	53.14	2.12	17.72	1.04	2.26	0.28	17.88	1.72
		25	51.18	1.36	10.11	0.73	42.83	1.71	68.92	3.95	27.23	2.88	46.56	4.35
12		200	56.92	1.51	11.48	0.83	50.82	2.04	20.22	1.18	1.86	0.23	20.52	2.10
		300	57.09	1.51	1.28	0.09	56.59	2.24	17.57	1.01	1.48	0.20	17.96	1.68
		800	57.88	1.54	1.76	0.13	58.43	2.38	19.27	1.11	5.42	0.60	18.53	1.86
12		24	51.79	1.37	9.62	0.70	41.78	1.72	72.58	4.14	28.94	3.05	50.29	4.56
		200	57.08	1.53	2.04	0.15	56.22	2.27	23.95	1.38	3.34	0.38	24.38	2.41
		400	57.11	1.52	2.13	0.15	56.83	2.24	22.34	1.31	5.44	0.60	19.23	1.66
		800	56.95	1.51	4.14	0.30	56.27	2.28	28.79	1.65	6.54	0.72	23.18	2.05

Table 2. Analytical results of $^{127}\text{I}/^{129}\text{I}$ atomic ratios and iodide/iodate molecular ratios in depth profile seawater from the central Arctic.

Station	Description	Depth [m]	$^{129}\text{I}/^{127}\text{I}$ ratio, $\times 10^{-10}$						I/IO_3^-	
			Total iodine		I^-		IO_3^-		^{127}I	^{129}I
			Mean	SD	Mean	SD	Mean	SD		
1	Canada Basin	25	6.03	0.45	6.55	1.78	4.91	0.56	0.352	0.469
		244	67.62	4.29	279.90	44.75	67.18	6.56	0.023	0.095
		370	23.01	1.48	122.75	32.17	21.41	2.16	0.013	0.076
2		25	62.88	4.07	73.80	9.99	72.03	6.88	0.622	0.637
		250	36.43	2.47	126.83	26.14	44.23	4.25	0.024	0.070
		400	10.59	0.71	43.44	28.57	10.70	1.10	0.013	0.051
3	Mendeleyev-Alpha Ridge	250	62.15	3.97	331.21	53.20	62.16	6.00	0.014	0.074
		390	47.54	3.02	185.73	32.95	47.73	4.56	0.018	0.068
		800	18.17	1.20	76.71	22.16	16.39	1.64	0.017	0.080
4		10	310.62	19.57	534.01	68.85	240.02	23.43	0.267	0.595
		248	117.64	7.44	371.77	50.88	131.58	13.96	0.034	0.095
		500	106.21	6.73	462.79	63.51	107.21	10.51	0.025	0.108
5	Makarov Basin	25	278.24	17.66	493.00	63.23	267.96	25.28	0.273	0.503
		250	88.34	5.59	254.12	36.56	83.45	7.95	0.037	0.112
		333	84.75	5.36	254.70	37.99	82.72	7.83	0.032	0.099
6		800	61.44	3.91	152.24	25.23	66.25	6.42	0.037	0.084
		250	77.05	4.89	290.20	42.51	78.09	7.43	0.026	0.096
		400	52.68	3.36	290.20	42.51	52.61	5.24	0.022	0.085
7	Lomonosov Ridge	800	49.62	3.15	199.38	32.25	59.50	6.40	0.020	0.079
		10	309.11	19.55	433.95	55.40	246.16	24.05	0.413	0.728
		200	92.82	5.87	401.02	54.63	99.08	10.14	0.032	0.131
8		266	82.65	5.25	320.58	44.67	89.45	8.70	0.033	0.120
		25	199.34	12.58	209.44	27.29	116.44	11.24	0.296	0.532
		250	97.29	6.16	268.08	40.22	91.70	9.00	0.035	0.104
9		278	88.17	5.57	321.12	49.30	92.28	9.09	0.031	0.108
		750	100.60	6.45	262.27	39.71	89.30	8.49	0.041	0.120
		199	80.98	5.20	219.08	30.80	74.86	7.32	0.035	0.104
10	Eurasian Basin	263	72.98	4.62	209.79	30.51	65.22	6.27	0.032	0.102
		800	85.67	5.41	216.32	30.92	74.91	7.29	0.034	0.100
		10	239.84	15.09	429.41	54.95	193.03	19.45	0.217	0.483
11		200	73.65	4.72	223.24	32.51	77.57	8.48	0.029	0.084
		700	67.42	4.35	126.01	17.98	70.99	7.40	0.071	0.126
		25	284.11	17.95	568.36	72.86	229.36	23.32	0.236	0.585
12		200	74.96	4.81	34.09	4.95	85.19	9.37	0.226	0.090
		300	64.91	4.11	245.27	36.93	66.97	6.81	0.023	0.083
		800	70.22	4.45	651.61	85.95	66.90	7.24	0.030	0.293
		24	295.67	18.61	634.24	81.12	253.90	25.30	0.230	0.575
		200	88.53	5.63	345.84	47.01	91.48	9.76	0.036	0.137
		400	82.53	5.31	538.05	70.80	71.38	6.79	0.038	0.283
		800	106.63	6.73	333.32	43.98	86.91	8.46	0.074	0.282

Table 3. Inventory of ^{129}I and its species in compartments of the central Arctic by 2011.

Location	Depth (m)	Surface Area ($\times 10^{11} \text{ m}^2$)	^{129}I inventory (kg)	Percentage of ^{129}I in total inventory, %
Eurasian Basin	0-200 m	20.83	450 ± 45	30.9
	200-800 m	20.83	538 ± 54	36.9
Makarov Basin	0-200 m	8.48	157 ± 16	10.8
	200-800 m	8.48	166 ± 17	11.4
Canada Basin	0-200 m	19.78	15 ± 2	1.0
	200-800 m	19.78	131 ± 13	9.0
PML and Halocline, 0-200 m			1457 ± 357	42.7
AWL, 200-800 m			622 ± 108	57.3
Total in upper 800 m			835 ± 145	100.0

Figure Captions

Figure 1. Map showing the sampling locations of the 12 water depth profiles (red dots with black numbers) in the central Arctic Ocean. The circulation schematic diagram of Atlantic-origin water (yellow lines) was showed according to (Smith et al. 2011; Smith et al. 1999), which flows along the continental margin and Lomonosov and Alpha-Mendeleyev Ridges, and finally exits through the Fram Strait. The section contour indicated by the green dot line showed the topography of the Arctic Basin (below).

Figure 2. Lateral distribution of concentrations of ^{129}I and ^{127}I (in parenthesis) in seawater of the Polar mixed Layer.

Figure 3. Depth profiles of ^{127}I (top) and ^{129}I (bottom) in the central Arctic. The PML has lower ^{127}I concentration but much higher ^{129}I concentration. The ^{129}I concentrations in the Eurasian and Makarov Basin were significantly higher than those in the Canada Basin.

Figure 4. Typical depth profiles of ^{127}I (left) and ^{129}I (right) in the three Arctic Basins, showing depletion of ^{127}I in the surface layer, and ^{129}I concentrations decrease with depth in the Eurasian and Makarov Basins, but peak value at 250m depth in the Canada Basin.

Figure 5. Lateral distribution of iodide to iodate ratios for ^{127}I (upper) and ^{129}I (bottom) in seawater of the polar mixed layer.

Figure 6. Depth profiles of iodide to iodate ratios for ^{129}I and ^{127}I in the central Arctic, showing the highest value at the Eurasian Basin margin, and the lowest at the Canada Basin and Mendeleyev-Alpha Ridge.

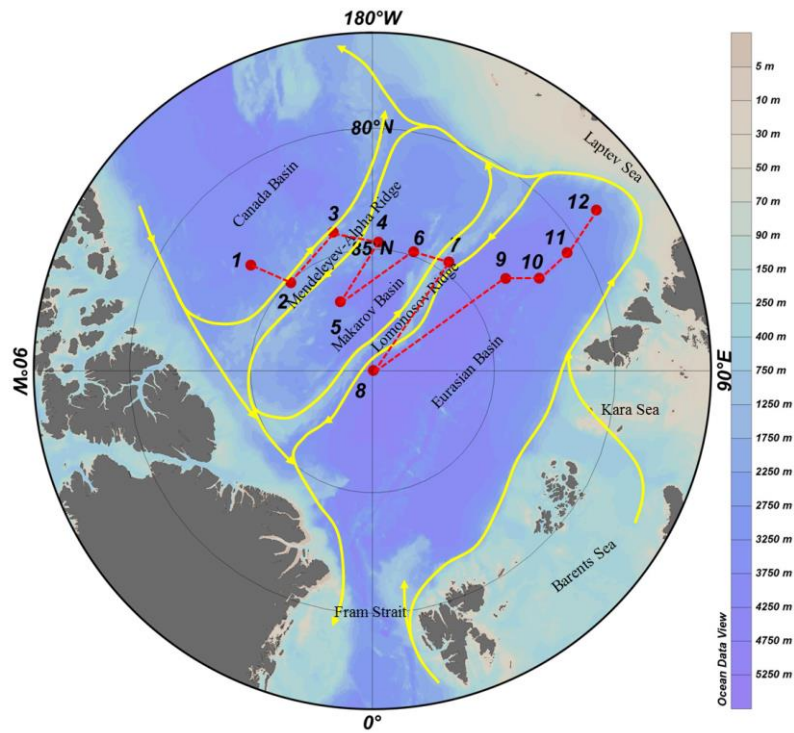


Figure 1. Map showing the sampling locations of the 12 water depth profiles (red dots with black numbers) in the central Arctic Ocean. The circulation schematic diagram of Atlantic-origin water (yellow lines) was shown according to (Smith et al. 2011; Smith et al. 1999), which flows along the continental margin and Lomonosov and Alpha-Mendeleyev Ridges, and finally exits through the Fram Strait. The section contour indicated by the green dot line showed the topography of the Arctic Basin (below).

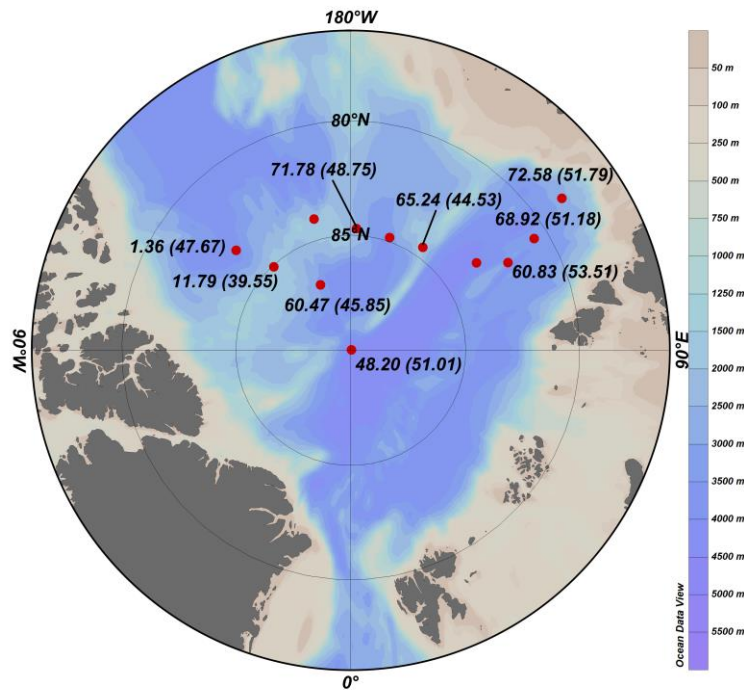


Figure 2. Lateral distribution of concentrations of ^{129}I and ^{127}I (in parenthesis) in seawater of the Polar mixed Layer.

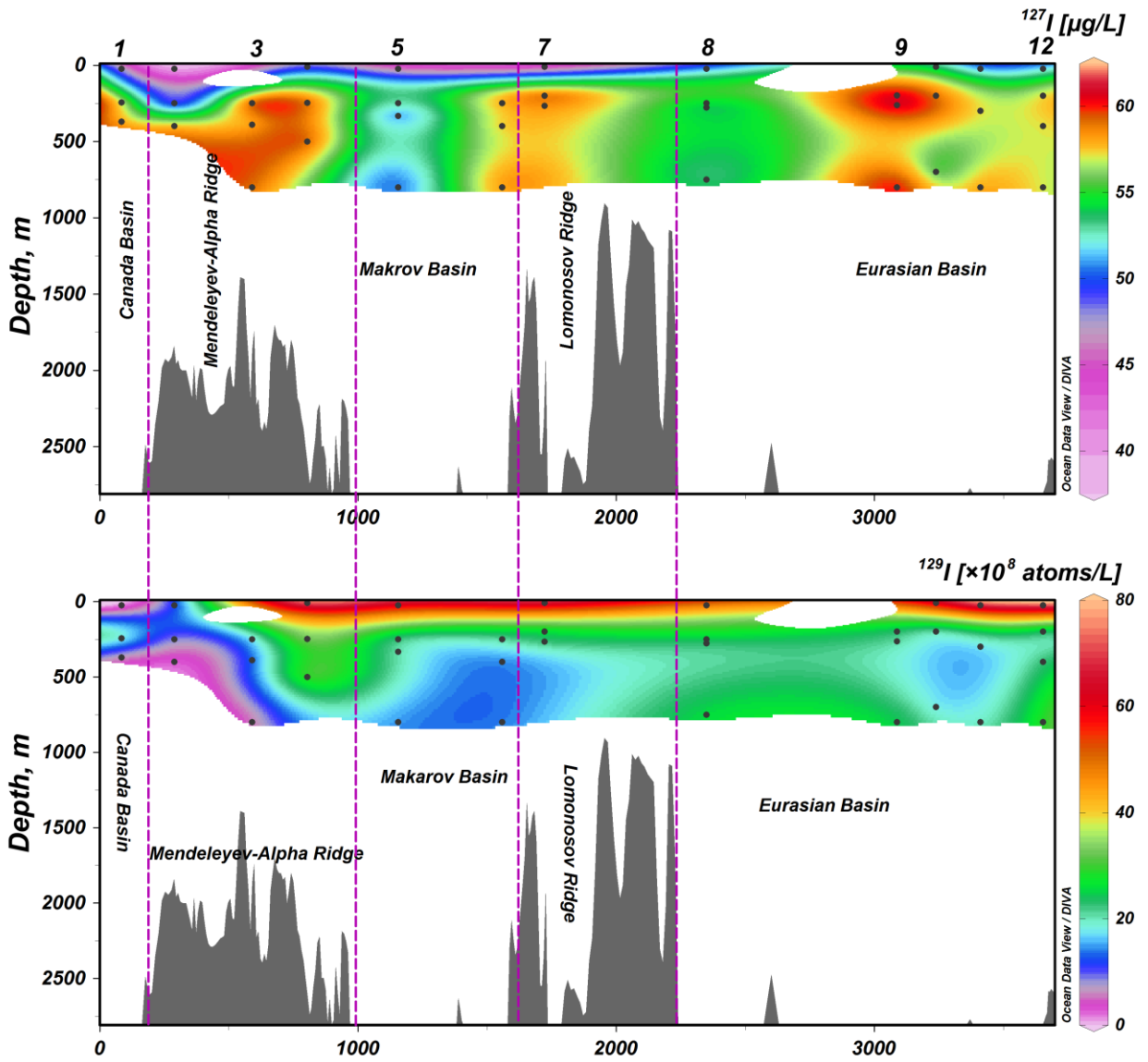


Figure 3. Depth profiles of ^{127}I (top) and ^{129}I (bottom) in the central Arctic. The PML has lower ^{127}I concentration but much higher ^{129}I concentration. The ^{129}I concentrations in the Eurasian and Makarov Basin were significantly higher than those in the Canada Basin.

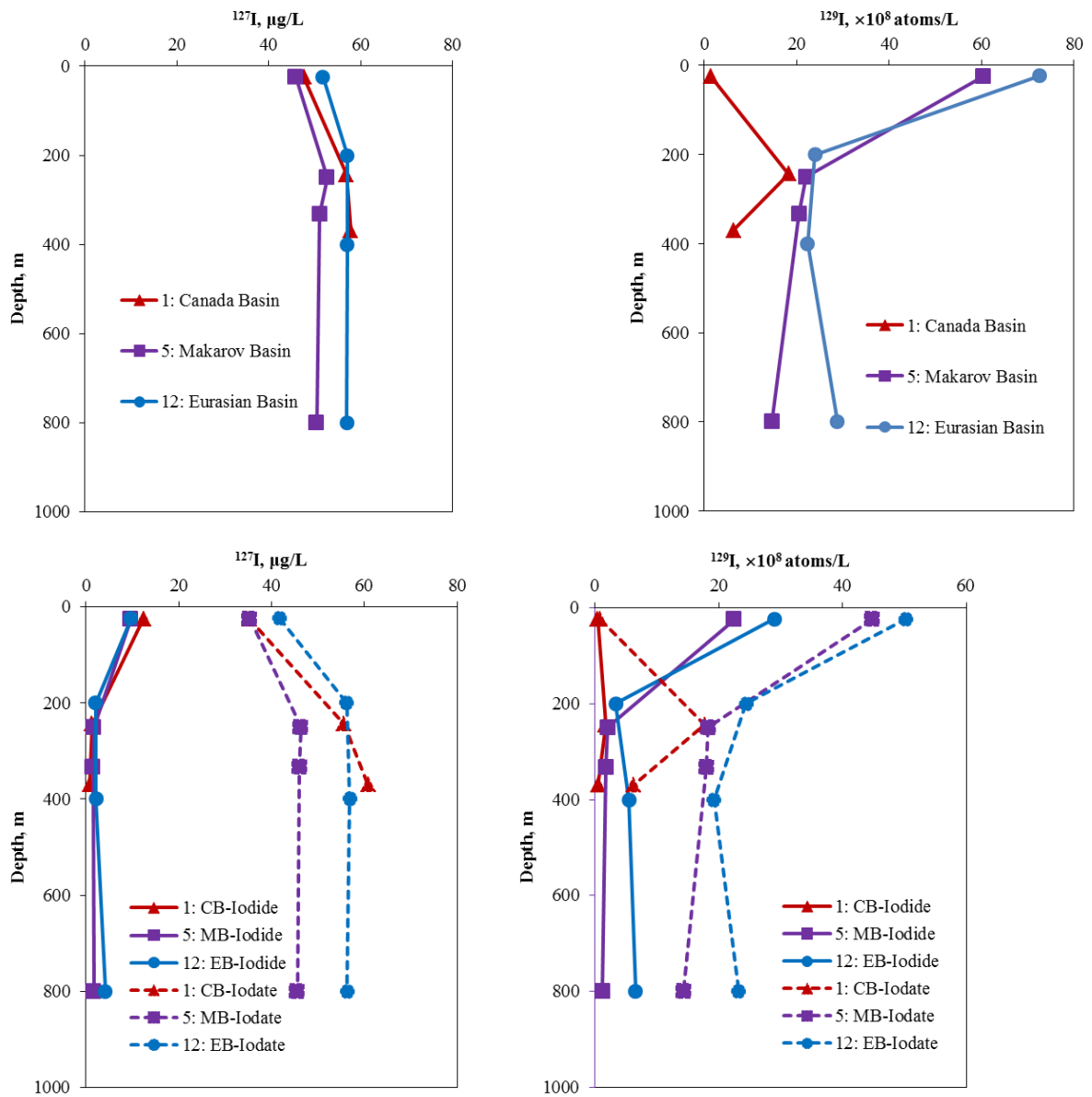


Figure 4. Typical depth profiles of ^{127}I (left) and ^{129}I (right) in the three Arctic Basins, showing depletion of ^{127}I in the surface layer, and ^{129}I concentrations decrease with depth in the Eurasian and Makarov Basins, but peak value at 250m depth in the Canada Basin.

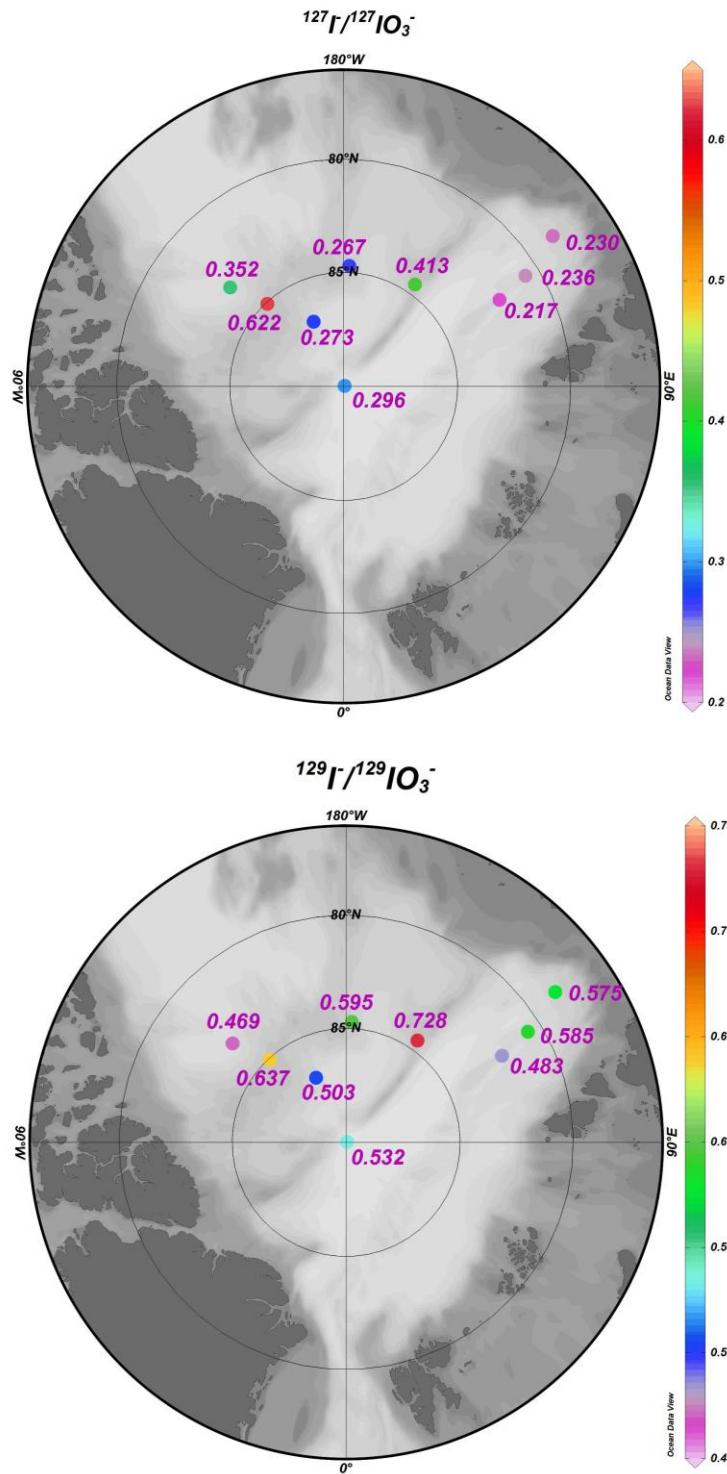


Figure 5. Lateral distribution of iodide to iodate ratios for ^{127}I (upper) and ^{129}I (bottom) in seawater in the Polar mixed layer.

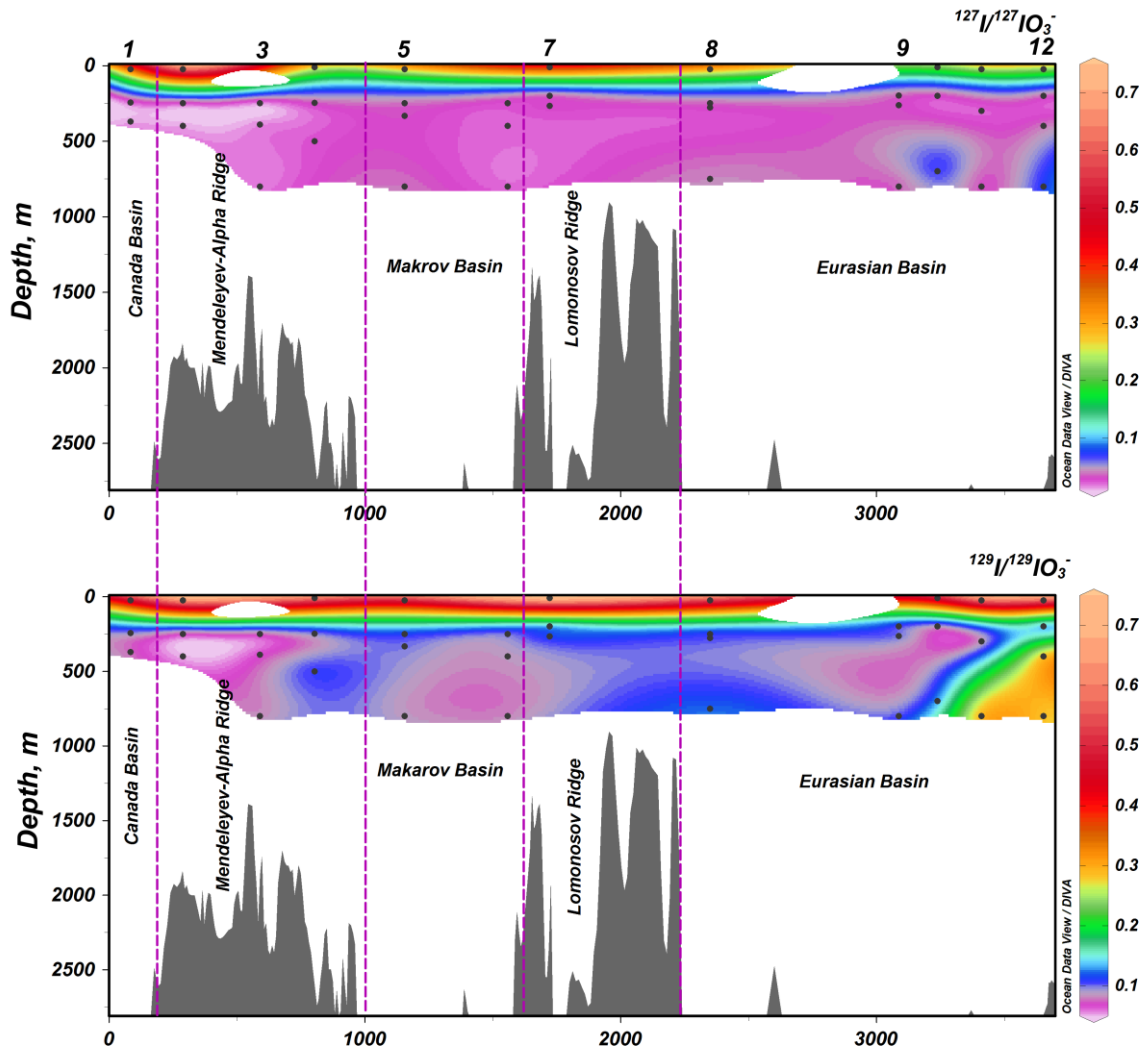


Figure 6. Depth profiles of iodide to iodate ratios for ^{129}I and ^{127}I in the central Arctic, showing the highest value at the Eurasian Basin margin, and the lowest at the Canada Basin and Mendeleev-Alpha Ridge.

Supporting information

Depth Profile of Chemical Species of ^{129}I and ^{127}I and Implication for Water Circulation and Marine Environmental Chemistry in the Central Arctic

Luyuan Zhang ¹, Xiaolin Hou ^{1,2*}, Justin P. Gwynn ³, Michael Karcher ^{4,5}, Weijian Zhou ², Yukun Fan ², Qi Liu ²

1) Center for Nuclear Technologies, Technical University of Denmark, Risø Campus, Roskilde 4000, Denmark

2) Xi'an AMS Center, State Key Laboratory of Loess and Quaternary Geology, Shanxi Key Laboratory of Accelerator Mass Spectrometry Technology and Application, Institute of Earth Environment, Chinese Academy of Sciences, Xi'an 710075, China

3) Norwegian Radiation Protection Authority, The Fram Centre, Tromsø 9296, Norway

4) O.A.Sys - Ocean Atmosphere Systems GmbH, Hamburg 22767, Germany

5) Alfred Wegener Institute for Polar and Marine Research, Bremerhaven 27515, Germany

This supporting information describes the details of the analytical methods for chemical separation of different species of iodine and measurement for ^{129}I , ^{127}I . The estimation of ^{129}I inventory in the central Arctic is also presented in detailed. It includes three tables and six figures.

Methods

Separation of inorganic iodine species.

An anion exchange chromatography with a long column was applied for the separation of iodate and iodide to prevent breakthrough of iodide from the column due to high chloride concentration in the high salinity seawater samples. The experiment using ^{125}I spike showed that no iodide leakage occurred when 600 mL of seawater with a salinity of 35 psu was loaded onto a column 30 cm in height and 1 cm in diameter. All reagents in this work were analytical grade except when otherwise stated.

600 mL of seawater was taken to a beaker and 2000 Bq ^{125}I was spiked, the sample was then loaded onto an anion exchange chromatography columns (AG 1×4, 50 mesh, Bio-Rad Laboratories Inc., Hercules, California, USA) which was transformed from Cl^- type to NO_3^- type using 2 M NaNO_3 . Iodate passed through the column due to its low affinity with anion exchange resin, while iodide was absorbed onto the resin. 30 mL of 0.2 M NaNO_3 and 20 mL of ultrapure water were used to wash the column in turn and integrated with the effluent. Iodide on the column was eluted with the addition of 100 mL of 5% NaClO and 30 mL of 3 M HNO_3 . The chemical yield of iodide was estimated by comparing ^{125}I in eluate with the standard solution.

Due to addition of HNO_3 , the iodide fraction was neutralized with concentrated $\text{NH}_3\cdot\text{H}_2\text{O}$ to pH 7 prior to ICP-MS measurement. 1 mL of the original seawater and the iodate and iodide fractions were diluted by factors of 10-20 with 1% $\text{NH}_3\cdot\text{H}_2\text{O}$ for ^{127}I measurement by ICP-MS (Thermo Fisher, X Series II) using Xt cone under normal mode (Hou et al. 2007). Cesium (CsNO_3) was added the solutions to a final concentration of 2 ng/g as an internal standard to monitor the ionization efficiency of iodine. Iodine was separated from the original seawater and the iodate and iodide fractions by solvent extraction after addition of 2 mg ^{127}I carrier (Woodward Company, Colorado, USA). Iodine as iodide in the extracted solutions was precipitated with 0.5M AgNO_3 as AgI , which was then dried at 70°C in an oven, mixed with niobium powder and pressed into copper target holders. The AgI target

*Corresponding author.

E-mail address: xiho@dtu.dk

was measured for ^{129}I by AMS (3MV, HVEE, Netherland) at Xi'an AMS Center, China. Pentavalent iodine (I^{5+}) was selected for the measurement of ^{127}I by Faraday cup and ^{129}I using gas ionization detector (Zhou et al. 2010). Directly pressed Nb powder was used to characterize the instrumental blank. Procedure blanks were prepared using the same procedure as the samples, and prepared as AgI targets for AMS measurement, $^{129}\text{I}/^{127}\text{I}$ values of less than 5×10^{-13} in the blanks (including iodide and iodate), which was 2 orders of magnitude lower than sample targets.

Nutrient and Chlorophyll a data.

The concentration of nutrients (nitrate and phosphate) in seawater samples in the central Arctic were measured with colorimetric autoanalysis (Kattner and Ludwichowski. 2014) (Fig. S-3). The concentration of chlorophyll a was obtained on the Arctic System Science Primary Production (ARCSS-PP) database (<http://www.nodc.noaa.gov/cgi-bin/OAS/prd/accession/details/63065>) (Fig. S-4).

Mapping method.

Free software Ocean Data view version 4 (ODV) was used to map the lateral and vertical profiles of iodine distribution and nutrients, as well as chlorophyll a distribution. For more information about ODV, see <http://odv.awi.de/>.

Estimation of ^{129}I inventory in the central Arctic.

The raw data obtained in this work and from the data of Smith et al. (Smith et al. 2011) with time correction were plotted and performed curve fitting using software OriginPro 9 (Fig. S-6). The parameters for the fitting functions were listed in Table S-3. The fitting curves were shown in Fig. S-6. The fitting results were in a good agreement with the observations ($r > 0.94$). The functions were integrated with an online integral calculator (<http://zh.numberempire.com/definiteintegralcalculator.php>) to estimate the integral values in difference intervals, 0-200 m, 0-800 m. The inventory was estimated by multiplying the surface area of basins with the integrated values.

Reference

- Hou X, Aldahan A, Nielsen SP, Possnert G, Nies H, Hedfors J. Speciation of I-129 and I-127 in seawater and implications for sources and transport pathways in the North Sea. *Environ Sci Technol* 2007;41:5993-9.
- Zhou WJ, Hou X, Chen N, Zhang LY, Liu Q, He CH et al. Preliminary study of radioisotope ^{129}I application in China using Xi'an accelerator mass spectrometer. *ICNS News* 2010; 25: 8-23.
- Online integral calculator. <http://zh.numberempire.com/definiteintegralcalculator.php>.
- Alfred Wegener Institute (<http://expedition.awi.de/expeditions>).

Table S-1. Sampling information and physical parameters of seawater samples from the central Arctic in 2011. Data is obtained from the web page of the Alfred Wegener Institute (<http://expedition.awi.de/expeditions>).

Station	Latitude Longitude	Station information	Sampling Date	Depth, m	Salinity, psu	T _{pot} , a °C	O ₂ ^b [μmol/l]
1	83°22.75 N 131°01.23 W	Southern slope of the Alpha Ridge	2011-09-02	25	30.23	-1.33	397.52
				244	34.49	-0.18	299.47
				370	34.83	0.64	297.95
2	85°03.70 N 137°16 W	Over the Alpha Ridge	2011-08-31	25	29.83	-1.40	402.09
				250	34.66	0.24	290.79
				400	34.84	0.43	294.48
3	84°04.44 N 164°13.08 W	Over the Mendelejev Ridge	2011-09-06	250	34.77	0.59	299.21
				390	34.85	0.78	304.31
				800	34.87	0.04	304.91
4	84°42.17 N 177°23.18 E	The Makarov Basin side of the Mendelejev Ridge	2011-09-08	10	31.06	-1.62	399.16
				248	34.79	0.76	303.55
				500	34.84	0.57	310.01
5	86°51.63 N 155°03.55 W	In the southwest of the Makarov basin	2011-08-29	25	31.90	-1.61	390.75
				250	34.78	0.75	301.75
				333	34.84	0.90	303.93
				800	34.87	0.03	308.50
6	84°49.35 N 161°02.14 E	In the southeast of the Makarov basin	2011-09-09	250	34.84	1.05	303.86
				400	34.86	0.75	305.62
				800	34.87	-0.08	309.31
7	84°32.44 N 145°04.70 E	The Amundsen Basin side of the Lomonosov Ridge	2011-09-10	10	28.26	-1.53	390.76
				200	34.81	0.92	306.32
				266	34.86	1.18	306.58
8	89°57.91 N 136°44.78 E	At the North Pole (Amundsen Basin)	2011-08-22~23	25	32.56	-1.72	354.71
				250	34.83	1.11	305.23
				278	34.87	1.28	305.98
				750	34.89	0.06	314.42
9	83°20.46 N 124°52.28 E	In the southeast of the Amundsen basin	2011-09-13	199	34.81	1.09	302.22
				263	34.88	1.36	303.41
				800	34.89	-0.07	313.97
10	82°09.88 N 119°08.18 E	Over the Nansen-Gakkel Ridge	2011-09-19	10	31.71	-1.65	383.13
				200	34.83	1.43	302.72
				700	34.89	0.17	311.59
11	80°38.30 N 121°20.3 E	In the south of the Nansen Basin	2011-09-20	25	32.88	-1.66	376.15
				300	34.89	1.56	304.40
				800	34.89	-0.12	312.68
12	78°29.68 N 125°46.09 E	The Nansen Basin margin close to the Laptev Sea	2011-09-22	24	32.89	-1.40	375.24
				200	34.86	1.17	308.64
				400	34.88	0.50	312.84
				800	34.88	-0.35	317.77

a. T_{pot}, potential temperature; b. O₂, dissolved oxygen concentration.

Table S-2. Molecular ratios of iodide to iodate for ^{129}I and ^{127}I in different water bodies

NO	Station	Sampling date	Depth (m)	Iodide/Iodate Ratio		Reference
				^{127}I	^{129}I	
1	Central Arctic Ocean	Aug-Oct, 2011	10-25	0.217 - 0.622	0.469 - 0.728	This study
			199-80		0.051 -	
			0	0.013 - 0.074	0.293	This study (Hou et al. 2007)
2	North Sea	Aug-Sep, 2005	surface	0.11 - 0.50	0.51 - 1.64	(Yi et al. 2012)
3	Skagerrak, Kattegat and Baltic Proper	Aug, 2006	25-240	0.5 - 13.1	0.5 - 67	(Yi et al. 2012)
	Skagerrak, Kattegat and Baltic Proper	April, 2007	30-300	0.1 - 33.1	0.4 - 44.9	(Yi et al. 2012)
4	Northern Atlantic Ocean	Oct-Nov, 2010	surface	0.06 - 0.25	0.14 - 0.70	(He et al. 2013)

Table S-3. Functions and results of curve fitting by OriginPro 9

Location	Fitting Function	Formula	Adj. R-Square
Eurasian Basin	ExpDec1	$y=17.26+64.71*\exp(-0.007752*x)$	0.940
Makarov Basin	ExpDec1	$y=11.07+56.18*\exp(-0.006256*x)$	0.984
Canada Basin	Extreme	$y=1.70+17.86*\exp(-(-\exp(-z)-z+1), z=(x-265.90)*0.02323)$	0.987

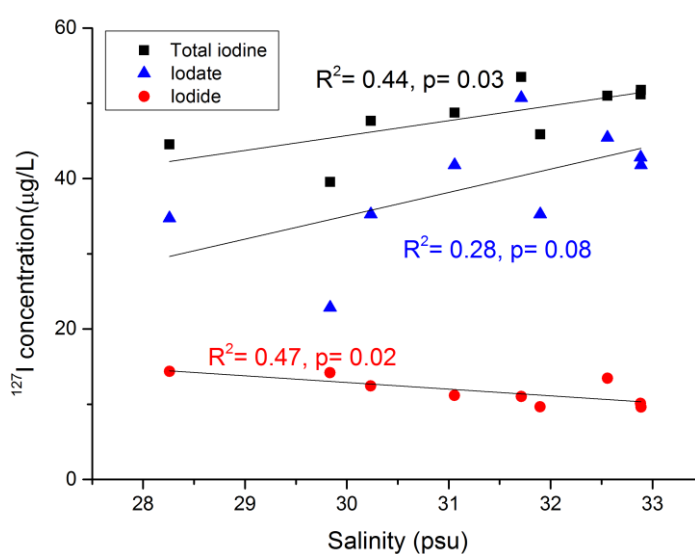


Figure S-1. Correlation of salinity with total iodine and iodine species in the polar mixed layer of the Arctic Ocean.

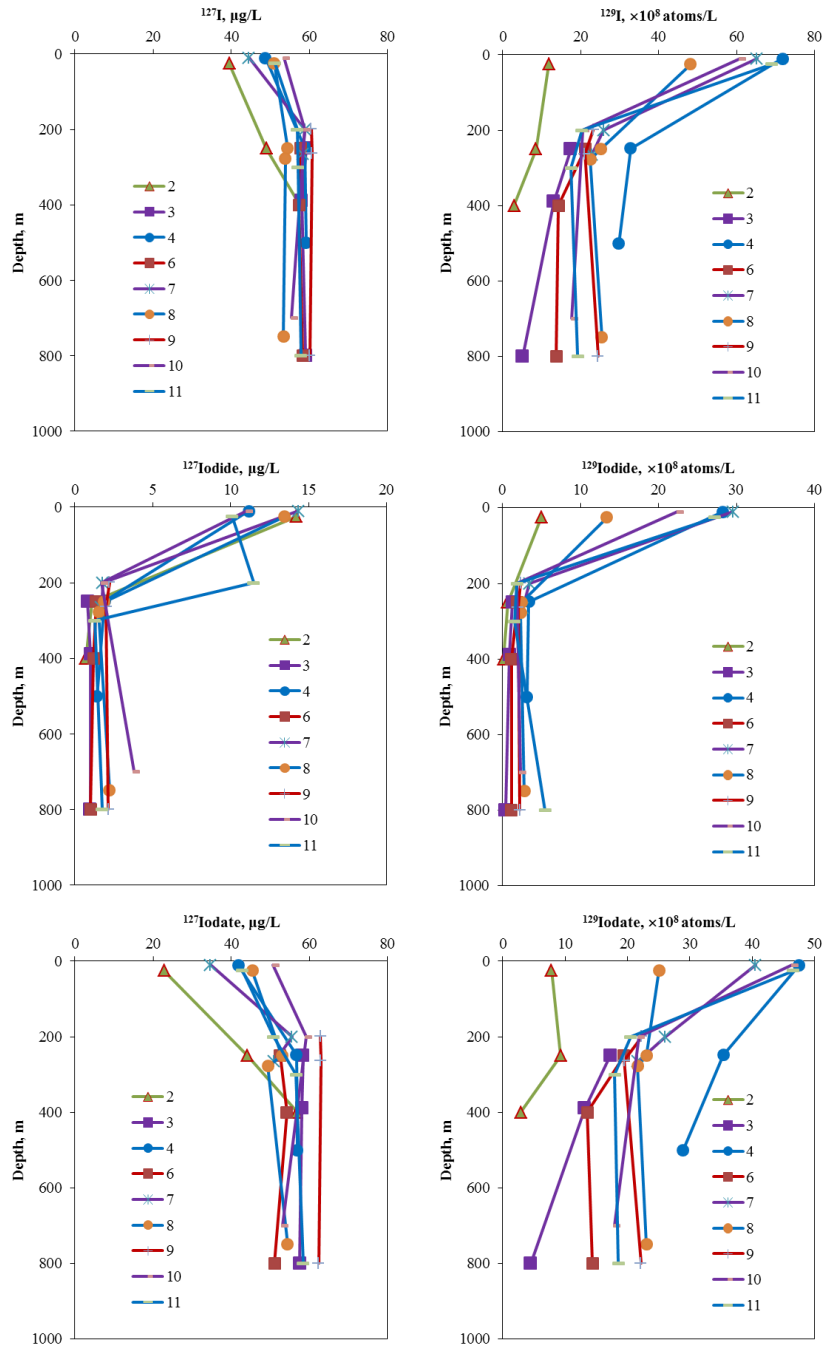


Figure S-2. Depth profiles of ^{127}I (left) and ^{129}I (right) in the three Arctic Basins, showing depletion of ^{127}I in the surface layer, and ^{129}I concentrations decrease with depth in the Eurasian and Makarov Basins, but peak value at 250m depth in the Canada Basin.

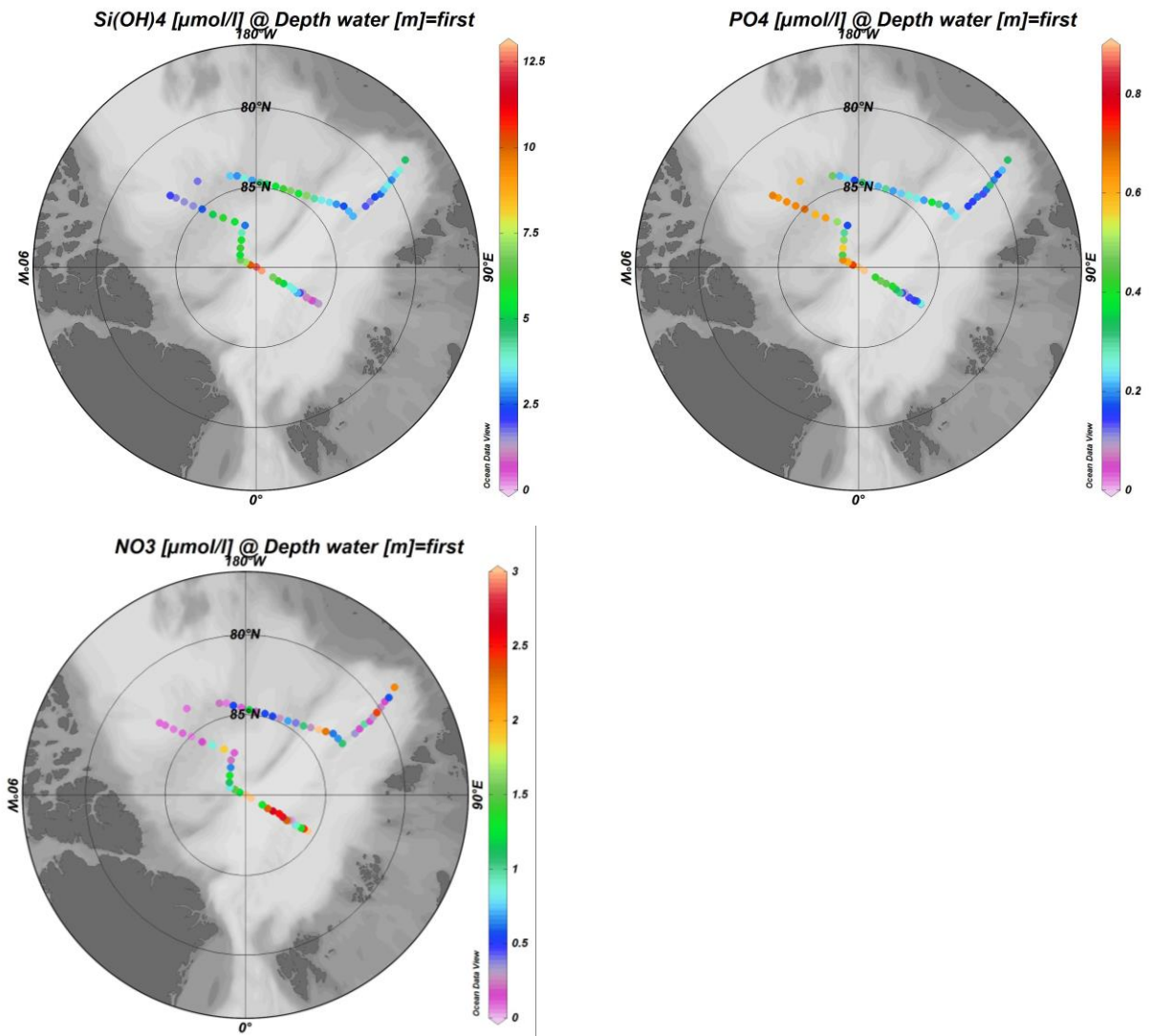


Figure S-3. Distribution of silicate, phosphate and nitrate at 20-25 m in the central Arctic Ocean. Data are available from (Kattner and Ludwichowski. 2014).

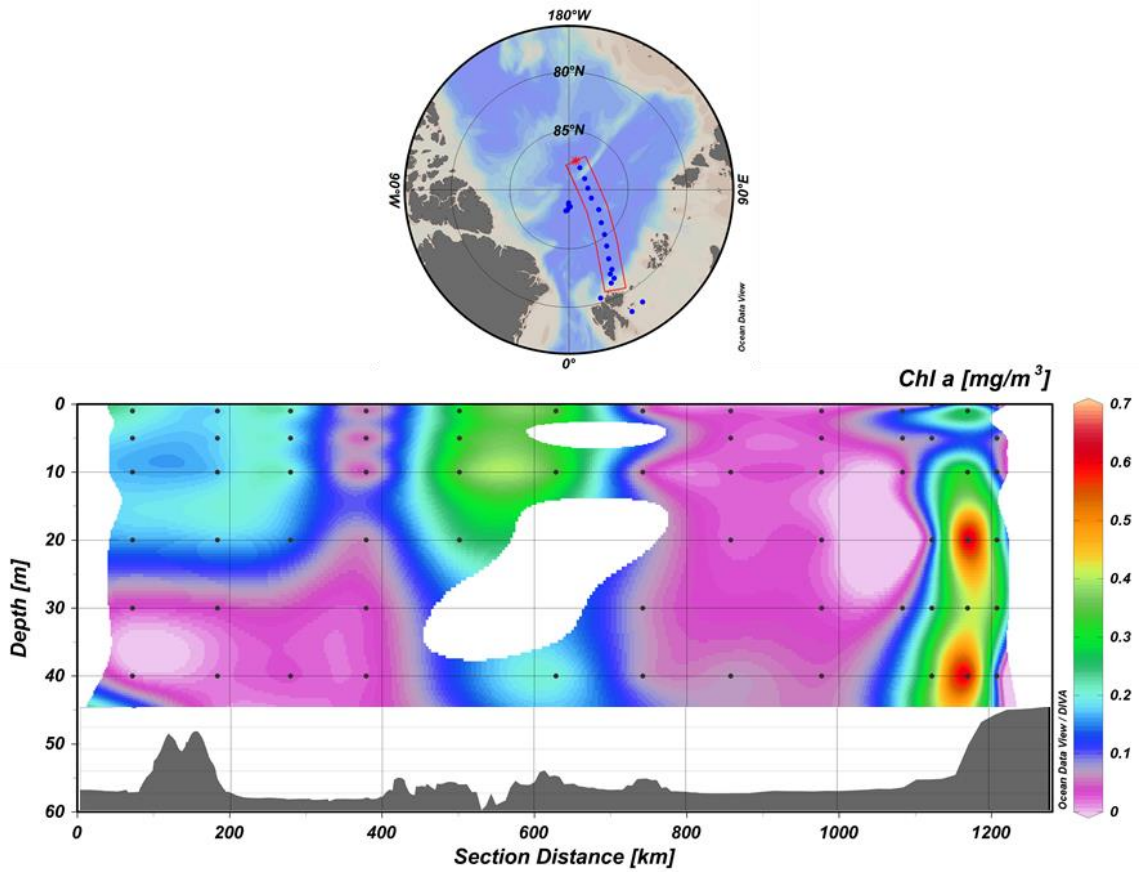


Figure S-4. Section of chlorophyll a concentration across the Eurasian Basin. Insert at the bottom shows the bathymetry of the sampling section. Sampling was conducted on July 2001. Data are available on Arctic System Science Primary Production (ARCSS-PP) database (<http://www.nodc.noaa.gov/cgi-bin/OAS/prd/accession/details/63065>).

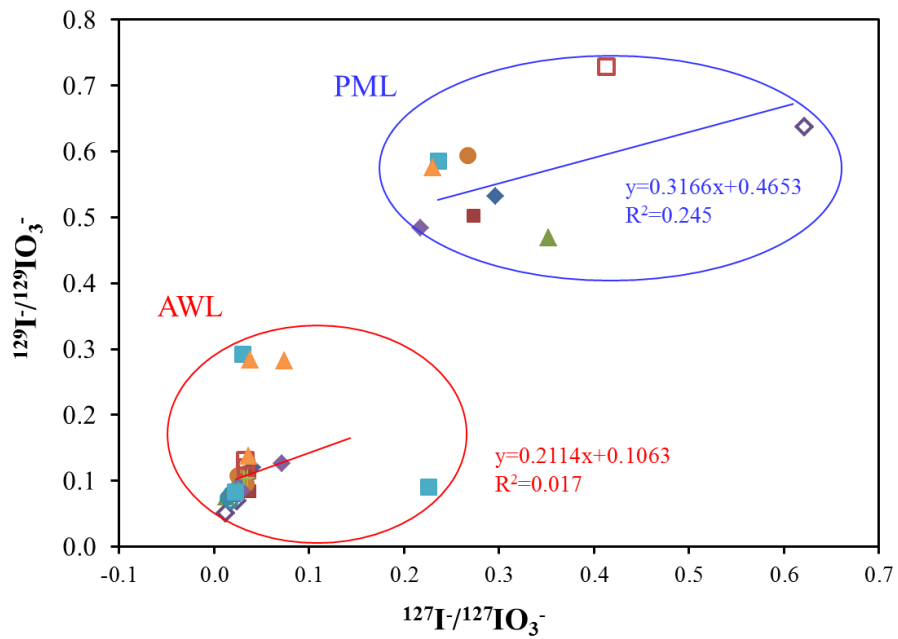


Figure S-5. Plot of $^{127}\text{I}/^{127}\text{IO}_3^-$ as a function of $^{129}\text{I}/^{129}\text{IO}_3^-$ in the polar mixed layer (PML) and the Atlantic water layer (AWL).

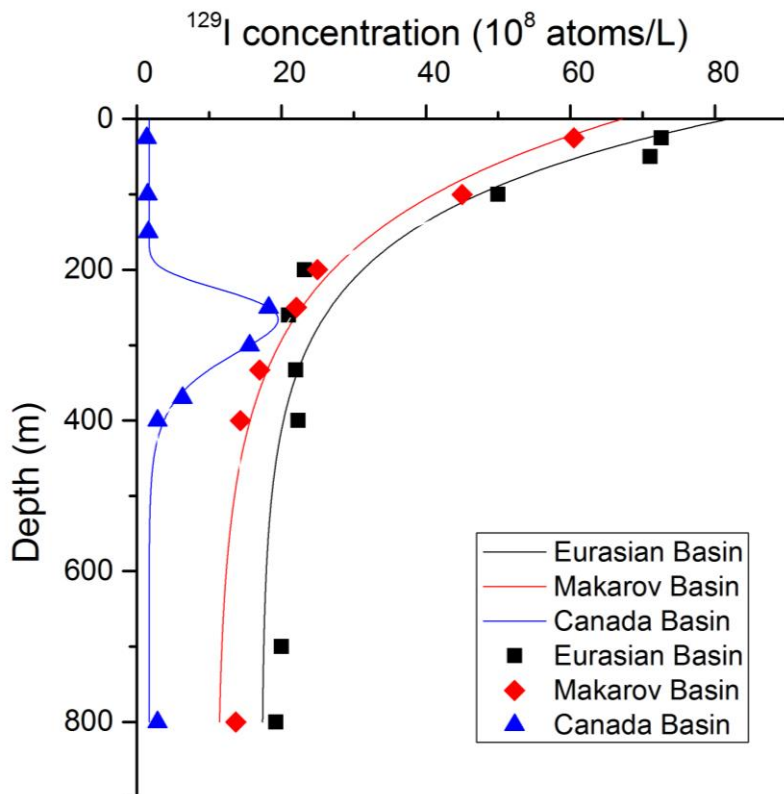


Figure S-6. Depth profiles of ^{129}I concentration in the central Arctic. Symbols are observed values and lines are the fitting curves for the three basins.

Paper IV

Iodine-129 in Seawater Offshore Fukushima: Distribution, Inorganic Speciation, Sources, and Budget

Xiaolin Hou,^{*,†,‡} Pavel P. Povinec,[§] Luyuan Zhang,[†] Keliang Shi,[†] Dana Biddulph,^{||,\$} Ching-Chih Chang,^{▼,\$} Yukun Fan,[‡] Robin Golser,[⊥] Yingkun Hou,[#] Miroslav Jeřkovský,^{⊥,\$} A. J. Tim Jull,^{||,▼,\$} Qi Liu,[‡] Maoyi Luo,^{†,¶} Peter Steier,[⊥] and Weijian Zhou[‡]

[†]Center for Nuclear Technology, Technical University of Denmark, Risø Campus, DK-4000 Roskilde, Denmark

[‡]Xi'an AMS Center, SKLLQG, Institute of Earth Environment, CAS, Xi'an 710075, China

[§]Department of Nuclear Physics and Biophysics, Comenius University, Bratislava, Slovakia

^{||}Department of Physics, University of Arizona, Tucson, Arizona 85721, United States

[⊥]Faculty of Physics, University of Vienna, Währingerstrasse 17, 1090 Vienna, Austria

[#]Department of Chemistry, Imperial College London, United Kingdom

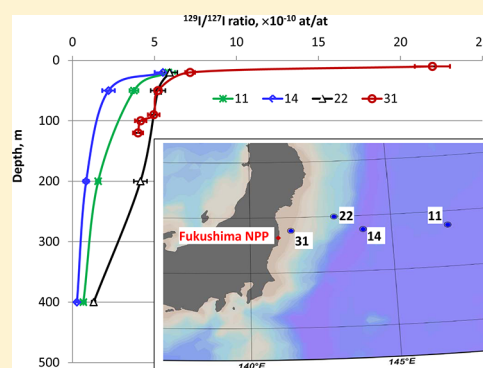
[¶]Department of Nuclear Science and Technology, Xian Jiaotong University, China

[▼]Department of Geosciences, University of Arizona, Tucson, Arizona 85721, United States

^{\$}NSF Arizona AMS Laboratory, University of Arizona, Tucson, Arizona 85721, United States

Supporting Information

ABSTRACT: The Fukushima nuclear accident in March 2011 has released a large amount of radioactive pollutants to the environment. Of the pollutants, iodine-129 is a long-lived radionuclide and will remain in the environment for millions of years. This work first report levels and inorganic speciation of ¹²⁹I in seawater depth profiles collected offshore Fukushima in June 2011. Significantly elevated ¹²⁹I concentrations in surface water were observed with the highest ¹²⁹I/¹²⁷I atomic ratio of 2.2×10^{-9} in the surface seawater 40 km offshore Fukushima. Iodide was found as the dominant species of ¹²⁹I, while stable ¹²⁷I was mainly in iodate form, reflecting the fact that the major source of ¹²⁹I is the direct liquid discharges from the Fukushima NPP. The amount of ¹²⁹I directly discharged from the Fukushima Dai-ichi nuclear power plant to the sea was estimated to be 2.35 GBq, and about 1.09 GBq of ¹²⁹I released to the atmosphere from the accident was deposited in the sea offshore Fukushima. A total release of 8.06 GBq (or 1.2 kg) of ¹²⁹I from the Fukushima accident was estimated. These Fukushima-derived ¹²⁹I data provide necessary information for the investigation of water circulation and geochemical cycle of iodine in the northwestern Pacific Ocean in the future.



INTRODUCTION

A nuclear accident at the Fukushima Dai-ichi nuclear power plant (1FNPP), Japan, occurred in March 2011 due to failure of the cooling system after the Tohoku earthquake and the Tsunami on March 11, 2011. Hydrogen explosions occurred in unit 1 on March 12 and unit 3 on March 14, and in the spent fuel storage building in unit 4 on March 15, as well as an internal explosion in reactor 3 on March 15, 2011.^{1–3} Significant quantities of radioactive materials were emitted to the atmosphere from March 12 through 24, with estimated atmospheric releases of 150–160 PBq (peta becquerels, or 10^{15} Bq) of ¹³¹I and 10–15 PBq of ¹³⁷Cs.^{4–6} These radionuclides were transported and deposited over large areas of the northern hemisphere; radioisotopes of cesium and iodine have been observed in the atmosphere over America, Europe, and Asia. Fortunately, due to the dominant westerly wind, the radio-

nuclides were transported and deposited mainly in the Pacific Ocean, with less than 20% of them deposited over the land of Japan.^{1,6,7}

The damage in the containment vessel of the reactor of unit 2 at the 1FNPP due to an internal hydrogen explosion caused a leakage of highly contaminated water to the sea from March 25 to April 5.^{3,8,9} Large volumes of contaminated water were produced during cooling of the reactors using fresh water and seawater, and some of this water was intentionally discharged directly to the sea April 4–20, 2011 to leave space for more highly contaminated water. In addition, some contaminated

Received: November 1, 2012

Revised: March 4, 2013

Accepted: March 5, 2013

Published: March 5, 2013

groundwater was also directly discharged to the sea.^{2,8,10} This direct discharge of contaminated water to the sea has significantly elevated ¹³⁷Cs and ¹³¹I concentrations in seawater at the coast as well as offshore, starting from March 21 and rapidly increasing from March 27, with peak values on March 30 (47 kBq/L of ¹³⁷Cs) and on April 6 (68 kBq/L) at the discharge point of the 1FNPP.⁹ Therefore liquid discharge directly to the sea was another major source of radionuclides to the environment, especially to the ocean.

¹³⁷Cs and ¹³¹I, which were two major radionuclides released from the Fukushima accident, have been intensively investigated. However, many other radionuclides have also been released to the environment, especially through the liquid discharge to the sea, because of high leaching efficiency of radionuclides from the damaged fuel rod materials when corrosive brine water was used to cool the reactor. Among these radionuclides, ¹²⁹I is a fission product with relative high fission yields of 0.6%. However, few data on ¹²⁹I from the Fukushima accident have been reported, especially in the sea surrounding Fukushima.

¹²⁹I is a long-lived radioisotope of iodine with a half-life of 15.7 Ma. It is a soft beta-emitter with maximum beta-energy of 154 keV. Therefore, ¹²⁹I is less radiologically harmful, and less important in view of radiation protection. However, due to its high solubility and the long residence time of iodine in the ocean, ¹²⁹I is an ideal oceanographic tracer for investigation of water circulation in the ocean,¹¹ and a useful environmental tracer for the investigation of the interaction of atmosphere and seawater, as well as for the biochemical cycle of stable iodine through chemical speciation analysis of ¹²⁹I,^{12,13} ¹³¹I ($t_{1/2} = 8$ days) is the most harmful radionuclide from the nuclear accident, due to its large release during the accident, and the high uptake and enrichment in human thyroid. Its short half-life prevents it from being well measured in the environment to evaluate the radiation risk to humans exposed to the radioactive contamination. The long-lived ¹²⁹I provides a good analogue to reconstruct levels and distribution of short-lived ¹³¹I in the environment.¹⁴ In addition, iodine is highly concentrated in seaweed, and some types of seaweed are popular seafood in Japan and other Asian countries.¹⁵ ¹²⁹I discharged to the sea will be concentrated in the seaweed and some sea fish,¹⁶ which might cause an increased radiation to humans who consume seafood from a highly contaminated area.

This work aims to investigate the levels and distribution of ¹²⁹I in the sea offshore Fukushima by determination of ¹²⁹I in depth profiles of seawater, and to evaluate the source term and budget of ¹²⁹I by chemical speciation of ¹²⁹I and ¹²⁷I for iodide and iodate in seawater profiles.

MATERIALS AND METHODS

Samples and Reagents. Seawater samples were collected from offshore Fukushima during the research cruise organized by American scientists June 3–17, 2011 using the research vessel Kaimikai-O-Kanaloa of the University of Hawaii.³ The samples were stored in dark at ambient temperature before analysis. Of these samples, depth profiles from 4 sampling stations with distances of 40–530 km from Fukushima Dai-ichi nuclear power plant (Figure S-1 and Table S-1 in the Supporting Information) were used for ¹²⁹I.

All chemical reagents used were of analytical grade and all solutions were prepared using deionized water (18.2 MΩ cm⁻¹). ¹²⁹I standard (NIST-SRM-4949c), carrier free ¹²⁵I (Amersham Pharmacia Biotech, Little Chalfout, Buckingham-

shire, UK), ¹²⁷I carrier (Woodward iodine, MICAL Specialty Chemicals, New Jersey, USA), and Bio-Rad AG1-×4 anion exchange resin (50–100 mesh, Cl form, Bio-Rad laboratories, Richmond, CA, USA) were used in the experiments.

Analytical Methods for Determination of ¹²⁹I Species.

Anion exchange chromatography was used for separation of iodide, iodate, and total inorganic iodine from seawater. A schematic diagram of the separation procedure is shown in Figure S-2, and the separation methods are presented in the Supporting Information. The detailed methods for speciation analysis of ¹²⁹I in seawater have been reported elsewhere.¹³

Filtered seawater (0.5–1 L) was transferred to a beaker, and ¹²⁵I⁻ was added. After loading the prepared solution to an anion exchange column (AG1-×4 resin, NO₃⁻ form), and washing with 0.2 mol/L NaNO₃, iodide on the column was eluted with 5% NaClO; effluent and wash were combined for iodate separation. A 1.0 mL solution of the iodide fraction, the iodate fraction, and the original seawater were taken to a vial for ¹²⁷I measurement using ICP-MS. Iodine in the remaining solutions of the iodide and iodate fractions, as well as in the original seawater, was separated using CHCl₃ extraction based on adjusting the oxidation state of iodine. The separated iodine from each fraction in iodide form was used to prepare AgI sputter target by adding AgNO₃ solution for AMS measurement of ¹²⁹I.

Before extraction, the eluate of iodide from the anion exchange column was also measured for ¹²⁵I by gamma-spectrometer to monitor chemical recovery of iodide during column separation. This measurement is used to correct the ¹²⁷I⁻ and ¹²⁹I⁻ concentrations in seawater.^{12,13}

An ICP-MS system (X Series II, Thermo, Waltham, MA) equipped with an Xs-skimmer cone and standard concentric nebulizer was used for the measurement of ¹²⁷I. A 1.0 mL portion of the separated fractions or the original seawater was diluted to 20 mL using 1% ammonium solution, and spiked with Cs⁺ (to 2.0 ppb) as internal standard. The detection limit of the method for ¹²⁷I was calculated as 3 SD of the procedure blank to be 0.03 ng/mL.

The ¹²⁹I/¹²⁷I ratios in total iodine samples were determined by AMS at the Vienna Environmental Research Accelerator (VERA)¹⁷ and the University of Arizona AMS Laboratory, both using a 3MV National Electrostatics Corporation AMS.¹⁸ The ¹²⁹I/¹²⁷I ratios in iodide and iodate samples were measured using the 3 MV AMS facility at the Xi'an AMS center.¹⁹ The machine backgrounds of the ¹²⁹I/¹²⁷I ratio are around (2–4) × 10⁻¹⁴. Procedure blanks using the same procedure as the samples were also prepared; the highest measured ¹²⁹I/¹²⁷I ratio is 2.8 × 10⁻¹³, which is significantly lower than measured ¹²⁹I/¹²⁷I ratios in the samples. No seawater from uncontaminated deep ocean with ¹²⁹I/¹²⁷I close to preanthropogenic level of 2 × 10⁻¹² in marine environment has yet been analyzed.²⁰ However, a ¹²⁹I/¹²⁷I ratio as low as 3 × 10⁻¹³ (or 5 × 10⁵ atoms for a target with 0.5 mg ¹²⁷I) has been measured in a procedure background sample, which was produced by addition of ¹²⁷I carrier to deionized water and separation of iodine and measuring it using the same procedure and method as for the samples analyzed in this work.²¹ The ¹²⁹I levels for any species presented in this work (>7.7 × 10⁶ at/L for ¹²⁹I concentration in >0.5 L water or 2.6 × 10⁻¹¹ for ¹²⁹I/¹²⁷I atomic ratio) are 1–2 orders of magnitude higher than the procedure plank, confirming that the applied method is well suitable for the analysis of these samples.

Table 1. Distribution of ^{129}I , ^{127}I , $^{129}\text{I}/^{127}\text{I}$ Ratios, and Speciation of ^{129}I and ^{127}I in Four Seawater Profiles Offshore Fukushima Collected in June 2011^a

sampling station	depth (m)	total ^{129}I concn ($\times 10^7$ atoms/L)	^{127}I concn ($\mu\text{g/L}$)	$^{129}\text{I}/^{127}\text{I}$ ($\times 10^{-10}$ at/at)	iodide/iodate (mol/mol)	
					^{129}I	^{127}I
11	400	1.89 ± 0.40	60.44 ± 1.29	0.66 ± 0.14	NM	NM
11	200	4.46 ± 0.36	60.32 ± 1.30	1.56 ± 0.13	2.89 ± 0.47	0.074 ± 0.001
11	50	9.87 ± 0.65	55.53 ± 1.24	3.75 ± 0.26	6.01 ± 0.52	0.162 ± 0.004
11	20	15.63 ± 1.07	56.40 ± 1.08	5.84 ± 0.42	8.54 ± 2.11	0.173 ± 0.005
14	400	0.77 ± 0.09	61.64 ± 1.22	0.26 ± 0.03	NM	NM
14	200	2.30 ± 0.16	58.68 ± 1.00	0.83 ± 0.06	NM	NM
14	50	5.68 ± 0.38	54.60 ± 1.15	2.19 ± 0.15	3.61 ± 0.28	0.185 ± 0.004
14	20	14.75 ± 0.50	56.42 ± 1.21	5.51 ± 0.22	6.08 ± 0.78	0.181 ± 0.004
22	400	3.74 ± 0.34	61.38 ± 1.36	1.28 ± 0.12	NM	NM
22	200	11.80 ± 1.12	60.05 ± 1.42	4.14 ± 0.40	NM	NM
22	50	14.31 ± 1.20	57.88 ± 1.18	5.21 ± 0.45	3.74 ± 0.46	0.067 ± 0.002
22	20	16.14 ± 1.25	57.46 ± 1.08	5.92 ± 0.47	3.81 ± 0.71	0.115 ± 0.003
31	120	10.47 ± 0.76	55.23 ± 1.32	4.00 ± 0.30	NM	NM
31	100	10.68 ± 0.87	54.20 ± 1.10	4.15 ± 0.35	2.28 ± 0.51	0.262 ± 0.007
31	90	13.61 ± 0.93	57.95 ± 1.18	4.95 ± 0.35	3.35 ± 0.34	0.235 ± 0.006
31	50	13.31 ± 0.49	53.83 ± 1.14	5.21 ± 0.22	3.77 ± 0.40	0.270 ± 0.007
31	20	20.70 ± 0.75	60.87 ± 1.21	7.17 ± 0.30	7.40 ± 1.33	0.194 ± 0.005
31	10	62.90 ± 2.72	60.40 ± 1.39	21.95 ± 1.08	8.74 ± 0.33	0.255 ± 0.008

^aNM: not measured; the uncertainties shown in the table are 2σ analytical uncertainty. The distances from the sampling stations 31 (37.52° N, 141.44° E), 22 (38.00° N, 143.0° E), 14 (37.50° N, 144.00° E), and 11 (37.50° N, 147.00° E) to the Fukushima NPP are about 40, 180, 260, and 530 km, respectively.

RESULTS AND DISCUSSION

Distribution of ^{129}I in Seawater Offshore Fukushima.

In 4 seawater profiles offshore Fukushima, the highest concentration of ^{129}I up to 62×10^7 atoms/L was measured in the surface water from the station 31 about 40 km from the 1FNPP (Table 1). In the other 3 stations (11, 14, and 22), similar ^{129}I concentrations of $(14\text{--}16) \times 10^7$ atoms/L at depth 20 m were observed, which is slightly lower than that at station No. 31 with the value of 20×10^7 atoms/L at the same depth (Table 1). At station 31, the ^{129}I concentrations decrease with increasing depth to about $(10\text{--}13) \times 10^7$ atoms/L in the depth 50–120 m (Figure 1). The decreasing ^{129}I concentrations with depth were observed at all stations. The lowest ^{129}I

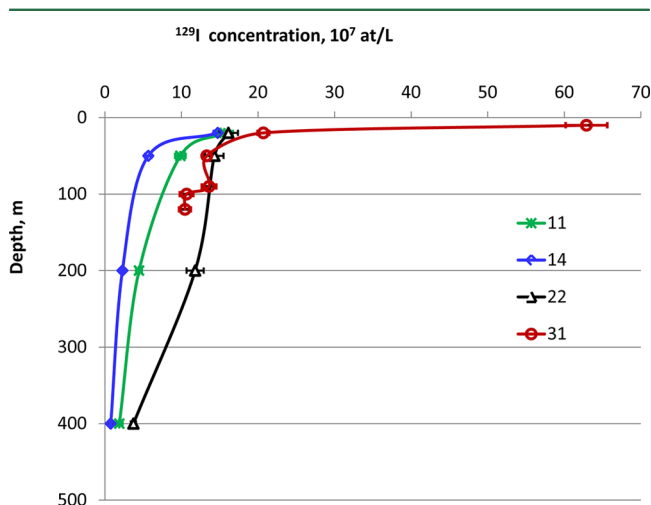


Figure 1. Depth distribution of ^{129}I concentration in 4 seawater profiles (at stations 11, 14, 22, and 31; refer to Table S-1 and Figure S-1 for precise locations) offshore Fukushima, error bars showing analytical uncertainty.

concentration of 0.77×10^7 atoms/L was observed at a depth of 400 m at station 14, which is about 260 km offshore Fukushima. A similar low ^{129}I concentration of 1.9×10^7 atoms/L was measured at depth of 400 m at station 11 (the most distant location 530 km from Fukushima). These values are 30–80 times lower than that of the surface water at station 31. Relative lower concentrations of ^{129}I in subsurface water (50–400 m depth) from station 14 compared to those at station 11 were measured, although station 11 is relatively far from Fukushima (530 km) compared to station 11 (260 km), these might be attributed to the pathway of water current as well as the contaminated water plume in this area.

Relatively constant ^{127}I concentrations of 55–61 $\mu\text{g/L}$ were observed in these seawater samples (Table 1). The distribution of the $^{129}\text{I}/^{127}\text{I}$ ratios (Figure 2, Table 1) is the same as for the ^{129}I concentrations; the highest $^{129}\text{I}/^{127}\text{I}$ ratio of 22×10^{-10} was observed at the 10 m depth in station 31, while the lowest $^{129}\text{I}/^{127}\text{I}$ ratio is only 0.26×10^{-10} in the water from station 14 at a depth of 400 m (Figure 2).

Inorganic Speciation of ^{129}I and ^{127}I in Seawater Profiles.

In seawater, especially offshore and in the open sea, iodine mainly exists as iodide and iodate and to a minor extent as organic iodine,^{22,23} although a high fraction of iodine in coastal and estuarine seawater and river and lake water was observed in organic form,²⁴ and increased level of organic iodine was reported in some open sea waters.²⁵ Two seawater samples collected in the North Sea (open seawater) and offshore Fukushima (surface water at station 31), respectively, were analyzed for both total inorganic ^{129}I and total ^{129}I using a method recently developed in our lab.²⁶ In this method, organic matter was first decomposed using $\text{K}_2\text{S}_2\text{O}_8$ at pH 1–2 to convert any organic associated iodine to inorganic form, followed by solvent extraction after addition of ^{127}I carrier. The results showed no significant difference between total inorganic ^{129}I and total ^{129}I , confirming that negligible amount of ^{129}I was present in organic form in these open sea and offshore seawater

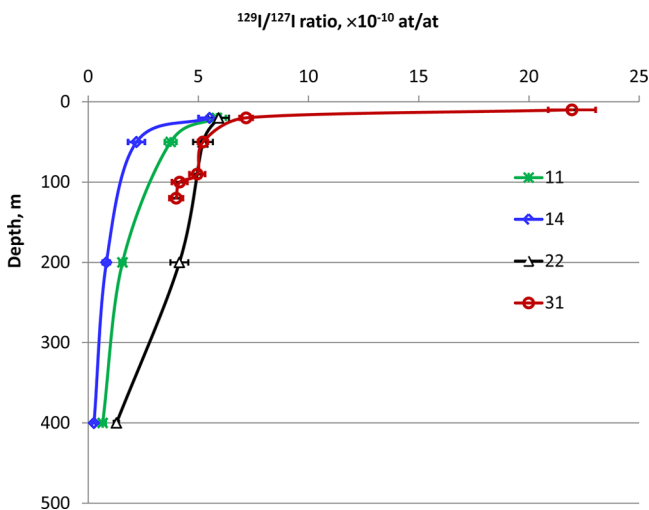


Figure 2. Depth distribution of $^{129}\text{I}/^{127}\text{I}$ atomic ratios in 4 seawater profiles (at stations 11, 14, 22 and 31; refer to Table S-1 and Figure S-1 for precise locations) offshore Fukushima, error bars showing analytical uncertainty.

samples. It is therefore shown that the measured total inorganic ^{129}I concentrations represent the total ^{129}I in the seawater measured in this work.

The analytical results of iodide, iodate, and total iodine for both ^{129}I and ^{127}I (Table S-2) show a completely different distribution of ^{129}I compared to ^{127}I in all seawater analyzed (Figure 3). ^{129}I is mainly in iodide form, with an iodide/iodate

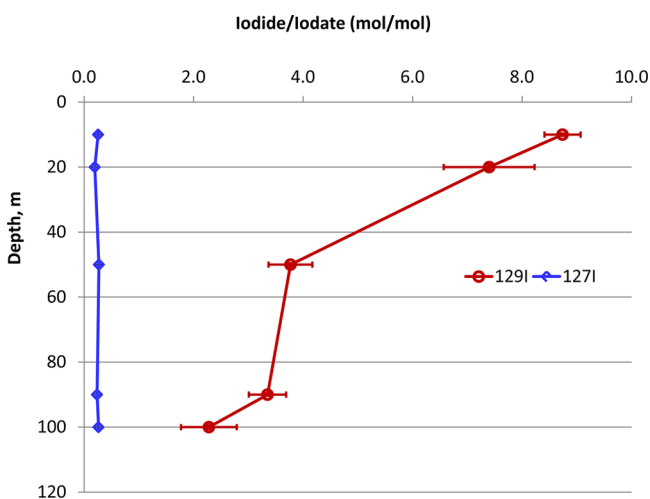


Figure 3. Distribution of ^{129}I and ^{127}I species (iodide/iodate, mol/mol) in seawater profile of station 31 (refer to Table S-1 and Figure S-1 for precise location) offshore Fukushima, error bars showing analytical uncertainty.

molecular ratio up to 8.7 in surface water (< 20 m) and about 2–3 in subsurface water (> 50 m). However, iodate is the dominant species of ^{127}I , with a relative constant molecular ratio of iodide/iodate of about 0.2 (range of 0.07–0.27) (Table 1). In the water profile at station 31, a trend of gradually decreasing iodide/iodate ratios from 8.7 in the surface water (at depth of 10 m) to 2.2 in subsurface water (at depth of 120 m) is observed (Figure 3). $^{129}\text{I}/^{127}\text{I}$ ratios show a significantly different distribution for iodide and iodate, with much higher isotopic ratio for iodide compared to iodate (Table S-2). The

$^{129}\text{I}/^{127}\text{I}$ ratios for iodide increase from 14×10^{-10} in the subsurface water to 104×10^{-10} in the surface water at station 31, while $^{129}\text{I}/^{127}\text{I}$ ratios for iodate are more than 45 times lower compared to those for iodide, only $(0.04\text{--}0.31) \times 10^{-10}$ (Table S-2).

The different distribution of ^{129}I species compared to ^{127}I can be attributed to two reasons: (1) the different sources of ^{127}I and ^{129}I ; (2) relatively long time to reach equilibrium among iodine oxidation states in the open sea. The ocean is the main source of iodine (^{127}I), which accounts for more than 80% of iodine in the earth's crust. Distribution of ^{127}I species in seawater depends on many parameters. In the open sea (oxygenated seawater), iodine mainly occurs as iodate; iodide concentrations might increase in the coastal water and surface water by reduction of iodate through biological, chemical, and photochemical approaches.²² Seawaters analyzed in this work were collected from an open sea, and the measured iodide/iodate ratios in these samples are typical values for the open sea.^{22,27}

Although the oxidation of iodide to iodate is a favored process in view of chemical dynamics of redox reactions of iodine in oxygenated seawater, investigation in the North Sea, Nordic seas, and the Arctic has shown, however, that oxidation of iodide to iodate in the open sea is a slow process,¹³ and chemical species of ^{129}I in offshore water and in the open sea have not significantly changed during their transport from the North Sea to the Norwegian Sea, and further to the Arctic, which takes 1–4 years. The seawater investigated in this work was collected June 9–15, about 2.5 months after direct liquid discharges of contaminated water from 1FNPP. Therefore, the dominant iodide species of ^{129}I should result from its source, i.e. that ^{129}I was discharged to the seawater from the 1FNPP mainly in iodide form. Chemical species of radioiodine in neither the liquid discharges from the 1FNPP nor irradiated fuel in the reactor have been reported. However, it has been observed that radioiodine (^{131}I , ^{123}I , or ^{124}I) in trap solution thermally released from the irradiated uranium or tellurium is mainly in iodide form (Syed M. Qaim, 2012, communication in NRC-9, 2012). This might imply that radioiodine in the contaminated water from the damaged reactor in 1FNPP might be mainly in iodide form. The chemical species of radioiodine in the precipitation of Fukushima are not yet available.

Source Terms of ^{129}I in Seawater Offshore Fukushima.

There are 4 possible sources of ^{129}I in the seawater offshore Fukushima: (1) direct liquid discharges from 1FNPP to the sea; (2) atmospheric fallout of ^{129}I from Fukushima accident; (3) runoff of ^{129}I deposited on the land to the sea; (4) global fallout of ^{129}I .

In a seawater profile collected offshore Kushiro (42°N , 146°E) before Fukushima accident in 2007, it has been observed that the $^{129}\text{I}/^{127}\text{I}$ ratios decreased with increasing depth from 0.7×10^{-10} in surface water, 0.18×10^{-10} in depth of 500 m, to $<0.07 \times 10^{-10}$ in the deeper water (> 1000 m), corresponding to ^{129}I concentration of 2×10^7 atoms/L in the surface water to 0.5×10^7 atoms/L at depth about 500 m, and then $<0.2 \times 10^7$ atoms/L in deeper water (> 1000 m).²⁸ Similar levels of ^{129}I concentrations of $(0.8\text{--}2) \times 10^7$ atoms/L in surface and subsurface (> 1000 m) have also been reported in two water profiles collected from the Northwestern Pacific Ocean (35°N , 152°E and 31°N , 170°E) in 1997.²⁹ Because there is no other source of ^{129}I in the Pacific Ocean except global fallout (and possibly local fallout from the nuclear weapons testing at Bikini and Enewetak atolls²⁹) before the Fukushima accident, the ^{129}I

level in these waters should be a representative level of ^{129}I in the Pacific Ocean. The ^{129}I level (for both ^{129}I concentrations and $^{129}\text{I}/^{127}\text{I}$ ratios) in the surface seawater (< 20 m) offshore Fukushima analyzed in this work is 5–30 times higher than the global fallout value, and 1.5–7 times higher in the subsurface water (> 400 m). A significantly decreased ^{129}I level with the increased depth in the water columns, especially in the top 100 m, was observed (Figures 1 and 2). At station 31, more than 3 times higher ^{129}I level at 10 m compared to at 20 m depth water was measured, this might imply that ^{129}I at surface (<10 m) is even higher, and difference of the ^{129}I concentration at surface water comparing to the pre-accident level is even bigger than just comparing with 20 m and 10 m depth water. Investigation of ^{129}I in seawater nearby the discharge point of nuclear power plants in China (the Pacific Ocean) has shown no significant influence of the operation of NPP on the ^{129}I levels in the seawater,³⁰ and the ^{129}I concentrations of $(0.7\text{--}2.5) \times 10^7$ atoms/L in surface water collected in 2–10 km distance from the discharge point of the NPP, corresponding to $^{129}\text{I}/^{127}\text{I}$ ratios of $(0.8\text{--}2.6) \times 10^{-10}$. It can be assumed that there was no significant influence of the operation of the Fukushima NPP on ^{129}I levels in seawater before the accident. The elevated ^{129}I levels in the surface seawater offshore Fukushima can therefore not be attributed to global fallout and the discharges from the ordinary operation of the Fukushima NPP. However, the global fallout contribution to the ^{129}I levels in the subsurface waters could not be ignored.

During the Fukushima accident in March 2011, huge amounts of radionuclides including 150–160 PBq of ^{131}I and 10–15 PBq of ^{137}Cs were released to the atmosphere.^{4–6} The half-lives of these radionuclides are very much different from a few hours (e.g., ^{132}I) to millions of years (e.g., ^{129}I). For easy discussion, all concentrations and ratios of the radionuclides discussed in this work (i.e., ^{137}Cs , ^{131}I , and ^{129}I) are decay-corrected to March 13, 2011, the beginning of the radioactive releases from the nuclear accident at the Fukushima Dai-ichi nuclear power plant, if not otherwise specified. It has been estimated that a total of 5.6 PBq of ^{137}Cs released to the atmosphere has been deposited over Japan and the surrounding ocean (130–150° E and 30–46° N),⁶ and a similar value of 5 PBq of ^{137}Cs deposited in the Ocean surrounding Japan has also been estimated by another group.⁵ This means that 30–50% of ^{137}Cs released to the atmosphere during the accident was deposited in the ocean surrounding Japan, indicating the deposition of radionuclides from the atmosphere to the ocean is one of important sources of radionuclides in seawater offshore Fukushima. Up to 77 Bq/L of ^{131}I and 24 Bq/L of ^{137}Cs were measured in seawater 30 km offshore Fukushima on March 23, 2011; this is more than 10^4 times higher than the background level of 1 mBq/L of ^{137}Cs in the Pacific Ocean,^{8,9} indicating a notable contribution of atmospheric deposition into the sea offshore Fukushima.

It is difficult to estimate the amount of radionuclide runoff from the land to the Sea *via* rivers, because no sufficient data on radionuclide concentrations in rivers are available. It has been reported that iodine can be easily absorbed in soil components, especially in the soil with high organic matter.³¹ It can be estimated that only very small fraction of iodine deposited on the lands can be quickly removed to the sea through rain and river runoff. Considering that only 13% of radioiodine released to the atmosphere was deposited on the land of Japan,⁷ the runoff of ^{129}I from the land to the sea would not be a significant source of ^{129}I in the seawater offshore Fukushima.

Direct liquid discharges of 3.5–4 PBq of ^{137}Cs from 1FNPP to the sea from 21 March to 30th April 2011 have been estimated.^{5,9} Much higher releases of ^{137}Cs of 27 PBq (12–41 PBq) have been estimated using a simple interpolation model of sparsely observed data and relatively coarse horizontal resolution,^{32,33} But a small release of ^{137}Cs of only 0.94 PBq in 1–6 April 2011 was estimated by Japanese government.³³ Therefore the direct discharge from 1FNPP to the sea is another important source of ^{129}I in the seawater offshore Fukushima.

The seawater samples investigated in this work have also been analyzed for ^{137}Cs ³⁴ using AMP (ammonium molybdophosphate) preconcentration and gamma spectrometry measurement,³⁵ and 0.01–1.1 Bq/L of ^{137}Cs were measured in these waters, i.e. 60–1100 times higher ^{137}Cs concentrations compared to the global fallout level, indicating its dominant Fukushima source. The $^{129}\text{I}/^{137}\text{Cs}$ atomic ratios in the analyzed seawater samples are calculated to be 0.41–0.62 in the top 50 m water column and 0.8–1.7 in subsurface seawaters (> 50 m) at 4 stations. Cesium is considered to be a relatively conservative element in oceans and ^{137}Cs has been widely applied as an oceanographic tracer for water circulation,^{36,37} although the residence time of ^{137}Cs is much shorter than ^{129}I due to the shorter physical half-life of ^{137}Cs and relatively higher adsorption of ^{137}Cs to the particulates (especially clay minerals) suspending in the water column. The high $^{129}\text{I}/^{137}\text{Cs}$ ratios in the subsurface water might be attributed to the fact that a relatively high fraction of ^{129}I in the subsurface seawater originates from global fallout. Based on the fact that the ^{129}I concentrations in subsurface water measured in this work are 1.5–7 times higher than pre-accident values, it can be estimated that 12–75% ^{129}I in subsurface water of >400 m depth originates from the global fallout. In addition, the higher analytical uncertainty of ^{137}Cs in subsurface water samples with low ^{137}Cs concentration also influences this value. By measurement of soil samples collected around the 1FNPP, a $^{129}\text{I}/^{131}\text{I}$ atomic ratio of (26.6 ± 7.5) has been reported.³⁸ Therefore $^{131}\text{I}/^{137}\text{Cs}$ atomic ratios in the surface water (<50 m depth) offshore Fukushima can be derived to be 0.015–0.023, or an activity ratio of 21–32. This values are close to the measured $^{131}\text{I}/^{137}\text{Cs}$ activity ratio of about 17.8 in coastal waters near the discharge point in the 1FNPP after March 25, 2011.^{8,9} Based on the estimated atmospheric releases of ^{131}I (150 PBq) and ^{137}Cs (13 PBq), $^{131}\text{I}/^{137}\text{Cs}$ activity ratio in the atmosphere released from the Fukushima accident can be calculated to be 11.5. Measurement of ^{131}I and ^{137}Cs in precipitation (rain and dust) over Japan from March 18 to April 29 has resulted in $^{131}\text{I}/^{137}\text{Cs}$ activity ratios ranging from 3.2 to 500 with a median of 15; the higher ratios occurred at downstream inland sites of radioactive plume.³⁹ The large variation of $^{131}\text{I}/^{137}\text{Cs}$ ratio might also result from the different ratios of $^{131}\text{I}/^{137}\text{Cs}$ in different reactors. The measured $^{131}\text{I}/^{137}\text{Cs}$ ratios in air samples collected over Europe during March 22 to April 11, 2011 also highly varied, with an average of 40–100 for aerosol samples. Considering that only about 20% of ^{131}I occurred in particle-associated forms, the $^{131}\text{I}/^{137}\text{Cs}$ ratio in the atmosphere is likely higher than 200.³⁹ In addition, increased $^{131}\text{I}/^{137}\text{Cs}$ ratios with sampling date from March 19, 2011 onward have been observed in aerosols from the Fukushima area,⁴⁰ indicating that the radioactive cloud contained more radioiodine at the beginning of the accident. This could be attributed to the properties of higher volatility and longer residence time of iodine in the atmosphere compared to ^{137}Cs . In atmosphere,

iodine exists in both gaseous and particle-associated forms, while ^{137}Cs is mainly in particle-associated form. Removal rate of particles from the atmosphere by dry and wet deposition is much higher than gaseous form of iodine due to less efficiency of gaseous iodine capture to droplets. Consequently, residence time of radioiodine in atmosphere is longer than ^{137}Cs (particle), and therefore decreased ^{137}Cs concentrations compared to ^{131}I in the atmosphere or increased $^{131}\text{I}/^{137}\text{Cs}$ ratios with the increased time after accident were observed in the atmosphere or precipitation. The relatively high $^{129}\text{I}/^{137}\text{Cs}$ ratios measured in surface seawater can therefore be attributed to the contribution of the atmospheric deposition in the seawater offshore Fukushima.

In summary, ^{129}I in the surface water likely mainly originated from the liquid discharges from the Fukushima 1FNPP to the sea; however, the atmospheric deposition has also a visible contribution, and in subsurface waters the contribution from global fallout is not negligible.

Amount of ^{129}I Discharged to the Sea from the Fukushima Daiichi NPP. As described above, ^{129}I in the seawater offshore Fukushima has two major sources, i.e. direct liquid discharge from 1FNPP, and the atmospheric deposition subsequent to the accident. From March 21, 2011, ^{131}I and ^{137}Cs concentrations in coastal seawater samples collected at 3 sites at the discharge channel of 1FNPP and 10 km and 16 km south of the 1FNPP, as well as at 8 sites 30 km off the Fukushima coastline, have been monitored by the operator of 1FNPP, the Tokyo Electric Power Company (TEPCO), and the Ministry of Education, Culture, Sports, Science and Technology (MEXT). A quite constant activity ratio of $^{131}\text{I}/^{137}\text{Cs}$ of 17.6 has been observed in the seawater from all coastal sites near to the 1FNPP from March 26, 2011, while scattered and higher $^{131}\text{I}/^{137}\text{Cs}$ ratios of >28 have been observed in the seawater from the sites 10 and 16 km south of 1FNPP March 21–25, 2011. A large scatter of $^{131}\text{I}/^{137}\text{Cs}$ ratios of 6–20 have been observed in seawater collected at 30 km offshore Fukushima before April 2.^{8,9} Similarly lower $^{131}\text{I}/^{137}\text{Cs}$ ratios of 3–18 have also been observed at sites >5 km from the coast of Fukushima before April 2.²³ The large scatter before March 25 in coastal sites and before April 2 at sites offshore Fukushima can be attributed to the atmospheric deposition from the Fukushima accident.^{8,9} Large variations in the $^{131}\text{I}/^{137}\text{Cs}$ activity ratios in atmospheric and precipitation samples have been observed in Japan as well as at far locations in Europe after the Fukushima accident.^{39,40} This is attributed to different ratios of $^{131}\text{I}/^{137}\text{Cs}$ from different reactors in the 1FNPP, as well as to different behaviors of ^{131}I and ^{137}Cs in the atmosphere. ^{137}Cs is mainly associated with particles, while radioiodine can be in both gaseous and particle-associated form,⁴⁰ which cause different dispersion and deposition patterns of ^{131}I and ^{137}Cs . Therefore the $^{131}\text{I}/^{137}\text{Cs}$ ratios vary in seawater, to which the atmospheric deposition has a significant contribution (together with liquid discharges). The constant $^{131}\text{I}/^{137}\text{Cs}$ ratio (17.6) in the seawater collected from the coastal sites within 16 km of the 1FNPP confirms that the ^{131}I and ^{137}Cs in seawater offshore Fukushima is dominated by the direct liquid discharges from the damaged nuclear reactor 2 in the 1FNPP after March 25, 2011.^{8,9,33} Because of the same chemical properties and environmental behaviors of ^{131}I and ^{129}I , the amount of ^{129}I directly discharged to the sea from the 1FNPP can be estimated from the measured $^{131}\text{I}/^{137}\text{Cs}$ ratio, and estimated amount of ^{137}Cs directly discharged to the sea

from the 1FNPP. Here, we applied the estimated value of 3.5 PBq for direct liquid discharge of ^{137}Cs to the sea,⁹ the amount of ^{131}I directly discharged to the sea can be estimated to be 61.6 PBq. Based on these data and the measured $^{129}\text{I}/^{131}\text{I}$ atomic ratio of (26.6 ± 7.5) for released radioiodine from the 1FNPP,³⁸ the amount of ^{129}I directly discharged to the sea from the 1FNPP can be estimated to be 2.35 GBq (or 0.35 kg).

Of the total 150 PBq of ^{131}I and 13 PBq of ^{137}Cs released to the atmosphere from the Fukushima accident,^{1,4} it has been estimated that more than 80% of ^{137}Cs has been deposited in the ocean, 18% in Japanese land area, and only 1.9% was deposited over land areas outside Japan.⁴¹ A similar percentage of radionuclide deposition has been estimated by Morino et al.⁷ using a 3-dimensional chemical transport model; they reported that 13% of ^{131}I and 22% of ^{137}Cs fell over the land of Japan, 19% ^{131}I and 10% of ^{137}Cs were deposited over the Ocean in the area of 34–41° N and 137–145° E (700 km \times 700 km), and the rest was transported and deposited in other areas, mainly in the Pacific Ocean. It can be estimated that about 120 PBq of ^{131}I was deposited in the Ocean, mostly in the Pacific Ocean; of this, 28.5 PBq of ^{131}I was deposited in the sea area of 34–41° N and 137–145° E, mainly offshore Fukushima. Based on the reported $^{129}\text{I}/^{127}\text{I}$ atomic ratio of 26.6,³⁸ about 4.57 GBq (0.68 kg) of ^{129}I released to the atmosphere was deposited in the Ocean, and about 1.09 GBq of ^{129}I (0.16 kg) was deposited in the sea area of 34–41° N and 137–145° E, most in the sea offshore Fukushima. This estimation indicates that liquid discharges from 1FNPP are the major source of ^{129}I in the sea offshore Fukushima, and the atmospheric deposition is the minor source, accounting for about 32% of the total ^{129}I .

If we assume the liquid discharges still remained in the 700 \times 700 km area offshore Fukushima and mainly in the top 50 m water column, and it was homogeneously distributed in this area, ^{129}I concentration in the top 50 m seawater can be calculated to be about 1×10^8 atom/L, or a $^{129}\text{I}/^{127}\text{I}$ isotopic ratio of about 3.5×10^{-10} . This value agrees relatively well with the measured ^{129}I concentration ($(0.5\text{--}2) \times 10^8$ atoms/L) and $^{129}\text{I}/^{127}\text{I}$ ratios $(2\text{--}7) \times 10^{-10}$ in the surface water (10–50 m depth) offshore Fukushima.

It has been estimated that Chernobyl accident released about 1.3–6 kg of ^{129}I to the atmosphere.^{23,42} A total release of 1.2 kg of ^{129}I from the Fukushima accident estimated in this work is comparable to that released from the Chernobyl accident. However, the ^{129}I released from Chernobyl accident was deposited in the terrestrial area, mainly in European countries, whereas ^{129}I released from Fukushima accident was mainly deposited to the ocean.

Reprocessing plants have released large amounts of ^{129}I to the environment, especially from the two European reprocessing plants at La Hague (France) and Sellafield (UK), which have discharged about 5200 kg of ^{129}I to the sea and 440 kg to the atmosphere (up to 2007).²³ The ^{129}I released from the Fukushima accident accounts therefore to less than 0.3% of the total ^{129}I released from reprocessing plants. However, the ^{129}I from the European reprocessing plants has been mainly discharged and transported to the European seas, and further to the Arctic.^{11,13,42} The contribution of ^{129}I from the Fukushima accident to the Pacific Ocean is remarkable, as it has influenced the total inventory of ^{129}I in the Pacific Ocean. The Fukushima-derived ^{129}I will be therefore a useful tracer for oceanographic research in this area.

■ ASSOCIATED CONTENT

■ Supporting Information

Detailed chemical procedure for separation of iodine species in seawater samples; detailed sampling information and analytical results of ^{129}I and ^{127}I in 4 seawater profiles (Table S-1); analytical results of inorganic speciation of ^{129}I and ^{127}I in 4 seawater profiles (Table S-2); a map showing sampling stations and water depth (Figure S-1); and a schematic diagram of chemical procedure for speciation analysis of ^{129}I and ^{127}I (Figure S-2). This material is available free of charge via the Internet at <http://pubs.acs.org>.

■ AUTHOR INFORMATION

Corresponding Author

*E-mail: xiho@risoe.dtu.dk; phone:+45-21325129; fax:+45-46775347.

Notes

The authors declare no competing financial interest.

■ ACKNOWLEDGMENTS

We acknowledge Dr. Ken Buesseler (WHOI) and Dr. Harmut Nies (IAEA-EL) for provision of seawater samples. X.L.H. acknowledges financial support provided by Innovation Method Fund China (2012IM030200). P.P.P. acknowledges support provided by the EU Research and Development Operational Program funded by the ERDF (26240220004). Equipment support at the University of Arizona was provided in part by a grant from the National Science Foundation (EAR0929458).

■ REFERENCES

- (1) Yoshida, N.; Kanda, J. Tracking the Fukushima Radionuclides. *Science* **2012**, *336*, 1115–1116.
- (2) Wakeford, R. Fukushima. *J. Radiol. Protect.* **2011**, *31*, 167–176.
- (3) Buesseler, K. O.; Jayne, S. R.; Fisher, N. S.; Rypina, I. I.; Baumann, H.; Baumann, Z.; Breier, C. F.; Douglass, E. M.; George, J.; Macdonald, A. M.; Miyamoto, H.; Nishikawa, J.; Pike, S. M.; Yoshida, S. Fukushima-derived radionuclides in the ocean and biota off Japan. *Proc. Natl. Acad. Sci., U. S. A.* **2012**, *109* (16), 5984–5988.
- (4) Chino, M.; Nakayama, H.; Nagai, H.; Terada, H.; Katata, G.; Yamazawa, H. Preliminary estimation of release amounts of ^{131}I and ^{137}Cs accidentally discharged from the Fukushima Daiichi nuclear power plant into the atmosphere. *J. Nucl. Sci. Technol.* **2012**, *48* (7), 1129–1134.
- (5) Kawamura, H.; Kobayashi, T.; Furuno, A.; In, T.; Ishikawa, Y.; Nakayama, T.; Shima, S.; Awaji, T. Preliminary numerical experiment on oceanic dispersion of ^{131}I and ^{137}Cs discharged into the ocean because of the Fukushima Daiichi nuclear power plant disaster. *J. Nucl. Sci. Technol.* **2012**, *48* (11), 1349–1356.
- (6) Yasunari, T. J.; Stohl, A.; Hayano, R. S.; Hayano, R. S.; Burkhardt, J. F.; Eckhardt, S.; Yasunari, T. Cesium-137 deposition and contamination of Japanese soil due to the Fukushima nuclear accident. *PNAS* **2011**, *108* (49), 19530–19534.
- (7) Morino, Y.; Ohara, T.; Nishizawa, M. Atmospheric behavior, deposition, and budget of radioactive materials from the Fukushima Daiichi nuclear power plant. *Geophys. Res. Lett.* **2011**, *38*, L00G11.
- (8) Buesseler, K.; Aoyama, M.; Fukasawa, M. Impact of the Fukushima nuclear power plants on marine radioactivity. *Environ. Sci. Technol.* **2011**, *45*, 9931–9935.
- (9) Tsumune, D.; Tsubono, T.; Aoyama, M.; Hirose, K. Distribution of oceanic ^{137}Cs from the Fukushima Dai-ichi nuclear power plant simulated numerically by a regional ocean model. *J. Environ. Radioact.* **2012**, *111*, 100–108.
- (10) Povinec, P. P.; Hirose, K.; Aoyama, M. Radiostronium in the western North Pacific: Characteristics, Behavior, and the Fukushima Impact. *Environ. Sci. Technol.* **2012**, *46*, 10356–10363.
- (11) Raisbeck, G. M.; Yiou, F. ^{129}I in the oceans: Origins and applications. *Sci. Total Environ.* **1999**, *237/238*, 31–41.
- (12) Hou, X. L.; Aldahan, A.; Nielsen, S. P.; Possnert, G. Time series of ^{129}I and ^{127}I speciation in precipitation from Denmark. *Environ. Sci. Technol.* **2009**, *43*, 6532–6528.
- (13) Hou, X. L.; Aldahan, A.; Nislen, S. P.; Possnert, G.; Nies, H.; Hedfords, J. Speciation of ^{129}I and ^{127}I in seawater and implications for sources and transport pathways in North Sea. *Environ. Sci. Technol.* **2007**, *41*, 5993–5999.
- (14) Straume, T.; Anspaugh, L. R.; Marchetti, A. A.; Voigt, G.; Minenko, V.; Gu, F.; Men, P.; Trofimik, S.; Tretyakevich, S.; Drozdovitch, V.; Shagalova, E.; Zhukova, O.; Germenchuk, M.; Berlovich, S. Measurement of ^{129}I and ^{137}Cs in soil from Belarus and reconstruction of ^{131}I deposition from the Chernobyl accident. *Health Phys.* **2006**, *91*, 7–19.
- (15) Hou, X. L.; Yan, X. J. Study on the concentration and seasonal variation of inorganic elements in 35 species of marine algae. *Sci. Total Environ.* **1998**, *222*, 141–156.
- (16) Manley, S. L.; Lowe, G. Canopy-Forming kelps as California's dosimeter: ^{131}I from damaged Japanese reactor measured in *Macrocystis pyrifera*. *Environ. Sci. Technol.* **2012**, *46*, 3731–3736.
- (17) Wallner, G.; Steier, P.; Brandl, T.; Friesacher, M. E.; Hille, P.; Kutschera, W.; Tatzber, M.; Ayromlou, S. Developments toward the measurement of I-129 in lignite. *Nucl. Instrum. Methods* **2007**, *B 259*, 714–720.
- (18) Biddulph, D. L.; Beck, J. W.; Burr, G. S.; Donahue, D. J.; Hatheway, A. L.; Jull, A. J. T. Measurement of the radioisotope ^{129}I at the NSF-Arizona AMS laboratory. *Nucl. Instrum. Methods* **2000**, *B 172*, 693–698.
- (19) Hou, X. L.; Zhou, W. J.; Chen, N.; Zhang, L. Y.; Liu, Q.; Luo, M. Y.; Fan, Y. K.; Liang, W. G.; Fu, Y. C. Determination of ultralow level $^{129}\text{I}/^{127}\text{I}$ in natural samples by separation of microgram carrier free iodine and accelerator mass spectrometry detection. *Anal. Chem.* **2010**, *82*, 7713–7721.
- (20) Fehn, U.; Snyder, G.; Egeberg, P. Dating of Pore Waters with ^{129}I : Relevance for the Origin of Marine Gas Hydrates. *Science* **2000**, *289*, 2332–2335.
- (21) Zhou, W. J.; Chen, N.; Hou, X. L.; Zhang, L. Y.; Liu, Q.; He, C. H.; Luo, M. Y.; Fan, Y. K.; Fu, Y. C. Analytical methods of ^{129}I and a case study of ^{129}I environmental tracing in Xi'an Accelerator Mass Spectrometry Centre. *Nucl. Instrum. Methods* **2013**, *B 294*, 147–151.
- (22) Wong, G. T. F. The marine Geochemistry of iodine. *Rev. Aquat. Sci.* **1991**, *45*, 45–73.
- (23) Hou, X. L.; Hansen, V.; Aldahan, A.; Possnert, G.; Lind, O. C.; Lujaniene, G. A review on speciation of iodine-129 in the environmental and biological samples. *Anal. Chim. Acta* **2009**, *632*, 181–196.
- (24) Schwehr, K. A.; Santschi, P. H.; Elmore, D. The dissolved organic iodine species of the isotopic ratio of $^{129}\text{I}/^{127}\text{I}$: A novel tool for tracing terrestrial organic carbon in the estuarine surface water of Galveston Bay, Texas. *Limnol. Oceanogr.: Methods* **2005**, *3*, 326–337.
- (25) Huang, Z.; Ito, K.; Morita, I.; Yokota, K.; Fukushi, K.; Timerbaev, A. R.; Watanabe, S.; Hirokawa, T. Sensitive monitoring of iodine species in sea water using capillary electrophoresis: Vertical profiles of dissolved iodine in the Pacific Ocean. *J. Environ. Monitor.* **2005**, *7*, 804–808.
- (26) Dang, H. J.; Hou, X. L.; Roos, P.; Nielsen, S. P. Release of iodine from organic matter in natural water by $\text{K}_2\text{S}_2\text{O}_8$ oxidation for ^{129}I determination. *Anal. Methods* **2013**, *5*, 449–456.
- (27) Truesdale, V. W.; Bale, A. J.; Woodward, E. M. S. The meridional distribution of dissolved iodine in near surface water of the Atlantic Ocean. *Prog. Oceanogr.* **2000**, *45*, 387–400.
- (28) Suzuki, T.; Minakawa, M.; Amano, H.; Togawa, O. The vertical profiles of iodine-129 in the Pacific Ocean and the Japan Sea before the routine operation of a new nuclear fuel reprocessing plant. *Nucl. Instrum. Methods* **2010**, *B 268*, 1229–1231.

(29) Povinec, P. P.; Lee, S. H.; Liong Wee Kwong, L.; Oregioni, B.; Jull, A. J. T.; Kieser, W. E.; Morgenstern, U.; Top, Z. Tritium, radiocarbon, ^{90}Sr and ^{129}I in the Pacific and Indian Oceans. *Nucl. Instrum. Methods* **2010**, *B268*, 1214–1218.

(30) He, C. H.; Hou, X. L.; Zhao, Y. L.; Wang, Z. W.; Li, H. B.; Chen, N.; Lu, Q.; Zhang, L. Y.; Luo, M. Y.; Liang, W. G.; Fan, Y. K.; Zhao, X. L. ^{129}I level in seawater near a nuclear power plant determined by accelerator mass spectrometry. *Nucl. Instrum. Methods* **2011**, *A632*, 152–156.

(31) Shetya, W. H.; Young, S. D.; Watts, M. J.; Ander, E. L.; Bailey, E. H. Iodine dynamics in soil. *Geochim. Cosmochim. Acta* **2012**, *77*, 457–473.

(32) Masumoto, Y.; Miyazawa, Y.; Tsumune, D.; Tsubono, T.; Kobayashi, T.; Kawamura, H.; Estournel, C.; Marsaleix, P.; Lanerolle, L.; Mehra, A.; Garraffo, Z. D. Oceanic dispersion simulations of ^{137}Cs released from the Fukushima Daiichi nuclear power plant. *Elements* **2012**, *8*, 207–212.

(33) Bailly du Bois, P.; Laguionie, L.; Boust, D.; Korsakissok, I.; Didier, D.; Fievet, B. Estimation of marine source term following Fukushima Dai-ichi accident. *J. Environ. Radioact.* **2012**, *114*, 2–9.

(34) NERH. *Report of Japanese Government to the IAEA Ministerial Conference on Nuclear Safety, The Accident at TEPCO's Fukushima Nuclear Power Stations*; 2011. http://www.kantei.go.jp/foreign/kan/topics/201106/iaea_houkokusho_e.html.

(35) Povinec, P. P.; Aoyama, M.; Biddulph, D.; Breier, R.; Buesseler, K.; Chang, C. C.; Golser, R.; Hou, X. L.; Jěskovský, M.; Jull, A. J. T.; Kaizer, J.; Nakano, M.; Nies, H.; Palcsu, L.; Papp, L.; Pham, M. K.; Steier, P.; Zhang, L. Y. Cesium, iodine and tritium in NW Pacific waters – A comparison of the Fukushima impact with global fallout. *Biogeosciences* **2013**, under review.

(36) Aarkrog, A.; Dahlgaard, H.; Hallstadius, L.; Hansen, H.; Holm, E. Radiocaesium from Sellafield effluents in Greenland water. *Nature* **1983**, *304*, 49–51.

(37) Volpe, A. M.; Bandong, B. B.; Esser, B. K.; Bianchini, G. M. Radiocaesium in North San Francisco Bay and Baja California coastal surface waters. *J. Environ. Radioact.* **2002**, *60*, 365–380.

(38) Miyake, Y.; Matsuzaki, H.; Fujiwara, T.; Saito, T.; Yamagata, T.; Honda, M.; Muramatsu, Y. Isotopic ratio of radioactive iodine ($^{129}\text{I}/^{131}\text{I}$) released from Fukushima Daiichi NPP accident. *Geochem. J.* **2012**, *46*, 327–333.

(39) Hirose, K. 2011 Fukushima Dai-ichi nuclear power plant accident: Summary of regional radioactive deposition monitoring results. *J. Environ. Radioact.* **2012**, *111*, 13–17.

(40) Masson, O.; Baeza, A.; Bieringer, J.; et al. Tracking of Airborne Radionuclides from the Damaged Fukushima Dai-Ichi Nuclear Reactors by European Networks. *Environ. Sci. Technol.* **2011**, *45*, 7670–7677.

(41) Stohl, A.; Seibert, P.; Wotawa, G.; Arnold, D.; Burkhart, J. F.; Eckhart, S.; Tapia, C.; Vargas, A.; Yasunari, T. J. Xenon-133 and Caesium-137 releases into the atmosphere from the Fukushima Daiichi nuclear power plant: Determination of the source term, atmospheric dispersion and deposition. *Atmos. Chem. Phys.* **2012**, *12*, 2313–2343.

(42) Aldahan, A.; Alfimov, V.; Possnert, G. ^{129}I anthropogenic budget: Major source and sink. *Appl. Geochem.* **2007**, *22*, 606–618.

Iodine-129 in Seawater Offshore Fukushima: Distribution, Speciation, Sources, and Budget

Xiaolin Hou^{1,3*}, Pavel P. Povinec², Luyuan. Zhang¹, Keliang Shi¹, Dana Biddulph^{4,9}, Ching-Chih Chang^{8,9}, Yukun. Fan³, Robin Golser⁵, Yingkun Hou⁶, Miroslav. Jeřkovský^{5,2}, A.J. Tim Jull^{4,8,9}, Qi Liu³, Maoyi Luo^{1,7}, Peter Steier⁵, Weijian. Zhou³

- 1) Center for Nuclear Technology, Technical University of Denmark, Risø Campus, DK-4000 Roskilde, Denmark
- 2) Department of Nuclear Physics and Biophysics, Comenius University, Bratislava, Slovakia
- 3) Xi'an AMS Center, SKLLQG, Institute of Earth Environment, CAS, Xi'an 710075, China
- 4) Department of Physics, University of Arizona, Tucson, AZ 85721 USA
- 5) Faculty of Physics, University of Vienna, Währingerstr. 17, 1090 Vienna, Austria
- 6) Department of Chemistry, Imperial College London, United Kingdom
- 7) Department of Nuclear Science and Technology, Xi'an Jiaotong University, China
- 8) Department of Geosciences, University of Arizona, Tucson, AZ 85721 USA
- 9) NSF Arizona AMS Laboratory, University of Arizona, Tucson, AZ 85721 USA

Chemical procedure for separation of ¹²⁹I species

0.5-1 L filtered seawater was transferred to a beaker; ¹²⁵I solution (about 100 Bq, in NaI form) was added to the seawater. The prepared solution was then loaded to an anion exchange column (AG1-×4 resin, NO₃⁻ form, 1.0 cm in diameter and 15 cm length), the column was washed with 50 mL 0.2 mol/L NaNO₃, the effluent and wash were combined for iodate separation. The column was then eluted with 150 mL 5% NaClO and then 50 mL of 3M HNO₃, and the eluate was combined for iodide separation.

1.0 mL of solution of iodide fraction, iodate fraction and original seawater were taken into a vial for ¹²⁷I measurement using ICP-MS. The remaining solution of iodate fraction (Effluent + washes of 0.2 mol/L NaNO₃) or 200-500 mL of original seawater samples (for total ¹²⁹I) was transferred to a beaker; ¹²⁵I tracer (200 Bq), 0.5 mg ¹²⁷I carrier, and 1M NaHSO₃ solution were added. The solution was adjusted to pH 1-2 using 3 mol/L HNO₃ to convert all iodine to iodide. The solution was then transferred to a separation funnel, 50 mL CHCl₃ was added and then 1.0 mol/L NaNO₂

solution was added to oxidize iodide to I_2 to be extracted to $CHCl_3$ phase by shaking. I_2 is then back-extracted to the water phase by add 5 mmol/L $NaHSO_3$ solution. This extraction and back-extraction steps were repeated once. The back-extracted aqueous phase was used for preparation of AgI target.

The remaining solution of iodide fraction was transferred to a separatory funnel. After addition of 0.5 mg of ^{127}I carrier, 3.0 mol/L HNO_3 was added to adjust pH1-2. 50 mL of $CHCl_3$ and 5 mL of 1 mol/L $NH_2OH \cdot HCl$ solution were added to reduce iodate to I_2 to be extracted to $CHCl_3$ phase by shaking. I_2 in $CHCl_3$ phase was then back-extracted using 5mM $NaHSO_3$ solution.

0.5 mL of 1.0 mol/L $AgNO_3$ solution was added to the back-extracted aqueous phases to precipitate iodide as AgI, which was separated using a centrifuge. The resulting AgI precipitate was dried at 70 °C and used for AMS measurement of ^{129}I . ^{125}I in the precipitate was counted using a NaI gamma-detector to monitor the chemical yield of iodine in the separation. Before extraction, the eluate of iodide from the anion exchange column was also measured for ^{125}I by gamma-detector to monitor chemical recovery of iodide during column separation. This is used to correct ^{127}I iodide and ^{129}I iodide concentrations in seawater. ¹

References

- (1) Hou, X.L.; Aldahan, A.; Nislen, S.P.; Possnert, G.; Nies, H.; Hedfords, J. Speciation of ^{129}I and ^{127}I in seawater and implications for sources and transport pathways in North Sea. *Environ. Sci. Technol.* 2007, 41, 5993–5999.

Table S-1 Distribution of ^{129}I and ^{127}I and the $^{129}\text{I}/^{127}\text{I}$ ratios in 4 seawater profiles offshore Fukushima

Sampling station	Depth		Coordinate	^{129}I conc., 10^7 at/L		^{127}I conc., $\mu\text{g/L}$		$^{129}\text{I}/^{127}\text{I}$, 10^{-10} at/at	
	m	Sampling date		Value	Uncertainty	Value	Uncertainty	Value	Uncertainty
11	400	09/06/2011	37.50008° N, 147.0000° E	1.89	0.40	60.44	1.29	0.66	0.14
11	200	09/06/2011	37.50008° N, 147.0000° E	4.46	0.36	60.32	1.30	1.56	0.13
11	50	09/06/2011	37.50008° N, 147.0000° E	9.87	0.65	55.53	1.24	3.75	0.26
11	20	09/06/2011	37.50008° N, 147.0000° E	15.63	1.07	56.40	1.08	5.84	0.42
14	400	10/06/2011	37.50287° N, 143.9992°E	0.77	0.09	61.64	1.22	0.26	0.03
14	200	10/06/2011	37.50287° N, 143.9992°E	2.30	0.16	58.68	1.00	0.83	0.06
14	50	10/06/2011	37.50287° N, 143.9992°E	5.68	0.38	54.60	1.15	2.19	0.15
14	20	10/06/2011	37.50287° N, 143.9992°E	14.75	0.50	56.42	1.21	5.51	0.22
22	400	13/06/2011	37.99908° N, 142.9998° E	3.74	0.34	61.38	1.36	1.28	0.12
22	200	13/06/2011	37.99908° N, 142.9998° E	11.80	1.12	60.05	1.42	4.14	0.40
22	50	13/06/2011	37.99908° N, 142.9998° E	14.31	1.20	57.88	1.18	5.21	0.45
22	20	13/06/2011	37.99908° N, 142.9998° E	16.14	1.25	57.46	1.08	5.92	0.47
31	120	15/06/2011	37.51953° N, 141.4431° E	10.47	0.76	55.23	1.32	4.00	0.30
31	100	15/06/2011	37.51953° N, 141.4431° E	10.68	0.87	54.20	1.10	4.15	0.35
31	90	15/06/2011	37.51953° N, 141.4431° E	13.61	0.93	57.95	1.18	4.95	0.35
31	50	15/06/2011	37.51953° N, 141.4431° E	13.31	0.49	53.83	1.14	5.21	0.22
31	20	15/06/2011	37.51953° N, 141.4431° E	20.70	0.75	60.87	1.21	7.17	0.30
31	10	15/06/2011	37.51953° N, 141.4431° E	62.90	2.72	60.40	1.39	21.95	1.08

Table S-2 Chemical speciation of ^{129}I and ^{127}I in seawater offshore Fukushima

Sampling station	Depth m	Iodate						Iodide				Iodide/Iodate, mol/mol					
		^{127}I Conc, ppb		^{129}I Conc, $\times 10^7$ atoms/L		$^{129}\text{I}/^{127}\text{I}$ ratio, $\times 10^{-10}$, at/at		^{127}I Conc, ppb		^{129}I Conc, $\times 10^7$ atoms/L		$^{129}\text{I}/^{127}\text{I}$ ratio, $\times 10^{-10}$ at/at		^{129}I		^{127}I	
		Value	Unc.	Value	Unc.	Value	Unc.	Value	Unc.	Value	Unc.	Value	Unc.	Value	Unc.	Value	Unc.
11	200	54.21	0.83	1.15	0.12	0.045	0.005	4.03	0.04	3.32	0.42	17.37	2.19	2.89	0.47	0.074	0.001
11	50	49.71	1.00	1.41	0.10	0.060	0.004	8.07	0.14	8.46	0.43	22.10	1.19	6.01	0.52	0.162	0.004
11	20	48.76	0.72	1.64	0.39	0.071	0.017	8.42	0.18	13.99	1.03	35.02	2.68	8.54	2.11	0.173	0.005
14	50	49.82	0.77	1.23	0.07	0.052	0.003	9.24	0.16	4.45	0.24	10.16	0.57	3.61	0.28	0.185	0.004
14	20	51.25	0.88	2.08	0.19	0.086	0.008	9.28	0.14	12.67	1.14	28.76	2.64	6.08	0.78	0.181	0.004
22	50	55.48	0.83	3.02	0.30	0.115	0.012	3.72	0.08	11.29	0.79	64.03	4.65	3.74	0.46	0.067	0.002
22	20	52.24	0.77	3.35	0.52	0.135	0.021	6.02	0.13	12.79	1.35	44.80	4.82	3.81	0.71	0.115	0.003
31	100	46.13	0.74	3.26	0.65	0.080	0.016	12.09	0.26	7.42	0.75	15.55	1.61	2.28	0.51	0.262	0.007
31	90	50.09	0.77	3.13	0.23	0.132	0.010	11.75	0.21	10.48	0.73	18.81	1.35	3.35	0.34	0.235	0.006
31	50	47.72	0.82	2.60	0.18	0.155	0.011	12.88	0.24	9.80	0.79	16.05	1.34	3.77	0.40	0.270	0.007
31	20	45.87	0.82	2.46	0.41	0.113	0.019	8.89	0.14	18.24	1.21	43.24	2.94	7.40	1.33	0.194	0.005
31	10	44.51	0.78	6.46	0.21	0.306	0.012	11.35	0.30	56.44	1.07	104.82	3.38	8.74	0.33	0.255	0.008

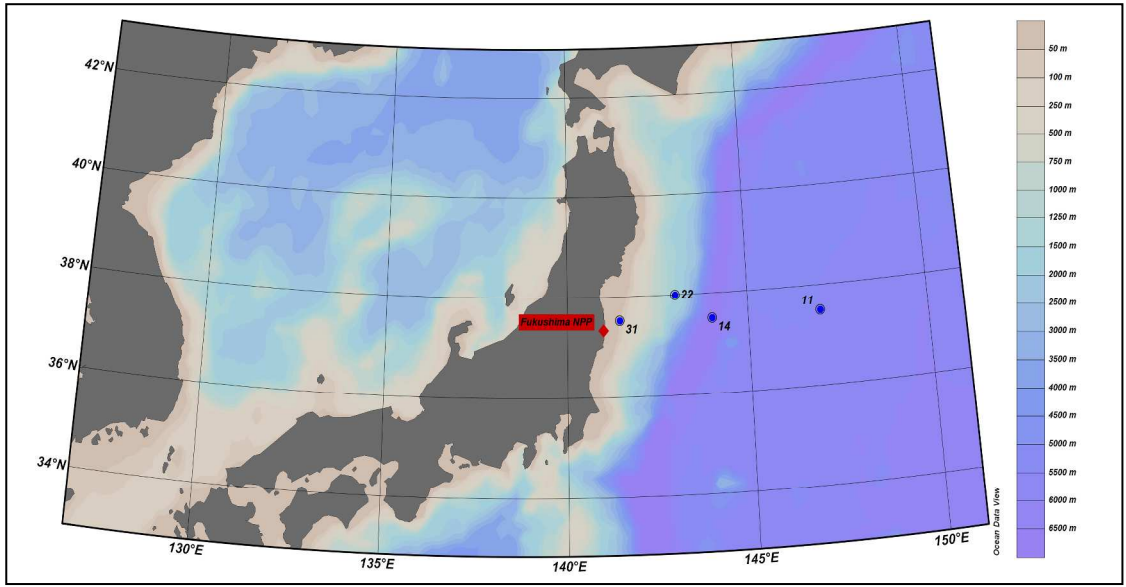


Fig. S-1 Sampling stations of seawater profile collected offshore Fukushima in June 2011

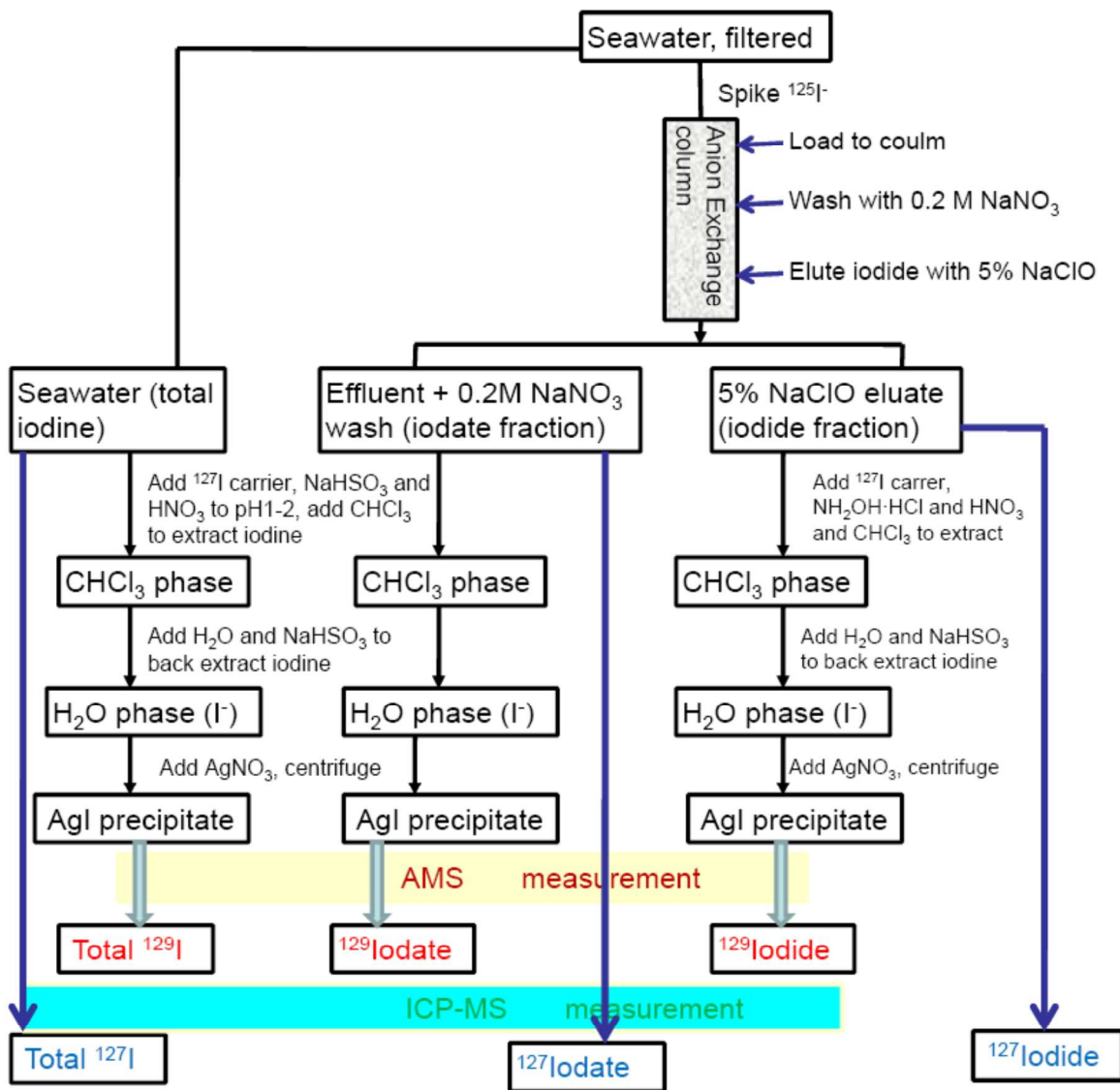


Fig. S-2 Schematic diagram of chemical procedure for speciation analysis of ^{129}I and ^{127}I .

Paper V

Speciation of Radiocesium and Radioiodine in Aerosols from Tsukuba after the Fukushima Nuclear Accident

Sheng Xu,^{*,†} Luyuan Zhang,[‡] Stewart P. H. T. Freeman,[†] Xiaolin Hou,[‡] Yasuyuki Shibata,[§] David Sanderson,[†] Alan Cresswell,[†] Taeko Doi,[§] and Atsushi Tanaka[§]

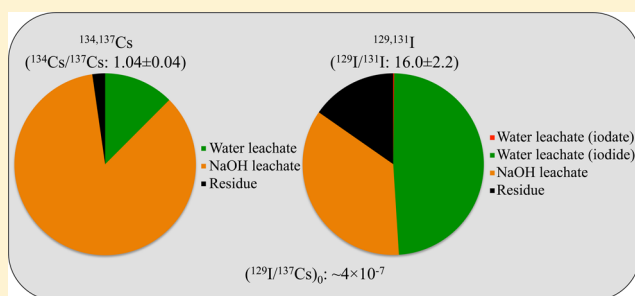
[†]Scottish Universities Environmental Research Center, East Kilbride, G75 0QF, United Kingdom

[‡]Center for Nuclear Technologies, Technical University of Denmark, Risø Campus, 4000 Roskilde, Denmark

[§]NIES-TERRA, National Institute for Environmental Studies, Tsukuba, Ibaraki 305-8506, Japan

S Supporting Information

ABSTRACT: Aerosol samples were collected from Tsukuba, Japan, soon after the 2011 Fukushima nuclear accident and analyzed for speciation of radiocesium and radioiodine to explore their chemical behavior and isotopic ratios after the release. Most ^{134}Cs and ^{137}Cs were bound in organic matter (53–91%) and some in water-soluble fractions (5–15%), whereas a negligible proportion of radiocesium remained in minerals. This pattern suggests that sulfate salts and organic matter may be the main carrier of Cs-bearing particles. The ^{129}I in aerosol samples is contained in various proportions as soluble inorganic iodine (I^- and IO_3^-), soluble organic iodine, and unextractable iodine. The measured mean $^{129}\text{I}/^{131}\text{I}$ atomic ratio of 16.0 ± 2.2 is in good agreement with that measured from rainwater and consistent with ratios measured in surface soil samples. Together with other aerosols and seawater samples, an initial $^{129}\text{I}/^{137}\text{Cs}$ activity ratio of $\sim 4 \times 10^{-7}$ was obtained. In contrast to the effectively constant $^{134}\text{Cs}/^{137}\text{Cs}$ activity ratios (1.04 ± 0.04) and $^{129}\text{I}/^{131}\text{I}$ atomic ratios (16.0 ± 2.2), the $^{129}\text{I}/^{137}\text{Cs}$ activity ratios scattered from 3.5×10^{-7} to 5×10^{-6} and showed temporally and spatially different dispersion and deposition patterns between radiocesium and radioiodine. These findings confirm that ^{129}I , instead of ^{137}Cs , should be considered as a proxy for ^{131}I reconstruction.



INTRODUCTION

After the Fukushima Dai-ichi nuclear power plant (FDNPP) accident on March 11, 2011, a large amount of radioactive substances were released into the atmosphere. The release caused serious radioactive contamination in a large area of eastern Japan. Among the released radionuclides, short-lived radionuclides, such as ^{134}Cs , ^{137}Cs , and ^{131}I are the major concerns. In particular, ^{131}I is regarded as one of the most important radionuclides, because of its high fission yield and high radiation risk to humans, especially to children. When it is taken up through food and inhalation, it mainly concentrates in the thyroid gland resulting in a high radiation risk. As ^{131}I is difficult to detect after several months because of its very short half-life (8.02 days), assessment of radiation risk of ^{131}I is only possible using an initial ratio between ^{131}I and other long-lived radionuclides. Although ^{137}Cs can be potentially considered as a proxy for ^{131}I ,¹ the different chemical properties and behaviors in the environment of the two elements means that ^{137}Cs may not be a suitable proxy.^{2,3} In the Fukushima area, variations of a few orders of magnitude in $^{131}\text{I}/^{137}\text{Cs}$ activity ratios have been measured in the atmospheric samples collected in the early stage of the accident.^{4–6} Thus, accurate reconstruction of ^{131}I most likely relies on calculations based on ^{129}I measurement and an initial $^{129}\text{I}/^{131}\text{I}$ ratio which is currently poorly known.

After the Chernobyl accident in 1986, a number of $^{129}\text{I}/^{131}\text{I}$ ratios were estimated based on the measurements of different environmental samples and theoretical calculations.⁷ Among the wide range of $^{129}\text{I}/^{131}\text{I}$ ratios from 9 to 89, a mean ratio of 13.6 ± 2.8 estimated through analysis of the soil samples from Belarus were considered to be the best estimate.^{1,2,7}

Numerous measurements of the Fukushima-derived radionuclides in the worldwide environments have been recently reported.^{4–6,8,9} However, these studies mainly focused on radiocesium and other gamma-emitting nuclides including ^{131}I . Measurements of the long-lived ^{129}I ($t_{1/2} = 1.57 \times 10^7$ years) are still relatively limited except for a few studies on soil,^{10,11} seawater,^{12–15} and rainwater.¹⁶ $^{129}\text{I}/^{131}\text{I}$ isotopic ratios of 22.3 ± 6.3 and 18.3 were estimated by analyzing ^{131}I and ^{129}I in 109 surface soil samples within 60 km from the FDNPP.^{10,11} A similar ratio of 16 ± 1 was also obtained from the monthly rainwater collected in Fukushima city during March 2011.¹⁶ Although these ratios overlap within the large uncertainty estimates, as compared with studies after the Chernobyl

Received: September 10, 2014

Revised: December 15, 2014

Accepted: December 18, 2014

Published: December 18, 2014

Table 1. Speciation of ^{134}Cs and ^{137}Cs in Aerosols from Tsukuba, Japan^a

sample	speciation	^{134}Cs in the fraction (Bq)	^{134}Cs species fraction (%)	^{137}Cs in the fraction (Bq)	^{137}Cs species fraction (%)	$^{134}\text{Cs}/^{137}\text{Cs}$
no. 1	total aerosol	8.24 ± 0.04		8.03 ± 0.04		1.03 ± 0.07
	water leachate	0.432 ± 0.039	5	0.389 ± 0.030	5	1.11 ± 0.13
	NaOH leachate	7.28 ± 0.37	88	6.90 ± 0.35	86	1.06 ± 0.01
	residue	0.073 ± 0.008	1	0.077 ± 0.004	1	0.95 ± 0.12
no. 2	total aerosol	9.17 ± 0.46		9.19 ± 0.46		1.00 ± 0.07
	water leachate	1.06 ± 0.06	12	0.988 ± 0.055	11	1.08 ± 0.09
	NaOH leachate	5.14 ± 0.26	56	4.91 ± 0.25	53	1.05 ± 0.07
	residue	0.080 ± 0.013	1	0.073 ± 0.005	1	1.10 ± 0.20
no. 3	total aerosol	3.95 ± 0.20		3.83 ± 0.19		1.03 ± 0.07
	water leachate	0.479 ± 0.037	12	0.435 ± 0.029	11	1.10 ± 0.11
	NaOH leachate	3.37 ± 0.17	85	3.49 ± 0.18	91	0.97 ± 0.07
	residue	0.147 ± 0.019	4	0.128 ± 0.009	3	1.15 ± 0.17
no. 4	total aerosol	2.90 ± 0.15		2.67 ± 0.13		1.08 ± 0.08
	water leachate	0.448 ± 0.034	15	0.379 ± 0.026	14	1.18 ± 0.12
	NaOH leachate	1.99 ± 0.10	69	1.81 ± 0.009	68	1.09 ± 0.08
	residue	0.062 ± 0.018	2	0.045 ± 0.005	2	1.37 ± 0.43

^aCorrected to March 11th, 2011 at 14:46.

Table 2. Speciation of ^{127}I and ^{129}I in Aerosols from Tsukuba, Japan

sample	speciation	^{127}I (ng/m ³) ^a	^{129}I (× 10 ⁶ atom/m ³)	^{129}I species fraction (%)	$^{129}\text{I}/^{127}\text{I}$ (× 10 ⁻⁶)
no. 1	IO_3^-	ND	2.04 ± 0.05	0.4	
	I^-	28.4 ± 0.2	231.9 ± 4.9	44.5	1.75 ± 0.04
	NaOH leachate	ND	166.7 ± 4.9	32.0	
	residue	ND	120.1 ± 3.5	23.1	
	sum		520.8 ± 27.6		
no. 2	IO_3^-	ND	0.078 ± 0.002	0.03	
	I^-	14.8 ± 0.1	142.8 ± 3.4	47.4	2.07 ± 0.05
	NaOH leachate	ND	133.4 ± 3.4	44.3	
	residue	ND	24.8 ± 0.6	8.2	
	sum		301.1 ± 15.1		
no. 3	IO_3^-	ND	0.089 ± 0.002	0.04	
	I^-	10.8 ± 0.1	90.1 ± 2.6	42.4	1.78 ± 0.06
	NaOH leachate	ND	67.9 ± 1.7	32.0	
	residue	ND	54.3 ± 1.4	25.5	
	sum		212.4 ± 10.7		
no. 4	IO_3^-	ND	0.61 ± 0.02	0.3	
	I^-	3.70 ± 0.04	142.2 ± 3.8	60.9	8.27 ± 0.24
	NaOH leachate	ND	80.4 ± 2.3	34.4	
	residue	ND	10.4 ± 0.3	4.5	
	sum		233.6 ± 13.3		

^aND, not detectable.

accident, more measurements at Fukushima are required to confidently assess the initial ratios of short and long-lived radionuclides. For this purpose, the atmospheric samples collected in the early stage of the accident are generally considered to be the best estimate.

The chemical species of the radionuclides released into the environment are not well-known.¹⁷ However, understanding the chemical species of radionuclides is essential to evaluating their formation process, behaviors in the environment, and potential health impacts. In practice, such knowledge is helpful in designing effective ways to decontaminate the radioactive materials from the environment and to prevent further resuspension of the contaminated materials. After the Fukushima accident, few studies were focused on the speciation of radiocesium. For instance, the sulfate aerosol ($\sim 0.5 \mu\text{m}$) was considered as a potential transport medium of radiocesium.¹⁸ It was also reported that the spherical Cs-bearing particles are

physically large ($\sim 2 \mu\text{m}$) and chemically water insoluble.¹⁹ However, to our knowledge, similar investigations have not been done for radioiodine-bearing materials, except for one study of inorganic iodine speciation in offshore seawater.¹² In this study, we analyzed speciation of both the radioiodine and radiocesium of aerosol samples collected from Tsukuba, Japan, soon after the Fukushima accident. We aim to update the database of important and poorly known initial $^{129}\text{I}/^{131}\text{I}$ and $^{129}\text{I}/^{137}\text{Cs}$ ratios in addition to well-documented $^{134}\text{Cs}/^{137}\text{Cs}$ ratio, and to provide basic knowledge to understand the environmental behaviors and risks of the radiocesium and radioiodine released from the nuclear accident.

MATERIALS AND METHODS

Aerosol samples were collected on the rooftop of a building at the National Institute for Environmental Studies (NIES) at Tsukuba ($36^\circ 02' 56''\text{N}$, $140^\circ 07' 06''\text{E}$), Japan, located $\sim 170 \text{ km}$

Table 3. Fukushima-Derived Nuclide Isotopic Ratios^a

aerosol	¹²⁹ I (10 ⁸ atom/m ³)	¹³¹ I (10 ⁷ atom/m ³)	¹³⁴ Cs (Bq/m ³)	¹³⁷ Cs (Bq/m ³)	¹²⁹ I/ ¹³¹ I (atomic ratio)	¹³⁴ Cs/ ¹³⁷ Cs (activity ratio)	¹²⁹ I/ ¹³⁷ Cs (10 ⁻⁷ activity ratio)
no. 1	5.21 ± 0.27	3.30 ± 0.01	3.09 ± 0.16	3.01 ± 0.15	15.8 ± 0.8	1.03 ± 0.07	2.42 ± 0.17
no. 2	3.01 ± 0.15	2.18 ± 0.01	0.668 ± 0.034	0.670 ± 0.034	13.8 ± 0.7	1.00 ± 0.07	6.29 ± 0.45
no. 3	2.12 ± 0.11	1.11 ± 0.08	0.540 ± 0.027	0.523 ± 0.026	19.1 ± 1.7	1.03 ± 0.07	5.68 ± 0.41
no. 4	2.34 ± 0.13	1.51 ± 0.01	0.126 ± 0.006	0.116 ± 0.006	15.5 ± 0.9	1.08 ± 0.08	28.1 ± 2.1
mean ± sd.					16.0 ± 2.2	1.04 ± 0.04	10.8 ± 11.8

^aData of ¹³¹I activity were from ref 6. ¹³¹I activity in sample No. 3 was estimated from measured ¹³³I and extrapolated ¹³³I/¹³¹I ratio (see text). All ¹³¹I, ¹³⁴Cs, and ¹³⁷Cs activities were corrected to March 11th, 2011 at 14:46.

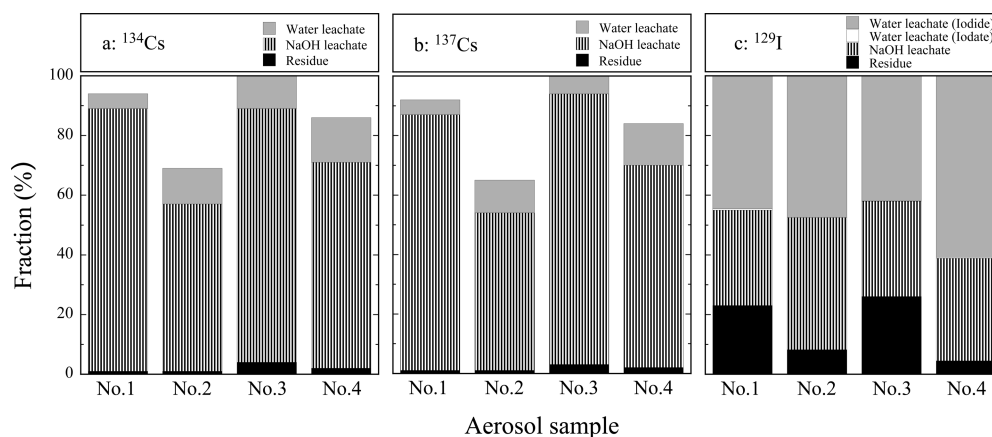


Figure 1. Speciation of radiocesium and radioiodine in aerosol samples from Tsukuba, Japan. Note that the water leachate (iodate) is not visible due to small fractions (see Table 2).

southwest of the FDNPP. The sampling details are listed in Supporting Information (SI) Table S1. Samples used in this study were collected during periods (local time) from 14:39 (March 15th) to 17:34 (March 15th), from 17:48 (March 15th) to 8:48 (March 16th), from 9:08 (March 16th) to 17:08 (March 16th), and from 10:00 (March 22nd) to 11:10 (March 23rd) after the cessation of the reactors at 14:46 of March 11th, 2011. In this study, a small piece (20 × 50 mm²) was cut from the original quartz fiber air filter (203 × 254 mm²).

Detailed experiments including chemical leaching and extraction for cesium and iodine speciations, ^{134,137}Cs detection by gamma-ray spectrometer, ¹²⁷I analysis by inductively coupled plasma-mass spectrometer (ICP-MS), and ¹²⁹I measurement by accelerator mass spectrometry (AMS) are separately described in the SI.

RESULTS AND DISCUSSION

Table 1 lists ¹³⁴Cs and ¹³⁷Cs activities as well as ¹³⁴Cs/¹³⁷Cs activity ratios in both the bulk aerosol samples and different fractions of aerosol samples. Table 2 shows ¹²⁷I and ¹²⁹I concentrations, and ¹²⁹I/¹²⁷I atomic ratios in different species of iodine separated from the aerosol samples. Table 3 summarizes the Fukushima-derived radionuclide ratios.

Fraction of Radiocesium in Aerosols. The measured activity in the aerosol samples for both ¹³⁴Cs and ¹³⁷Cs scattered from 0.1 to 3.0 Bq/m³. In comparison with those measured in the whole filter sample,⁶ the ¹³⁴Cs and ¹³⁷Cs activities in sample No. 1 are 21–22% low, whereas those in the other three samples agree within 5%. This discrepancy in sample No.1 may suggest uneven distribution of the Cs-bearing particles in the filter, which is consistent with the observation by an imaging plate analysis.¹⁹ However, such a discrepancy would not change the ¹³⁴Cs/¹³⁷Cs ratio, because isotopic

fractionation is insignificant. Therefore, the ¹³⁴Cs/¹³⁷Cs activity ratios in the four samples are constant with a small variation between 1.00 and 1.08, with an average of 1.04 ± 0.04. This value is consistent with observations in whole filter and the aerosol samples collected worldwide after the Fukushima accident.^{6,9}

¹³⁴Cs and ¹³⁷Cs have a similar fraction pattern (Figure 1a,b). The NaOH leachate (organic-bounded Cs) consists of 56–88% and 53–91% of the total ¹³⁴Cs and ¹³⁷Cs, respectively, whereas the water leachate contains 5–15% of the total ¹³⁴Cs and 5–14% of the total ¹³⁷Cs. The residue contains only 1–4% of the total ¹³⁴Cs and 1–3% of the total ¹³⁷Cs. It should be noted that the sum of all fractions of radiocesium in samples Nos. 1, 2, and 4 are lower than the radiocesium in total bulk aerosol samples by 6–8%, 31–35%, and 14–16%, respectively (Table 1). The difference in the sample No. 1 and 4 can be attributed to analytical uncertainties, while the significantly lower value of the sum of all fractions of radiocesium compared with that measured for total radiocesium in sample No. 2 is beyond the analytical uncertainty. This may be attributable to a process of NaOH leaching. In sample No. 2, the volume of the first NaOH leachate was significantly lower than that of the other samples due to the evaporation of the leachate at 60 °C for 4 h. Although cesium and iodine in the leachate should not be lost during evaporation, the reduced volume of the leachate in this sample might have caused a deviation of gamma spectrometry measurement of ¹³⁴Cs and ¹³⁷Cs.

The mean ¹³⁴Cs/¹³⁷Cs activity ratios in water-soluble, NaOH leachate, and residue fractions are 1.12 ± 0.04, 1.04 ± 0.05, and 1.14 ± 0.17, respectively. These values are consistent with those of the total aerosols within the analytical uncertainties, confirming no significant isotopic fractionation during

processes of the aerosol formation and transport after the accident.

The percentages of water-soluble $^{134,137}\text{Cs}$ fraction are comparable with those observed on the aerosol samples collected in Vilnius, Lithuania during the 2 weeks after the Chernobyl accident.²⁰ It is also compatible with the qualitative analysis of aerosol samples collected from Tsukuba, which includes large spherical Cs-bearing particles containing Fe and Zn that are water insoluble.¹⁹ By comparing the size distribution of Cs-bearing particles also collected in Tsukuba, it was suggested that the radiocesium is mainly associated with sulfate salts such as ammonium sulfate and ammonium bisulfate.¹⁸ As ammonium sulfate is chemically water-soluble, it can be concluded that the water-soluble $^{134,137}\text{Cs}$ observed in this study might be associated with sulfate. In addition, a coincidence in the size distributions of radiocesium activity and mass of the thermal-organic carbon was also reported.¹⁸ This caused the authors to “withhold a decisive conclusion that sulfate aerosol is the only transport medium of radiocesium until the time-series data for both the radionuclides and the aerosol chemical components, if they exist, are reported”. Our results show that NaOH solution leached 53–91% of total radiocesium, while water-soluble radiocesium only accounted for <15% of total radiocesium. These results clearly suggest that the sulfate salts are only a minor carrier of radiocesium. Instead, the organic substance is considered to be the dominated carrier of radiocesium and to play a key role in the transport and dispersion of radiocesium in the atmosphere. At present, the detailed species of organic substances that were associated with radiocesium, and the mechanism by which the organic-bounded radiocesium species were formed, are not clear. However, the relatively coarse vegetation-related organic particles abundant in the spring season (March) might be responsible for the high load of the organic particles in the atmosphere, which would adsorb small radiocesium particles and form radiocesium associated organic particles.

Speciation of ^{127}I and ^{129}I in Aerosols. The total ^{129}I concentrations in the aerosol samples varied from 2×10^8 to 5×10^8 atoms/m³. These values are more than 2 orders of magnitude higher than those observed in the European atmosphere from 1987 to 2008.²¹ It is also 2 orders of magnitude higher than that observed in Tokaimura (1987–1989), 160 km south of the FDNPP where a spent nuclear fuel reprocessing plant is located.²² The highest value in this study reaches into the upper range of highly contaminated environments of the reprocessing plants at Hanford, U.S.A., during the period of 1986–2003.²³

^{127}I was only detectable in the iodide fraction. The measured ^{127}I concentrations and $^{129}\text{I}/^{127}\text{I}$ atomic ratios varied from 3.7 to 28.4 ng/cm³ and from 1.7×10^{-6} to 8.3×10^{-6} , respectively. The $^{129}\text{I}/^{127}\text{I}$ ratios are 1–2 orders of magnitude higher than those in the European atmosphere.²¹ The $^{129}\text{I}/^{127}\text{I}$ ratios in the atmospheric fallout in Tsukuba from 1986 to 2005 have been reported.²⁴ The observed high $^{129}\text{I}/^{127}\text{I}$ ratios were $2\text{--}23 \times 10^{-8}$ in 1986–1992, while the low $^{129}\text{I}/^{127}\text{I}$ ratios were obtained since 1993 ($0.7\text{--}11 \times 10^{-8}$). In Fukushima, $^{129}\text{I}/^{127}\text{I}$ atomic ratios in surface soil before the accident were reported to be below 3×10^{-8} .¹⁰ Compared to these values, the $^{129}\text{I}/^{127}\text{I}$ ratio in aerosol from Tsukuba in March 2011 is 1–2 orders of magnitude higher than the baseline level for this region. Stable ^{127}I in the aerosols originate from releases from both sea and land. The ^{127}I on land was accumulated by deposition from both the atmosphere and natural weathering of the rocks;

however, deposition from the atmosphere is considered as the major source to land proximal to the sea. Although ^{127}I could have been produced in the nuclear reactor and released with ^{129}I , ^{131}I , and other radioiodine during the Fukushima accident, the total amount of ^{127}I in the aerosol samples originating from the reactor is considered negligible compared to the ^{127}I that originated from natural processes. It has been estimated that about 0.68 kg ^{129}I was released to the atmosphere during the Fukushima accident,¹² which is much higher than the other source in the region. Therefore, the high $^{129}\text{I}/^{127}\text{I}$ ratios observed in aerosols is attributed to the significant releases of ^{129}I during the accident.

Among the ^{129}I species (Table 2 and Figure 1c), water-soluble iodide (I^-) and NaOH leachable iodine account for 42–61% and 32–44%, respectively. Water-soluble iodate (IO_3^-) corresponds to only less than 0.5% of the total ^{129}I in the aerosols, whereas the residue fraction contains 4–23% of the total ^{129}I . The NaOH leachable iodine is normally responsible for organic associated iodine, because the organic matter in the aerosol, soil, and sediment is easily dissolved in alkaline solution. The iodine in the residue might account for those associated with oxides and/or minerals.²⁵ This distribution pattern with ^{129}I enriched in iodide and depleted in iodate form is similar to that observed in four aerosol samples collected soon after the Chernobyl accident at Oak Ridge, Tennessee.²⁶ It is also similar to those reported for natural ^{127}I in the aerosol.²⁷ However, this pattern differs from that reported for natural ^{127}I in marine aerosols enriched in iodate.²⁸ Such a discrepancy suggests different formation process for the Fukushima-derived ^{129}I compared to the natural ^{127}I . The large fraction of inorganic ^{129}I -iodide in Tsukuba aerosols might be attributed to a major form of ^{129}I as $^{129}\text{I}_2$ released from the damaged nuclear reactor during the Fukushima accident. This also agrees with the finding in the seawater samples from offshore Fukushima, where most of ^{129}I in the seawater is in the form of iodide, while most of the ^{127}I is in iodate form.¹² However, the large fraction of ^{129}I in the NaOH leachate fraction (organic-bounded) might be attributed to the $^{129}\text{I}_2$ released from the damaged reactors, which has a high reactivity with the vegetation-related organic particles as mentioned above, and consequently I_2 is converted to organic associated iodine in the atmosphere. A higher organic associated ^{127}I in aerosol samples has also been reported previously.^{29,30}

$^{129}\text{I}/^{131}\text{I}$ Ratio of Fukushima-Derived Radioiodine. The $^{129}\text{I}/^{131}\text{I}$ atomic ratios were calculated based on the particulate ^{131}I radioactivity concentration measured in ref 6 and ^{129}I concentration measured in this work from the same sample. It was found that the $^{129}\text{I}/^{131}\text{I}$ atomic ratios vary from 5 to 16 (decay-corrected to March 11th, 2011), and the lowest $^{129}\text{I}/^{131}\text{I}$ atomic ratio of 5 was observed in the sample No. 3. Figure 2 shows temporal variations of the selected Fukushima-derived radionuclides (radiocesium and radioiodine) in the Tsukuba air samples of gaseous and particulate forms.⁶ It is evident that all radionuclides except for the particulate ^{131}I have a similar pattern after the first radioactive plume on March 15. This pattern is consistent with those observed at Oarai and Inage, 120 km and 220 km south of the FDNPP, respectively.^{4,5} In Figure 4 in ref 6, with the exception of two outliers, temporal variation of the $^{133}\text{I}/^{131}\text{I}$ ratios in Tsukuba and Inage coincides with a curve that is consistent with a decay constant ($\lambda_{133}\text{--}\lambda_{131}$). The sample No. 3 in this study, which is one of the two outliers, has a significantly lower $^{133}\text{I}/^{131}\text{I}$ ratio than the corresponding

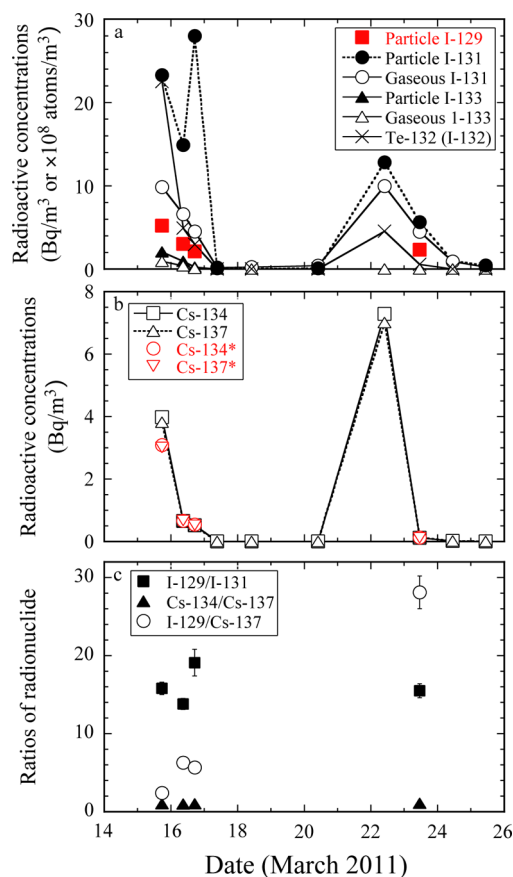


Figure 2. Temporal variation of selected Fukushima-derived radionuclides in aerosol samples from Tsukuba, Japan. Data of the particulate ^{129}I in (a) and $^{134,137}\text{Cs}^*$ in (b) are from this study and those of the other radionuclides from ref 6. Note that unit of radioactive concentrations for ^{129}I is atoms/ m^3 , while that for the other nuclides is Bq/m^3 . The $^{129}\text{I}/^{131}\text{I}$ in (c) is atomic ratio, while the others are activity ratios.

value on the decay curve, indicating that the ^{131}I activity reported in the sample No. 3 might be anomalous. Particulate ^{135}I and ^{129}I , and gaseous ^{131}I and ^{133}I all show a simple decrease, and other radionuclides such as ^{132}Te and $^{134,137}\text{Cs}$ are also similar. Therefore, even though it may be theoretically possible for a high ^{131}I value due to resuspension of the deposited material, the long-lived ^{129}I data do not support this. Therefore, taking the initial particulate ^{133}I activity ($15.5 \pm 0.3 \text{ Bq}/\text{m}^3$ on March 11th calculated from decay correction of the measured $0.256 \pm 0.005 \text{ Bq}/\text{m}^3$ on March 16th) and the extrapolated initial $^{133}\text{I}/^{131}\text{I}$ ratio (1.4 ± 0.1),⁶ the initial ^{131}I activity in sample No. 3 can be estimated to be $11.1 \pm 0.8 \text{ Bq}/\text{m}^3$, which is nearly 4-fold lower than the reported value. On the basis of this data, the $^{129}\text{I}/^{131}\text{I}$ atomic ratio in sample No. 3 can be recalculated to be 19.1 ± 1.7 (Table 3), which overlaps with the other samples within the uncertainties. Therefore, all aerosol samples in this study result in an average $^{129}\text{I}/^{131}\text{I}$ ratio of 16.0 ± 2.2 for the Fukushima-derived radioiodine, which shows an effectively constant value from March 15th to 23rd, 2011.

In the Fukushima area, a $^{129}\text{I}/^{131}\text{I}$ atomic ratio of 22.3 ± 6.3 (decay-corrected to March 11, 2011) has been estimated from 27 surface soil samples collected around the FDNPP in April 2011.¹⁰ The best fitting of ^{131}I and ^{129}I data measured from 82 surface soil samples collected in June 2011 resulted in a slope of

18.3 ($R^2 = 0.85$), which gives the $^{129}\text{I}/^{131}\text{I}$ atomic ratio (decay-corrected on March 11, 2011).¹¹ In addition, a $^{129}\text{I}/^{131}\text{I}$ atomic ratio of 16 ± 1 was also obtained from a monthly rainwater sample collected in Fukushima city in March 2011.¹⁶ In comparison with these values, the estimated $^{129}\text{I}/^{131}\text{I}$ ratio from four aerosol samples in this study is in good agreement with that from rainwater and also consistent with that from soil samples within the analytical uncertainty. The reliability of the effectively constant $^{129}\text{I}/^{131}\text{I}$ ratio obtained from this study is also supported by previous findings from other elements of Fukushima-derived radionuclides that also have an almost constant isotopic ratio (i.e., $^{133}\text{I}/^{131}\text{I}$, $^{134}\text{Cs}/^{137}\text{Cs}$, $^{136}\text{Cs}/^{137}\text{Cs}$ and $^{129\text{m}}\text{Te}/^{132}\text{Te}$).^{6,9}

$^{129}\text{I}/^{131}\text{I}$ ratios scattered largely among different environmental samples collected shortly after the Chernobyl accident.^{1,2,7,31} One $^{129}\text{I}/^{131}\text{I}$ ratio was reported to be 9 ± 4 for aerosols collected in Israel in May 5–18, 1986.³¹ The rainwater samples showed $^{129}\text{I}/^{131}\text{I}$ ratios from 19 ± 5 in Munich (May 5, 1986) to 35 ± 9 in Israel (May 3–4, 1986). The $^{129}\text{I}/^{131}\text{I}$ ratios in soil samples largely scattered from 10 to 89.⁷ A mean ratio of 13.6 ± 2.8 were considered to be the best estimate of the Chernobyl-derived radioiodine.⁷ Thus, it can be seen that the Fukushima-derived $^{129}\text{I}/^{131}\text{I}$ ratio is comparable with the Chernobyl-derived value.

Four reactors at FDNPP were damaged in succession due to hydrogen explosions, core damage, and a major leak on the 13th of March (15:36), 14th of March (11:01), 14th of March (~20:00) and 15th of March (6:14). The emission rates of radionuclides certainly varied during different events. Thus, it has been pointed out that the variation of $^{129}\text{I}/^{131}\text{I}$ ratios measured in rainwater and soil samples may suggest the radioiodine was released from multiple reactors with different $^{129}\text{I}/^{131}\text{I}$ ratios due to different operating histories.¹⁶ However, our effectively constant $^{129}\text{I}/^{131}\text{I}$ ratio does not show any temporal variation from March 15 to 23, which implies the similar or indistinguishable $^{129}\text{I}/^{131}\text{I}$ ratio in the radioactive substances released from the multiple reactors during the FDNPP accident. In general, it is necessary to consider the contribution of background ^{129}I , including preaccident ^{129}I released from worldwide nuclear weapon tests and the spent fuel reprocessing plants, if the radioiodine deposition is not high. However, as the measured $^{129}\text{I}/^{127}\text{I}$ ratios in the 4 aerosol samples are 1–2 orders of magnitude higher than the background value reported in the environmental samples in Japan before the Fukushima accident, the contribution of background ^{129}I to the estimated $^{129}\text{I}/^{131}\text{I}$ is negligible. Large corrections for decay of ^{131}I during the long time spans of the emission and low ^{131}I signal due to its rapid decay might also contribute some uncertainties. Therefore, more analyses of the time series of materials collected soon after each accident event is needed to clarify detailed variation of the $^{129}\text{I}/^{131}\text{I}$ ratio related to their specific sources (e.g., different damaged reactors).

Initial $^{129}\text{I}/^{137}\text{Cs}$ Ratio and Fractionation between Cesium and Iodine. It is likely that the $^{129}\text{I}/^{137}\text{Cs}$ ratio in a reactor should be a constant value, because the ^{129}I and ^{137}Cs are both fission products with a fixed fission yield. In general, the $^{129}\text{I}/^{137}\text{Cs}$ activity ratio in the released radioactive substance reflects the operation history of the damaged reactors and the chemical forms of the released radiocesium and radioiodine. This ratio would remain constant if there is no significant elemental fractionation between iodine and cesium during their formation, migration, deposition, etc. An initial $^{129}\text{I}/^{137}\text{Cs}$

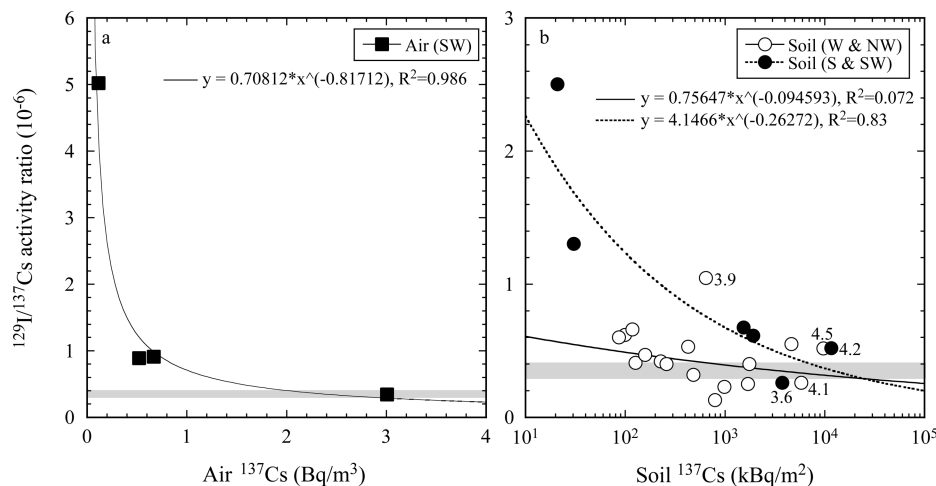


Figure 3. Relationship between $^{129}\text{I}/^{137}\text{Cs}$ activity ratio and ^{137}Cs activity concentration in aerosol samples from Tsukuba in this study and surface soils within 60 km from the FDNPP in ref 10 and 32. The aerosol ^{129}I used in the calculation of the $^{129}\text{I}/^{137}\text{Cs}$ activity ratio are sum of the particulate and gaseous ^{129}I which was estimated from the measured particulate ^{129}I in this study and its percentage in the total ^{131}I from ref 6. Numbers beside the data points denote the distance (km) from the FDNPP.

activity ratio of 2.75×10^{-7} has been reported for the fourth block of Chernobyl NPP at the time of that accident.¹ Although the $^{129}\text{I}/^{137}\text{Cs}$ activity ratios in soils with high fallout radiocesium differed little from the Chernobyl source value, the $^{129}\text{I}/^{137}\text{Cs}$ activity ratios in soils with lower radiocesium from distances further from the damaged reactor were significantly higher than the source value.¹ This pattern can be explained if the I/Cs ratio might have changed with the dispersion of the plume, because $^{134,137}\text{Cs}$ is mainly in particle associated form, whereas $^{129,131}\text{I}$ can be in both aerosol and gaseous form. Even in the aerosols, the attached iodine might be converted to gaseous form and be lost, and some gaseous radioiodine might be attached to aerosols later. A similar distribution pattern can be observed after the Fukushima accident: that is, higher $^{131}\text{I}/^{137}\text{Cs}$ ratios in sites further away have been reported compared to those in the site closer to the Fukushima reactor.⁹ For example, a systematic review of the available air and soil monitoring data both in the highly contaminated areas of Japan and worldwide shows that the mean $^{131}\text{I}/^{137}\text{Cs}$ activity ratio is 22.7 ± 3.7 ($n = 1844$) and 31.8 ± 12.9 ($n = 90$) in soil and air, respectively, within 80 km from FDNPP. The air samples showed $^{131}\text{I}/^{137}\text{Cs}$ ratios of 70.9 ± 63.5 ($n = 234$), 69.5 ± 26.9 ($n = 457$) and 77.1 ± 16.6 ($n = 196$) at distances of 80–2000 km (Japan), 2000–12 000 km (Pacific Ocean) and >12 000 km (Europe), respectively.⁹ Even at the short distance scale, an inhomogeneous spatial distribution has been observed in surface soils within a distance of <60 km from the FDNPP.³² The $^{131}\text{I}/^{137}\text{Cs}$ ratios show three distinctive patterns. The first group locating in the south, and to some extent southwest, of the FDNPP is characterized with an increasing pattern of the activity ratio with increasing distance from the NPPs. The second group includes the locations close to the NPPs in the northwest direction, where the contaminated soils are relatively rich in ^{131}I . The third group is from areas northwest to southwest of FDNPP and exhibits nearly constant $^{131}\text{I}/^{137}\text{Cs}$ ratio regardless of the distance from the NPPs.

Indeed, unlike the effectively constant $^{134}\text{Cs}/^{137}\text{Cs}$ and $^{129}\text{I}/^{131}\text{I}$ ratios observed in the environmental samples contaminated by the Fukushima accident, the particulate $^{129}\text{I}/^{137}\text{Cs}$ activity ratios in the aerosol from Tsukuba scattered

largely from 2.4×10^{-7} to 2.8×10^{-6} with a mean value 1.1×10^{-6} and standard deviation 1.2×10^{-6} (Table 3), suggesting significant elemental fractionation between cesium and iodine and/or source differences. Taking into account the fraction of gaseous ^{131}I ,⁶ the total (particulate and gaseous) $^{129}\text{I}/^{137}\text{Cs}$ activity ratios were estimated to be from 3.5×10^{-7} to 5.0×10^{-6} (Figure 3). This range is similar to the wide variation of $^{131}\text{I}/^{137}\text{Cs}$ (8–1000), $^{132}\text{Te}/^{137}\text{Cs}$ (4–65), and $^{99}\text{Mo}/^{137}\text{Cs}$ (0.14–12.3) in the Tsukuba atmospheric samples.⁶ The large variations of the isotopic ratios of different elements was also observed worldwide.⁹ Therefore, the largely variable $^{129}\text{I}/^{137}\text{Cs}$ ratios in the Tsukuba atmosphere can be generally attributed to elemental fractionation during the transport from the sources with a fixed initial $^{129}\text{I}/^{137}\text{Cs}$ ratio. The measured $^{129}\text{I}/^{137}\text{Cs}$ activity ratio in the aerosol in Tsukuba on the 15th of March (the first radioactive plume) is 3.5×10^{-7} . Within the analytical uncertainties, this value is consistent with the $^{129}\text{I}/^{137}\text{Cs}$ activity ratio of 4.4×10^{-7} for the effluent from Fukushima derived from seawater.¹⁴ In fact, the atmospheric $^{131}\text{I}/^{137}\text{Cs}$ activity ratios varied much wider compared with the limited data set of $^{129}\text{I}/^{137}\text{Cs}$. For instance, the range of $^{131}\text{I}/^{137}\text{Cs}$ activity ratios from Oarai, Tsukuba, and Inage are 0.2–100, 8–1000, and 10–500, respectively.^{4–6} The $^{131}\text{I}/^{137}\text{Cs}$ ratio is apparently negatively correlated with ^{137}Cs activity concentration in each locality. Although each location has slightly different $^{131}\text{I}/^{137}\text{Cs}$ ratio distribution patterns, the lowest $^{131}\text{I}/^{137}\text{Cs}$ ratios are from 8 to 15 (mean 11 ± 2) for the peak releases (March 15/16 and 22/23) with a radiocesium radioactivity concentration of >3 Bq/m³. Taking into account the $^{129}\text{I}/^{131}\text{I}$ atomic ratio of 16.0 ± 2.2 discussed above, the mean atmospheric $^{129}\text{I}/^{137}\text{Cs}$ activity ratio of the early stage of the accident observed in Oarai, Tsukuba, and Inage would be $(2.6 \pm 0.5) \times 10^{-7}$. Therefore, based on these data sets, the initial Fukushima-derived $^{129}\text{I}/^{137}\text{Cs}$ activity ratio can be considered to be around 4×10^{-7} .

Figure 3 shows the $^{129}\text{I}/^{137}\text{Cs}$ activity ratio and ^{137}Cs activity concentration in the Tsukuba atmosphere from this study and available surface soil samples within 60 km of the FDNPP.^{10,32} Overall, an inverse correlation between the $^{129}\text{I}/^{137}\text{Cs}$ activity ratio and ^{137}Cs activity concentration can be found for both the aerosol and soil samples. In particular, there is a highly

significant negative correlation between the $^{129}\text{I}/^{137}\text{Cs}$ ratio and ^{137}Cs activity concentration in the limited aerosol samples.

Like the large variation of $^{129}\text{I}/^{137}\text{Cs}$ activity ratios in air, the soil samples have $^{129}\text{I}/^{137}\text{Cs}$ activity ratios of $0.2\text{--}3 \times 10^{-6}$.^{10,32} It has been found that the radiocesium activity concentrations in the west, northwest, and north of the FDNPP are significantly higher than those to the south of the FDNPP, whereas the radioiodine shows an opposite distribution.^{9,33} This resulted in a different spatial distribution of $^{129}\text{I}/^{137}\text{Cs}$ activity ratios in soil samples. As shown in Figure 3, the $^{129}\text{I}/^{137}\text{Cs}$ activity ratio in the south and southwest of the FDNPP apparently has a negative correlation with the ^{137}Cs radioactivity concentration. The $^{129}\text{I}/^{137}\text{Cs}$ activity ratios scattered from 3×10^{-7} to 2.5×10^{-6} , apparently showing a distance dependence. In comparison with the soil samples from the southern and southwestern direction, no clear correlation can be found for the soil samples from the west and northwest of the FDNPP. The mean $^{129}\text{I}/^{137}\text{Cs}$ activity ratio is $4.6 \pm 2.1 \times 10^{-7}$. Although the $^{129}\text{I}/^{137}\text{Cs}$ activity ratios in soil samples show a geographic distribution at a short distance scale, the samples closest to the FDNPP (<5 km) have $^{129}\text{I}/^{137}\text{Cs}$ activity ratios of $3\text{--}10 \times 10^{-7}$ with a mean $^{129}\text{I}/^{137}\text{Cs}$ activity ratio of $(5.2 \pm 3.2) \times 10^{-7}$.^{10,32} It can be seen that this value is consistent with the initial $^{129}\text{I}/^{137}\text{Cs}$ activity ratio deduced from the first radioactive plume on March 15/16 and from seawater. This coincidence likely reflects the fact that the radioactive deposition in the surface soil with low $^{129}\text{I}/^{137}\text{Cs}$ activity ratio was from the peak release on March 15/16. Rainfall observed in Fukushima Prefecture and adjacent areas from the evening of March 15 to early morning of March 16 coincides with the deposition of wet and dry deposition of the first peak release. The relatively uniform $^{129}\text{I}/^{137}\text{Cs}$ activity ratios to the west and northwest of the FDNPP suggest negligible elemental fractionation, while the higher and variable $^{129}\text{I}/^{137}\text{Cs}$ activity ratios observed in the south and southwest of the FDNPP are most likely caused by the elemental fractionation during the migration and deposition of the radioactive plume.

Therefore, the wide variation of $^{129}\text{I}/^{137}\text{Cs}$ and $^{131}\text{I}/^{137}\text{Cs}$ activity ratios in the air and soil near the FDNPP suggests significant fractionation can occur between radiocesium and radioiodine at some sites, although negligible fractionation was observed in soils distributed in the west and northwest of the FDNPP. Sites with significant fractionation between iodine and cesium could cause highly inaccurate reconstruction of ^{131}I if ^{137}Cs were used as a proxy at Fukushima. Instead, this study demonstrates that the $^{129}\text{I}/^{131}\text{I}$ ratios observed in the aerosol samples collected from the early stage of the Fukushima accident are relatively constant, which implies that ^{129}I is a potentially more robust proxy for accurate reconstructions of ^{131}I .¹¹ Further work is needed to add observations covering the early periods of the accident, if suitable air filters are available. Also, further work is needed to verify the biodynamics of ^{129}I over the first year of postdepositional behavior, and to identify spatially variable samples that can be used to reconstruct the ^{131}I depositional history.

■ ASSOCIATED CONTENT

Supporting Information

Text describes detailed experimental procedures. One table summarizes detailed information on materials. This material is available free of charge via the Internet at <http://pubs.acs.org>.

■ AUTHOR INFORMATION

Corresponding Author

*E-mail: s.xu@suerc.gla.ac.uk.

Notes

The authors declare no competing financial interest.

■ ACKNOWLEDGMENTS

We thank A. Dougass and P. Gallacher of SUERC for laboratory assistance during AMS measurements.

■ REFERENCES

- (1) Mironov, V.; Kudrjashov, V.; Yiou, F.; Raisbeck, G. M. Use of ^{129}I and ^{137}Cs in soils for the estimation of ^{131}I deposition in Belarus as a result of the Chernobyl accident. *J. Environ. Radioact.* **2002**, *59*, 293–307.
- (2) Straume, T.; Marchetti, A. A.; Anspaugh, L. R.; Kthrough, V. T.; Gavrilin, Y. I.; Shinkarev, S. M.; Drozdovitch, V. V.; Ulanovsky, A. V.; Korneev, S. V.; Brekeshew, M. K.; Leonov, E. S.; Voight, G.; Panchenko, S. V.; Minenko, V. M. The feasibility of using ^{129}I to reconstruct ^{131}I deposition from the Chernobyl reactor accident. *Health Phys.* **1996**, *71*, 733–740.
- (3) Hou, X. L.; Fogh, C. L.; Kucera, J.; Andersson, K. G.; Dahlgard, H.; Nielsen, S. P. Iodine-129 and caesium-137 in Chernobyl contaminated soil and their chemical fractionation. *Sci. Total Environ.* **2003**, *308*, 97–109.
- (4) Furuta, S.; Sumiya, S.; Watanabe, H.; Nakano, M.; Imaizumi, K.; Takeyasu, M.; et al. Results of the environmental radiation monitoring following the accident at the Fukushima Daiichi nuclear power plant—Interim report (ambient radiation dose rate, radioactivity concentration in the air and radioactivity concentration in the fallout). *JAEA-Rev.* **2011**, *1–84*, 2011–035.
- (5) Amano, H.; Akiyama, M.; Chunlei, B.; Kawamura, T.; Kishimoto, T.; Kuroda, T.; Muroi, T.; Odaira, T.; Ohta, Y.; Takeda, K.; Watanabe, Y.; Morimoto, T. Radiation measurements in the Chiba Metropolitan area and radiological aspects of fallout from the Fukushima Dai-ichi Nuclear Power Plants accident. *J. Environ. Radioact.* **2012**, *111*, 42–52.
- (6) Doi, T.; Matsumoto, K.; Toyoda, A.; Tanaka, A.; Shibata, Y.; Hirose, K. Anthropogenic radionuclides in the atmosphere observed at Tsukuba: characteristics of the radionuclides derived from Fukushima. *J. Environ. Radioact.* **2013**, *122*, 55–62.
- (7) Michel, R.; Handl, J.; Ernst, T.; Botsch, W.; Szidat, S.; Schmidt, A.; Jakob, D.; Beltz, D.; Romantschuk, L. D.; Synal, H.-A.; Schnabel, C.; Lépez-Gutiérrez, J. M. Iodine-129 soils from Northern Ukraine and the retrospective dosimetry of the iodine-131 exposure after the Chernobyl accident. *Sci. Total Environ.* **2005**, *340*, 35–55.
- (8) Masson, O.; Baeza, A.; Bieringer, J.; Brudecki, K.; Bucci, S.; Cappai, M.; Carvalho, F. P.; Connan, O.; Cosma, C.; Dalheimer, A.; Didier, D.; Depuydt, G.; De Geer, L. E.; De Vismes, A.; Gini, L.; Groppi, F.; Gudnason, K.; Gurriaran, R.; Hainz, D.; Halldorsson, O.; Hammond, D.; Hanley, O.; Holey, K.; Homoki, Zs.; Ioannidou, A.; Isajenko, K.; Jankovick, M.; Katzlberger, C.; Kettunen, M.; Kierepko, R.; Kontro, R.; Kwakman, P. J. M.; Lecomte, M.; Leon Vintro, L.; Leppänen, A. P.; Lind, B.; Lujaneni, G.; Mc Ginnity, P.; Mc Mahon, C.; Mala, H.; Manenti, S.; Manolopoulos, M.; Mattila, A.; Mauring, A.; Mietelski, J. W.; Möller, B. S.; Nielsen, P.; Nikolick, J.; Overwater, R. M. W.; Palsson, S. E.; Papastefanou, C.; Penev, I.; Pham, M. K.; Povinec, P. P.; Rameback, H.; Reis, M. C.; Ringer, W.; Rodriguez, A.; Rulík, P.; Saey, P. R. J.; Samsonov, V.; Schlosser, C.; Sgorbati, G.; Silobritiene, B. V.; Söderström, C.; Sogni, R.; Solier, L.; Sonck, M.; Steinhäuser, G.; Steinkopff, T.; Steinmann, P.; Stoulos, S.; Sykora, I.; Todorovic, D.; Tooloutalaie, N.; Tositti, L.; Tschiersch, J.; Ugroun, A.; Vagena, E.; Vargas, A.; Wershofen, H.; Zhukova, O. Tracking of airborne radionuclides from the damaged Fukushima Dai-Ichi nuclear reactors by European networks. *Environ. Sci. Technol.* **2011**, *45*, 7670–7677.

- (9) Chaisan, K.; Smith, J. T.; Bossew, P.; Kirchner, G.; Laptev, G. V. Worldwide isotope ratios of the Fukushima release and early-phase external dose reconstruction. *Sci. Rep.* **2013**, *3*, 2520.
- (10) Miyake, Y.; Matsuzaki, H.; Fujiwar, T.; Saito, T.; Yamagata, T.; Honda, M.; Muramatsu, Y. Isotopic ratio of radioactive iodine ($^{129}\text{I}/^{131}\text{I}$) released from Fukushima Daiichi NPP accident. *Geochem. J.* **2012**, *46*, 327–333.
- (11) Muramatsu, Y.; Matsuzaki, H.; Toyama, C.; Ohno, T. Analysis of ^{129}I in the soils of Fukushima Prefecture: preliminary reconstruction of ^{131}I deposition related to the accident at Fukushima Daiichi Nuclear Power Plant (FDNPP). *J. Environ. Radioact.* **2014**, DOI: 10.1016/j.jenvrad.2014.05.007.
- (12) Hou, X. L.; Povinec, P. P.; Zhang, L. Y.; Shi, K. L.; Biddulph, D.; Chang, C. C.; Fan, Y. K.; Golser, R.; Hou, Y. K.; Jeskovec, M.; Jull, A. J. T.; Liu, Q.; Luo, M. Y.; Steier, P.; Zhou, W. J. Iodine-129 in seawater offshore Fukushima: Distribution, inorganic speciation, sources, and budget. *Environ. Sci. Technol.* **2013**, *47*, 3091–3098.
- (13) Suzuki, T.; Otsuka, S.; Kuwabara, J.; Kawamura, H.; Tobayashi, T. Iodine-129 concentration in seawater near Fukushima before and after the accident at the Fukushima Daiichi nuclear power plant. *Biogeosciences Discuss.* **2013**, *10*, 1401–1419.
- (14) Tumey, S. J.; Guilderson, T. P.; Brown, T. A.; Broek, T.; Buesseler, K. O. Input of ^{129}I into the western Pacific ocean resulting from the Fukushima nuclear event. *J. Radioanal. Nucl. Chem.* **2013**, *296*, 957–962.
- (15) Guilderson, T. P.; Tumey, S. J.; Brown, T. A.; Buesseler, K. O. The 129-Iodine content of subtropical Pacific waters: impact of Fukushima and other anthropogenic ^{129}I sources. *Biogeosci. Discuss.* **2013**, *10*, 19935–19968.
- (16) Xu, S.; Freeman, S. P. H. T.; Hou, X. L.; Watanabe, A.; Yamaguchi, K.; Zhang, L. Y. Iodine isotopes in precipitation: temporal responses to ^{129}I emissions from the Fukushima nuclear accident. *Environ. Sci. Technol.* **2013**, *47*, 10851–10859.
- (17) Burns, P. C.; Ewing, R. C.; Navrotsky, A. Nuclear fuel in a reactor accident. *Science* **2012**, *335*, 1184–1188.
- (18) Kaneyasu, N.; Ohashi, H.; Suzuki, F.; Okuda, T.; Ikemori, F. Sulfate aerosol as a potential transport medium of radiocesium from the Fukushima nuclear accident. *Environ. Sci. Technol.* **2012**, *46*, 5720–5726.
- (19) Adachi, K.; Kajino, M.; Zaizen, Y.; Igarashi, Y. Emission of spherical cesium-bearing particles from an early stage of the Fukushima nuclear accident. *Sci. Rep.* **2013**, *3*, 2554.
- (20) Lujanienė, G.; Lujanas, V.; Jankunaite, D.; Ogorodnikov, B. I.; Mastauskas, A.; Ladygiene, R. Speciation of radionuclides of the Chernobyl origin in aerosol and soil samples. *Czech. J. Phys.* **1999**, *49*, 107–114.
- (21) Jabbar, T.; Wallner, G.; Steier, P. A review on ^{129}I analysis in air. *J. Environ. Radioact.* **2013**, *126*, 45–54.
- (22) Tsukada, H.; Ishida, J.; Narita, O. Particle size distribution of atmospheric ^{129}I and ^{127}I aerosols. *Atmos. Environ.* **1991**, *25A*, 905–908.
- (23) Fritz, B. G.; Paton, G. W. Monitoring iodine-129 in air and milk samples collected near the Hanford Site: an investigation of historical iodine monitoring data. *J. Environ. Radioact.* **2006**, *86*, 64–77.
- (24) Toyama, C.; Muramatsu, Y.; Igarashi, Y.; Aoyama, M.; Matsuzaki, H. Atmospheric fallout of ^{129}I in Japan before the Fukushima accident: regional and global contributions (1963–2005). *Environ. Sci. Technol.* **2013**, *47*, 8383–8390.
- (25) Englund, E.; Aldahan, A.; Hou, X. L.; Petersen, R.; Possnert, G. Speciation of iodine (^{127}I and ^{129}I) in lake sediments. *Nucl. Instrum. Methods Phys. Res. Sect. B* **2010**, *268*, 1102–1105.
- (26) Bondiotti, E. A.; Brantley, J. N. Characteristics of Chernobyl radioactivity in Tennessee. *Nature* **1986**, *322*, 313–314.
- (27) Baker, A. R. Inorganic iodine speciation in tropical Atlantic aerosol. *Geophys. Res. Lett.* **2004**, *31*, L23S02 DOI: 10.1029/2004GL020144.
- (28) Xu, S. Q.; Xie, Z. Q.; Li, B.; Liu, W.; Sun, L. G.; Kang, H.; Yang, H. X.; Zhang, P. E. Iodine speciation in marine aerosols along a 15 000-km round-trip cruise path from Shanghai, China, to the Arctic Ocean. *Environ. Chem.* **2010**, *7*, 406–412.
- (29) Baker, A. R. Marine aerosol iodine chemistry: the importance of soluble organic iodine. *Environ. Chem.* **2005**, *2*, 295–198.
- (30) Lai, S. C.; Hoffmann, T.; Xie, Z. Q. Iodine speciation in marine aerosols along a 30,000 km round-trip cruise path from Shanghai, China to Prydz Bay, Antarctica. *Geophys. Res. Lett.* **2008**, *35*, L21803 DOI: 10.1029/2008GL035492.
- (31) Paul, M.; Fink, D.; Hollos, G.; Kaufman, A.; Kutschera, W.; Magaritz, M. Measurement of ^{129}I concentration in the environment after the Chernobyl reactor accident. *Nucl. Instrum. Methods Phys. Res. Sect. B* **1987**, *29*, 341–345.
- (32) Fujiwara, T.; Saito, T.; Muroya, Y.; Yamashita, Y.; Nagasaki, S.; Katsumura, Y.; Tanaka, S.; Uesaka, M. Isotopic ratio and vertical distribution of radionuclides in soil affected by the accident of Fukushima Daiichi nuclear power plants. *J. Environ. Radioact.* **2012**, *113*, 37–44.
- (33) Saito, K.; Tanihata, I.; Fujiwara, M.; Saito, T.; Shimoura, S.; Otsuka, T.; Onda, Y.; Hoshi, M.; Ikeuchi, Y.; Takahashi, F.; Kinouchi, N.; Saegusa, J.; Seki, A.; Takemiya, H.; Shibata, T. Detailed deposition density maps constructed by large-scale soil sampling Nuclear Power Plant accident. *J. Environ. Radioact.* **2014**, DOI: 10.1016/j.jenvrad.2014.02.014.

1
2
3
4
5

Supporting Information

The Supporting Information consists of 6 pages and 1 table

6 **Radiocesium and radioiodine speciation in aerosols from Tsukuba**
7 **after the Fukushima nuclear accident**

8
9
10 Sheng Xu^{1,*}, Luyuan Zhang², Stewart P.H.T. Freeman¹, Xiaolin Hou²,
11 Yasuyuki Shibata³, David Sanderson¹, Alan Cresswell¹, Taeko Doi³ and Atsushi Tanaka³

12
13
14
15 ¹Scottish Universities Environmental Research Center
16 East Kilbride, G75 0QF, UK

17
18 ²Center for Nuclear Technologies, Technical University of Denmark
19 Risø Campus, 4000 Roskilde, Denmark

20
21 ³NIES-TERRA, National Institute for Environmental Studies
22 Tsukuba, Ibaraki 305-8506, Japan

23
24
25 *Corresponding author: s.xu@suerc.gla.ac.uk
26
27

28 S1. Materials and Experiments

29 The aerosol samples were collected on the rooftop of a building at the National Institute for
30 Environmental Studies (NIES) at Tsukuba (36°02'56"N, 140°07'06"E), located about 170 km
31 southwest of the FDNPP. Detailed sampling methods were described previously.¹ In this
32 study, a small piece (20 × 50 mm) of the quartz fibre filter was cut from the original one (203
33 mm × 254 mm).

34 A procedure reported for the speciation of radiocesium and iodine in soil and sediment
35 samples,² was modified for analysis of aerosol samples in this work. A method reported for
36 the speciation of ¹²⁹I and ¹²⁷I in rainwater samples,³ was referred for the separation of water
37 soluble iodine fraction. Detailed procedures of chemical leaching and extraction, together
38 with ^{134,137}Cs detection by gamma-ray spectrometer, ¹²⁷I analysis by inductively coupled
39 plasma-mass spectrometer (ICP-MS), and ¹²⁹I measurement by accelerator mass spectrometer
40 (AMS), are described as follows.

41

42 (1) Water leaching

43 After being measured for the total ^{134,137}Cs activity, the aerosol was cut into small pieces,
44 put into a beaker and 20 mL deionized water (18.2 MΩ·cm) was added. The mixture was
45 stirred using a magnetic stirring apparatus under room temperature for 24 hours. The water
46 leachate was separated from the residue by filtration. Another aliquot of 20 mL deionized
47 water was added to the residue and stirred for 0.5 hours to wash the residue. The second
48 leachate was filtered. The wash step was repeated once. The three water leachates were
49 combined and measured for ^{134,137}Cs activity. An aliquot of 1mL was reserved for ¹²⁷I
50 measurement. The aerosol residue combined with the filter was used for NaOH leaching.

51 After being measured for the ^{134,137}Cs activity of water leachate, separation of inorganic
52 iodine from water leachate was carried out. The water leachate, after the addition of 2000 Bq
53 ¹²⁵I tracer as iodide form, was loaded onto a strong basic anion exchange column with 10 cm
54 height and 1 cm diameter. Based on the affinity properties of iodide and iodate with anion
55 exchange resin, iodate can pass through the resin due to its low affinity with resin particles,
56 while iodide will be absorbed onto the resin. 10 mL 0.2 M NaNO₃ and 10 mL water were
57 used to wash the column in the order and the washes were combined with the effluent. An
58 aliquot of 5 mL was reserved for ¹²⁷IO₃⁻ measurement. 30 mL 1% NaClO and 10 mL 3 M
59 HNO₃ were used in order to elute the iodide from the column. The pH of the eluate was
60 adjusted to neutral with NH₃·H₂O. 6 g of the eluate was taken out to measure the ¹²⁵I counts

61 by a NaI detector to calculate the chemical yield of iodide. An aliquot of 1 mL was reserved
62 for $^{127}\text{I}^-$ measurement.

63

64 (2) NaOH leaching

65 The aerosol residue, together with the filter after water leaching, was placed into a beaker.
66 20 mL 0.5 M NaOH solution was added, and the suspension was heated to 60°C and stirred
67 for 4 hours with a watch glass cover to prevent the loss of the solution during heating. After
68 cooling down, the leachate was separated from the residue by filtration. Another aliquot of 20
69 mL 0.5 M NaOH solution was added into the residue and the suspension was stirred under
70 60°C for 0.5 hours to wash the residue. The second leachate was filtered when it was cooled
71 down. This wash step was repeated once. The three NaOH leachates were combined and
72 measured for $^{134,137}\text{Cs}$ activity. An aliquot of 1mL was reserved for ^{127}I measurement. The
73 aerosol residue combined with the filter was ready for combustion.

74

75 (3) Residue combustion

76 After the $^{134,137}\text{Cs}$ determination for the residues, the aerosol residue together with filter
77 was transferred into a quartz boat for separation of the remained iodine using combustion.
78 2000 Bq of ^{125}I tracer was added to monitor the chemical yield of combustion. The
79 temperature was slowly increased to avoid rapid inflammation of the air filter that may result
80 in an explosion. 35 mL trap solution (mixture of 0.4 M NaOH and 0.01 M $\text{K}_2\text{S}_2\text{O}_5$) was used
81 to absorb iodine released by the aerosol residue. An aliquot of 6 g trap solution was measured
82 by a NaI detector for ^{125}I counts to calculate the chemical yield of combustion. 1g of the trap
83 solution was reserved for ^{127}I measurement.

84

85 (4) Measurement of ^{134}Cs and ^{137}Cs in total aerosol and species

86 The total aerosol sample was placed into plastic tubes (Φ 8 mm) and pressed with a rod to
87 the bottom of the tube. ^{134}Cs and ^{137}Cs in the prepared samples were measured by gamma
88 spectrometry equipped with a high purity germanium (HPGe) detector and Gennie 2000
89 software, which were used for spectrum acquire and analysis at the Center for Nuclear
90 Technologies, Technical University of Denmark (TUD) at Risø. The total uncertainty is made
91 up of calibration uncertainty and statistic uncertainty. Cs isotopes in water leachate, NaOH
92 leachate and aerosol residue in appropriate containers were also measured by gamma
93 spectrometry.

94

95 (5) Measurement of ^{127}I in species

96 All fractions (leachate or trap solution) were diluted using deionized water by a factor of 1-
97 10 depending on the salinity of the solution. For ^{127}I measurement, Cs^+ as an internal standard
98 was added to solutions to a final concentration of 2 ppb, and $\text{NH}_3\cdot\text{H}_2\text{O}$ was added to a final
99 concentration of 1%. ^{127}I in sample was measured by ICP-MS (Series XII, Thermo, USA) at
100 the Center for Nuclear Technologies, Technical University of Denmark.

101

102 (6) ^{129}I extraction and precipitation

103 A certain amount of the diluted solution above was used for ^{129}I preparation depending on
104 ^{129}I level in the fractions. 2 mg Woodward iodine (WWI, Woodward Company, USA) was
105 added as a carrier. The solution was acidified to $\text{pH}<2$ using 3 M HNO_3 after the addition of 1
106 M $\text{K}_2\text{S}_2\text{O}_5$ solution to convert all inorganic iodine to iodide, which was extracted with CHCl_3
107 after being oxidized to iodine using NaNO_2 . The extraction step was repeated to obtain a high
108 recovery of iodine. Iodine in the CHCl_3 phase was then back extracted to the water phase
109 using $\text{K}_2\text{S}_2\text{O}_5$ solution. This extraction and back extraction procedure was repeated once. The
110 separated iodide was precipitated as AgI by the addition of 0.5 M AgNO_3 as the procedure
111 reported elsewhere.⁴ The AgI precipitate was dried at 70°C , ground to fine powder, mixed
112 with silver powder (Aldrich, USA) in weight ratio of 1:2 for AgI to Ag powder, and pressed
113 into a copper holder.

114

115 (7) ^{129}I measurement

116 The ^{129}I were measured using 5 MV AMS (NEC Corporation, USA) at the Scottish
117 Universities Environmental Research Center.⁵ The mixed AgI and Ag were pressed into an
118 aluminum target holder with a 1 mm diameter and loaded into the ion source. Negative I^- ions
119 were extracted by a Cs-sputtering ion source. Due to the low melting point of AgI , the ion
120 source was adjusted to a relatively lower power. 3 MV was chosen as the terminal voltage and
121 the I^{5+} was chosen for detection, which resulted in about 1 % ion transmission efficiency. The
122 $^{127}\text{I}^{5+}$ was detected using a Faraday cup mounted at the exit of the high-energy analyzing
123 magnet, while $^{129}\text{I}^{5+}$ was counted using ionization detector with 100 nm thick SiN detector
124 window. Although the $^{97}\text{Mo}^{4+}$, which were produced by dissociation of the injected MoO_2^-
125 and had a similar magnetic rigidity (ME/q^2) to $^{129}\text{I}^{5+}$, may interfere with $^{129}\text{I}^{5+}$, they can be
126 completely separated from $^{129}\text{I}^{5+}$ in the detector. The measured $^{129}\text{I}/^{127}\text{I}$ ratios were corrected
127 against a standard material with $^{129}\text{I}/^{127}\text{I}$ ratios of 1.138×10^{-10} , prepared by ^{127}I addition to the

128 original NIST 4949B standard. The measured $^{129}\text{I}/^{127}\text{I}$ ratios in samples were 10^{-12} - 10^{-10} ,
129 which are more than 1-2 orders of magnitude higher than that of the procedure blank (10^{-13}).
130 Due to possible memory effects in the ion source, care was taken to measure samples in
131 sequence from low to high $^{129}\text{I}/^{127}\text{I}$ ratios. Repeat measurements of secondary standards
132 indicated better than 2 % reproducibility.

133

134 **References**

- 135 (1) Doi, T.; Matsumoto, K.; Toyoda, A.; Tanaka, A.; Shibata, Y.; Hirose, K.
136 Anthropogenic radionuclides in the atmosphere observed at Tsukuba: characteristics
137 of the radionuclides derived from Fukushima. *J. Environ. Radioact.* 2013, 122, 55–62.
- 138 (2) Hou, X.L.; Fogh, C. L.; Kucera, J.; Andersson, K. G.; Dahlgard, H.; Nielsen, S. P.
139 Iodine-129 and caesium-137 in Chernobyl contaminated soil and their chemical
140 fractionation. *Sci. Total Environ.* 2003, 308, 97–109.
- 141 (3) Hou, X.L.; Aldahan, A.; Nielsen, S.P.; Possnert, G. Time series of ^{129}I and ^{127}I
142 speciation in precipitation from Denmark, *Environ. Sci. Technol.* 2009, 43, 6522–
143 6528.
- 144 (4) Zhang, L. Y.; Zhou, W. J.; Hou, X. L.; Chen, N.; Liu, Q.; He, C. H.; Fan, Y. K.; Luo,
145 M. Y.; Wang, Z. W.; Fu, Y. C. Level and source of ^{129}I of environmental samples in
146 Xi'an region, China. *Sci. Total Environ.* 2011, 409, 3780–3788.
- 147 (5) Xu, S.; Freeman, S. P. H. T.; Hou, X. L.; Watanabe, A.; Yamaguchi, K.; Zhang, L. Y.
148 Iodine isotopes in precipitation: temporal responses to ^{129}I emissions from the
149 Fukushima nuclear accident. *Environ. Sci. Technol.* 2013, 47, 10851–10859.
- 150

Table S1. Comparison of ^{134}Cs and ^{137}Cs measurements in NIES and TUD*

Sample	Sample collection (2011)				Volume (m ³)	Institution	Filter size (mm x mm)	^{134}Cs (Bq/m ³)	^{137}Cs (Bq/m ³)	$^{134}\text{Cs}/^{137}\text{Cs}$
	Start		Stop							
	Month-day	Time	Month-day	Time						
No. 1	Mar 15	14:39	Mar 15	17:34	105	NIES	203 x 254	3.99±0.01	3.82±0.02	1.04±0.01
						TUD	20 x 50	3.09±0.16	3.01±0.15	1.03±0.07
No. 2	Mar 15	17:48	Mar 16	08:48	540	NIES	203 x 254	0.661±0.006	0.648±0.007	1.02±0.01
						TUD	20 x 50	0.668±0.034	0.670±0.034	1.00±0.07
No. 3	Mar 16	09:08	Mar 16	17:08	288	NIES	203 x 254	0.518±0.005	0.498±0.006	1.04±0.02
						TUD	20 x 50	0.540±0.027	0.523±0.026	1.03±0.07
No. 4	Mar 22	10:00	Mar 23	11:10	906	NIES	203 x 254	0.124±0.002	0.117±0.002	1.06±0.02
						TUD	20 x 50	0.126±0.006	0.116±0.006	1.08±0.08

*Activity was corrected to March 11, 2011 at 14:46. Data of NIES are from Ref.¹ and TUD from this study.

Paper VI

Speciation of ^{127}I and ^{129}I in atmospheric aerosols at Risø, Denmark: Insight into sources of iodine isotopes and their species transformation

Luyuan Zhang¹, Xiaolin Hou^{1,2,*}, Sheng Xu³

¹ Center for Nuclear Technologies, Technical University of Denmark, Risø Campus, Roskilde 4000, Denmark

² Xi'an AMS Center, SKLLQG, Shaanxi Key Laboratory of AMS Technology and Application, Institute of Earth Environment, CAS, Xi'an 710075, China

³ Environmental Research Center, Scottish University, United Kingdom

Abstract

Speciation analysis of iodine in aerosols is an effective approach to understand the biogeochemical cycling of iodine in the atmosphere. Overall iodine species, including water soluble iodine species (iodide, iodate and water soluble organic iodine), NaOH soluble iodine and insoluble iodine have been measured in aerosols collected at Risø, Denmark during March-May 2011 (shortly after the Fukushima nuclear accident) and December 2014. The concentrations of total iodine are in ranges of 1.04-2.48 ng/m³ for ^{127}I and $(11.3-97.0)\times 10^5$ atoms/m³ for ^{129}I , resulting in $^{129}\text{I}/^{127}\text{I}$ atomic ratios of $(17.8-86.8)\times 10^{-8}$. The contribution of Fukushima-derived ^{129}I (peak value of 6.3×10^4 atoms/m³) is estimated to be negligible (less than 6% of the total ^{129}I) in the northern Europe. The concentrations and species of ^{129}I and ^{127}I in aerosols are found to be strongly related with their sources and pathways of the carrier air. The air from the ocean on the west contributed higher ^{129}I concentration in aerosols compared to that from European continent on the east. The high ^{129}I concentration in aerosols is attributed to the secondary emission of the heavily ^{129}I -contaminated seawater in the North Sea to the west, rather than direct gaseous release of ^{129}I from nuclear reprocessing plants. Water soluble iodine was found to be a minor fraction to total iodine for both natural ^{127}I (7.8-13.7%) and ^{129}I (6.5-14.1%) in ocean-derived aerosols, which increased to 20.2-30.3% for ^{127}I and 25.6-29.5% for ^{129}I in land-derived aerosols. Iodide was the predominant form in the water soluble iodine, accounting for more than 97% of the water soluble iodine. NaOH soluble iodine seems to be independent on the source of aerosols. The significant proportion of ^{129}I and ^{127}I found in NaOH soluble fractions is likely bound with organic substances. In contrast to water soluble iodine,

*Corresponding author: xiho@dtu.dk; Tel: +45 46775357; Fax: +45 4677 5347

however, the sources of air mass exerted distinct influences on insoluble iodine for both ^{129}I and ^{127}I , i.e. which enriched in oceanic air and depleted in land-ocean mixed air.

Introduction

Atmospheric chemistry of iodine has attracted increasing attention in recent years, not only because of its crucial role in geochemical cycling of iodine, but also due to the significant effects on tropospheric ozone depletion and formation of primary particles, which could indirectly influence global climate by regulating solar radiation (Carpenter 2003; O'Dowd et al., 2002; Saiz-Lopez et al., 2012). However, most of the studies concentrated on laboratory smog chamber experiments and modeling prediction, apparently lack of field and laboratory measurements on real atmospheric samples. Significant fraction of iodine exists in atmospheric particles, which makes aerosol become a potent tool to study atmospheric chemistry of iodine. Speciation analysis of iodine in aerosol, furthermore, could provide intensive knowledge on comprehensively understanding biogeochemical cycling of iodine.

Most of work on iodine speciation of aerosol focused on water soluble iodine (WSI) in aerosols (Baker 2004; Baker 2005; Gilfedder et al., 2008). Early modelling work predicted that aerosol iodate may be a by-product of the production of higher iodine oxides and is believed to be the only stable iodine species, while iodide concentration is negligible due to transformation into gaseous iodine (McFiggans et al., 2000; Vogt et al., 1999). However, this prediction went against with several observations, which showed significant magnitude of iodide and soluble organic iodine, together accounting for 10%-100% of WSI in aerosol (Baker 2004; Baker 2005; Gabler and Heumann 1993; Wimschneider and Heumann 1995). An updated model was presented recently for better prediction primarily by elevating the proportion of iodide in aerosols (Pechtl et al., 2007). Only few works noticed water insoluble iodine in aerosol (Gilfedder et al., 2010; Tsukada et al., 1987), which might be hardly converted back to gaseous iodine but enter into next cycle stage being deposited to the Earth's surface. The existing observational data have suggested that the insoluble iodine is abundant in aerosol particles, representing 17-53% of total iodine (Gilfedder et al., 2010). However, there is no comprehensive investigation on iodine species in aerosol encompassing aqueous soluble and insoluble iodine species, which leaves a big vacancy for fully understanding interaction of iodine species both in aerosol as well as in gas-aerosol interface.

A difficulty on investigation of geochemical cycling of iodine is identification of the source of natural iodine. Due to the discernible source terms, ^{129}I , the only long-lived radioisotope of iodine ($T_{1/2}=15.7$ Ma), has been proved to be a ideal geochemical tracer

and successfully applied in investigations of various environmental processes (Hou et al., 2007; Jabbar et al., 2012; Michel et al., 2012). Large amount of ^{129}I has been released to the environment, predominantly from nuclear reprocessing plants (NRPs) with an amount of 6000 kg by 2009, especially the Sellafield (United Kingdom) and La Hague (France) (Hou et al., 2007; Raisbeck et al., 1995). In the present environment, the anthropogenic ^{129}I is distributed unevenly in water, atmosphere and terrestrial systems (Hou et al., 2009b). To the atmosphere, explosions of nuclear bombs aboveground produced radioactive aerosols containing ^{129}I that was ejected even to the stratosphere and mixed globally before back to troposphere. Larger particles remained in the troposphere for about 20 days and finally deposited to the earth's surface (Tölgýessy 1993). Gaseous releases from reprocessing plants and accidents are primary sources of ^{129}I to local environment (Hou et al., 2009a; Xu et al., 2013). Re-emission of iodine from the marine boundary layer plays an important role to transfer ^{129}I to the air (Englund et al., 2010b). As with stable iodine (^{127}I), ^{129}I participates in geochemical cycling and is attached with particles in various chemical species. Particulate ^{129}I has been successfully applied to investigate transportation of air mass and monitor of radioiodine in nuclear activity zones as well as background areas without close-in ^{129}I source (Englund et al., 2010b; Jabbar et al., 2012; Santos et al., 2005; Tsukada et al., 1987). Investigation on speciation analysis of ^{129}I in aerosols is extremely scarce with only one our previous work (Xu et al., 2015), which didn't focus on conversion among iodine species in aerosols.

Here, we present the results of speciation analysis of soluble and insoluble stable ^{127}I and radioactive ^{129}I in aerosols collected at a coastal site in Denmark, in order to investigate the transformation mechanisms among the iodine species in aerosols and gas-aerosol exchange processes of iodine.

Materials and methods

Aerosol sampling

Eight aerosol samples were collected using 0.45 μm polypropylene filter (www.pti-ficher.com) that was attached to an in-house aerosol collector at Risø campus, Technical University of Denmark, Denmark (55°41.77'N, 12°05.39'E) (Fig. 1). The sampling filter is normally replaced every week, but during the Fukushima nuclear accident, the changing frequency was increased to every 3-4 days. Seven aerosols were sampled during 31st March - 2nd May, 2011, shortly after the Fukushima accident on 11th March, 2011. One sample was collected during 8-15th December 2014. The samples were put into plastic bags and stored in dark until analysis. Sample information is listed in Table 1.

Speciation analysis of ^{127}I and ^{129}I in aerosols

Separation of iodine species from aerosol. The aerosol samples were analyzed using a newly developed method (Zhang et al. submitted, 2015). In brief, iodine in aerosols was extracted sequentially using deionized water and sodium hydroxide solution for water soluble and NaOH soluble iodine (WSI and NSI). Total iodine (TI) and residual insoluble iodine (RII) were separated by alkaline ashing from the original air filters and the residual filters after NaOH solution leaching. Iodide and iodate in the water leachate were separated using anion exchange chromatography. Fig.1 shows a diagram of separation procedure for speciation analysis of iodine isotopes.

Determination of ^{127}I by ICP-MS and ^{129}I by AMS. ^{127}I in all fractions were diluted by a factor of 1-20 using ammonium to 1% $\text{NH}_3\cdot\text{H}_2\text{O}$. Cesium was added to a final concentration of 2 ng/g as internal standard to monitor the ionization efficiency of iodine. For measurement of ^{127}I in ash leachates of total iodine and insoluble fraction, standard addition method was employed. Iodine standard solution (NaI, NIST, USA) was spiked into the reserved aliquots and diluted to a final concentration of 2 ng/g. ^{127}I in the diluted solution was measured by ICP-MS (Thermo Fisher, X Series II) using Xt cone under normal mode as described elsewhere (Hou et al., 2007).

^{129}I was measured using a 5 MV accelerator mass spectrometry (NEC, Wisconsin, USA) at Scottish University Environmental Research Center, UK (Xu et al., 2013). The prepared AgI precipitates were mixed with silver powder (Sigma-Aldrich Co., USA) in mass ratio of 1:2 and pressed into copper holder using a manual pressure machine. The terminal voltage of 3.5 MV and I^{5+} were chosen for detection of ^{129}I . The measured $^{129}\text{I}/^{127}\text{I}$ ratios were corrected against a standard with $^{129}\text{I}/^{127}\text{I}$ ratio of 1.138×10^{-10} prepared by NIST 4949C and ^{127}I carrier. The analytical accuracies for standards and samples are within 5%. The procedure blanks are 5×10^{-13} , 1-3 orders of magnitude lower than that in the samples. All results were corrected for procedure blanks.

Results

The concentrations of total iodine in aerosols from Risø, Denmark ranged at 1.04-2.48 ng/m^3 (1.79 ± 0.52 ng/m^3 in average) for ^{127}I and $11.3-73.0\times 10^5$ atoms/m^3 (43.65 ± 18.88) $\times 10^5$ atoms/m^3 in average) for ^{129}I , during March-May 2011 (Table 2). Total ^{127}I concentration of 2.36 ng/m^3 during 8-15 December 2014 fell within the range in 2011, while ^{129}I concentration of 97.0×10^5 atoms/m^3 was about two times higher than the average value in 2011. Much lower values of ^{129}I and ^{127}I concentrations were observed during 18 April- 2 May compared to those before 18 April (Fig. 3), but ^{129}I level didn't show a synchronous variation with ^{127}I concentrations. The results of ^{127}I concentrations in the studied aerosols are compatible with those from an inland city, Regensburg, Germany and from some Pacific islands ((Gabler and Heumann 1993) and references

therein). $^{129}\text{I}/^{127}\text{I}$ atomic ratios in the investigated aerosols were $(17.84-86.84)\times 10^{-8}$, which are virtually consistent with those found at Foehr island, north of Germany in April 2002 (Michel et al., 2012) and in southern Sweden during 1983-2008 (Englund et al., 2010b; Michel et al., 2012). However, the measured ^{129}I concentrations and $^{129}\text{I}/^{127}\text{I}$ ratios are 1-2 orders of magnitude higher than those observed in Vienna, Austria during 2001-2002, and at high altitude eastern Alps (2700 m) during 2001 (Jabbar et al., 2011; Jabbar et al., 2012).

WSI in aerosols of year 2011 predominantly occurred as iodide for ^{127}I ranging at $0.12-0.33\text{ ng/m}^3$, and iodate concentrations of $0.02-0.03\text{ ng/m}^3$ were detectable in only two samples (AE11-12 during 4-7th April and AE11-17 during 26th April-2nd May) (Table 1 and Fig. 4). The highest ^{127}I concentration of 0.74 ng/m^3 was observed in the aerosols collected in year 2014. No water soluble organic iodine was measured. Water soluble ^{129}I shows a similar species pattern as ^{127}I except iodate that was below the detection limit. Concentrations of ^{129}I varied at $(3.26-5.91)\times 10^5\text{ atoms/m}^3$ with an average value of $4.41\times 10^5\text{ atoms/m}^3$ in aerosol of 2011, while the value in the sample collected in 2014 ($30.12\times 10^5\text{ atoms/m}^3$) is about 8 times higher than those in 2011. Apparently high concentrations of iodine species in all aerosols samples is the NSI species with an average of $0.64\pm 0.21\text{ ng/m}^3$ for ^{127}I and $(13.55\pm 10.12)\times 10^5\text{ atoms/m}^3$ for ^{129}I . The NSI are likely organically bound iodine, which can be soluble in NaOH solution, implying a large portion of iodine is associated with organic matter. RII is the dominant specie in aerosol samples for both iodine isotopes, with concentrations ranges of $0.34-1.66\text{ ng/m}^3$ for ^{127}I and $(4.27-39.94)\times 10^5\text{ atoms/m}^3$ for ^{129}I .

Since there is no available standard reference material for measurement of iodine isotopes in aerosol, the ratios of sum of all species to total iodine in whole samples were calculated to be 85%-110%, confirming the reliability of the analytical results (Fig. 5).

Before 18th April, the proportion of ^{129}I and ^{127}I species follows an order of RII > NSI > iodide, while for the samples in later April 2011 and winter 2014, the three iodine fractions for both ^{129}I and ^{127}I account for almost same proportion of total iodine (Fig. 5). Compared to the former sampling period (31 March-18 April 2011), the most apparent feature in the latter sampling period is that the RII fraction dramatically diminished by 38.7% for ^{127}I and 26.8% for ^{129}I , which is accompanied by increasing iodide fraction in aerosol particles. Iodate, as the least abundant iodine specie (< 3%), was only determined in two aerosol samples for ^{127}I , and no $^{129}\text{IO}_3^-$ was found.

The $^{129}\text{I}/^{127}\text{I}$ ratios range in $(15.56-102.36)\times 10^{-8}$ were observed for different iodine species in aerosols. Variation trends of $^{129}\text{I}/^{127}\text{I}$ atomic ratios in iodide, NSI and RII almost agree with those in total $^{129}\text{I}/^{127}\text{I}$ ratios that high values were found before 18 April 2011 and December 2014 (Table 2).

Discussion

Sources of ^{127}I and ^{129}I in aerosols

Analysis of the variation of ^{127}I and ^{129}I concentrations in aerosols against the meteorological parameters (i.e. wind direction, wind speed and temperature) during the sampling period shows that wind direction has a dominant influence on iodine concentrations (Fig. 3). Back trajectory model analysis shows that ^{127}I and ^{129}I in the aerosol is directly controlled by the source and pathways of the carrier air (Fig. 6 and Fig S-1, S-2 in supplementary material). The relatively high ^{127}I and ^{129}I concentrations in aerosols was observed in early April 2011 and December 2014, when the air mass mainly transported from the Atlantic Ocean and the North Sea by prevailing westerly wind. While low concentrations of iodine isotopes were observed in aerosols collected in later April, when the air masses were dominated by prevailing easterly wind, which passed over the European continent and the Baltic Sea.

Marine emission is a major source of iodine in the atmosphere, which generally results in higher ^{127}I concentration in marine atmosphere than terrestrial atmosphere (Saiz-Lopez et al., 2012). During the sampling period of 11-14th April, the westerly air mass was transported from a vast area of the northern Atlantic Ocean to the sampling site, which caused the highest ^{127}I concentration in this aerosol sample. Whereas, the most area of the northern Atlantic ocean containing low ^{129}I concentration in seawater (except the coastal water in the Norwegian Sea) (He et al., 2013) contributed low level of ^{129}I to these relative air masses, and consequently to this aerosol sample.

The highest ^{129}I concentrations ($(73-97)\times 10^5$ atoms/ m^3) were observed in aerosol samples collected in 4-7th April 2011 and 8-15th December 2014, when the air masses were transported from two directions, west/northwest and south/southwest (Fig. 6, Figure S-1 and S-2). The dominant south/southwesterly wind passed over the high ^{129}I areas, i.e. the entire North Sea, as well as the sites of Cap de La Hague and Sellafield. Distinct from ocean-origin ^{127}I , more than 95% of ^{129}I in the environment was discharged from Sellafield and La Hague, which locate at west and southwest of Denmark, respectively. Only a small fraction of ^{129}I in gaseous form (about 2-5 kg/year in the past 20 years) was released to the atmosphere, which was dispersed with air over a large area, especially in southern European (Ernst et al., 2003; Hou et al., 2007). However, large fraction of ^{129}I (200-300 kg/year since 1995) in liquid form was discharged to the English Channel and Irish Sea, then transported by water current to the North Sea, to the Kattegat and the Baltic Sea with a small proportion, and further to the Arctic along the Norwegian coast (Alfimov et al., 2004a; Buraglio et al., 1999; Hou et al., 2007; Raisbeck et al., 1995; Yi et al., 2012). Remarkably elevated ^{129}I concentrations have been observed up to 10^{10} - 10^{11} atoms/L in the North Sea, 10^9 - 10^{10}

atoms/L in the Norwegian coastal seawater and the Kattegat, and 10^8 - 10^9 atoms/L in the Baltic Sea (Aldahan et al., 2007; Alfimov et al., 2004b; He et al., 2014; Hou et al., 2007; Michel et al., 2012; Yi et al., 2011). Besides air release to the atmosphere from the two reprocessing plants, iodine emitted from seawater especially in the North Sea, as well as the Kattegat through sea-spray and biological activity of macroalgae and microalgae (McFiggans 2005; O'Dowd et al., 2002) could significantly increase the ^{129}I concentrations in the atmosphere as well as in the aerosol samples collected during these periods.

The lowest ^{129}I concentrations ($(11-13)\times 10^5$ atoms/ m^3) were observed in aerosol samples collected in 18-26th April and 26th April-2nd May. The back trajectory analysis (Fig. S-1) shows that in this period the air masses at the sampling site were mainly transported by easterly or northwesterly wind from the northeastern European continent. The lower terrestrial emission of iodine through the vegetation and microorganism compared to marine emission and the lower ^{129}I level in the land of the northeastern Europe compared to that in the North Sea should be therefore the reasons of low ^{129}I concentrations in these two aerosol samples. The much higher ^{210}Pb level (249-253 $\mu\text{Bq}/\text{m}^3$) (Table 1) in this period also reflected the aerosols mainly originated from the European continent. For the aerosol samples collected in 11-14th and 14-18th April, the ^{129}I concentrations of $(43-47)\times 10^5$ atoms/ m^3 were measured, which is lower than the one collected in 4-7th April (73×10^5 atoms/ m^3) by a factor of 1.6, but about 4-fold higher than that in the aerosol samples derived from the northeastern European continent during 18th April to 2nd May. The back trajectory analysis clearly shows that the dominant air masses during the sampling periods were transported westerly, i.e. from the Atlantic Ocean but cross a narrow area of the northern North Sea (Fig. 4 and Fig. S-1). The secondarily high ^{129}I concentrations in these aerosol samples should be attributed to the re-emission of ^{129}I from the highly contaminated seawater in the North Sea. It can be therefore concluded that besides the direct air releases of ^{129}I from the two European reprocessing plants, secondary emission of ^{129}I from the highly ^{129}I contaminated North Sea water is the dominant source of ^{129}I in the aerosols collected in Denmark. This is also supported by other investigation on ^{129}I concentrations in aerosols at European high altitude sites (Jabbar et al., 2012).

However, such result could not be observed in precipitation samples collected in central Sweden during 1998-1999 (Buraglio et al., 2001). This might be attributed to the different incorporation processes of iodine into particles and precipitation. Gaseous iodine species, e.g. I_2 , CH_2I_2 emitted by abundant iodine-rich seaweed are dominant precursors for the formation of new particles, due to their relatively rapid photolysis to active iodine oxides (e.g. IO, OIO) (McFiggans 2005; O'Dowd et al., 2002; Saiz-Lopez et al., 2012). This implies iodine in aerosols may participate in aerosol formation,

which is sensitive to iodine source terms. Whereas, iodine in precipitation originates from washout process of gaseous iodine and particulate iodine in the air, which is primarily in the forms of polar iodine compounds (e.g. HI, HOI, IO, I, IO₃⁻, I₂, unidentified organic iodine species) in H₂O molecules during precipitation events (Buraglio et al., 2001; Gilfedder et al., 2007). In addition, aerosol samples were collected in a long time scale (3-7 days), reflecting an accumulated signal during the sampling period, while precipitation normally takes a short time, reflecting the formation processes related to cloud and rainfall. Therefore the real source terms of iodine isotopes in the precipitation might not be simply revealed by the back trajectory analysis.

Species of ¹²⁹I and ¹²⁷I in aerosols

WSI is virtually only present as iodide in the aerosols investigated, the sum of iodate and water soluble organic iodine calculated by the difference between WSI and iodide accounting for less than 3% of total iodine, which were only measured in two samples. Iodate was once considered to be the only WSI species in aerosol (Vogt et al., 1999), which is supported by an earlier field observation that iodate was found to be the dominant form in size-segregated aerosols in the tropical Atlantic (Wimschneider and Heumann 1995). However, the iodate-dominant feature could not be observed in other aerosol samples, e.g. the northwest Atlantic Ocean and the tropical atmospheric aerosols (Baker 2004; Baker 2005), where the iodide was predominated in aerosol phase, which agrees well with the observation in this work. Significant amount of soluble organic iodine accounting for 83-97% of WSI has been reported in aerosols collected at the Mace Head atmospheric research station on the west coast of Ireland (Gilfedder et al., 2008). Soluble organic iodine accounting for 4%-75% of WSI were also measured in aerosols collected in a cruise from the UK to the Falkland Islands in 2003 (Baker 2005). This indicates that soluble organic iodine in aerosols might be related to the sampling areas, sources and formation processes of aerosols, as well as the analytical method used for speciation analysis (Zhang et al., submitted, 2015).

It is not clear how iodide is formed in the atmosphere with presence of oxidants, i.e. oxygen and ozone. Current models predict a negligible iodide concentration in particle phase based on an assumption that the iodide in aerosols only origins from the low level of gaseous HI (McFiggans et al., 2000; Vogt et al., 1999). This work in combination with other previous results (Baker 2004; Xu et al., 2015) suggests that there should be other wealthy sources contributing iodide in the observed levels. It's generally accepted that iodine atoms are photochemically produced by photolysis of gaseous iodinated compounds, and oxidized by ozone to reactive iodine oxides (Carpenter 2003; Saiz-Lopez et al., 2012; Vogt et al., 1999). The formation of iodide from iodine atoms and other reactive iodine compounds certainly relies on

electron-donors that are responsible for reduction of high valence of iodine species to iodide. It has been suggested that the global cycling of sulfur plays an important role on conversion of iodinated compounds to iodine atoms (Chatfield and Crutzen 1990). Therefore, it might be proposed that the formation of iodide is based on reduction reaction by sulfur compounds (Table 3, Equations 1-4). The reductive gaseous SO_2 is formed by reactions of dimethyl sulfate (DMS) with hydroxide and nitrate, and associated with H_2O to produce HSO_3^- and SO_3^{2-} (Equations 1 and 2). Iodine in the form of iodine atoms and other reactive species (not shown) can be reduced to I^- on gas-aerosol interface (Equation 3). Other iodine species in aerosols are also reduced by reductive sulfur compounds to iodide (Equation 4). The electron-donors are not limited to sulfur compounds, for example, nitrogen in the form of ammonia gas ($\text{NH}_3 \rightarrow \text{NO}_2/\text{NO}_3$) (McFiggans et al., 2000; Saiz-Lopez and Plane 2004) and elemental mercury ($\text{Hg}^0 \rightarrow \text{HgO}/\text{HgX}$, X is halogens I^- , Br^- , Cl^-) (Lindberg et al., 2002; Simpson et al., 2007) are also available candidates responsible for formation of iodide.

It can be observed that lower WSI (^{129}I and ^{127}I) was measured in marine sourced aerosols from the North Sea compared to the European continent sourced aerosols (Fig. 4 and 5). This is well consistent with the conclusion drawn from the iodine speciation in the coastal aerosol samples in England (Baker et al., 2001), where the concentrations of total water extractable iodine in continent-origin aerosols were significantly higher than those in aerosols derived from ocean.

A large proportion of ^{129}I and ^{127}I in the aerosol samples was observed in NaOH soluble form, which is consistent with the observation in the aerosols from Tsukuba, Japan collected shortly after the Fukushima nuclear accident in March 2011 (Xu et al., 2015). The abundant NaOH soluble ^{129}I (32%-44% of total ^{129}I) in Fukushima-derived aerosols was attributed to coarse vegetation-related organic particles rich in the spring season. The measured NaOH soluble iodine (NSI) fractions of ^{129}I and ^{127}I in the whole sampling period in spring 2011 and winter 2014 are similar. This indicates that NSI is relative stable and less affected by the source and pathways of air mass compared to the WSI. NaOH leaching is often used to extract organic substance in fractionation analysis of soil and sediment (Englund et al., 2010a; Hou et al., 2003) based on the high solubility of major organic matter, such as humic substances. Organic compounds are important contributors in aerosols, such as lipidic, saccharides, proteinaceous materials (O'Dowd et al., 2004; Quinn et al., 2014). A significant part of atmospheric aerosol was found to be humic-like substances (HULIS), named as its considerable similarities in structural properties to humic and fulvic acids (Havers et al., 1998). Most of these organic compounds are water-soluble including the fulvic acids in HULIS, but a significant water-insoluble fraction of HULIS, humic acids, having more hydrophobic and acidic character and higher molecular weight, can be dissolved in alkaline medium

like NaOH solution (Feczko et al., 2007; Havers et al., 1998). Therefore, NaOH soluble iodine is suggested to be most likely associated with HULIS in aerosols.

Besides NSI, RII in aerosols has been also less investigated (Gilfedder et al., 2010; Tsukada et al., 1987). The earliest report on insoluble iodine fraction in aerosol particles conducted by neutron activation analysis (NAA) showed that 27-58% of iodine was residual insoluble species in aerosols from Tokyo, Japan during 1983-84 (Tsukada et al., 1987). Similar result of 17-53% of total iodine as insoluble species has been reported for aerosols from west coast of Ireland during 2007 and from a ship transect from China to Antarctica during 2005-2006 (Gilfedder et al., 2010). If taking the alkaline leachable iodine in aerosols into account, these results well agrees with our observations in aerosols at Risø, Denmark (Fig. 6). Less insoluble ^{129}I fractions were reported to be 4-23% of total ^{129}I in Fukushima-derived aerosol particles (Xu et al., 2015). This discrepancy suggests different formation process of RII species for the NRPs-derived ^{129}I in this study compared to Fukushima-derived ^{129}I . Since ^{129}I discharged from the NRPs has been presented in the European environment for about 50 years, it has vastly participated in the geochemical cycling with natural ^{127}I and has incorporated into various environment components. Whereas, the RII in Fukushima-derived aerosols likely primarily consists of fine explosive debris during sampling period of 15-22 March, 2011, immediately after the Fukushima nuclear accident.

Iodine species in the residual insoluble fraction after water and NaOH leaching is also poorly understood at present. It's possible that RII is derived from the suspended soil particles (Xu et al., 2013). However, speciation analysis of ^{129}I in soil shows the residual iodine after NaOH leaching accounts for less than 10%, which is considered as mineral associated forms (Hou et al., 2003; Qiao et al., 2012). Soot and black carbon from combustion-related process are found in anthropogenic aerosols (Kondratyev et al., 2006; Rose et al., 2006), while the aerosols collected in early April 2011 and winter of 2014 were mainly marine aerosols with high RII. It has been reported that a relative large fraction of iodine in soil and sediment is associated with metal oxides (Hou et al., 2003), the RII in aerosols might be the iodine associated with metal oxides and minerals originated from the suspension of fine inorganic particles. Gaseous iodine in atmosphere might interact with these inorganic particles and to be firmly bound. The higher RII in the marine-originated aerosols (Fig. 5) might imply that some marine components can stimulate the association of gaseous iodine with these inorganic particles.

A significant positive correlation between ^{127}I iodide and ^7Be in aerosol samples ($R=0.76$, $p=0.05$) is observed (Fig. 7). ^7Be ($t_{1/2}=54$ days) is produced in the stratosphere by cosmic rays reactions with oxygen and nitrogen and transported to the troposphere by

vertical mixing processes to be finally deposited onto the earth. The production of ^7Be decreases with altitude in the troposphere because of the attenuation of the cosmic ray by interactions with atomic targets in the atmosphere (Turekian et al., 1983). This positive correlation might indicate the formation of iodide occur in air mass from higher altitude. No significant correlation between ^{129}I and ^7Be could be observed (Fig. 6) confirms that ^{129}I in the aerosol origins from atmosphere releases and secondary emission from contaminated seawater in the North Sea which is only present in lower layer of troposphere. The significant negative correlation of NSI for ^{129}I with ^7Be ($R=0.73$, $p=0.06$) likely reflects that association of iodine with organic matter occurs in low altitude, where organic matters liberated by biological activity from ocean and land.

Fukushima-derived ^{129}I signal in the European atmosphere

The Fukushima Dai-ichi nuclear power plant accident on March 11, 2011 has released large amount of radioiodine to the atmosphere, primarily as ^{131}I and ^{129}I , which dispersed mainly eastwards across the Pacific ocean, American continent and Atlantic Ocean, and some fractions arrived to the European continent after 1-2 weeks (Clemenza et al., 2012; Leon et al., 2011; Manolopoulou et al., 2011; Pittauerová et al., 2011). The ^{129}I concentrations have been reported in various environmental samples in Japan, such as soil, seawater, precipitation and aerosols (Buesseler et al., 2012; Hou et al., 2013; Muramatsu et al., 2015; Xu et al., 2013; Xu et al., 2015), in which the level of ^{129}I in aerosols collected in Tsukuba, about 170 km to the Fukushima Dai-ichi NPP reached up to 5×10^8 atoms/m³ (Xu, et al. 2015). While Fukushima-derived ^{129}I in environmental samples outside Japan and Fukushima offshore seawater was less investigated, ^{131}I and other gamma emitters such as ^{134}Cs in the aerosol samples collected at Risø, Denmark, 10 days after the Fukushima accident have been observed (Fig. 8) (Nielsen et al., 2011). The peak of ^{131}I ($763 \mu\text{Bq/m}^3$ in aerosol) reached at 24-30th of March 2011, then decreased to below detection limit for ^{131}I in the middle of May. Based on the measured ^{131}I radioactivity in the aerosol samples and a $^{131}\text{I}/^{129}\text{I}$ atomic ratio of 16.0 ± 2.2 deduced from the aerosol samples collected at Tsukuba, Japan shortly after the Fukushima accident (Xu et al., 2015), the Fukushima-derived ^{129}I signals in Denmark can be reconstructed (Fig. 8). The highest ^{129}I concentration in the aerosols in Denmark originated from Fukushima accident can be estimated to be 6.3×10^4 atoms/m³ on 30-31 of March 2011, which approximately accounts for less than 6% of total ^{129}I ($1.1-9.7 \times 10^6$ atoms/m³) in Denmark. Considering the significantly declined ^{129}I levels in aerosols and precipitation in Japan for a few orders of magnitude and nearly down to the pre-accident level two years after the accident (Xu et al., 2013), the contribution of Fukushima-derived ^{129}I signals to the ^{129}I level and inventory in Europe is negligible compared to the considerable amount of NRPs-derived ^{129}I in the European

atmosphere.

Dry deposition flux of iodine isotopes

Dry deposition fluxes of iodine can be estimated as $F_d = C_d \cdot v_d$ according to Baker et al. (Baker et al., 2001), where F_d is the flux ($\mu\text{g}/\text{m}^2/\text{yr}$ for ^{127}I and $\text{atoms}/\text{m}^2/\text{yr}$ for ^{129}I), C_d is the aerosol iodine concentrations in the atmosphere (ng/m^3 for ^{127}I and atoms/m^3 for ^{129}I), and v_d is the deposition velocity (cm/s). Dependent on the size of particles, the deposition velocities are employed as 0.1 cm/s for fine particles (Aerodynamic diameter $< 1 \mu\text{m}$) and 1.5 cm/s for larger particles (Duce et al., 1991). The aerosol samples in this work were collected on a PP filter with pore size of approximately 0.45 μm . According to the particle size distribution at Spieka-Neufeld, Germany, where received the atmospheric input of iodine from the North Sea and similar as the sampling site in this work, 67% of aerosol iodine was accumulated in particles larger than 1 μm and 33% in 0.45~1 μm particles (Gabler and Heumann 1993). Employing these parameters, dry deposition fluxes of iodine in Denmark can be estimated to be 342-815 $\mu\text{g}/\text{m}^2/\text{yr}$ for ^{127}I , and $0.4\text{-}3.2 \times 10^{12} \text{atoms}/\text{m}^2/\text{yr}$ for ^{129}I in the sampling period during 2011-2014. If the average values of 1.8 ng/m^3 and $43.7 \times 10^5 \text{atoms}/\text{m}^3$ are used as the representative concentrations of ^{127}I and ^{129}I in aerosol, respectively during 2011, average dry deposition fluxes of iodine during 2011 would be $591 \mu\text{g}/\text{m}^2/\text{yr}$ and $1.4 \times 10^{12} \text{atoms}/\text{m}^2/\text{yr}$ for ^{127}I and ^{129}I , respectively. The ^{127}I deposition flux falls within the range of natural stable iodine deposition flux of 460-830 $\mu\text{g}/\text{m}^2/\text{yr}$ observed at the north coast of Norfolk, United Kingdom (Baker et al., 2001). It is also comparable with that in southern Sweden, but higher than that in northern Sweden (Englund et al., 2010b). The dry deposition flux of ^{129}I for the aerosol samples collected in Sweden between 1983 and 2008 show a range of $0.33\text{-}6.6 \times 10^{11} \text{atoms}/\text{m}^2/\text{yr}$ in southern Sweden, and $0.008\text{-}1.6 \times 10^{11} \text{atoms}/\text{m}^2/\text{yr}$ in northern Sweden (Englund et al., 2010b), which are 1-3 orders of magnitude lower than the deposition fluxes in this work. This is attributed to the sampling locations much further away from the major point sources of aerosol ^{129}I . The wet deposition of ^{129}I at the same sample site as this work was calculated to be $(1.25 \pm 0.30) \times 10^{12} \text{atoms}/\text{m}^2/\text{yr}$ during 2001-2006 (Hou et al., 2009a), which is fairly consistent with the dry deposition flux of ^{129}I , indicating the contribution of ^{129}I transfer pathways are comparable via dry and wet deposition in the investigate area. However, it's noted that the estimated dry deposition flux was based on only one-month data in spring and on the modeled deposition velocity, which might introduce large uncertainty because of the temporal variation of ^{129}I in aerosols and particulate-size dependent velocity.

Conclusions

Based on the analytical results on speciation analysis of ^{129}I and ^{127}I in aerosols collected in Denmark immediately after Fukushima accident and the discussion above, the follow conclusions can be drawn:

- 1) Iodide is the dominant form (>97%) of the water soluble iodine in aerosol, its formation is related to atmospheric reductant, such as reductive SO_3 and disulfites. The most dominant species of iodine in aerosols are NSI and RII, accounting for up to 80% of total iodine, NSI is predominantly bound with organic matters, such as HULIS, while RII might be associated with inorganic components such as metal oxides and minerals.
- 2) The westerly-dominated air mass contributed high ^{127}I concentrations from the Atlantic Ocean compared to the easterly air from the northeastern European continent. ^{129}I in the aerosols in Denmark is mainly originated from the air releases of the European reprocessing plants, and secondary emission of ^{129}I from seawater in the North Sea and Kattegat heavily contaminated by the marine discharges of ^{129}I from two European reprocessing plants is another equally important source of ^{129}I in the aerosol in Denmark.
- 3) The contribution of Fukushima-derived ^{129}I signals is only less than 6 % of total ^{129}I to the European atmosphere immediately after the Fukushima accident, and negligible to the ^{129}I level and inventory in European environment compared to the considerable amount of ^{129}I released from Sellafield and La Hague nuclear reprocessing plants.

Water insoluble iodine in aerosol primarily associated with organic compounds is crucial for investigation of geochemical cycling of iodine in the atmosphere due to its large fraction. This requires more intensive studies through extending observations on time series and extensive spatial range.

Acknowledgement

LY Zhang is grateful for the supports from all of the colleagues in the Division of Radioecology (headed by Sven P. Niensen), Center for Nuclear Technologies, Technical University of Denmark for her PhD project. This work is partly supported by the projects of Innovation Methodology (No. 2012IM030200) and Fundamental Scientific Research (2015FY110800) from the Ministry of Science and Technology of China.

References

Aldahan, A., Possnert, Alfimov, V., Cato and Kekli: Anthropogenic ^{129}I in the Baltic Sea, Nucl. Instrum. Meth. B, 259, 491-495, 2007.

- Alfimov, V., Aldahan, A., Possnert, G. and Winsor, P.: Anthropogenic iodine-129 in seawater along a transect from the Norwegian coastal current to the North Pole, *Mar. Pollut. Bull.*, 49, 1097-1104, 2004a.
- Alfimov, V., Aldahan, A., Possnert, G., Kekli and Meili: Concentrations of ¹²⁹I along a transect from the North Atlantic to the Baltic Sea, *Nucl. Instrum. Meth. B*, 223-224, 446-450, 2004b.
- Baker, A. R., Tunnicliffe, C. and Jickells, T. D.: Iodine speciation and deposition fluxes from the marine atmosphere, *J. Geophys. Res.*, 106, 28743-28749, 2001.
- Baker, A. R.: Marine Aerosol Iodine Chemistry: The Importance of Soluble Organic Iodine, *Environ. Chem.*, 2, 295-298, 2005.
- Baker, A. R.: Inorganic iodine speciation in tropical Atlantic aerosol, *Geophys. Res. Lett.*, 31, - L23S02, 2004.
- Buesseler, K. O., Jayne, S. R., Fisher, N. S., Rypina, I. I., Baumann, H., Baumann, Z., Breier, C. F., Douglass, E. M., George, J., Macdonald, A. M., Miyamoto, H., Nishikawa, J., Pike, S. M. and Yoshida, S.: Fukushima-derived radionuclides in the ocean and biota off Japan, *Proc. Natl. Acad. Sci. U. S. A.*, 109, 5984-5988, 2012.
- Buraglio, N., Aldahan, A. and Possnert: Distribution and inventory of ¹²⁹I in the central Arctic Ocean, *Geophys. Res. Lett. (USA)*, 26, 1011-1014, 1999.
- Buraglio, N., Aldahan, A., Possnert, G. and Vintersved, I.: ¹²⁹I from the nuclear reprocessing facilities traced in precipitation and runoff in northern Europe, *Environ. Sci. Technol.*, 35, 1579-1586, 2001.
- Carpenter, L. J.: Iodine in the Marine Boundary Layer, *Chem. Rev.*, 103, 4953-4962, 2003.
- Chatfield, R. B. and Crutzen, P. J.: Are there interactions of iodine and sulfur species in marine air photochemistry?, *J. Geophys. Res. - Atmos.*, 95, 22319-22341, 1990.
- Clemenza, M., Fiorini, E., Previtali, E. and Sala, E.: Measurement of airborne ¹³¹I, ¹³⁴Cs and ¹³⁷Cs due to the Fukushima reactor incident in Milan (Italy), *J. Environ. Radioact.*, 114, 113-118, 2012.
- Duce, R. A., Liss, P. S., Merrill, J. T., Atlas, E. L., Buat-Menard, P., Hicks, B. B., Miller, J. M., Prospero, J. M., Arimoto, R., Church, T. M., Ellis, W., Galloway, J. N., Hansen, L., Jickells, T. D., Knap, A. H., Reinhardt, K. H., Schneider, B., Soudine, A., Tokos, J. J., Tsunogai, S., Wollast, R. and Zhou, M.: The atmospheric input of trace species to the world ocean, *Global Biogeochem. Cycles*, 5, 193-259, 1991.
- Englund, E., Aldahan, A., Hou, X., Petersen, R. and Possnert, G.: Speciation of iodine (¹²⁷I and ¹²⁹I) in lake sediments, *Nucl. Instrum. Meth. B*, 268, 1102-1105, 2010a.

- Englund, E., Aldahan, A., Hou, X., Possnert, G. and Soderstrom, C.: Iodine (I-129 and I-127) in aerosols from northern Europe, *Nucl. Instrum. Meth. B*, 268, 1139-1141, 2010b.
- Ernst, Szidat, Handl, Jakob, Michel, Schnabel, Synal, H. A., Arevalo, Benne, Boess, Gehrt, Capelle, Schneider, Schafer and Bottcher: Migration of iodine-129 and iodine-127 in soils, *Kerntechnik (Germany)*, 68, 155-167, 2003.
- Feczko, T., Puxbaum, H., Kasper-Giebl, A., Handler, M., Limbeck, A., Gelencsér, A., Pio, C., Preunkert, S. and Legrand, M.: Determination of water and alkaline extractable atmospheric humic-like substances with the TU Vienna HULIS analyzer in samples from six background sites in Europe, *J. Geophys. Res. - Atmos.*, 112, 1-9, 2007.
- Gabler, H. E. and Heumann, K. G.: Determination of particulate iodine in aerosols from different regions by size fractionating impactor sampling and IDMS, *Intern. J. Anal. Chem.*, 50(2), 129-146, 1993.
- Gilfedder, B. S., Chance, R., Dettmann, U., Lai, S. C. and Baker, A. R.: Determination of total and non-water soluble iodine in atmospheric aerosols by thermal extraction and spectrometric detection (TESI), *Anal. Bioanal. Chem.*, 398, 519-526, 2010.
- Gilfedder, B. S., Lai, S. C., Petri, M., Biester, H. and Hoffmann, T.: Iodine speciation in rain, snow and aerosols and possible transfer of organically bound iodine species from aerosol to droplet phases, *Atmos. Chem. Phys.*, 8, 6069-6084, 2008.
- Gilfedder, B. S., Petri, M. and Biester, H.: Iodine speciation in rain and snow: Implications for the atmospheric iodine sink, *J. Geophys. Res. - Atmos.*, 112, 2007.
- Havers, N., Burba, P., Lambert, J. and Klockow, D.: Spectroscopic Characterization of Humic-Like Substances in Airborne Particulate Matter, *J. Atmos. Chem.*, 29, 45-54, 1998.
- He, P., Hou, X., Aldahan, A., Possnert, G. and Yi, P.: Iodine isotopes species fingerprinting environmental conditions in surface water along the northeastern Atlantic Ocean, *Scientific Reports*, 3: 2685, 1-8, 2013.
- He, P., Aldahan, A., Possnert, G. and Hou, X.: Temporal Variation of Iodine Isotopes in the North Sea, *Environ. Sci. Technol.*, 48, 1419-1425, 2014.
- Hou, X., Aldahan, A., Nielsen, S. P. and Possnert, G.: Time Series of I-129 and I-127 Speciation in Precipitation from Denmark, *Environ. Sci. Technol.*, 43, 6522-6528, 2009a.
- Hou, X., Aldahan, A., Nielsen, S. P., Possnert, G., Nies, H. and Hedfors, J.: Speciation of I-129 and I-127 in seawater and implications for sources and transport pathways in the North Sea, *Environ. Sci. Technol.*, 41, 5993-5999, 2007.

- Hou, X., Fogh, C. L., Kucera, J., Andersson, K. G., Dahlgard, H. and Nielsen, S. P.: Iodine-129 and Caesium-137 in Chernobyl contaminated soil and their chemical fractionation, *Sci. Total Environ.*, 308, 97-109, 2003.
- Hou, X., Hansen, V., Aldahan, A., Possnert, G., Lind, O. C. and Lujanienė, G.: A review on speciation of iodine-129 in the environmental and biological samples, *Anal. Chim. Acta*, 632, 181-196, 2009b.
- Hou, X., Povinec, P. P., Zhang, L., Shi, K., Biddulph, D., Chang, C., Fan, Y., Jeřkovský, M., Liu, Q., Luo, M., Steier, P., Zhou, W. J., Hou, Y. and Golser, R.: Iodine-129 in Seawater Offshore Fukushima: Distribution, Inorganic Speciation, Sources, and Budget, *Environ. Sci. Technol.*, 47, 3091-3098, 2013.
- Jabbar, T., Steier, P., Wallner, G., Kandler, N. and Katzlberger, C.: AMS analysis of iodine-129 in aerosols from Austria, *Nucl. Instrum. Meth. B*, 269, 3183-3187, 2011.
- Jabbar, T., Steier, P., Wallner, G., Priller, A., Kandler, N. and Kaiser, A.: Iodine Isotopes (¹²⁷I and ¹²⁹I) in Aerosols at High Altitude Alp Stations, *Environ. Sci. Technol.*, 46, 8637-8644, 2012.
- Kondratyev, K. Y., Ivlev, L. S., Krapivin, V. F. and Varotsos, C. A.: Aerosol formation processes, in: *Atmospheric Aerosol Properties: Formation, Processes and Impacts*, ISBN: 978-3-540-26263-3 (Print) 978-3-540-37698-9 (Online), Kondratyev, K. Y., Ivlev, L. S., Krapivin, V. F. and Varotsos, C. A. (Eds.), Springer Berlin Heidelberg, 187-263, 2006.
- Leon, J. D., Jaffe, D. A., Kaspar, J., Knecht, A., Miller, M. L., Robertson, R. G. H. and Schubert, A. G.: Arrival time and magnitude of airborne fission products from the Fukushima, Japan, reactor incident as measured in Seattle, WA, USA, *J. Environ. Radioact.*, 102, 1032-1038, 2011.
- Lindberg, S. E., Brooks, S., Lin, C. -, Scott, K. J., Landis, M. S., Stevens, R. K., Goodsite, M. and Richter, A.: Dynamic Oxidation of Gaseous Mercury in the Arctic Troposphere at Polar Sunrise, *Environ. Sci. Technol.*, 36, 1245-1256, 2002.
- Manolopoulou, M., Vagena, E., Stoulos, S., Ioannidou, A. and Papastefanou, C.: Radioiodine and radiocesium in Thessaloniki, Northern Greece due to the Fukushima nuclear accident, *J. Environ. Radioact.*, 102, 796-797, 2011.
- McFiggans, G.: Atmospheric science: Marine aerosols and iodine emissions, *Nature*, 433, E13-E13, 2005.
- McFiggans, G., Plane, J. M. C., Allan, B. J., Carpenter, L. J., Coe, H. and O'Dowd, C.: A modeling study of iodine chemistry in the marine boundary layer, *Journal of Geophysical Research: Atmospheres*, 105, 14371-14385, 2000.
- Michel, R., Daraoui, A., Gorny, M., Jakob, D., Sachse, R., Tosch, L., Nies, H., Goroncy, I., Herrmann, J., Synal, H. A., Stocker, M. and Alfimov, V.: Iodine-129

- and iodine-127 in European seawaters and in precipitation from Northern Germany, *Sci. Total Environ.*, 419, 151-169, 2012.
- Muramatsu, Y., Matsuzaki, H., Toyama, C. and Ohno, T.: Analysis of ¹²⁹I in the soils of Fukushima Prefecture: preliminary reconstruction of ¹³¹I deposition related to the accident at Fukushima Daiichi Nuclear Power Plant (FDNPP), *J. Environ. Radioact.*, 139, 344-350, 2015.
- Nielsen, S. P., Anderson, K. P. and Miller, A.: December 2011 Radioactivity in the Risø District January-June 2011, Risø Report, Risø-R-1800(EN), 2011.
- O'Dowd, C. D., Facchini, M. C., Cavalli, F., Ceburnis, D., Mircea, M., Decesari, S., Fuzzi, S., Yoon, Y. J. and Putaud, J.: Biogenically driven organic contribution to marine aerosol, *Nature*, 431, 676-680, 2004.
- O'Dowd, C., D., Jimenez, J. L., Bahreini, R., Flagan, R. C., Seinfeld, J. H., Hämeri, K., Pirjola, L., Kulmala, M., Jennings, S. G. and Hoffmann, T.: Marine aerosol formation from biogenic iodine emissions, *Nature*, 417, 632-636, 2002.
- Pechtl, S., Schmitz, G. and von Glasow, R.: Modelling iodide – iodate speciation in atmospheric aerosol: Contributions of inorganic and organic iodine chemistry, *Atmos. Chem. Phys.*, 7, 1381-1393, 2007.
- Pittauerová, D., Hettwig, B. and Fischer, H. W.: Fukushima fallout in Northwest German environmental media, *J. Environ. Radioact.*, 102, 877-880, 2011.
- Qiao, J., Hansen, V., Hou, X., Aldahan, A. and Possnert, G.: Speciation analysis of ¹²⁹I, ¹³⁷Cs, ²³²Th, ²³⁸U, ²³⁹Pu and ²⁴⁰Pu in environmental soil and sediment, *Appl. Radial. Isot.*, 70, 1698-1708, 2012.
- Quinn, P. K., Bates, T. S., Schulz, K. S., Coffman, D. J., Frossard, A. A., Russell, L. M., Keene, W. C. and Kieber, D. J.: Contribution of sea surface carbon pool to organic matter enrichment in sea spray aerosol, *Nature Geosci*, 7, 228-232, 2014.
- Raisbeck, G. M., Yiou, F., Zhou, Z. Q. and Kilius, L. R.: ¹²⁹I from nuclear fuel reprocessing facilities at Sellafield (U.K.) and La Hague (France); potential as an oceanographic tracer, *J. Mar. Syst.*, 6, 561-570, 1995.
- Rose, D., Wehner, B., Ketzler, M., Engler, C., Voigtlander, J., Tuch, T. and Wiedensohler, A.: Atmospheric number size distributions of soot particles and estimation of emission factors, *Atmos. Chem. Phys.*, 6, 1021-1031, 2006.
- Saiz-Lopez, A., Gómez Martín, J. C., Plane, J. M. C., Saunders, R. W., Baker, A. R., Von Glasow, R., Carpenter, L. J. and McFiggans, G.: Atmospheric chemistry of iodine, *Chem. Rev.*, 112, 1773-1804, 2012.
- Saiz-Lopez, A. and Plane, J. M. C.: Novel iodine chemistry in the marine boundary layer, *Geophys. Res. Lett.*, 31, L04112 1-4, 2004.

- Santos, F. J., López-Gutiérrez, J. M., García-León, M., Suter, M. and Synal, H. A.: Determination of $^{129}\text{I}/^{127}\text{I}$ in aerosol samples in Seville (Spain), *J. Environ. Radioact.*, 84, 103-109, 2005.
- Simpson, W. R., von Glasow, R., Riedel, K., Anderson, P., Ariya, P., Bottenheim, J., Burrows, J., Carpenter, L. J., Frieß, U., Goodsite, M. E., Heard, D., Hutterli, M., Jacobi, H. -, Kaleschke, L., Neff, B., Plane, J., Platt, U., Richter, A., Roscoe, H., Sander, R., Shepson, P., Sodeau, J., Steffen, A., Wagner, T. and Wolff, E.: Halogens and their role in polar boundary-layer ozone depletion, *Atmos. Chem. Phys.*, 7, 4375-4418, 2007.
- Tölgyessy, J. (Ed.): *Chemistry and Biology of Water, Air and Soil-Environmental Aspects*, 1993.
- Tsukada, H., Hara, H., Iwashima, K. and Yamagata, N.: The iodine content of atmospheric aerosols as determined by the use of a fluoropore filter for collection, *Bull. Chem. Soc. Jpn.*, 60, 3195-3198, 1987.
- Turekian, K. K., Benninger, L. K. and Dion, E. P.: ^7Be and ^{210}Pb total deposition fluxes at New Haven, Connecticut and at Bermuda, *Journal of Geophysical Research: Oceans*, 88, 5411-5415, 1983.
- Vogt, R., Sander, R., von Glasow, R. and Crutzen, P.: Iodine Chemistry and its Role in Halogen Activation and Ozone Loss in the Marine Boundary Layer: A Model Study, *J. Atmos. Chem.*, 32, 375-395, 1999.
- Wimschneider, A. and Heumann, K. G.: Iodine speciation in size fractionated atmospheric particles by isotope dilution mass spectrometry, *Fresenius J. Anal. Chem.*, 353, 191-196, 1995.
- Xu, S., Freeman, S. P. H. T., Hou, X., Watanabe, A., Yamaguchi, K. and Zhang, L.: Iodine Isotopes in Precipitation: Temporal Responses to ^{129}I Emissions from the Fukushima Nuclear Accident, *Environmental Science and Technology*, 47, 2010851-10859, 2013.
- Xu, S., Zhang, L., Freeman, S. P. H. T., Hou, X., Shibata, Y., Sanderson, D., Cresswell, A., Doi, T. and Tanaka, A.: Speciation of Radiocesium and Radioiodine in Aerosols from Tsukuba after the Fukushima Nuclear Accident, *Environ. Sci. Technol.*, 49, 1017-1024, 2015.
- Yi, P., Aldahan, A., Hansen, V., Possnert, G. and Hou, X.: Iodine Isotopes (^{129}I and ^{127}I) in the Baltic Proper, Kattegat, and Skagerrak Basins, *Environ.Sci.Technol.*, 43, 903-909, 2011.
- Yi, P., Aldahan, A., Possnert, G., Hou, X., Hansen, V. and Wang, B.: ^{127}I and ^{129}I Species and Transformation in the Baltic Proper, Kattegat, and Skagerrak Basins, *Environ. Sci. Technol.*, 46, 10948-10956, 2012.

Table 1. Sampling information of aerosols collected at Risø, Denmark in 2011 and 2014. Data of ^{131}I , ^7Be and ^{210}Pb in the aerosol samples are adopted from the DTU Nutech report (Nielsen et al., 2011). The reference time was the mid-point of sampling period, and analytical uncertainties were 5% for ^{131}I , within 1% for ^7Be and ^{210}Pb .

Sample No	Sampling date	Air flux, m^3	Air flux, m^3/h	Weigh t, g	^{131}I , $\mu\text{Bq}/\text{m}^3$	^7Be , $\mu\text{Bq}/\text{m}^3$	^{210}Pb , $\mu\text{Bq}/\text{m}^3$
AE11-1	31 st Mar-4 th Apr, 2011	88833	2757	72.5	205	1925	66
AE11-2	4-7 th Apr, 2011	64339	2751	79.2	218	1482	47
AE11-3	7-11 th Apr, 2011	55911	1744	79.5	147	1482	47
AE11-4	11-14 th Apr, 2011	27083	1096	70.9	110	2750	172
AE11-5	14-18 th Apr, 2011	48317	1505	77.9	58.3	2750	172
AE11-6	18-26 th Apr, 2011	101400	1593	80.8	20.9	4528	249
AE11-7	26 th Apr-2 nd May, 2011	54600	1117	77.7	14.8	4027	253
AE14-1	8-15 th Dec, 2014	37917	2727	21.7	< D.L.	1499	54.9

Table 2. Analytical results of chemical species of ^{127}I and ^{129}I in aerosol collected from Risø, Denmark during spring 2011 and winter 2014.

Sample	TI	WSI	Iodate	Iodide	NSI	RII
^{127}I concentration, ng/m^3						
AE11-1	1.187 ± 0.062	0.152 ± 0.002	ND	0.158 ± 0.008	0.34 ± 0.019	0.606 ± 0.042
AE11-2	1.797 ± 0.116	0.141 ± 0.01	0.022 ± 0.012	0.119 ± 0.006	0.556 ± 0.037	0.977 ± 0.049
AE11-3	1.927 ± 0.115	0.264 ± 0.004	ND	0.259 ± 0.013	0.813 ± 0.027	0.983 ± 0.05
AE11-4	2.48 ± 0.129	0.258 ± 0.013	ND	0.276 ± 0.014	0.825 ± 0.049	1.664 ± 0.085
AE11-5	2.027 ± 0.104	0.221 ± 0.011	ND	0.237 ± 0.012	0.638 ± 0.036	1.308 ± 0.087
AE11-6	1.506 ± 0.112	0.305 ± 0.007	ND	0.327 ± 0.017	0.624 ± 0.033	0.585 ± 0.03
AE11-7	1.041 ± 0.055	0.316 ± 0.019	0.033 ± 0.024	0.283 ± 0.014	0.377 ± 0.027	0.343 ± 0.018
AE14-1	2.356 ± 0.127	0.618 ± 0.019	ND	0.739 ± 0.039	0.929 ± 0.057	0.802 ± 0.041
^{129}I concentration, $\times 10^5$ atoms/ m^3						
AE11-1	28.57 ± 1.11	3.07 ± 0.08	ND	3.60 ± 0.43	8.33 ± 0.84	14.14 ± 0.64
AE11-2	72.98 ± 5.64	4.72 ± 0.41	ND	4.63 ± 0.27	20.55 ± 1.43	39.94 ± 1.64
AE11-3	25.60 ± 0.98	3.60 ± 0.15	ND	4.11 ± 0.72	10.80 ± 0.40	13.49 ± 2.83
AE11-4	47.27 ± 1.55	4.78 ± 0.23	ND	5.27 ± 0.57	13.43 ± 1.24	30.26 ± 4.24
AE11-5	43.81 ± 1.28	5.55 ± 0.27	ND	5.91 ± 0.74	12.58 ± 0.46	27.51 ± 1.28
AE11-6	12.73 ± 0.42	3.26 ± 0.10	ND	3.26 ± 0.30	4.60 ± 0.49	5.91 ± 0.36
AE11-7	11.31 ± 0.43	3.34 ± 0.11	ND	4.08 ± 0.24	3.36 ± 0.25	4.27 ± 0.74
AE14-1	97.00 ± 3.01	26.85 ± 0.65	ND	30.12 ± 1.68	34.74 ± 0.80	39.01 ± 1.49
$^{129}\text{I}/^{127}\text{I}$ atomic ratio, $\times 10^{-8}$						
AE11-1	50.78 ± 3.31	42.73 ± 1.28	ND	48.04 ± 6.23	51.70 ± 5.98	49.19 ± 4.07
AE11-2	85.70 ± 8.63	70.73 ± 8.06	ND	81.93 ± 6.36	78.03 ± 7.50	86.21 ± 5.62
AE11-3	28.03 ± 1.99	28.82 ± 1.26	ND	33.49 ± 6.13	28.04 ± 1.40	28.94 ± 6.25
AE11-4	40.21 ± 2.48	39.11 ± 2.72	ND	40.29 ± 4.84	34.34 ± 3.78	38.37 ± 5.72
AE11-5	45.60 ± 2.70	52.85 ± 3.66	ND	52.50 ± 7.16	41.58 ± 2.79	44.36 ± 3.61
AE11-6	17.84 ± 1.46	22.59 ± 0.89	ND	21.08 ± 2.24	15.56 ± 1.85	21.32 ± 1.69
AE11-7	22.92 ± 1.48	22.30 ± 1.55	ND	30.43 ± 2.38	18.81 ± 1.93	26.28 ± 4.73
AE14-1	86.84 ± 5.40	91.70 ± 3.55	ND	86.03 ± 6.63	78.84 ± 5.20	102.63 ± 6.51

Analytical uncertainties were presented as 1σ .

Table 3. Possible pathways of formation of iodide by reduction of sulfur compounds

No.	Phase	Reactions	References
1	Gas	$\text{DMS} + \text{OH} \rightarrow \text{SO}_2$ $\text{DMS} + \text{NO}_3 \rightarrow \text{SO}_2$	(Chatfield and Crutzen 1990)
2	Gas/Aerosol	$\text{SO}_2 + \text{H}_2\text{O} \rightarrow \text{HSO}_3^-$ $\text{SO}_2 + \text{H}_2\text{O} \rightarrow \text{SO}_3^{2-}$	
3	Gas-Aerosol interface	$\text{I} + \text{HSO}_3^- \rightarrow \text{I}^- + \text{SO}_4^{2-}$ $\text{I} + \text{SO}_3^{2-} \rightarrow \text{I}^- + \text{SO}_4^{2-}$	
4	Aerosol	$\text{HOI} + \text{HSO}_3^- / \text{SO}_3^{2-} \rightarrow \text{I}^- + \text{SO}_4^{2-}$ $\text{HOI} + \text{SO}_3^{2-} \rightarrow \text{I}^- + \text{SO}_4^{2-}$ $\text{HOI}_2 + \text{HSO}_3^- / \text{SO}_3^{2-} \rightarrow \text{I}^- + \text{SO}_4^{2-}$ $\text{HOI}_2 + \text{SO}_3^{2-} \rightarrow \text{I}^- + \text{SO}_4^{2-}$	(Saiz-Lopez et al., 2012)

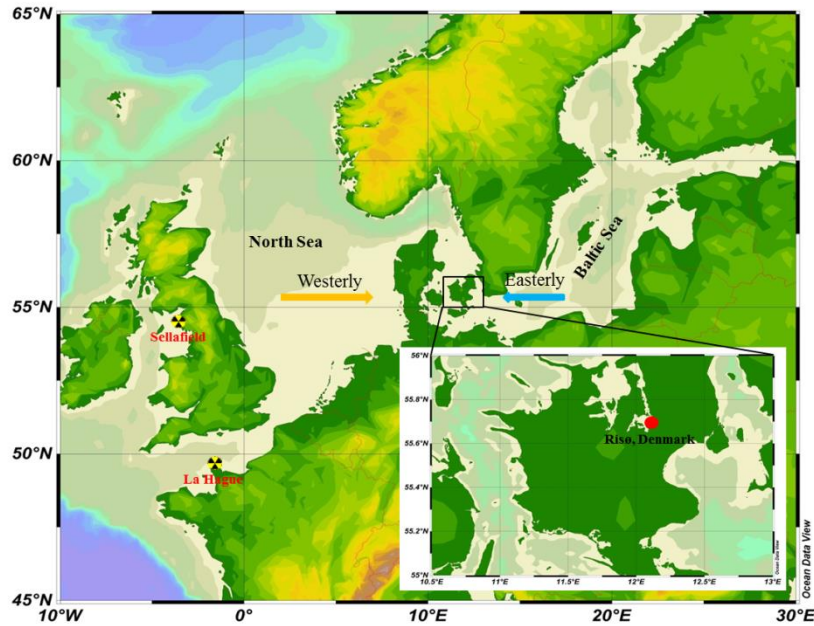


Figure 1. Map showing the sampling site (red dot) at Risø, Denmark for aerosol collection. The two nuclear reprocessing plants, Sellafield (United Kingdom) and La Hague (France) are indicated as radioactivity labels. Yellow arrow and blue arrow show the westerly wind and easterly wind, respectively.

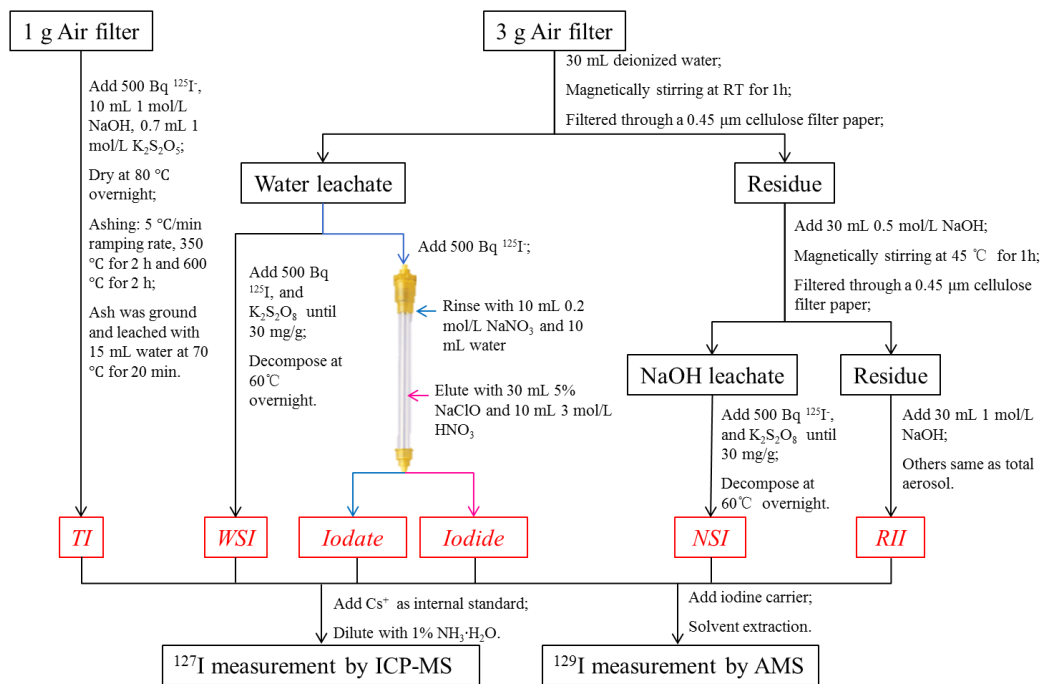


Figure 2. Schematic diagram of analytical procedure for determination of ^{127}I and ^{129}I species in aerosols. TI for total iodine, WSI for water soluble iodine, RII for residual insoluble iodine and NSI for NaOH soluble iodine.

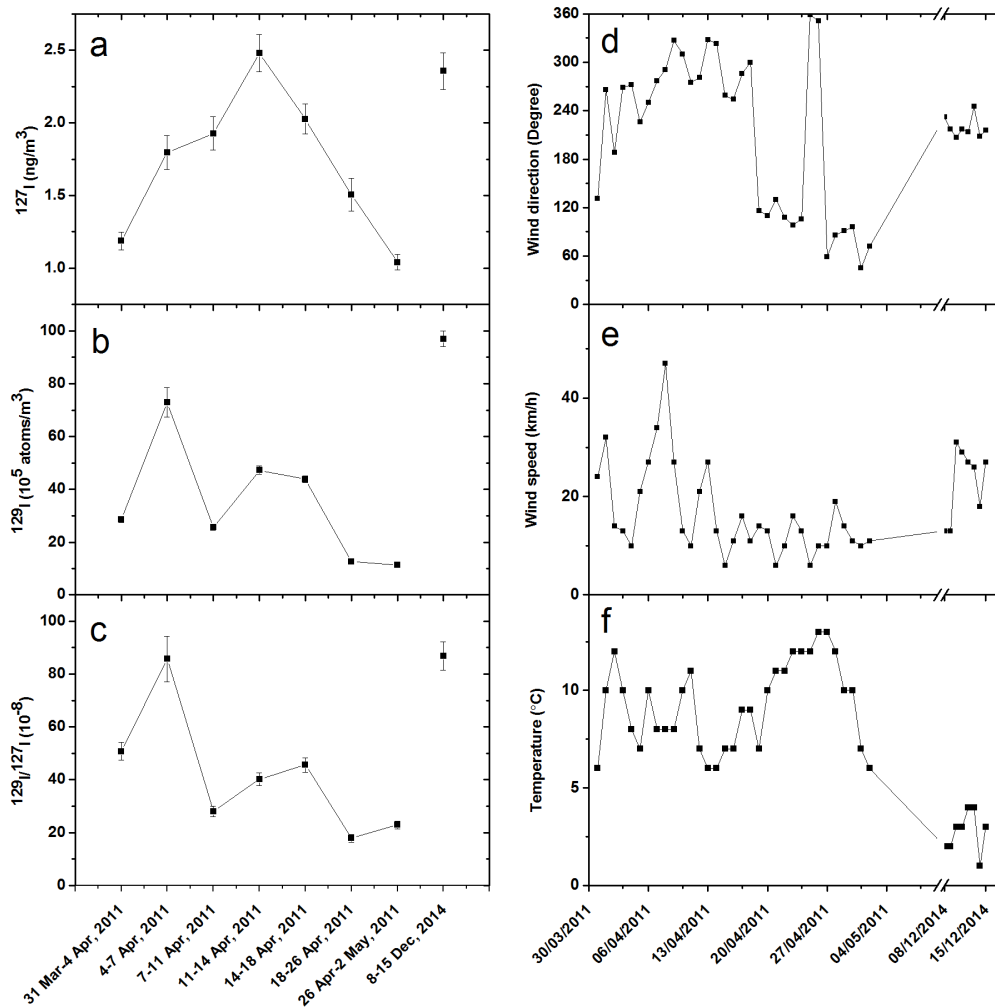


Figure 3. Variation of ^{127}I concentrations (a), ^{129}I concentrations (b), $^{129}\text{I}/^{127}\text{I}$ ratios (c) in aerosol, wind direction (d), wind speed (e) and temperature (f) during the sampling period. The historical meteorological data, including temperature, wind, precipitation were obtained from the observation station of Hangarvej in Roskilde, Denmark (55.594°N 12.128°E) based on 41 m ASL (<http://www.wunderground.com>).

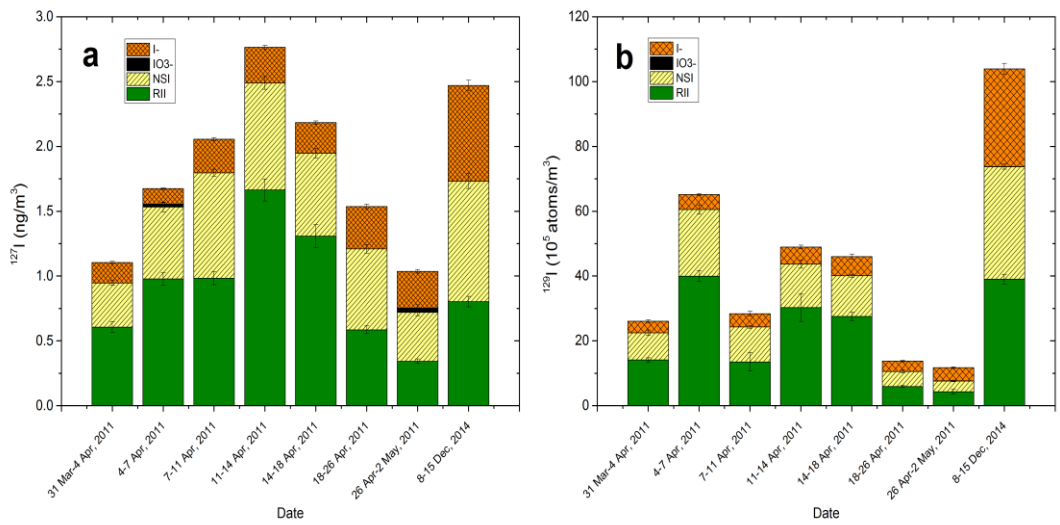


Figure 4. Concentration of different species of iodine in aerosol samples for ^{127}I (a) and ^{129}I (b), indicating NSI and RII are major species of iodine, and iodide is the predominant species of water soluble iodine species.

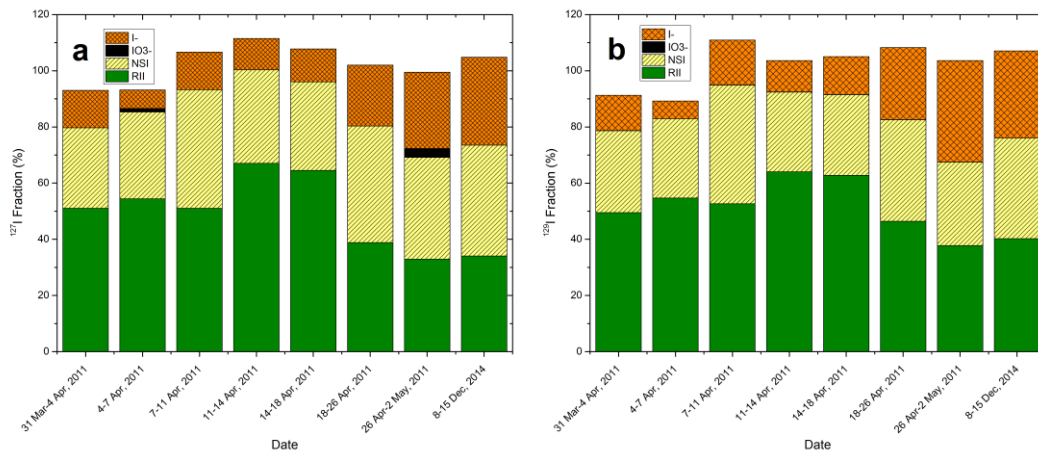


Figure 5. Distribution of iodine species in aerosol samples for ^{127}I (a) and ^{129}I (b).

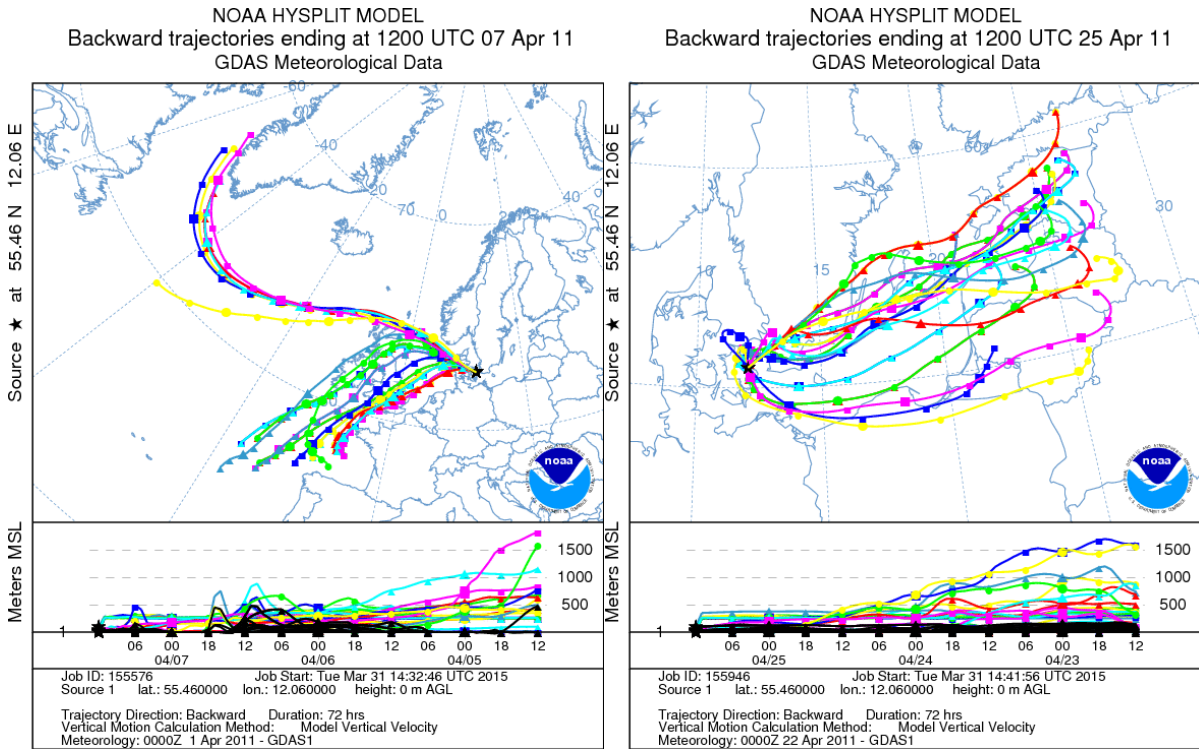


Figure 6. The 72 h (3 days) air mass back trajectories for starting altitudes of 0 m above ground level (AGL) calculated from the FNL database of the National Ocean and Atmospheric Administration (NOAA) and simulated by using the Hybrid Single-Particle Lagrangian Integrated Trajectory (HY-SPLIT) model. 4-7 April 2011 (left) and 21-25 April 2011 (right).

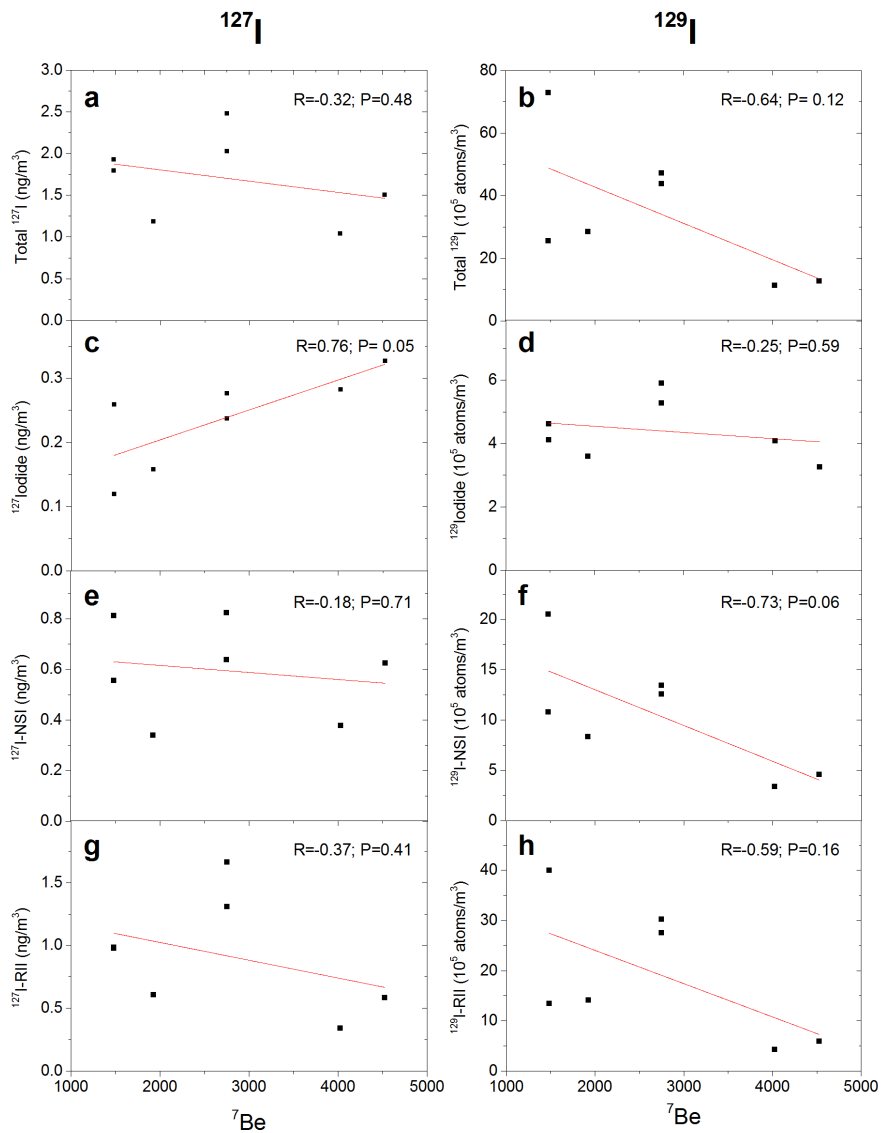


Figure 7. Correlation of aerosol ^7Be with iodine species including total ^{127}I (a) and ^{129}I (b), ^{127}I (c), ^{129}I (d), NSI for ^{127}I (e) and ^{129}I (f), as well as RII for ^{127}I (g) and ^{129}I (h).

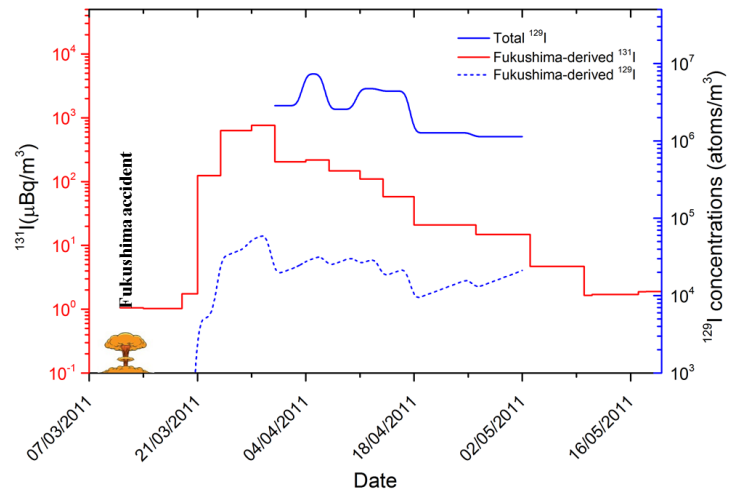


Figure 8. ^{131}I radioactivity (red), ^{129}I concentrations (blue) in aerosols from Risø, Denmark after the Fukushima accident (Nielsen et al., 2011). The Fukushima-derived ^{129}I concentrations are calculated based on $^{129}\text{I}/^{131}\text{I}$ atomic ratio of 16.0 ± 2.2 deduced from Fukushima-affected aerosol samples (Xu et al., 2015).

Supplementary material

The 72 h (3 days) air mass back trajectories for starting altitudes of 0 m above ground level (AGL) calculated from the FNL database of the National Ocean and Atmospheric Administration (NOAA) and simulated by using the Hybrid Single-Particle Lagrangian Integrated Trajectory (HY-SPLIT) model.

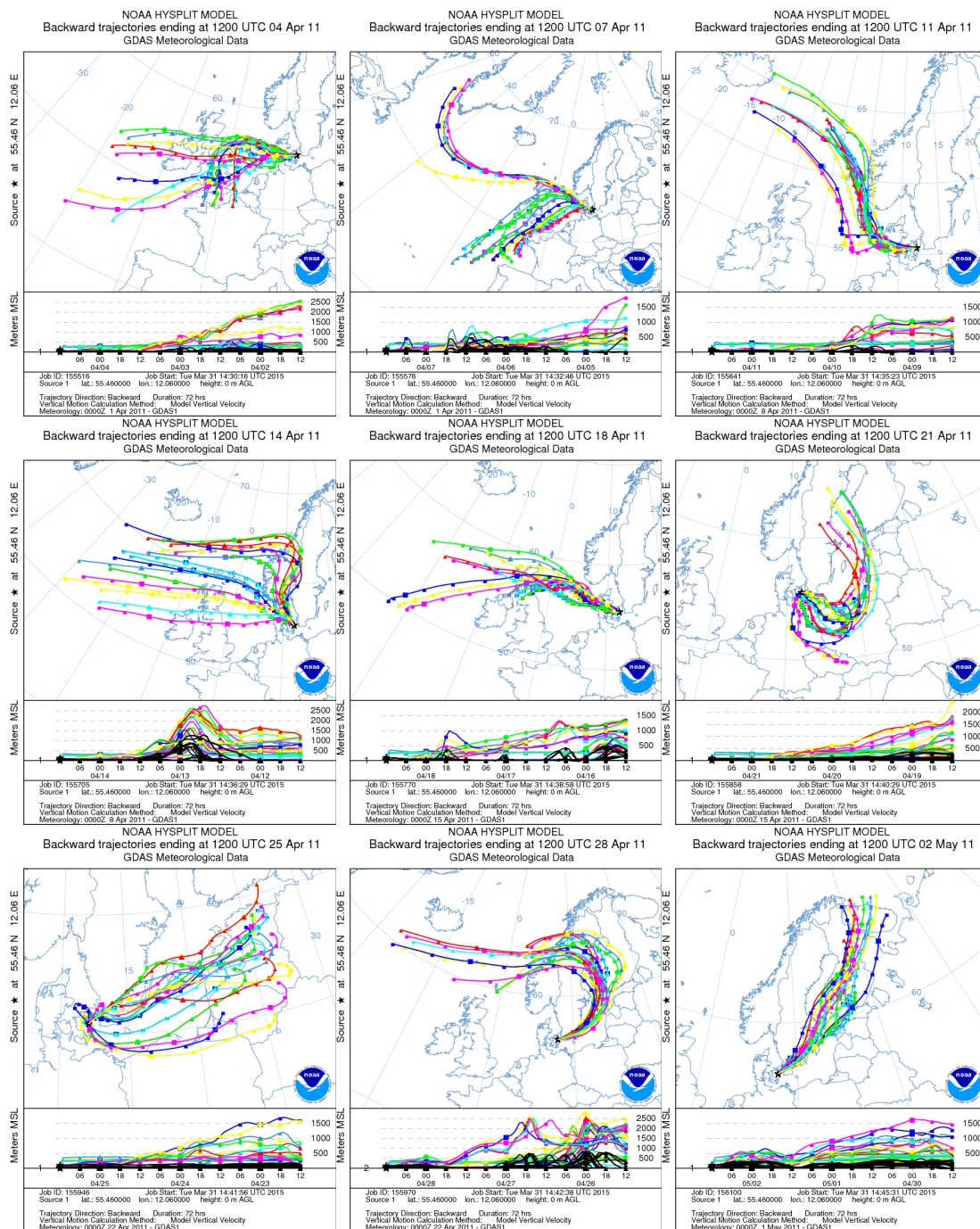


Figure S-1. Back trajectories from 4 April to 2 May, 2011

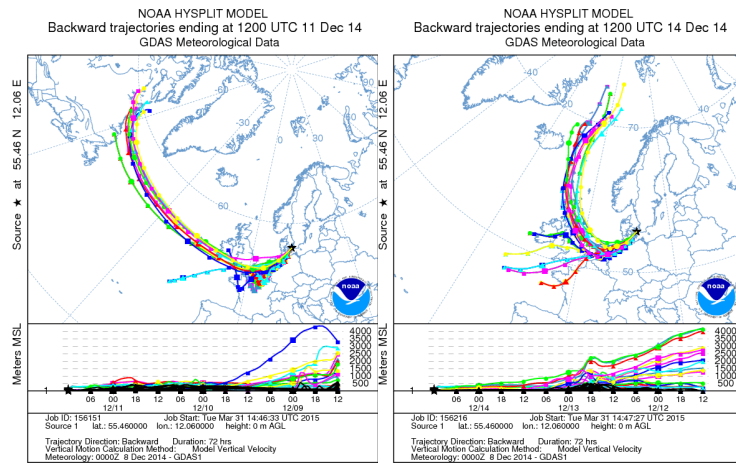


Figure S-2. Back trajectories from 8-15 December, 2014

DTU Nutech is the Danish national competence center for nuclear technologies. The aim of the center is to develop and utilize knowledge concerning radioactivity and ionizing radiation for the benefit of society.

DTU Nutech
Center for Nuclear Technologies
Technical University of Denmark

Frederiksborgvej 399
P.O. Box 49
4000 Roskilde, Denmark
Tel. +45 4677 4900
Fax +45 4677 4959

www.nutech.dtu.dk